AD-A081 864 GRUMMAN AEROSPACE CORP BETHPAGE NY F/G 1/3
INTEGRATED RACK CONCEPT STUDY FOR V/STOL TYPE AIRCRAFT.(U)
JAN 80 E V RAMIREZ, B BORGENSON, A CASERTA N62269-78-R-0294
NADC-78-11360
UNCLASSIFIED NL

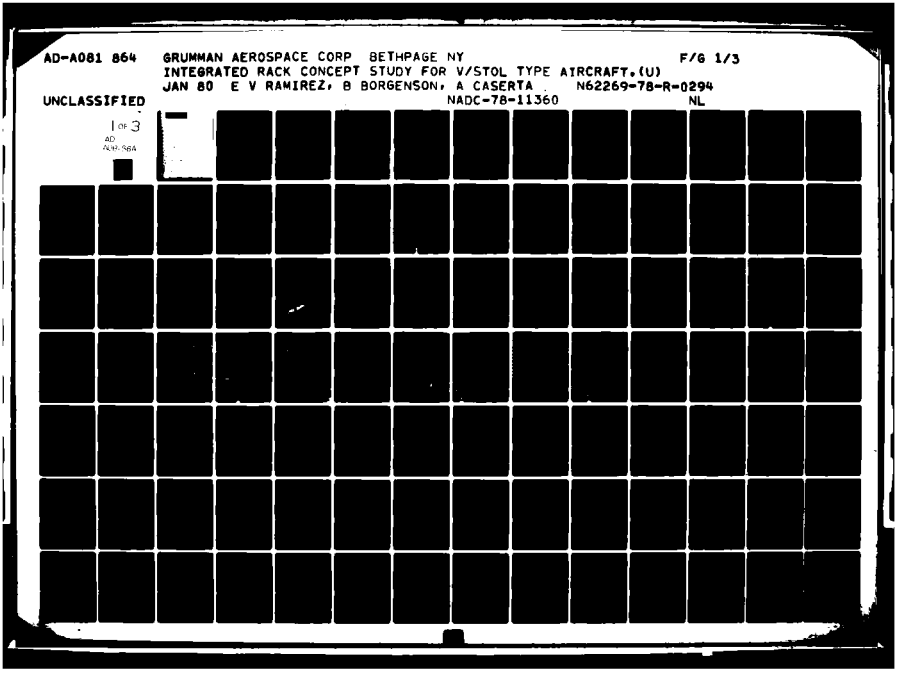

UNCLASSIFIED

SECURITY CLASSIFICATION OF THIS PAGE (When Data Entered)

REPORT DOCUMENTATION PAGE

READ INSTRUCTIONS BEFORE COMPLETING FORM

1. REPORT NUMBER: NADC-78-11360	2. GOVT ACCESSION NO.
3. RECIPIENT'S CATALOG NUMBER	
4. TITLE (and Subtitle): Integrated Rack Concept Study for V/STOL Type Aircraft	5. TYPE OF REPORT & PERIOD COVERED: Final Report for the Period 1 October 1978 to December 1979
6. PERFORMING ORG. REPORT NUMBER	
7. AUTHOR(s): E. V. Ramirez, B. Borgenson, A. Caserta, V. Cirrito, R. Dahl, B. Lijoi, J. Makowski, B. Steinberg	8. CONTRACT OR GRANT NUMBER(s): N62269-78-R-0294
9. PERFORMING ORGANIZATION NAME AND ADDRESS: Grumman Aerospace Corporation, Bethpage, New York 11714	10. PROGRAM ELEMENT, PROJECT, TASK AREA & WORK UNIT NUMBERS: 11 Jan 80
11. CONTROLLING OFFICE NAME AND ADDRESS: Naval Air Development Center, Warminster, PA 18974	12. REPORT DATE: 207
	13. NUMBER OF PAGES: 199
14. MONITORING AGENCY NAME & ADDRESS (if different from Controlling Office)	15. SECURITY CLASS. (of this report)
	15a. DECLASSIFICATION/DOWNGRADING SCHEDULE

16. DISTRIBUTION STATEMENT (of this Report)

Approved for Public Release; Distribution Unlimited

17. DISTRIBUTION STATEMENT (of the abstract entered in Block 20, if different from Report)

NADC/6011
NADC/8131
NASC
DDC

DTIC ELECTE MAR 17 1980 S A

18. SUPPLEMENTARY NOTES

19. KEY WORDS (Continue on reverse side if necessary and identify by block number)

Integrated Avionics Rack, Air Impingement, Conduction Cooled Heat Pipe, Primary and Secondary backplanes, Improved Standard Electronic Module (ISEM), Chip Carriers, Junction Temperature, Hollow Core Module, Thermal Analysis, SOSTEL, Parametric Thermal Analysis, Cross-Flow Heat Exchanger, Sensitivity Evaluation Program.

20. ABSTRACT (Continue on reverse side if necessary and identify by block number)

Six different rack concepts were investigated for determining the most optimum configuration of packaging the avionic equipment on A and B type V/STOL aircraft. The two basic approaches of cooling the rack considered were air impingement and conduction cooled. As a baseline, two module configurations were used; an Improved Standard Electronic Module-2A, and a Hollow Core Design with an ISEM-2A form factor. The modules, utilizing chip carrier semiconductor devices, were assumed to dissipate 5 to 10 watts. The rack power system makes use of Solid State Electric Logic (SOSTEL) power management elements. A parametric thermal analysis with junction temperatures from 60 to 125°C was performed. Each of the following disciplines, Mechanical, EMI, ECS, Reliability, Maintainability and Life Cycle Costs were also considered in the design of the racks. A Sensitivity Evaluation Program was used to select the most viable approaches.

DD FORM 1 JAN 73 1473 EDITION OF 1 NOV 65 IS OBSOLETE S/N 0102-014-6601

UNCLASSIFIED

SECURITY CLASSIFICATION OF THIS PAGE (When Data Entered)

388847

CONTENTS

CONTENTS (contd)

CONTENTS (contd)

ILLUSTRATIONS

ILLUSTRATIONS (contd)

ILLUSTRATIONS (contd)

ILLUSTRATIONS (contd)

ILLUSTRATIONS (contd)

ILLUSTRATIONS (contd)

TABLES

TABLES (contd)

1 - INTRODUCTION

This report contains the activities performed by Grumman Aerospace Corp., Bethpage, New York, on the Integrated Rack Concept Study for V/STOL type aircraft. The study identifies and evaluates conceptual integrated rack designs to support postulated V/STOL avionics systems. The study was performed for the Naval Air Development Center, Warminster, Pa., Contract No N62269-78-C-0294.

The objectives and technology assumptions of The Integrated Rack Study are summarized in the following portions of Section 1. Section 2 describes the requirements imposed on the designs of the integrated racks. Sections 3 and 4 contain the technical discussions on the rack configurations. The conclusions are in Section 5 while Section 6 lists the recommendations which were developed as a result of the study.

1.1 TECHNOLOGY ASSUMPTIONS

The approach taken in conducting this study was to identify technologies which would support the integrated rack concepts, provided they would be sufficiently mature by the 1982-1985 time frame. At present, there are several technologies which by their inclusion enhance the rack design concepts. However, it must be noted that none of these technology disciplines are essential in a near term point design of the rack. Each of the following disciplines is a preferred alternative which can be traded off with some other approaches. Their individual selection and combined usage result in a technology approach which has been identified as the baseline requirement for the integrated rack designs.

1.1.1 Standard Modules

The shipboard Navy has successfully demonstrated that standardization of shipboard electronics to the Standard Electronic Module (SEM) family will provide many benefits, one of the most important being reduced life cycle costs. Although a formal standardization program has not yet been developed for avionics,

a serious contender for the Standard Avionics Module is the ISEM-2A module. The ISEM-2A is an improved or modified SEM module of slightly different form factor than the SEM 2A unit. Both modules are shown in Figure 1. The ISEM, with its larger area, has increased the number of pins on its connector from 80 to 100. The ISEM module can utilize flatpacks, dual in line, or chip carrier LSI circuits. The ISEM card represents a transcended technology, which is capable of providing as many benefits to the avionics community as the SEM did for the shipboard branch. It is for this reason that all modules to be packaged in integrated racks are therefore assumed to be ISEM-2A modules.

1.1.2 Chip Carriers

It has been predicted that chip carriers will account for 80% of future LSI devices by 1985. Their projected use on a card will result in a 1/3 saving of active area when compared to Dual In Line Packages. All ISEM cards will be assumed to contain chip carriers.

1.1.3 Power Source

The V/STOL power source is assumed to be 270V dc. The development of the Advanced Aircraft Electric System (AAES) and Solid-State Electric Logic (SOSTEL) has been closely monitored by Grumman during the study. Portions of these systems have been included for control and generation.

1.1.4 Power Supplies

The technology projections that have been made to support the Integrated Rack Study indicate that most new technologies which are prime candidates for rack circuitry, such as Integrated Injection Logic (I^2L) and HMOS, will utilize +5V as the power source. The standardization to just one source simplifies the power requirements of the rack avionics. Thus, in performing the partitioning, it was assumed that:

- Only a single source voltage (+5V) will be adequate for all rack circuits
- Only two types of power supplies would be required; a 200-watt and a 90 watt unit.

1.1.5 Fiber Optics

The ALOFT program has successfully demonstrated the benefits of airborne fiber optics interconnections. The integrated rack design accomodates the use of

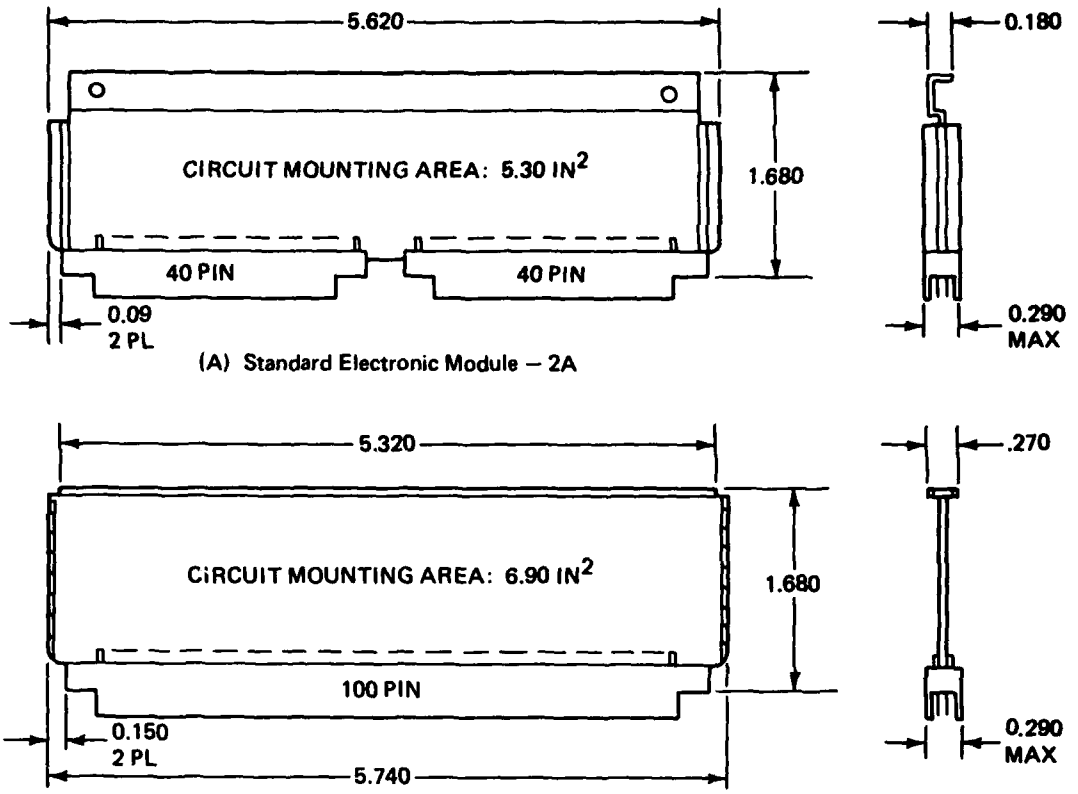

Figure 1 Electronic Module – Center Frame

fiber optics in its multiplex data buses for signal information transfer, thereby minimizing conducted interference to the rack electronics. Within the rack, space has been set aside for the 1553-type terminals required with the use of the fiber optics data buses.

2 - REQUIREMENTS

2.1 AVIONIC SYSTEMS

The Integrated Rack Study supports two V/STOL vehicle configurations: the AEW A V/STOL and the DLI B V/STOL. The avionic systems required for these missions will make full use of the Distributed Processing architecture. Distributed Processing represents an enhanced organization over present day avionic architectures. The key factors of this system are in the utilization of standard processing hardware and software elements, which provide processing flexibility of proportions to the throughput requirements. Figures 2 and 3 are the baseline architectures used in the identification of rack avionics for A and B V/STOL, respectively.

The partition of the avionics suite into rack equipment or conventionally packaged WRA's was generally predicated on the function, technology, and power required to implement the function. Functions which utilized digital and computer circuitry and low level analog signals were designated as prime candidate systems for the rack. Functions utilizing high power analog (RF circuitry) were not considered to be applicable to rack ISEM-2A packaging, primarily because these types of circuits have large components and/or dissipate an excessive amount of power. The exception to the selection of all digital hardware for rack circuitry is the Digital-Fly-By-Wire Flight Control System, which has strong safety of flight and vulnerability requirements. The study presumes that the packaging of this system is through conventional WRA's.

The projected time frame for the integrated rack avionics hardware is in the 1982-1985 time frame, which enables projected significant advances in technology to occur over present day circuits. One of the anticipated events is the wider utilization of low power technology such as Integrated Injection Logic (I^2L), which results in a significant decrease of the speed power product of present day circuits. With the anticipated advances in technology and a data base

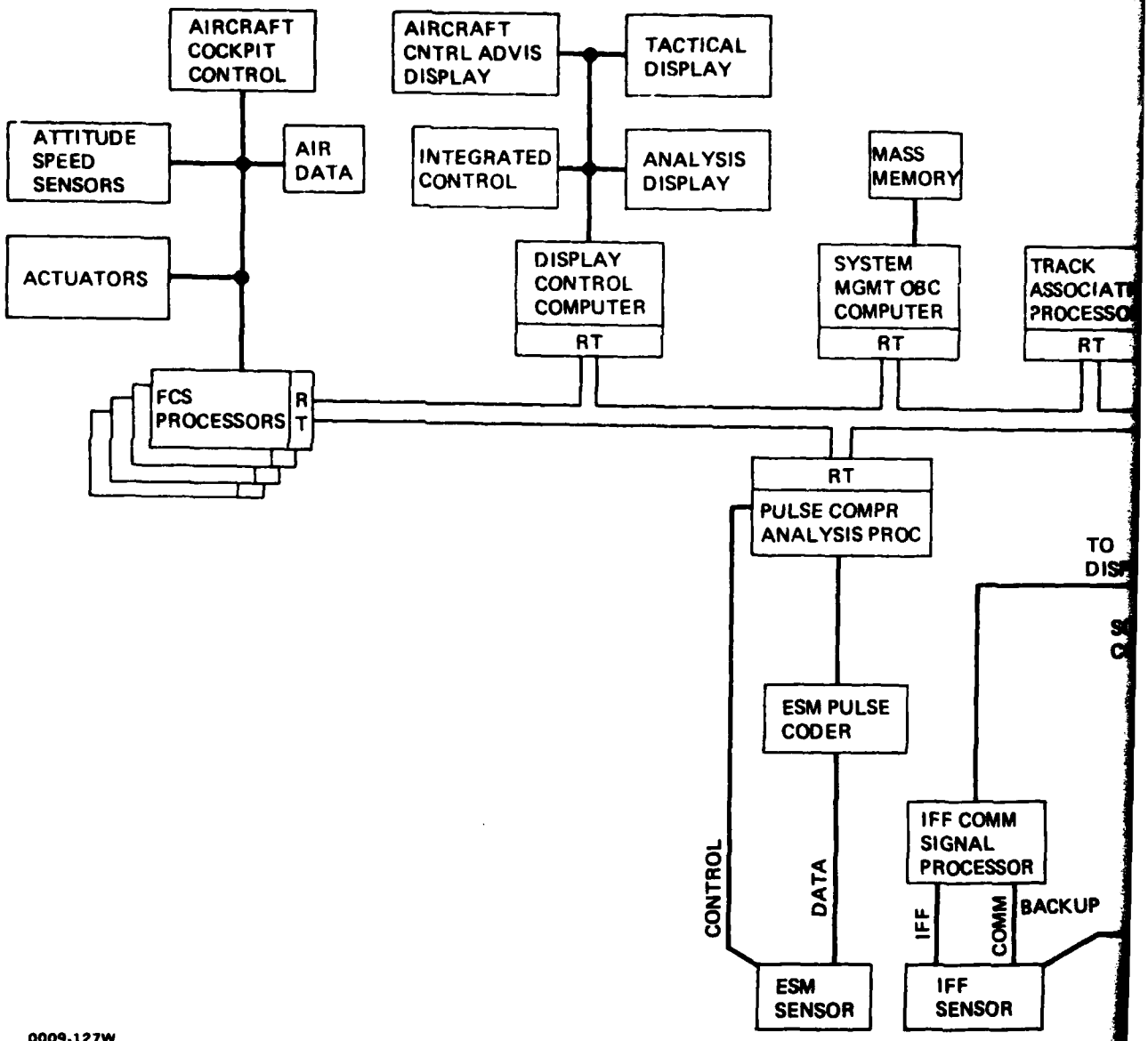
AIRCRAFT COCKPIT CONTROL
AIRCRAFT CNTRL ADVIS DISPLAY
TACTICAL DISPLAY
ATTITUDE SPEED SENSORS
AIR DATA
INTEGRATED CONTROL
ANALYSIS DISPLAY
MASS MEMORY
ACTUATORS
DISPLAY CONTROL COMPUTER
RT
SYSTEM MGMT OBC COMPUTER
RT
TRACK ASSOCIAT PROCESSO
RT
FCS PROCESSORS
R T
RT
PULSE COMPR ANALYSIS PROC
TO DISP
ESM PULSE CODER
IFF COMM SIGNAL PROCESSOR
CONTROL
DATA
IFF
COMM
BACKUP
ESM SENSOR
IFF SENSOR

0009-127W

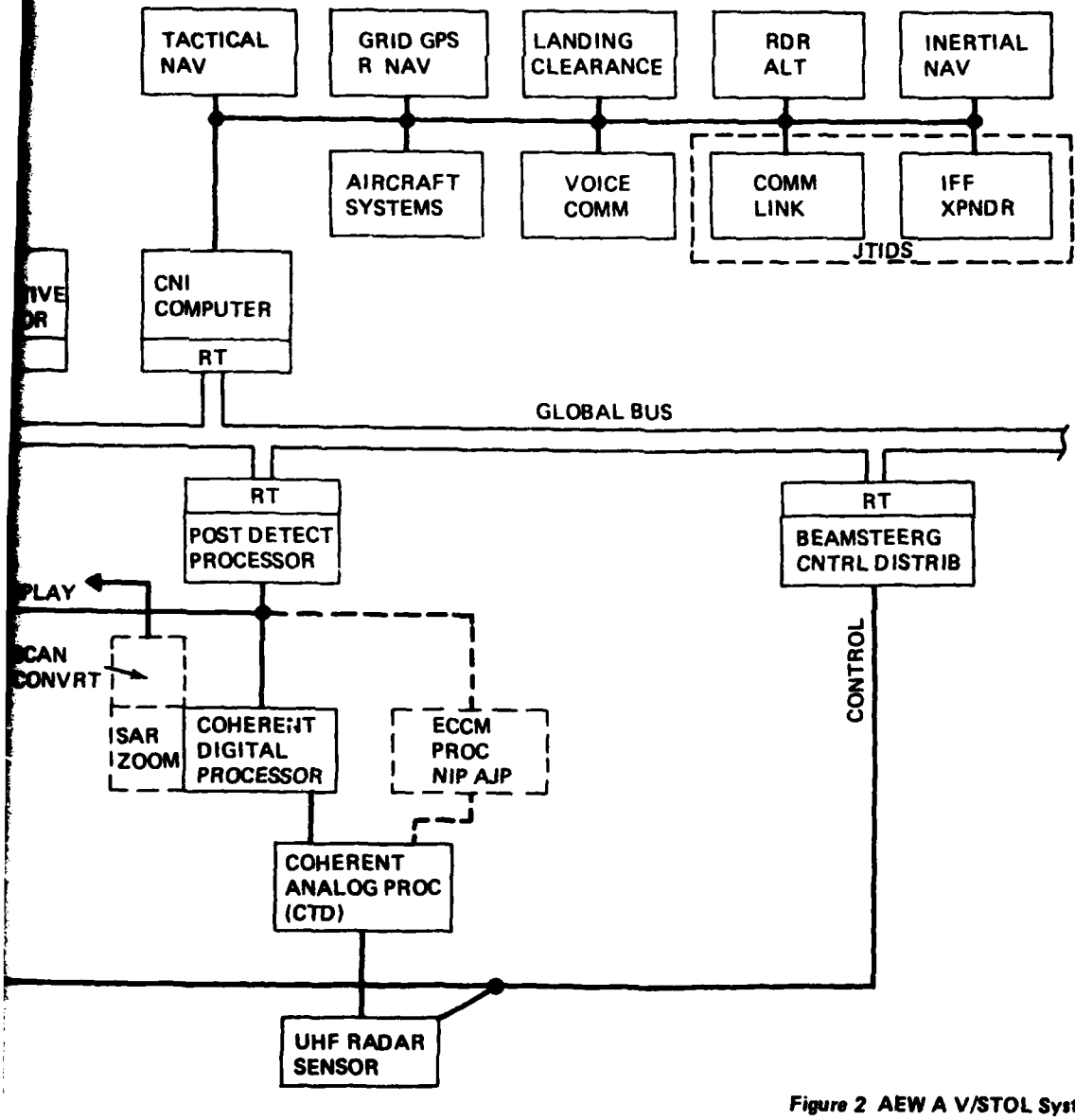

Figure 2 **AEW A V/STOL System Architecture**

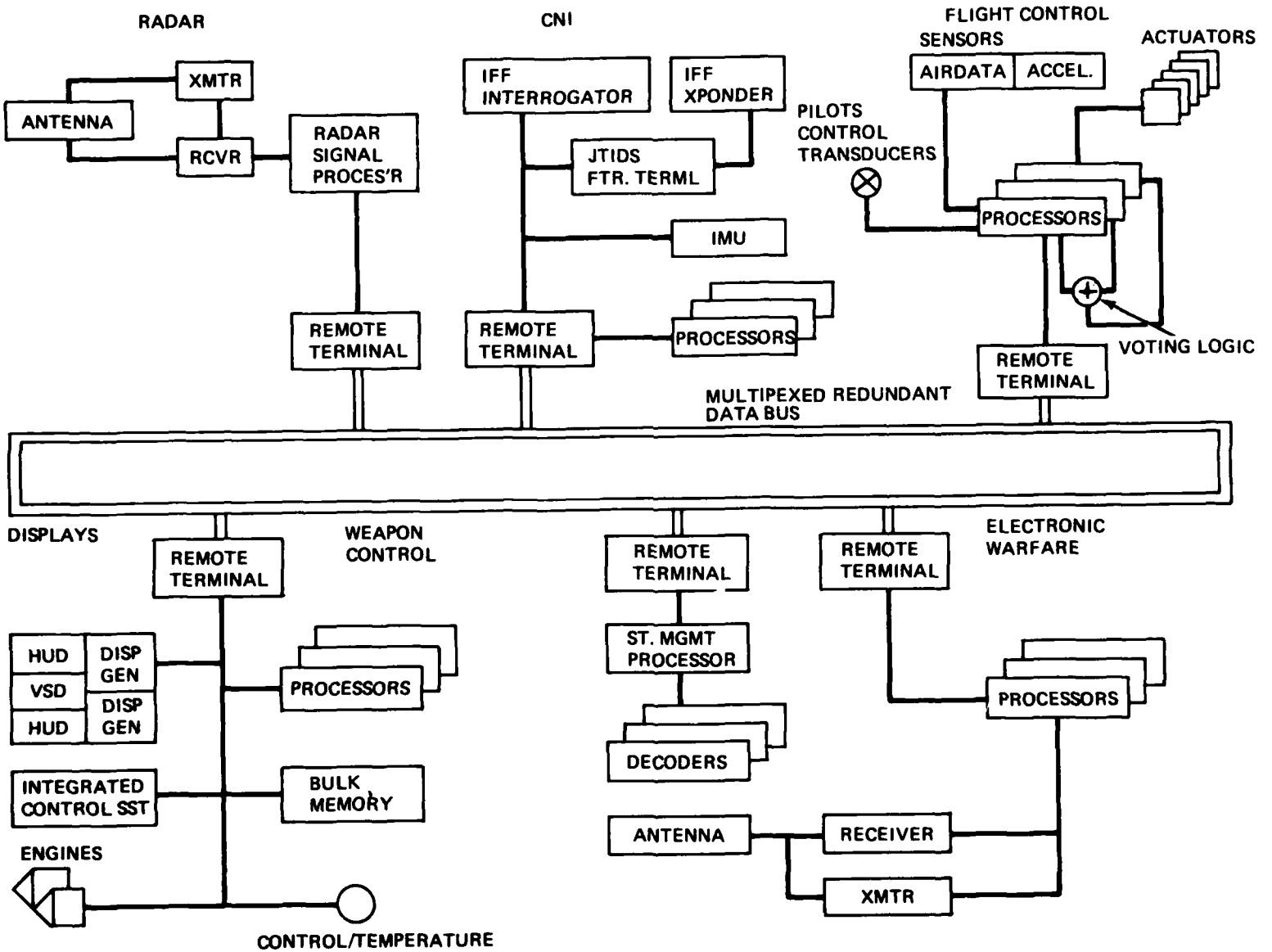

Figure 3 B V/STOL System Architecture

generated by other studies of V/STOL avionics, the partitioning portion of the study was conducted. The results presented in Section 2.2 describe all rack avionics in terms of total power per subsystem and the estimated number of ISEM cards required to implement the functions. Note that chip carriers mounted on both sides of the ISEM cards were presumed throughout the study.

2.2 ELECTRICAL POWER REQUIREMENTS

The A and B V/STOL power requirements of those subsystems designated for installation into integrated racks is presented in this section. To support these requirements, elements of the AAES currently under development by the Navy were utilized.

In the A V/STOL aircraft there are two areas which have been allocated as rack mounting areas (see Table 1). The power requirement for each subsystem in each area is the sum of the individual subsystem power dissipated, growth power, the power dissipated in the power supplies, and the power of the small fans used in the rack for humidity control. The estimated number of required power supplies are identified in the last two columns. These units, which are somewhat similar to the power supplies currently in development by the Naval Avionic Center, provide 2 watts of usable 5V power per cubic inch of rack volume. Active pursuit of improved 4 and 6 watts per cubic inch power supplies will reduce the space requirements for power supplies.

The B V/STOL integrated rack subsystems were distributed to four areas, as shown in Tables 2 and 3. In both V/STOL configurations, the SOSTEL power management concept was implemented. This encompasses the usage of the SOSTEL processor, multiplexing terminals, and power contactors (solid-state circuit breakers) for all voltages required. The power generating voltage was assumed to be 270V dc. Tables 1 through 3 also include power requirements for the standard 1553 data bus terminals.

Figures 4 and 5 present typical aircraft power profiles for typical missions of A and B V/STOL type aircraft. Variation in load profile versus mission time leads to the need for SOSTEL power management control to minimize power utilization in weight critical V/STOL vehicles.

Table 1 A V/STOL Power Requirements for Integrated Rack

SUBSYSTEM	NUMBER OF CARDS (SPACES)	POWER REQUIRED: POWER DISSIPATED BY CARDS	POWER REQUIRED: POWER DISSIPATED BY PWR SUPPLIES	POWER REQUIRED: POWER DISSIPATED BY MOTORS	GROWTH POWER	TOTAL REQUIRED POWER	NO. OF POWER SUPPLIES: 200 WATT	NO. OF POWER SUPPLIES: 90 WATT
RACK AREA 4								
IFF (+ MODE IV COMPUTER)	30	120	–	–	80	200	1	–
CNI	30	135	–	–	65	200	1	–
JTIDS	112	450	–	–	40	490	2	1
MASS MEMORY	72	240	–	–	50	290	1	1
DISPLAYS	134	534	–	–	66	600	3	–
TRACK PROCESSOR	80	240	–	–	50	290	1	1
DATA BUS TERM	32	264	–	–	26	290	1	1
SOSTEL	4	33	–	–	57	90	–	1
CONTACTOR	11	77	–	–	123	200	1	–
COOLING	–	–	–	800	0	800	4	–
PWR SUPPLY	455	–	1105	–	0	1105	–	–
	960	2093	1105	800	557	= 4555	15	5
RACK AREA 7								
COH DIG PROCESSOR	105	1050	–	–	40	1090	5	1
POST DETECT	225	900	–	–	100	1000	5	–
IFF PROCESSOR	120	480	–	–	10	490	2	1
EW	98	390	–	–	10	400	2	–
DATA BUS TERM	16	132	–	–	68	200	1	–
SOSTEL	4	33	–	–	57	90	–	1
CONTACTORS	14	98	–	–	102	200	1	–
COOLING	–	–	–	1000	0	1000	5	–
PWR SUPPLY	585	–	1443	–	0	1443	–	–
	1159	3083	1443	1000	387	5913	21	3

0009-003W

Table 2 B V/STOL Power Requirements for Integrated Racks (FORWARD)

SUBSYSTEM	NUMBER OF CARDS (SPACES)	POWER REQUIRED: POWER DISSIPATED BY CARDS	POWER DISSIPATED BY PWR SUPPLIES	POWER DISSIPATED BY MOTORS	GROWTH POWER	TOTAL REQUIRED POWER	NO. OF POWER SUPPLIES: 200 WATT	90 WATT
RACK AREA 1								
RADAR	80	375	–	–	25	400	2	–
DATA BUS TERM	8	66	–	–	24	90	–	1
SOSTEL	4	33	–	–	57	90	–	1
CONTACTOR	4	28	–	–	152	180	–	2
COOLING	–	–	–	200	–	200	1	–
POWER SUPPLY	130	–	299	–	–	299	–	–
	226	502	299	200	258	1259	3	4
RACK AREA 3								
CNI	100	535	–	–	65	600	3	–
DATA BUS TERM	8	66	–	–	24	90	–	1
SOSTEL	4	33	–	–	57	90	–	1
CONTACTORS	4	28	–	–	172	200	1	–
COOLING	–	–	–	200	–	200	1	–
POWER SUPPLY	156	–	377	–	–	377	–	–
	272	662	377	200	318	1557	5	2

0009-125W

Table 3 B V/STOL Power Requirements for Integrated Racks (AFT)

SUBSYSTEM	NUMBER OF CARDS (SPACES)	POWER REQUIRED: POWER DISSIPATED BY CARDS	POWER DISSIPATED BY PWR SUPPLIES	POWER DISSIPATED BY MOTORS	GROWTH POWER	TOTAL REQUIRED POWER	NO. OF POWER SUPPLIES: 200 WATT	90 WATT
RACK AREA 11a								
DISPLAY	117	592	–	–	8	600	3	–
DATA BUS TERM	8	66	–	–	24	90	–	1
SOSTEL	4	33	–	–	57	90	–	1
CONTACTORS	4	28	–	–	172	200	1	–
COOLING	–	–	–	200	–	200	1	–
POWER SUPPLIES	156	–	377	–	–	377	–	–
	289	719	377	200	261	1557	5	2
RACK AREA 11b								
EW	100	440	–	–	140	580	2	2
DATA BUS TERM	8	66	–	–	24	90	–	1
SOSTEL	4	33	–	–	57	90	–	1
CONTACTORS	5	35	–	–	165	200	1	–
COOLING	–	–	–	200	–	200	1	–
POWER SUPPLIES	156	–	364	–	–	468	–	–
	273	574	364	200	386	1524	4	4

1301-132W

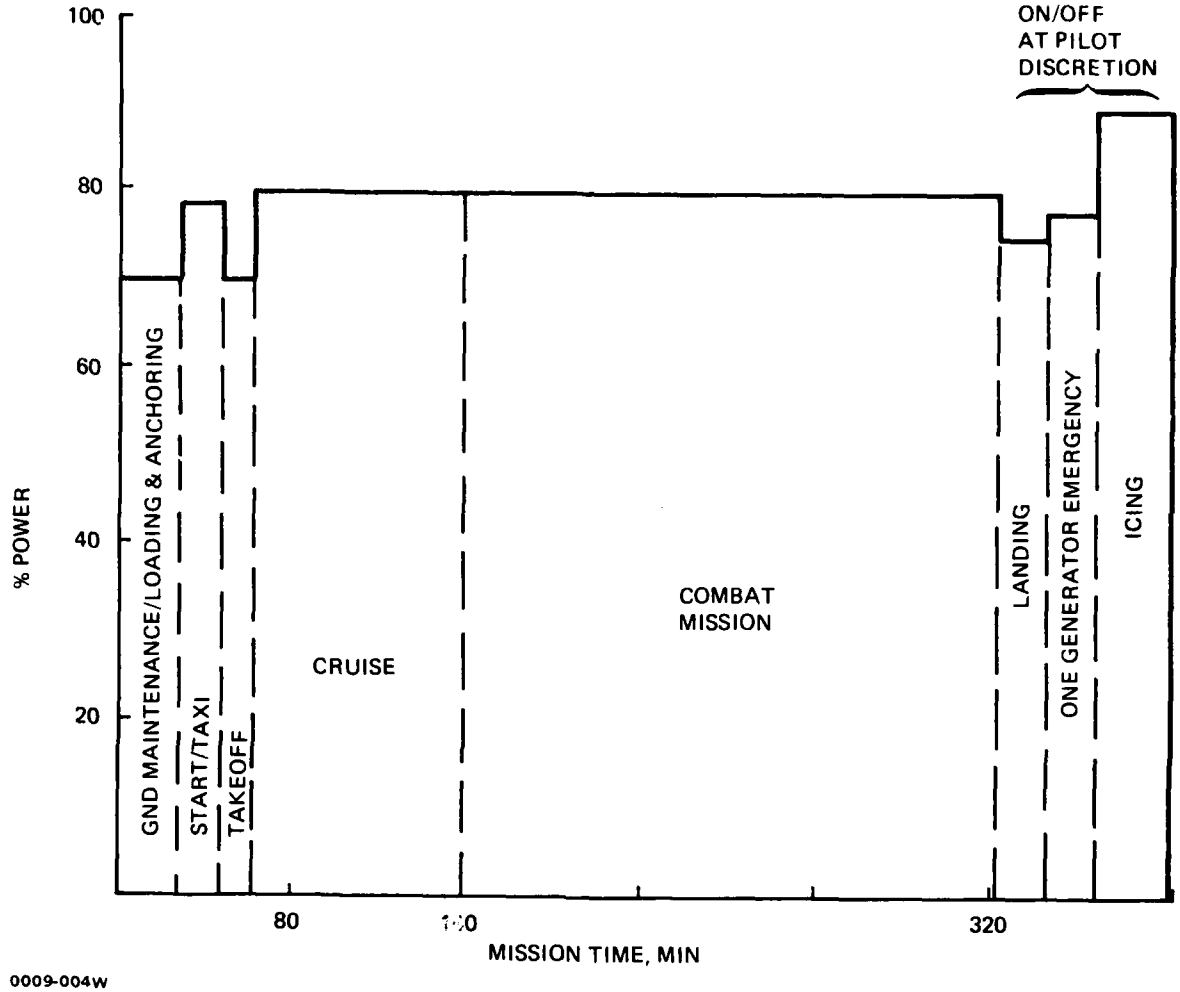

Figure 4 Typical AEW Mission A V/STOL

The selection of technology for the subsystems has a strong influence on the power requirements of the rack hardware. Power supplies for all subsystems of both missions were assumed to be 5V, which is consistent with the standardization objectives when using NMOS and HMOS technologies. For the circuits that demand Emitter Coupled Logic (ECL), the same supply was assumed. Although I^2L and CMOS/SOS were assumed to be used in the majority of subsystems, the same supply can be adapted for their use. With the chosen technologies, the estimated results indicate that an average value of 5 watts per card will be obtained.

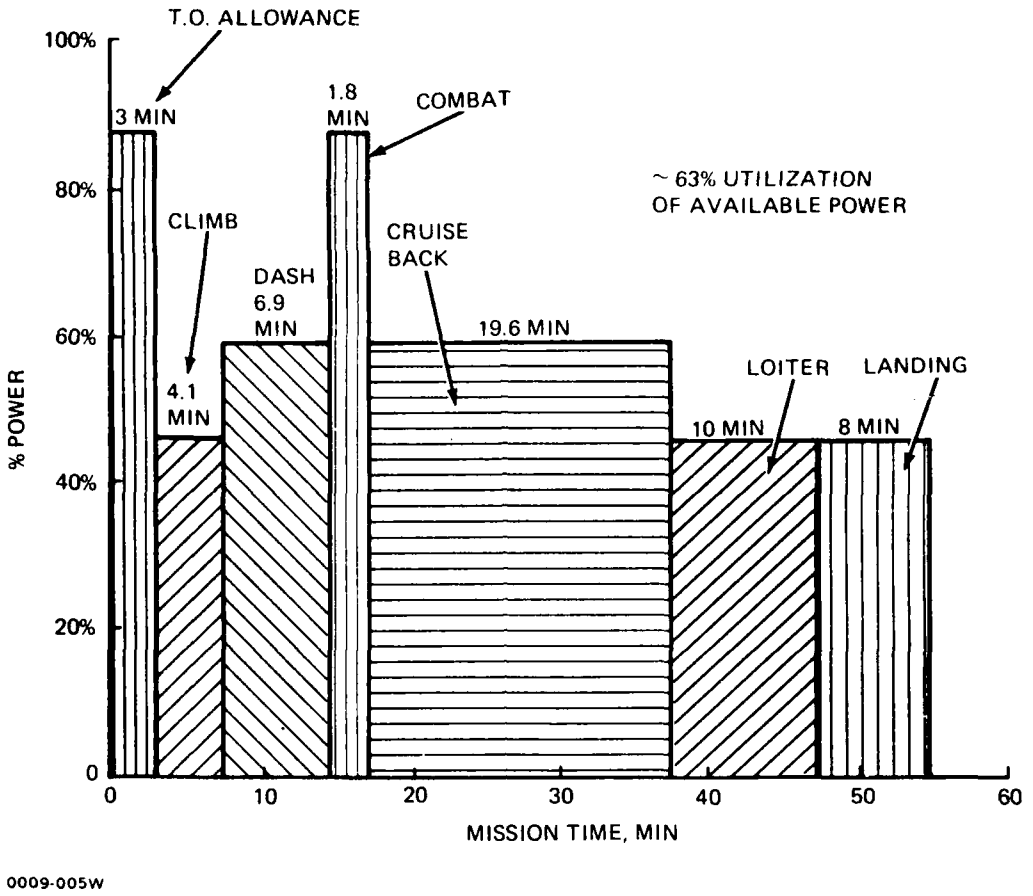

Figure 5 Integrated Rack Preliminary Power Requirements for B V/STOL vs Mission Time

This value will be used as a baseline for the study, however, analyses and rack designs were also developed when the average power per module was increased to 10 watts. For this latter case, keeping the same card count will require twice as many power supplies, and will result in a card volume exceeding the capability of the A and B V/STOL integrated rack equipment areas. Thus, no attempt was made to distribute the electrical power to the subsystems when 10 watts per module was considered.

2.3 EMI/EMP/RFI LIGHTNING REQUIREMENTS

The requirements of Mil Std 461/462 along with a preliminary Grumman composite aircraft lightning analysis were used as the starting point for the Inte-

grated Rack Study. Figure 6 shows that both emission limits and susceptibility limits must be considered for all electric components to control interference effects. These components act as generators and receptors of electromagnetic energy that are coupled via the radiated and conducted propagation paths seen in Figure 7.

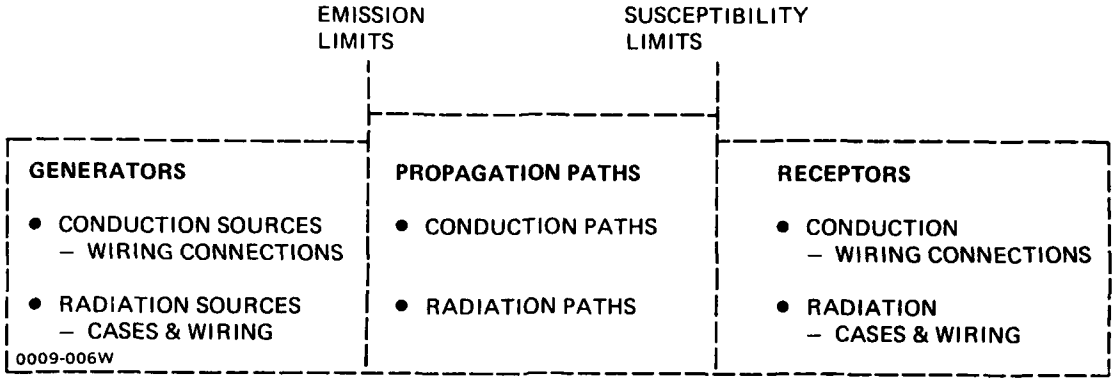

Figure 6 General Electromagnetic Interference Modeling Approach

The general approach for developing shielding requirements was to shield rack internal components and wiring for each tray from electromagnetic fields originating external to the rack, and also originating inside other trays within the same rack. This was accomplished by creating a six-sided Faraday cage (shielded enclosure) for each tray. The control of leakage fields via penetrations and apertures was addressed. Coupling of interference within a tray will be addressed by each vendor who will be assigned to a tray. Thus a tray is treated like today's black boxes. The electromagnetic interference may be associated with

- On-board aircraft drivers (electric generators, electromechanical motors, adjacent wires, transmitters/antennas, various circuit switches and oscillators)
- Phenomena in the environment of the aircraft (lightning, nuclear electromagnetic pulse, and directed energy weapon systems)
- Electrical devices in the environment of the aircraft carrier (radar, communication, motor generator, other aircraft, etc.)

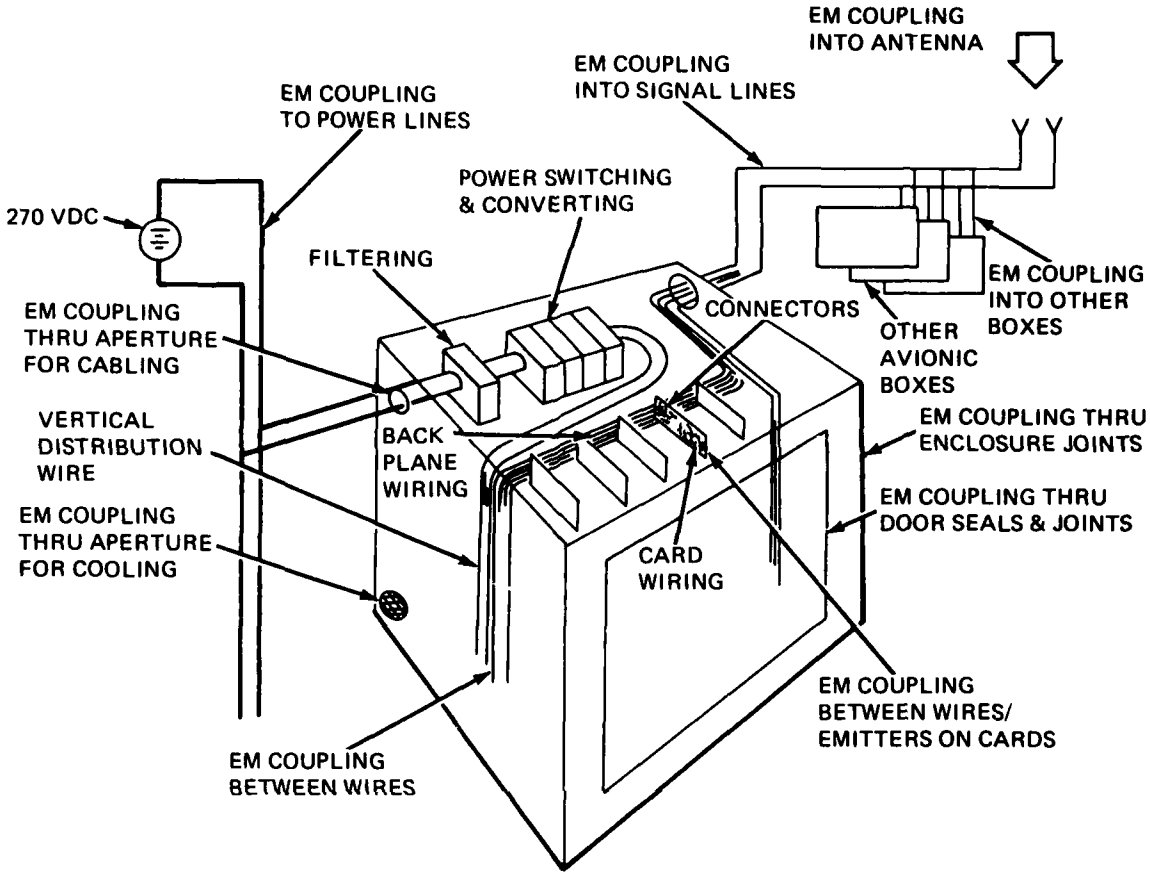

Figure 7 Rack EMI Considerations

- Items inside the rack (adjacent switching circuits, circuit oscillators, adjacent wires in backplanes, etc). The electromagnetic fields of interest range in frequency from 30 Hz to 40 GHz.

An initial examination of permissible tray to tray radiation and conducted levels in Mil Std 461/462 was undertaken. These limits and their associated test methods require appropriate modifications to assure EMI-free operation in a composite V/STOL configured with integrated racks. Further modifications result whenever several vendors are co-located within the same tray. Mil Std 461/462 radiated emission limits for electric fields (RE 02) and radiated susceptibility limits for electric fields (RS 02) are summarized in Table 4. As an example of

Table 4 Mil Std 461 Excerpts

TEST	SUBJECT	FREQ	LIMITS	NARROW BAND	BROAD BAND
RE 02	RADIATED EMISSION LIMITS (ELECTRIC FIELD)	14 kHz TO 200 MHz	100 dB$\frac{\mu V/m}{MHz}$ → 55 dB$\frac{\mu V/m}{MHz}$		X
		200 MHz TO 12.4 GHz	55 dB$\frac{\mu V/m}{MHz}$ → 70 dB$\frac{\mu V/m}{MHz}$		X
		14 kHz TO 25 MHz	35 dBμV/m → 20 dBμV/m	X	
		25 MHz TO 12.4 GHz	20 dBμV/m → 60 dBμV/m	X	
RS 02	RADIATED SUSCEPTIBILITY LIMITS (ELECTRIC FIELD)	14 kHz TO 35 MHz	10 V/m		
		35 MHz TO 10 GHz	5 V/m		
		10 GHz TO 42 GHz	20 V/m		

0009-008W

required changes, the 12.4 GHz upper frequency limit in RE 02 should be changed to 18 GHz, since current E2C hardware which is also planned for the V/STOL AEW configuration is operating at 18 GHz. As another example, current avionic black box to black box isolation is of the order of 60 dB. The current tray to tray isolation drops to approximately 40 dB. Therefore a net loss of 20 dB must somehow be made up either by lowering allowable emission limits and/or else raising the susceptibility limit to a total of 20 dB.

2.3.1 Co-Located Vendors

Since the integrated rack skin and tray support structure comprise the Faraday cage walls for individual trays, the preparation of EMI specifications for vendors requires special care to ensure electromagnetically compatible operation. Figure 8 identifies the possible interaction paths.

Each vendor's cards will be placed within one tray. The secondary backplane for that tray will be located within that tray's Faraday cage. The type of material and its thickness for each side of the six-sided Faraday cage plus the

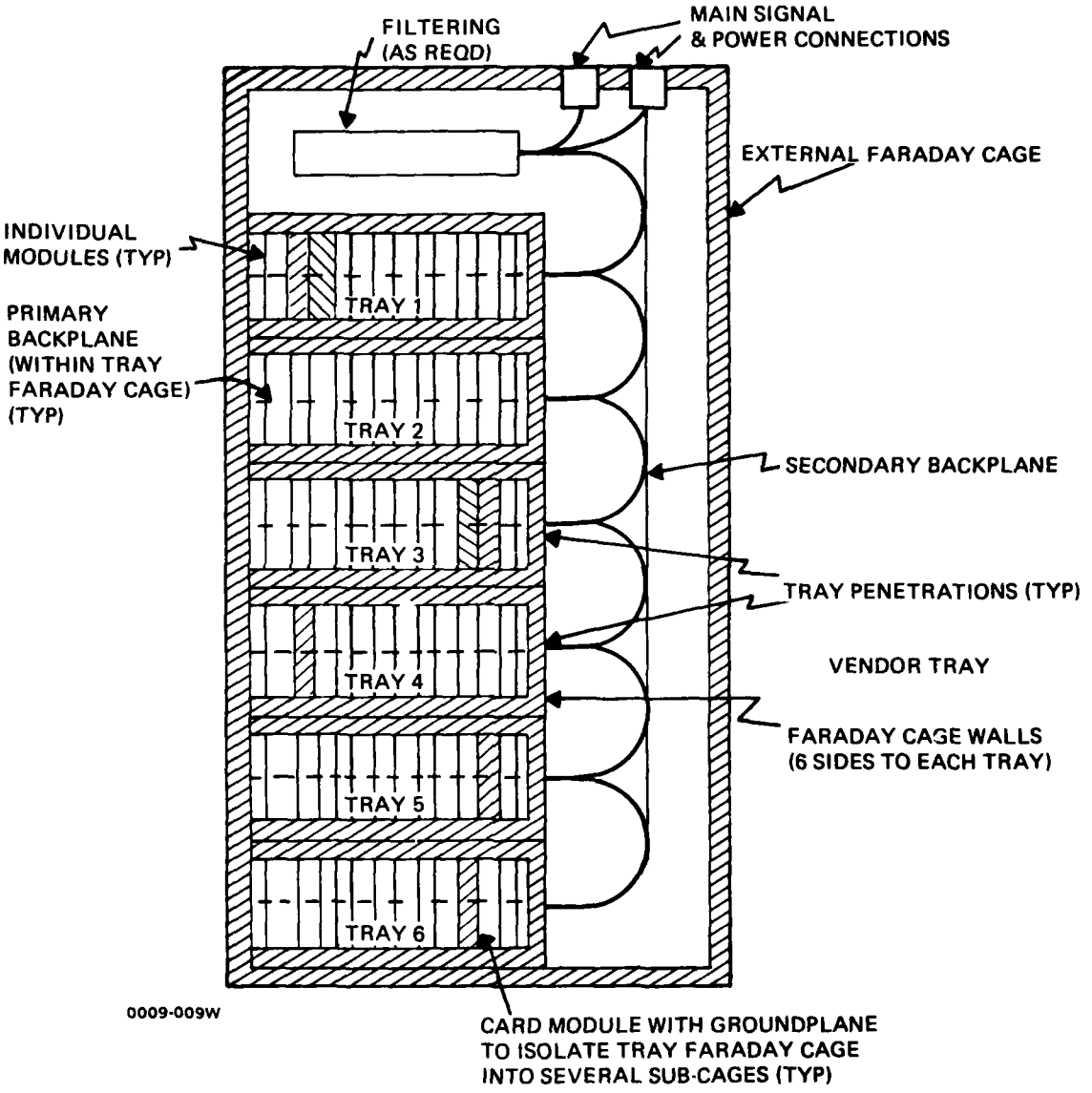

Figure 8 Integrated Rack EMI Interaction Paths

dimensions of the tray configuration will have to be specified to each vendor. Emission and susceptibility testing (radiation and conduction) using actual trays in racks will be a test requirement. Test results will demonstrate a self-compatible tray; and also compliance with EMI limits of Mil Std 461/462 for co-located trays and other on-board equipment. The use of conformal radar within a composite aircraft is expected to present an additional difficult EMI design control problem.

2.3.2 External EMI

In aluminum skinned aircraft, the external fuselage generally attentuates externally generated electromagnetic fields such as those resulting from lightning strikes, nuclear explosions, and aircraft carrier operations. Figure 9 shows a composite skinned B V/STOL aircraft. As an example, for lightning the SAE Lightning Committee AE-4 has taken the various measured lightning current waveforms (see Figure 10) and identified selected idealized waveforms for individualized spikes in the lightning stroke.

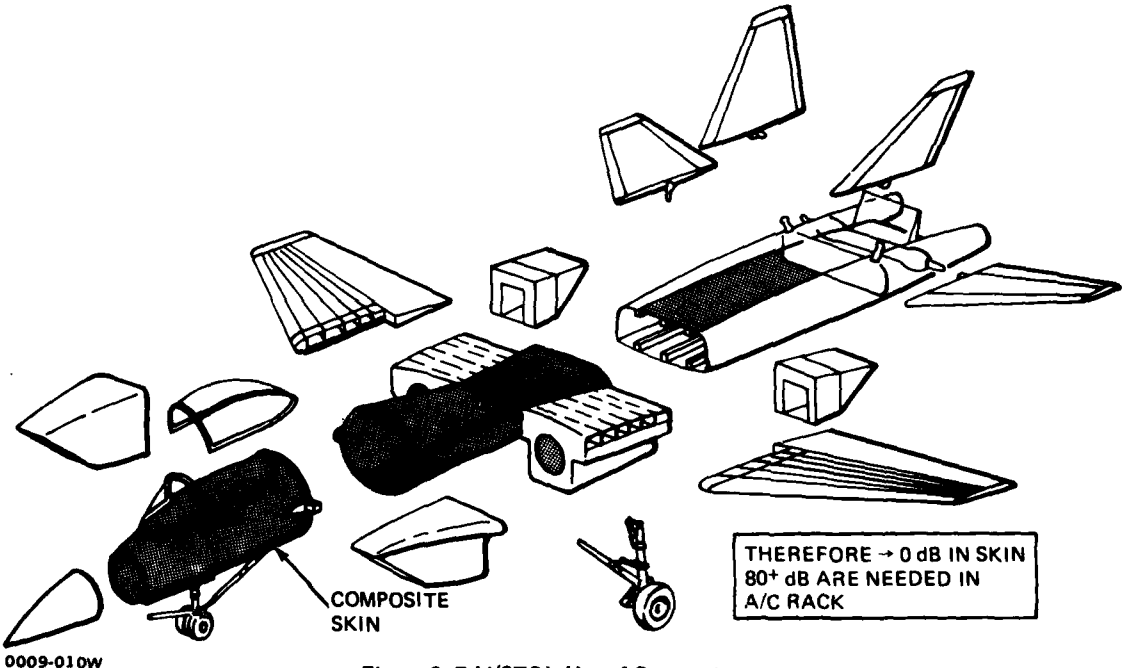

Figure 9 B V/STOL Use of Composites

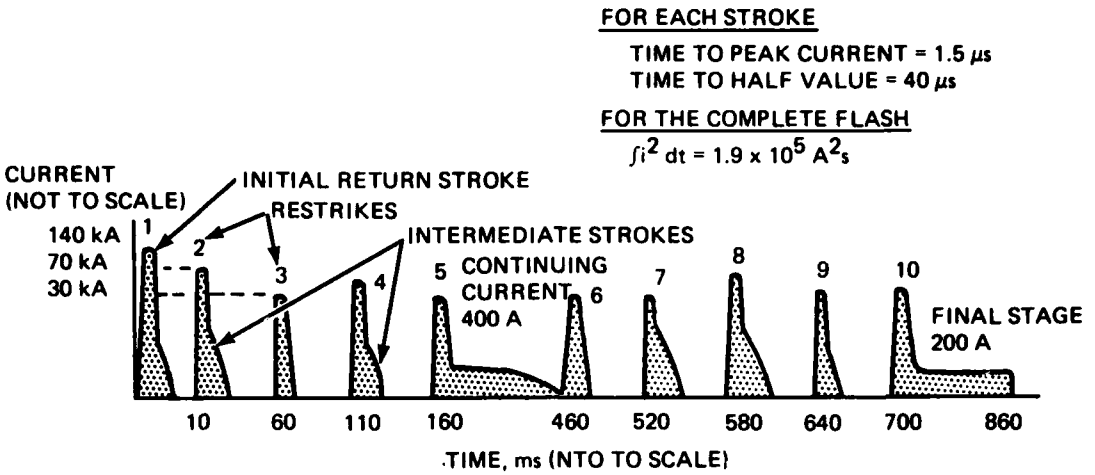

(A) Severe Negative Lightning Flash Current Waveform

(COURTESY OF CIANOS/PIERCE)

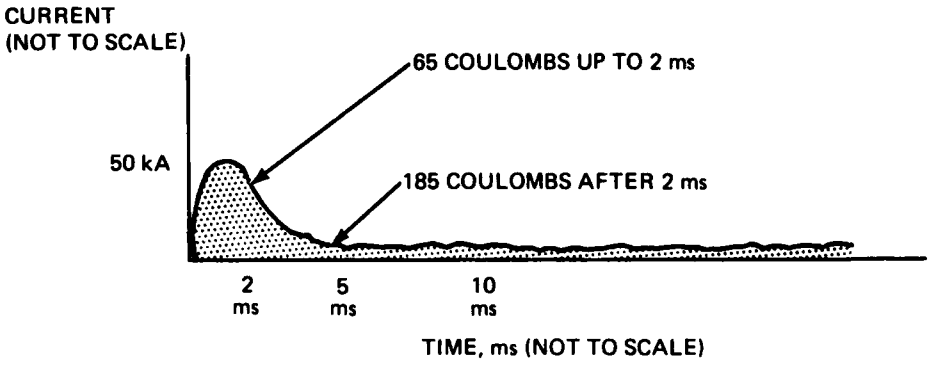

(B) Severe Positive Lightning Flash Current Waveform

0009-011W

Figure 10 Severe Lightning Flash Current Waveforms

Preliminary studies (GAC Report ADP20-03.78.1) have shown that in a lightning environment a composite aircraft provides less attenuation than an aluminum aircraft. Therefore in a composite aircraft the rack will be required to provide additional shielding. Figure 11 highlights the result of the Grumman study in terms of expected magnetic field strengths within both the aluminum and composite fuselages. Figure 12 provides the associated diffusion delay responses. The rack has to be designed to provide adequately lightning induced magnetic H field shielding for I^2L technology, since this technology is the most susceptible of the V/STOL candidate technologies (see Table 5).

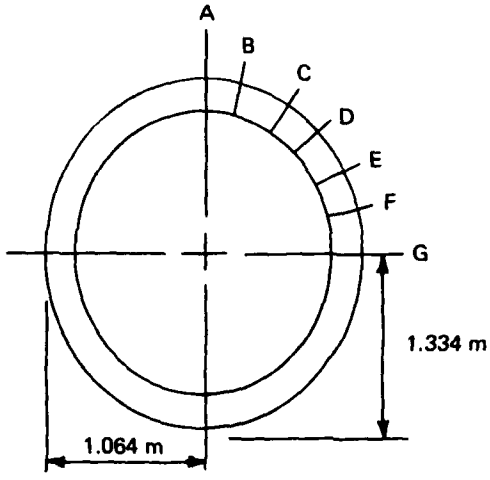

LOCATION	*FIELD, AMPS/m EXTERIOR	INTERIOR
ALUMINUM 0.040 IN.,		
A	4475	7.7
B	4366	7.5
C	4032	6.9
D	3818	6.5
E	3683	6.3
F	3607	6.2
G	3579	6.1
GRAPHITE COMPOSITE, 24 PLY		
A	4475	2200
B	4366	2146
C	4032	1982
D	3818	1876
E	3683	1811
F	3607	1773
G	3579	1759

$$*20 \log \frac{I_E}{I_I} = dB$$

0009-012W

Figure 11 Predicted Field Strengths

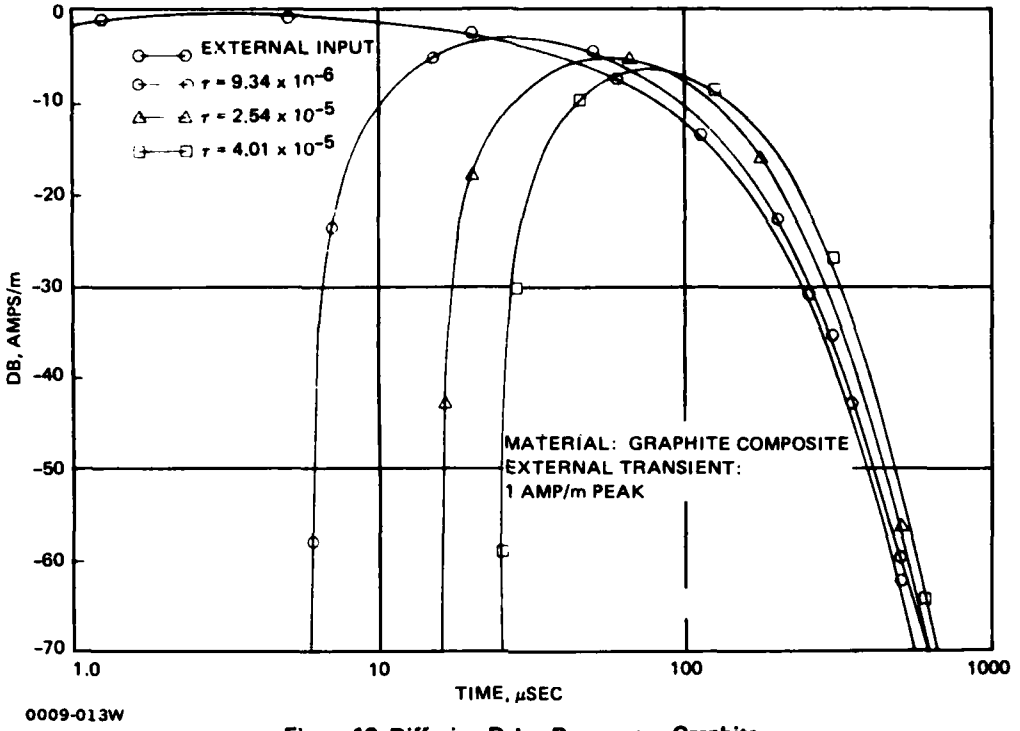

Figure 12 **Diffusion Delay Response – Graphite**

Table 5 Noise Immunity Typical Values

TECHNOLOGY	UPSET VOLTAGE
I^2L	100 MV OR 13 PICO JOULES @ Z=30 OHM
T^2L	400 MV
ECL	125 MV
CMOS	±2.25 VOLTS

0009-014W

As an alternate, the following requirement model for lightning was analyzed during the study:

- Assumed 30,000 ampere triangular pulse with a 2 μsec rise time and a 96 μsec fall time in accordance with SAE Lightning Committee AE-4 Test Wave form F (Note that for flight critical circuits a 200,000 ampere pulse width should be used)

- The fuselage was modeled as a straight wire with the rack located one foot away
- Calculated the magnetic shielding using the formulas for an infinite flat plate (absorption and main reflection)
- Calculated the induced voltage on a one square meter wire loop and compared the allowable noise impurity value.

2.4 AIRCRAFT SIZE CONTRAINTS

A major influence in the design of the Integrated Racks are the physical characteristics of the rack derived from the aircraft requirements. In both the A and B V/STOL aircrafts, all available volumes for avionics were defined and accessibility to each equipment area was identified. Four candidate areas where integrated racks can be mounted were selected for the B V/STOL, and 2 areas were selected for the A V/STOL. The equipment areas in both vehicle designs were studied to arrive at one basic dimensional requirement, which would be applicable to both vehicles in all candidate equipment areas.

A standard packaging size of approximately 10 in. wide by 5 in. deep was selected, with the exception of the Hollow Board Concept, where 15 in. by 5 in. was used. The height of the rack is variable to allow for flexibility in its application to different equipment areas. In addition to the height flexibility, it became apparent that stacking multiple racks side-by-side and back-to-back would better utilize the equipment compartment volume. Figure 13 depicts some possible rack arrangements which illustrate these flexibilities.

General aircraft mounting requirements suggest that mechanical interfaces be limited to the top and bottom surfaces, while all other interfaces are desirable on the top only. The B V/STOL design concept further impacts the mounting requirements, suggesting that the rack should be nonsensitive to mounting attitude, and should be mounted on extensible platforms to provide adequate accessibility for onboard servicing. A more detailed description of these requirements is covered in Section 3.

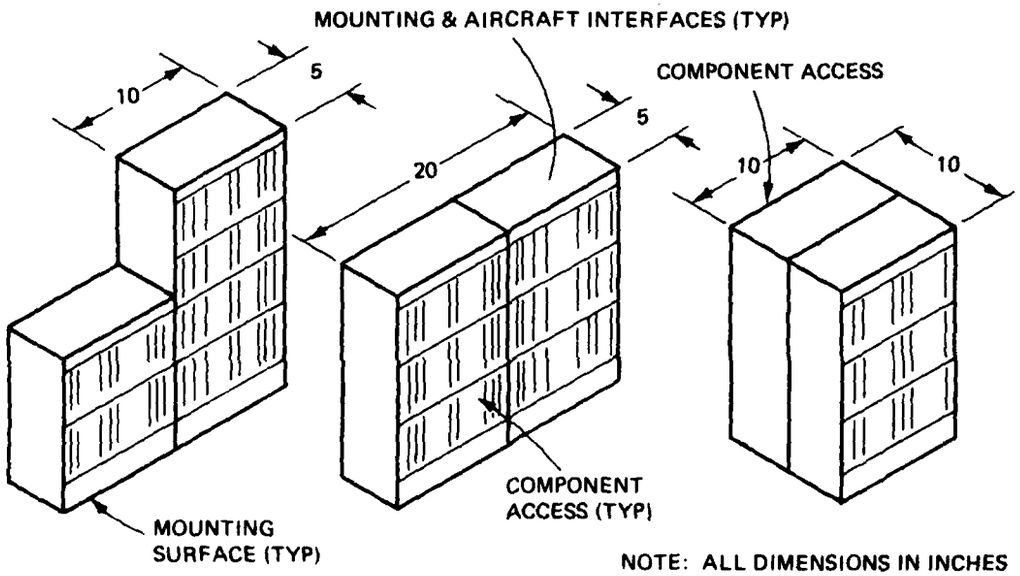

Figure 13 Basic IAR Size & Mounting Requirements

3 - RACK CONFIGURATION

The integrated rack is used as the interface between the airframe and the standard avionics module. As such, the rack must be compatible with the electrical, thermal, and mechanical functions of the module and the requirements of the airframe. The following are the functions considered in the candidate designs:

- Applicability to A and B type V/STOL aircraft of Grumman design
- Thermal interface between the ECS and the module
- Power and signal distribution
- Maintainability/reliability
- EMI/EMP
- Standardization of design
- Field changes
- Structural integrity.

3.1 CANDIDATE SYSTEMS

Six different rack candidates have been considered for this study. Candidates A_{21} and C utilize air-over-components, candidates B_{31}, B_{32}, and B_{33} utilize conduction cooling and concept D is air-cooled. All candidate racks have front accessibility. Module orientation is vertical, except for candidate C which is horizontal.

3.1.1 Candidate A_{21}

Candidate A_{21}, shown in Figure 14, is a combined conduction/direct air impingement cooling concept. Liquid coolant from the aircraft ECS is circulated through the individual heat exchangers. Air within the rack is circulated through the vertical finned areas of the heat exchanger, where it is cooled.

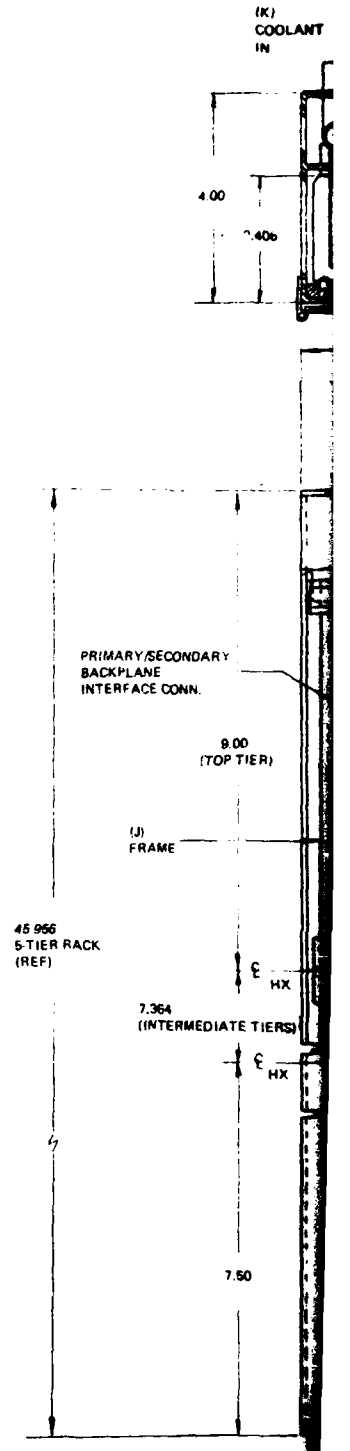
(K)
COOLANT
IN
4.00
PRIMARY/SECONDARY
BACKPLANE
INTERFACE CONN.
9.00
(TOP TIER)
(J)
FRAME
45.956
5-TIER RACK
(REF)
℄
HX
7.364
(INTERMEDIATE TIERS)
℄
HX
7.50

0009-016W

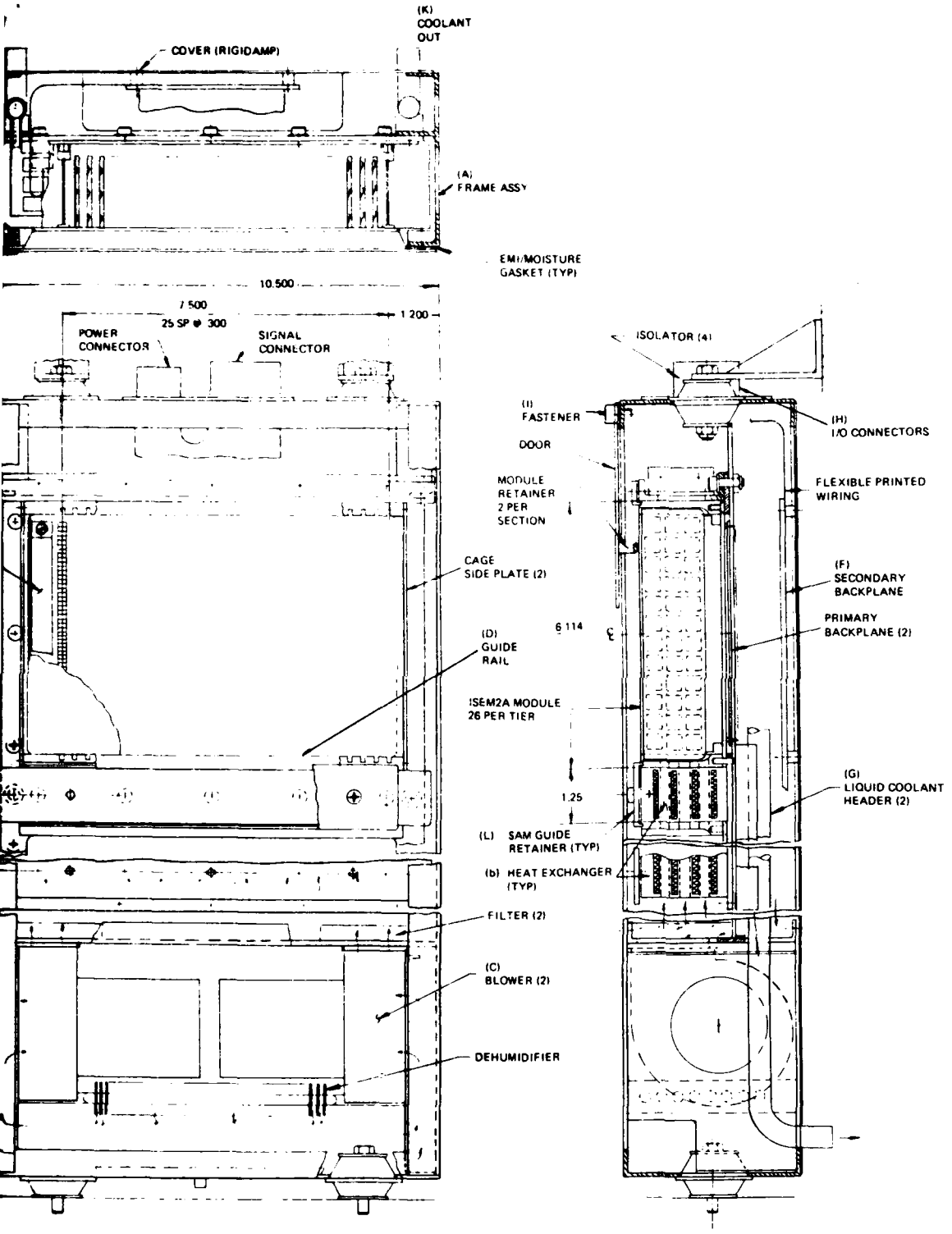

Figure 14 Candidate A_{21} Air-Over-Component Cooling, Liquid-Cooled Heat Exchanger

before flowing over the avionic components. Dehumidification coils located in the path of the return airflow remove the humidity that may be present within the rack. The major elements that make up the integrated rack are:

- Basic Frame Assembly (a)
- Heat exchangers (b)
- Blowers (c)
- Guide rails (d)
- Primary Backplane (e)
- Secondary Backplane (f)
- Liquid Coolant Headers (g).

Additional details on these items are found in Section 3.2.1

Two backplane configurations are used for power and signal distributions; The primary backplane (e), utilizing multilayer or wire wrap for interconnecting the modules within a subsystem, and the secondary backplane (f), used for interwiring the subsystems within the rack and the input/output (I/O) connectors (h). A typical secondary backplane is shown in Figure 15. The backplane is a hybrid circuit board consisting of a combination multilayer/flexible printed wiring. The power busing (a) located on one side of the circuit board is separated from the signal conductors. The flexible printed wiring (b) extends beyond the multilayers (c) to interface with the I/O connectors (d).

The number of I/O connectors that can be accommodated by this rack configuration is dependent on how the isolators are mounted. When the isolators are located as shown in Figure 14, it is possible to accommodate one power connector and two 155 pin connectors (type MIL-C-81511). When the isolators are located outboard of the rack, three 155 pin connectors and two shell size 14 connectors can be used (see Subsection 3.2.3.1, Figure 22).

3.1.2 Candidate B_{31}

Candidate B_{31}, shown in Figure 16, is a conduction cooled rack concept. Liquid coolant from the ECS is circulated through the guide rails to provide a

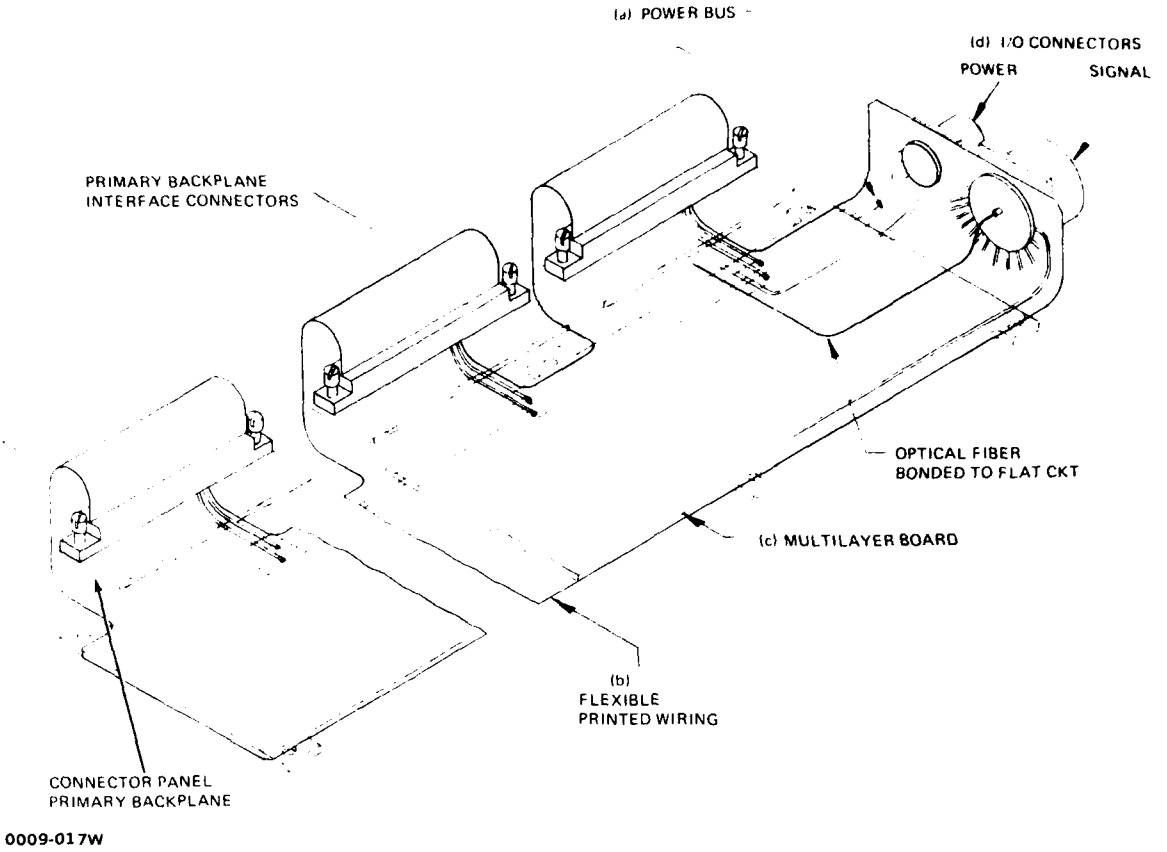

Figure 15 Secondary Backplane (Typical)

heat sink for the avionic modules. The avionic modules are securely held between the guide rails with beryllium copper retainers made by IERC. A dehumidifier and two vane axial fans with heaters are used to remove the condensation within the rack prior to start of mission. Primary and secondary backplane interwiring is same as in candidate A_{21}.

3.1.3 Candidate B_{32}

Candidate B_{32}, shown in Figure 17, is a conduction cooled rack concept with cold air flowing through the guide rails instead of liquid coolant. Except for the method of cooling the guide rails, candidates B_{31} and B_{32} are similar.

3.1.4 Candidate B_{33}

Candidate B_{33}, shown in Figure 18, is a conduction cooled rack concept which utilizes heatpipe guide rails (a) to conduct heat from the ISEM-2A mod-

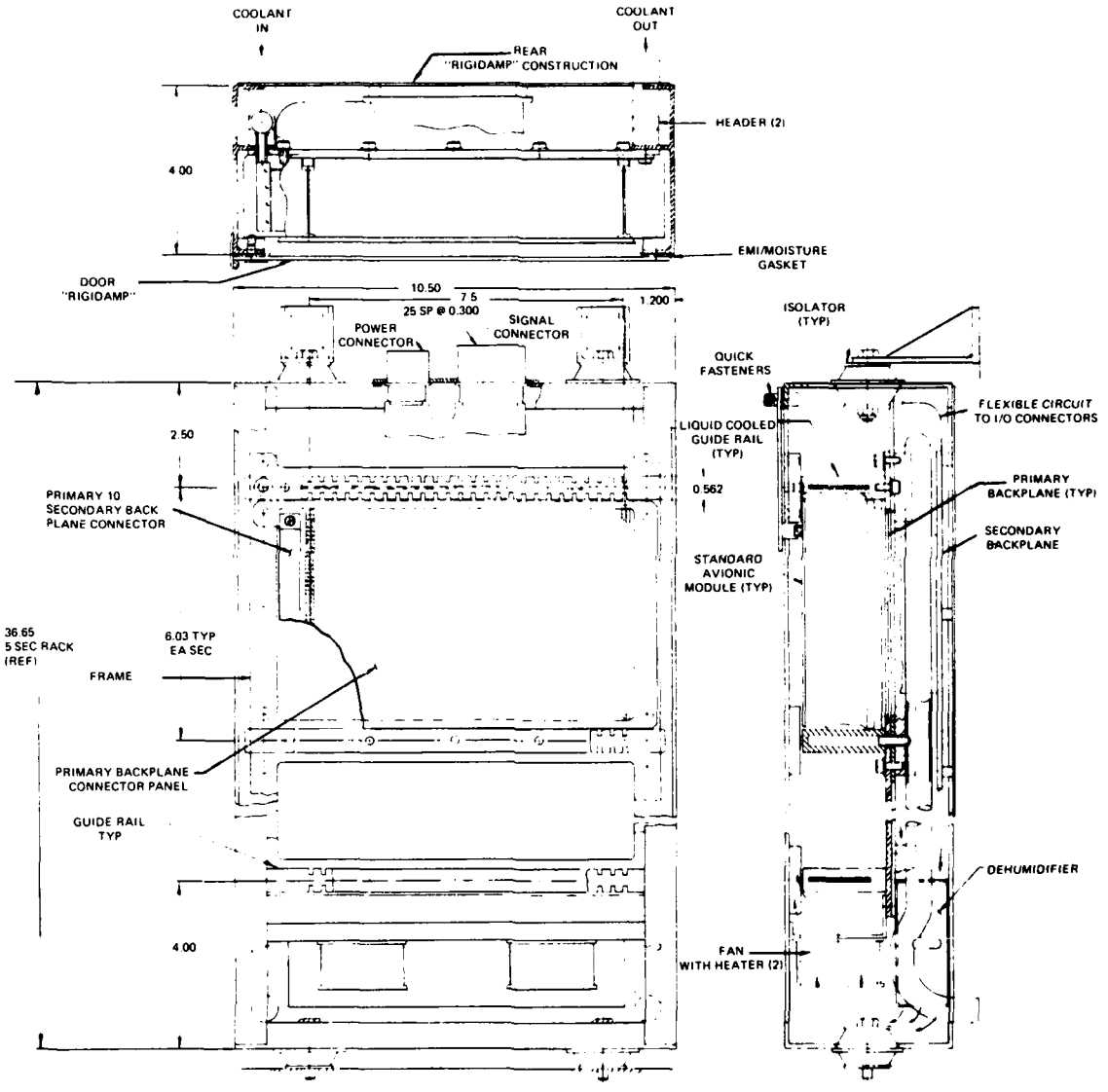

0009-018W

Figure 16 Candidate B_{31} Conduction Cooling/Liquid-Cooled Guide Rails

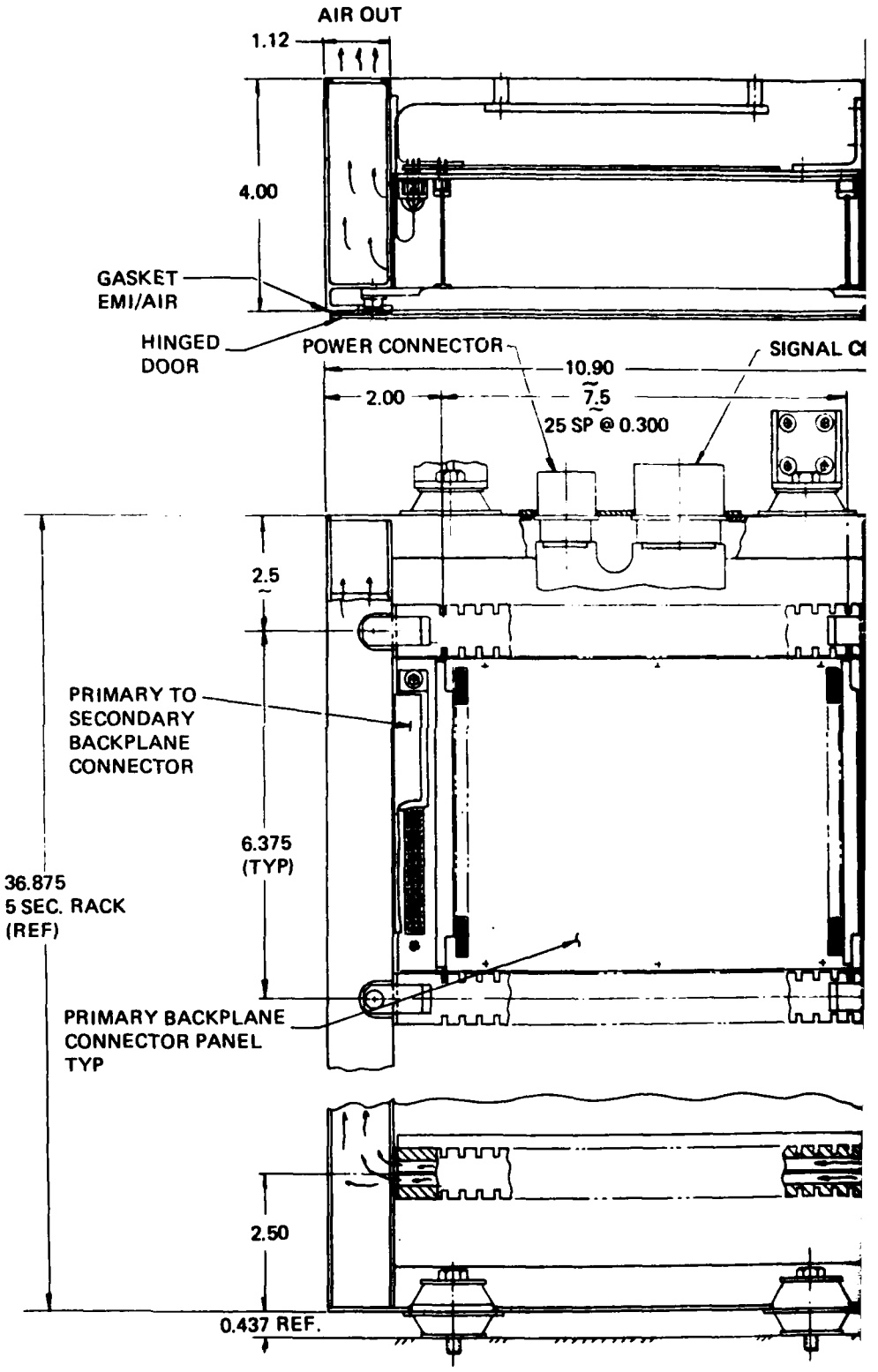
AIR OUT
1.12
4.00
GASKET
EMI/AIR
HINGED
DOOR
POWER CONNECTOR
SIGNAL C
10.90
2.00
7.5
25 SP @ 0.300
2.5
PRIMARY TO
SECONDARY
BACKPLANE
CONNECTOR
6.375
(TYP)
36.875
5 SEC. RACK
(REF)
PRIMARY BACKPLANE
CONNECTOR PANEL
TYP
2.50
0.437 REF.

0009-019W

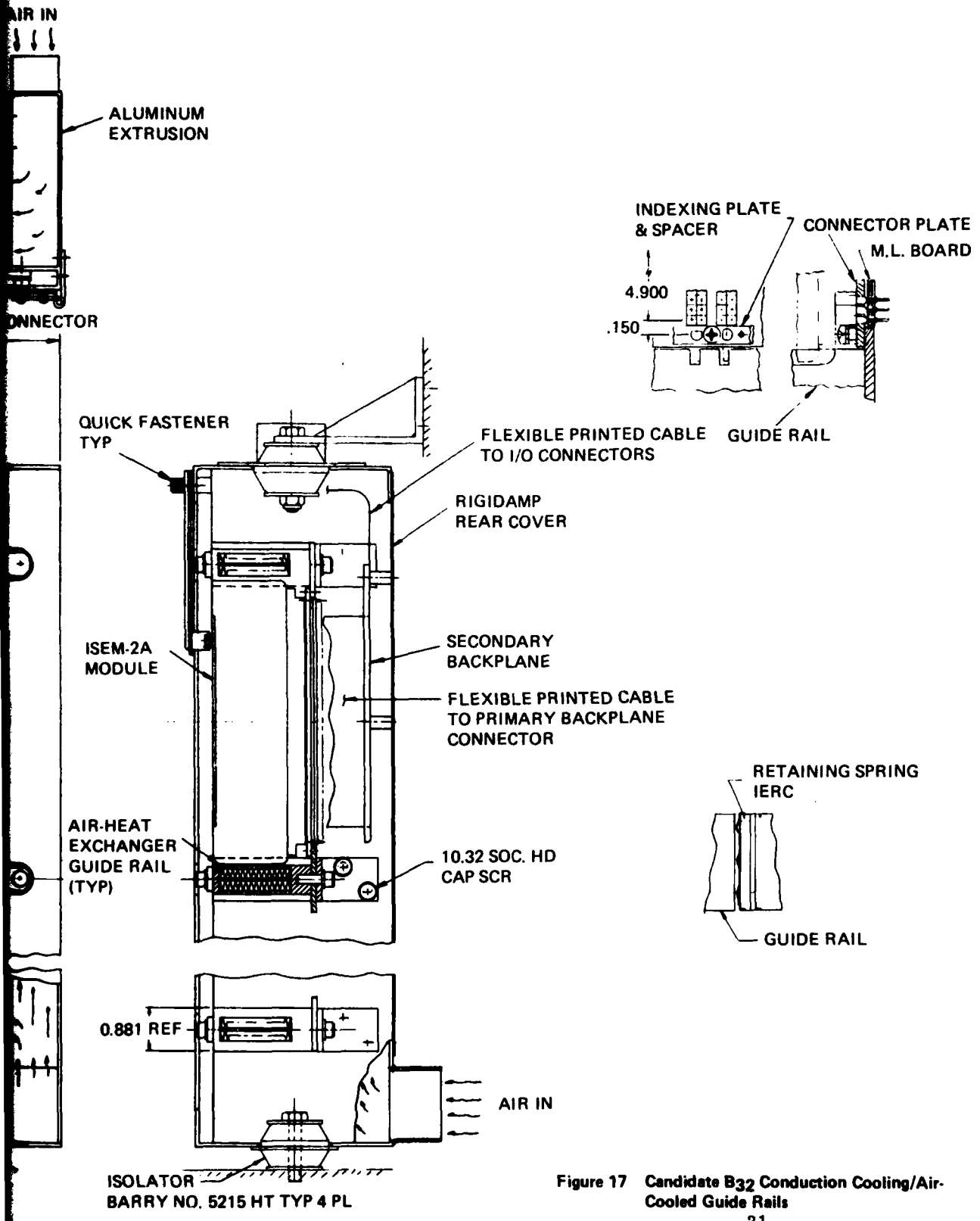

Figure 17 Candidate B_{32} Conduction Cooling/Air-Cooled Guide Rails

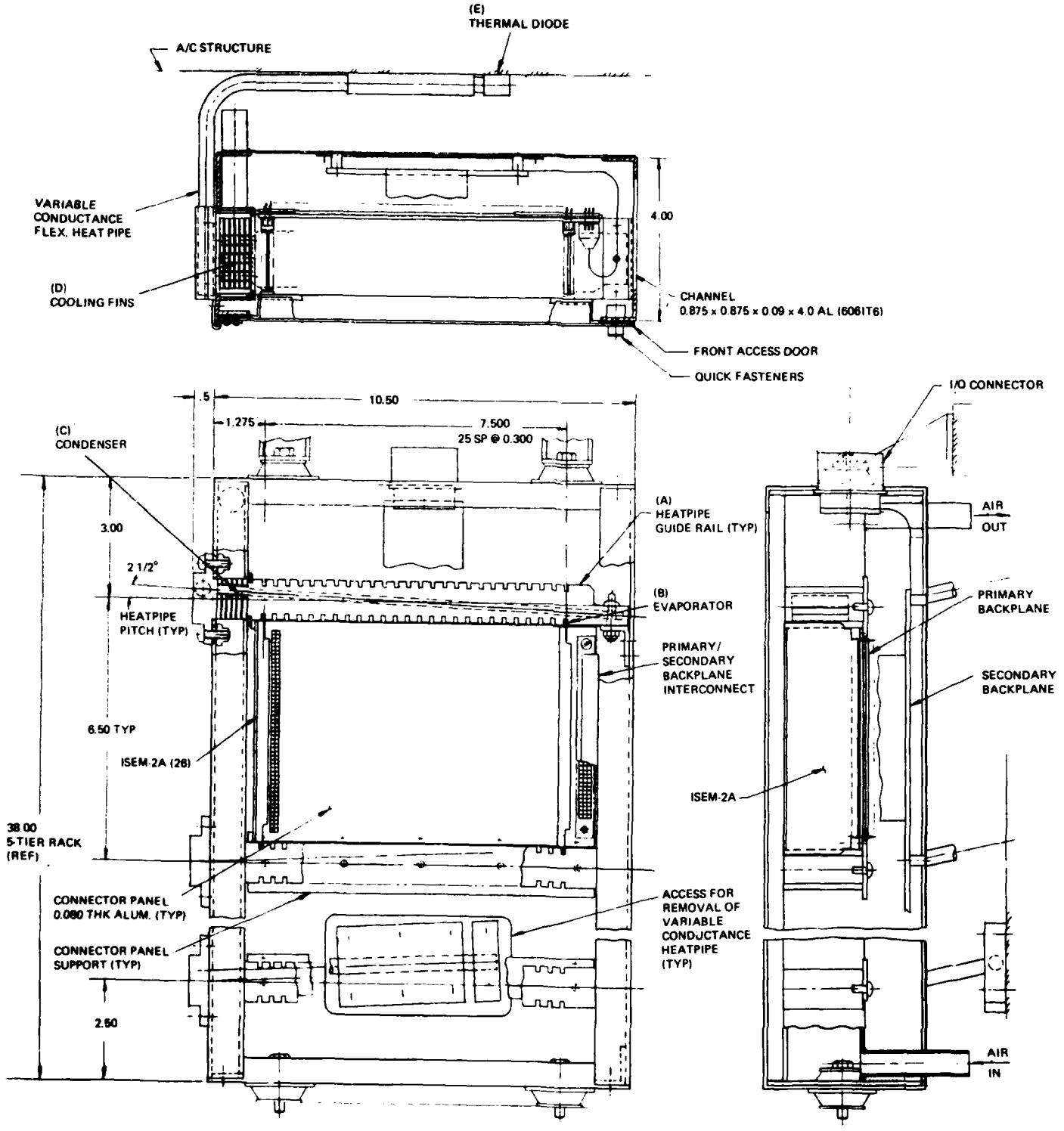

Figure 18 Candidate B33 Conduction Cooled/Heatpipe Guide Rail

ules. The evaporator section of the guide rail (b) is tilted 2½°, so that the condenser end of the heatpipe (c) is always above the horizontal. This orientation improves the pump action of the heatpipe, resulting in a more efficient heatpipe operation. Cooling fins (d) at the condenser end of the heatpipe are used to increase heat transfer from the heatpipe to the air coolant. In addition to the heatpipe guide rails, a variable conductance heatpipe system utilizes the aircraft structure as a heatsink. A thermal diode (e) will shut off the heatpipe action in case the structure temperature is greater than that of the electronic modules. This concept provides dual mode cooling, which could conserve fuel otherwise needed to power the ECS load. Humidity control (not shown in Fig. 18) is provided by heaters. The power and signal distribution system is similar to candidate A_{21}.

3.1.5 Candidate C

Candidate C, shown in Figure 19, is a front accessible rack which utilizes direct air impingement to cool the avionics. The upper section of the rack has two adjacent rows of horizontally oriented ISEM-2A modules. The base (d) contains the heat exchanger (a) with filter and two variable speed blowers. Air from the base flows through the center ducts (j) over the ISEM-2A modules, and back to the base through the side return air ducts (k). The primary backplane wiring (h) can be either multilayer or wire wrap. The secondary backplane is similar to candidate A_{21}. Humidity control in this candidate rack is accomplished by the heat exchanger located at the bottom of the rack.

3.1.6 Candidate D

Candidate D shown in Figure 20 is a concept developed for use with the hollow core ISEM-2A module (see Subsection 3.2.7, Figure 29). The rack assembly consists of a frame similar to candidate B_{32} and a number of tier assemblies having two guide rails (a), a connector plate (b), with the primary backplane, and two handles for removing and replacing the assembly. Two bullet type guide pins (e), located on the backside of the guide rails, position the tier assembly in the rack. The avionic modules are held in place by two sliding bars (f), one on each guide rail. The secondary backplane (g), used to interconnect the primary backplane with the I/O connectors on the top of the rack, is located on the rear rack cover. A typical secondary backplane is shown in Figure 15.

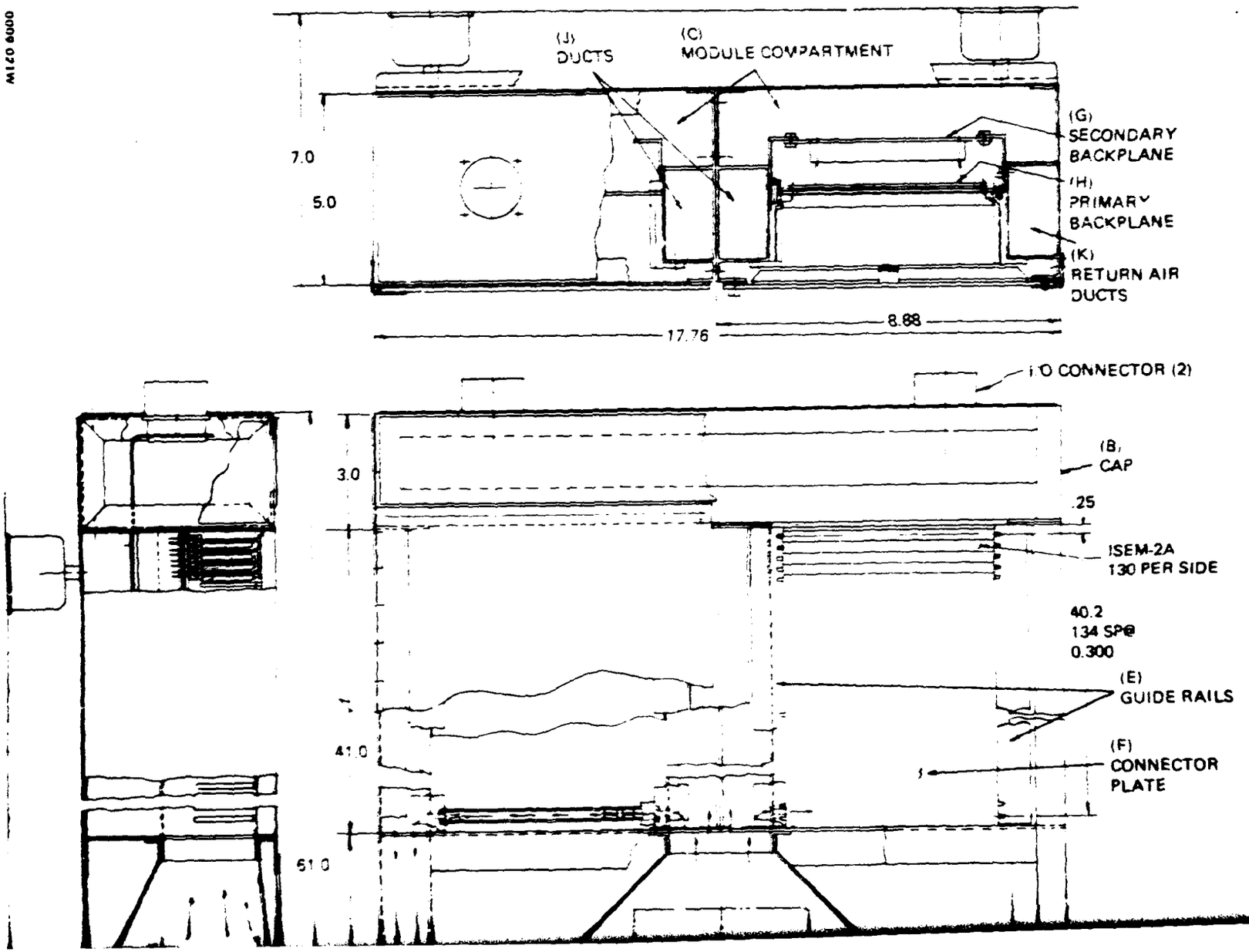
(J)
DUCTS
(C)
MODULE COMPARTMENT
(G)
SECONDARY
BACKPLANE
(H)
PRIMARY
BACKPLANE
(K)
RETURN AIR
DUCTS
7.0
5.0
17.76
8.88
I/O CONNECTOR (2)
(B)
CAP
3.0
.25
ISEM-2A
130 PER SIDE
40.2
134 SP@
0.300
(E)
GUIDE RAILS
(F)
CONNECTOR
PLATE
41.0
51.0

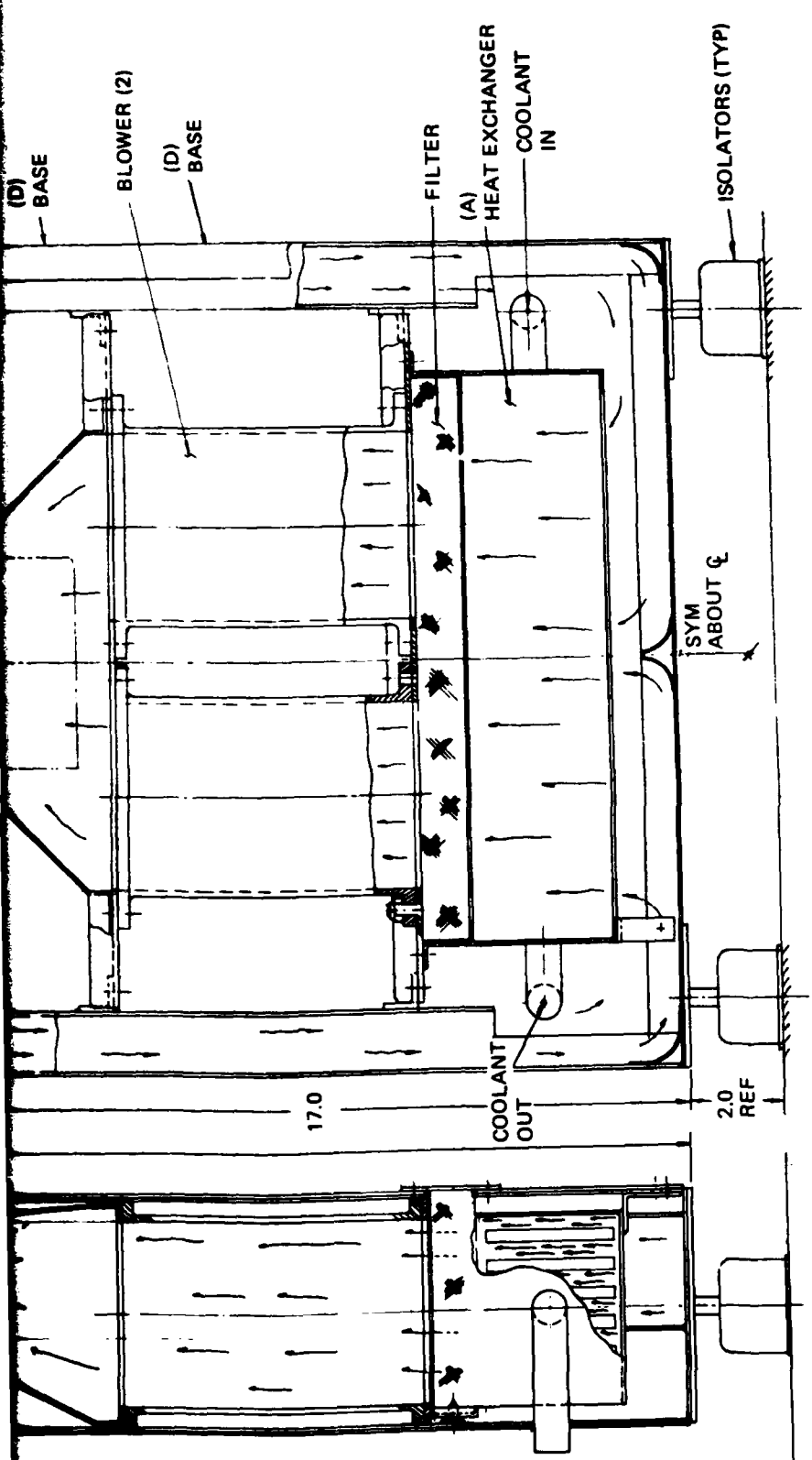

Figure 19 Candidate C Air-Over-Components/Central Heat Exchanger

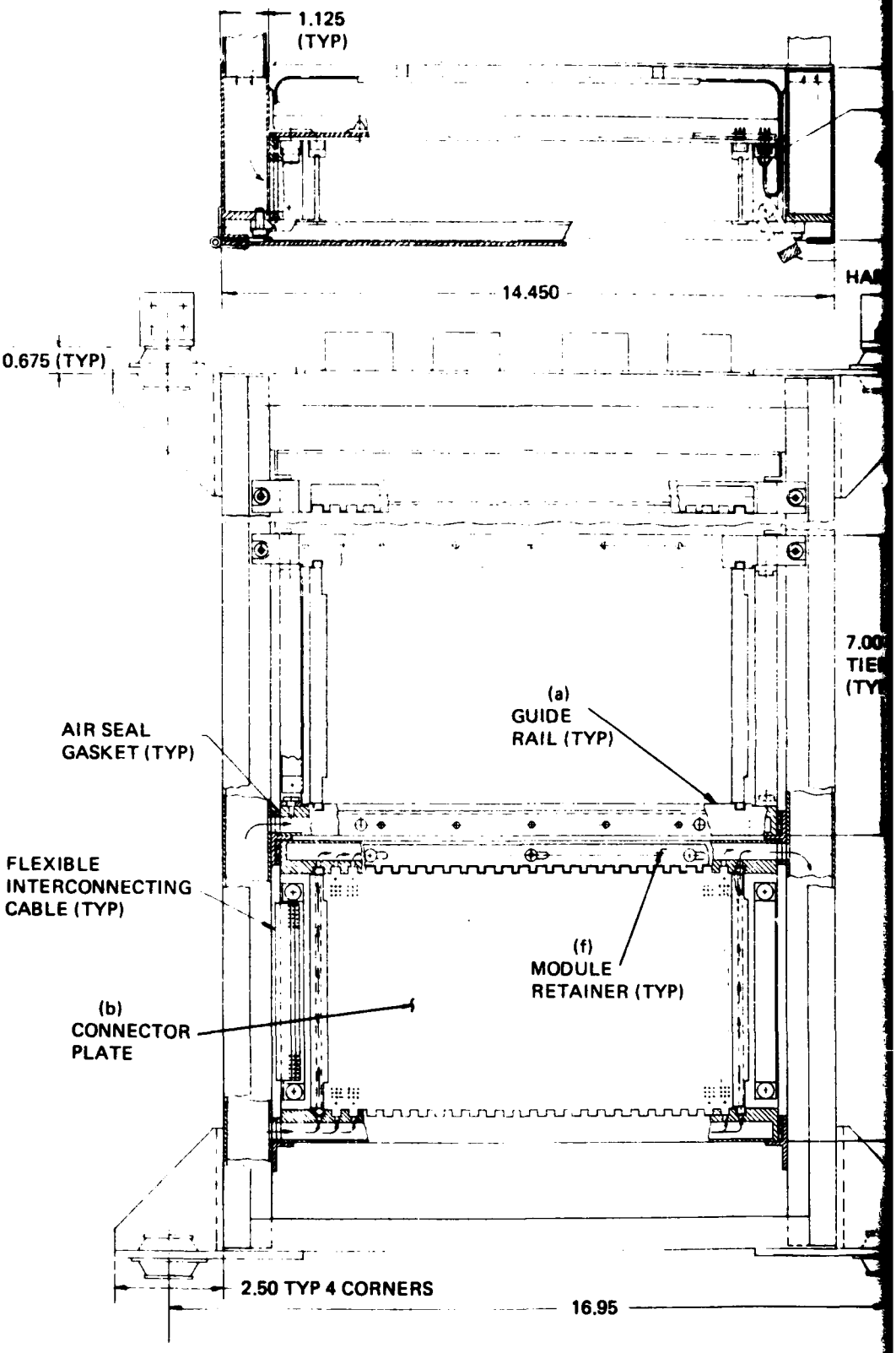
1.125
(TYP)
14.450
0.675 (TYP)
(a)
GUIDE
RAIL (TYP)
AIR SEAL
GASKET (TYP)
FLEXIBLE
INTERCONNECTING
CABLE (TYP)
(f)
MODULE
RETAINER (TYP)
(b)
CONNECTOR
PLATE
2.50 TYP 4 CORNERS
16.95

0009-022W

ARY/SECONDARY
PLANE CONNECTOR
AL BOTH ENDS

P)

R RACK

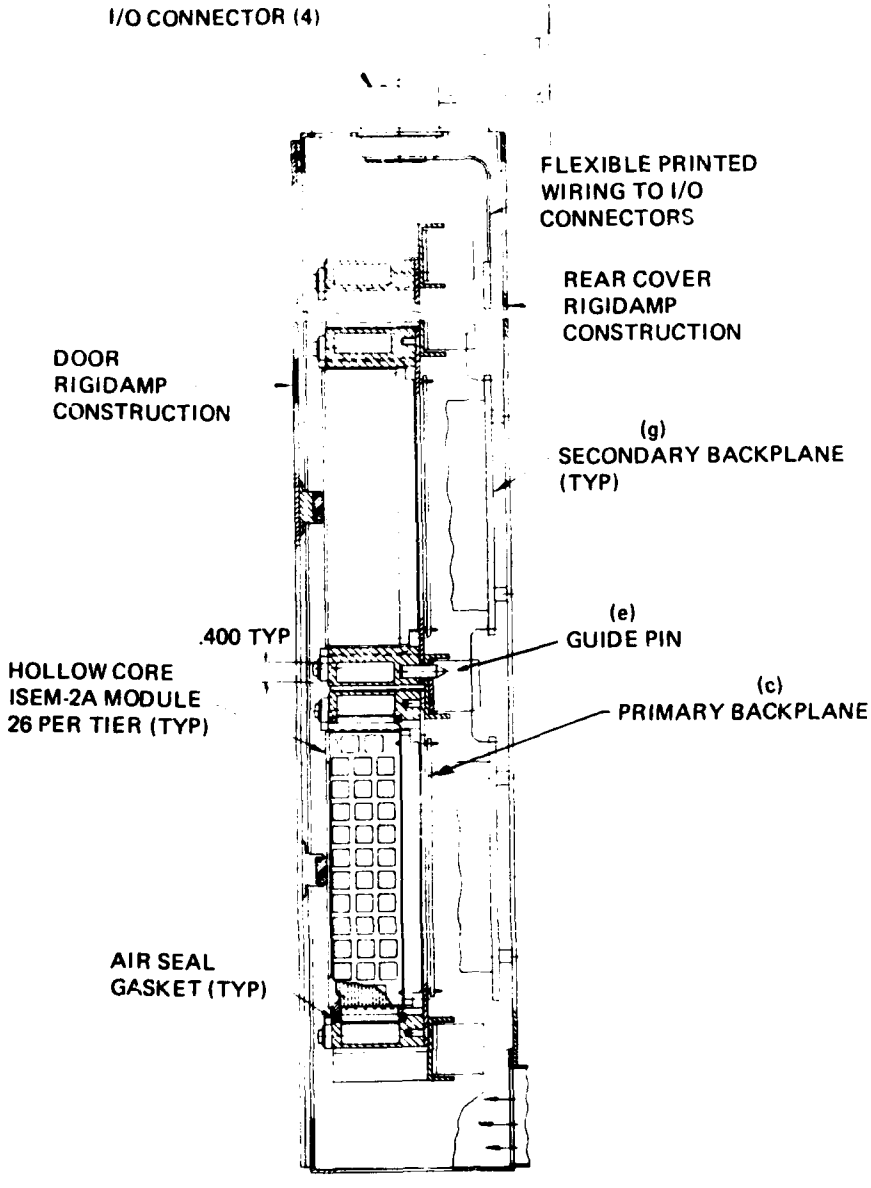

Figure 20 Candidate D Air Cooling Concept Hollow Core Module

Cooling of the avionic modules is accomplished by air flowing through the vertical duct on one side of the rack into the opening of the lower guide rail. The air is then metered out of the guide rail and into the hollow core module. The air passing through the hollow core module exits into the upper guide rail, and then out into the right side of the rack frame. Seals are used to prevent leakage between the vertical ducts of the rack and the guide rails, and also between avionic module and the guide rails. The dehumidification approach is similar to rack configuration B_{32}.

3.2 MECHANICAL DESIGN

The mechanical design concepts of the six candidate racks were based on the following:

- Use of the improved standard Electronic Module 2A (ISEM-2A) as the baseline module
- Adaptability to A and B type V/STOL aircraft
- Cooling system configuration to be direct air impingement or conduction cooling
- Direct module access from front of rack
- Primary and secondary backplane accessible from front of rack
- Ability to incrementally increase or decrease size of the integrated rack to suit available space in aircraft
- Standardization of rack elements.

The aircraft configurations used for this study are Grumman designs of A and B type V/STOL aircraft.

3.2.1 Basic Rack Structural Design

Two basic rack designs have been considered in this study. One rack design, candidate C, is applicable to A type V/STOL only. Candidates A_{21}, B_{31}, B_{32}, B_{33} and D are applicable to both A and B type V/STOL aircraft. For the purpose of obtaining comparable rack efficiencies, all candidate A and B type racks have been sized to accommodate 130 ISEM-2A modules, or 5 tiers at 26 modules per tier. This size rack is most commonly adaptable to both A and B type V/STOL.

3.2.1.1 Candidate A_{21} - Candidate A_{21} (Figure 14) is an integrated rack which utilizes the air-over-components cooling concept, and can be incrementally increased or decreased in size to fit available space. The rack is 10.50 in. wide by 4.00 in. deep. A typical five tier rack is 45.956 in. high.

The basic frame (a) consists of two "E" shaped aluminum extrusions which form the sides of the rack frame, and two aluminum channel extrusions which form the top and bottom of the rack. The rear cover is made from damping material, which is permanently secured to the aluminum frame. The damping material consists of a layer of viscoelastic material sandwiched between two sheets of aluminum. The front access door is made of the same damping material as the rear cover, and is hinged to the front of the rack. Quick fasteners (i) are used to secure the door to the frame. EMI/moisture gaskets are used to seal the door against moisture and EMI leakage. A 0.125 in. thick frame (j) is secured to the center flange of the "E" shaped extrusions, forming a partition to which the heat exchangers (b) are mounted. The heat exchangers in this candidate rack are combination liquid/air exchangers. Horizontal finned slots are used for circulating liquid coolant, while the vertical finned slots permit air to pass through the heat exchangers to the next tier of avionic modules (see Figure 21). Headers (k) on each side of the heat exchangers are used to provide coolant circulation. Two variable speed blowers (c) are located at the bottom of the rack to circulate air within the rack.

Since this candiate does not depend on conduction for cooling the avionic modules, the guide rails are independent of the heat exchangers, and therefore act only as a means of retaining the module within the rack. The guide rails, fitted with IERC spring module retainers, are assembled to the connector panel, forming a card cage assembly which fits between two heat exchangers. The card cage assembly, together with the avionic modules, can be removed as a unit. Retaining bars secured to the heat exchangers will hold the card cage in place. In addition, horizontal pressure bars built into the front access cover will prevent the avionic modules from loosening in case of severe shock.

The integrated rack is provided with four Barry isolation mounts type 5220 N. These are centrally located to permit the isolators to be partially recessed into the rack, thus reducing the overall package envelope. This method

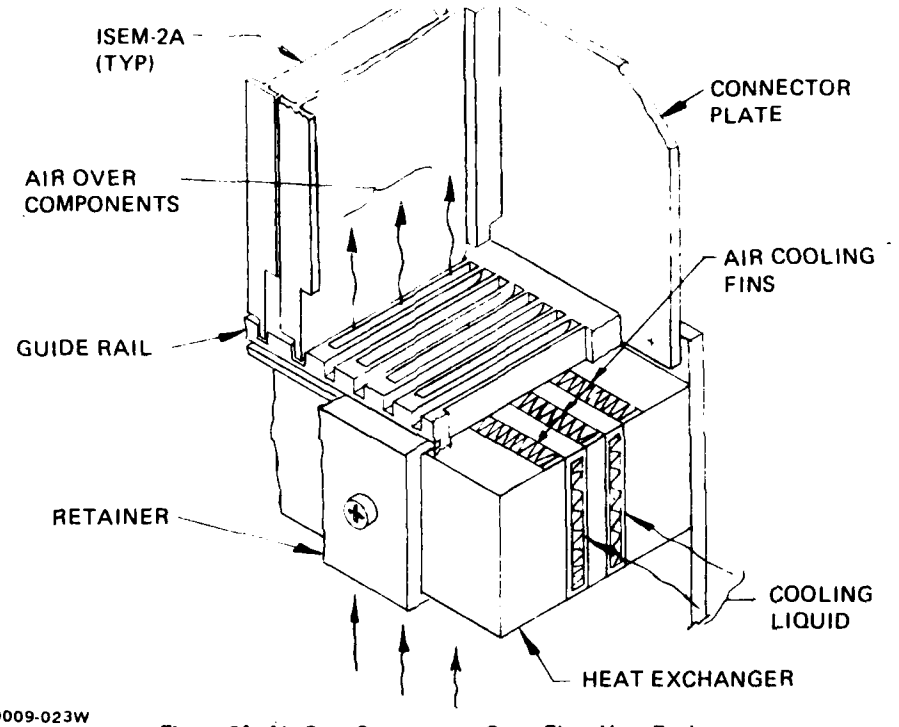

Figure 21 Air-Over-Components Cross-Flow Heat Exchanger

of isolation mounting necessitates opening the front access door of the rack to install it in the aircraft. An alternate method of mounting the isolators to the rack is shown in Figure 22. In this latter method, the isolators are mounted on the outside corners of the rack, making the mounting bolts accessible from the outside. However, the overall width of the rack increases by approximately 4 in. This will reduce the number of racks that can be accommodated by the A and B V/STOL. Where rack width does not present a problem, this method of isolation mounting is preferable. Two input connectors, power and signal, are mounted at the top of the rack.

3.2.1.2 Candidate B_{31} - Candidate B_{31} (Figure 16) uses a conduction cooling system with liquid coolant as the medium for cooling the guide rails. The rack is 10.50 in. wide by 4 in. deep. Because of the different mode of cooling used in this candidate, the pitch between guide rails is reduced from 7.364 in. in candidate A_{21} to 6.03 in. in candidate B_{31}. A typical five tier rack is 36.65 in. high. The rack basic structure and heat exchanger arrangement are the same as for candidate A_{21}.

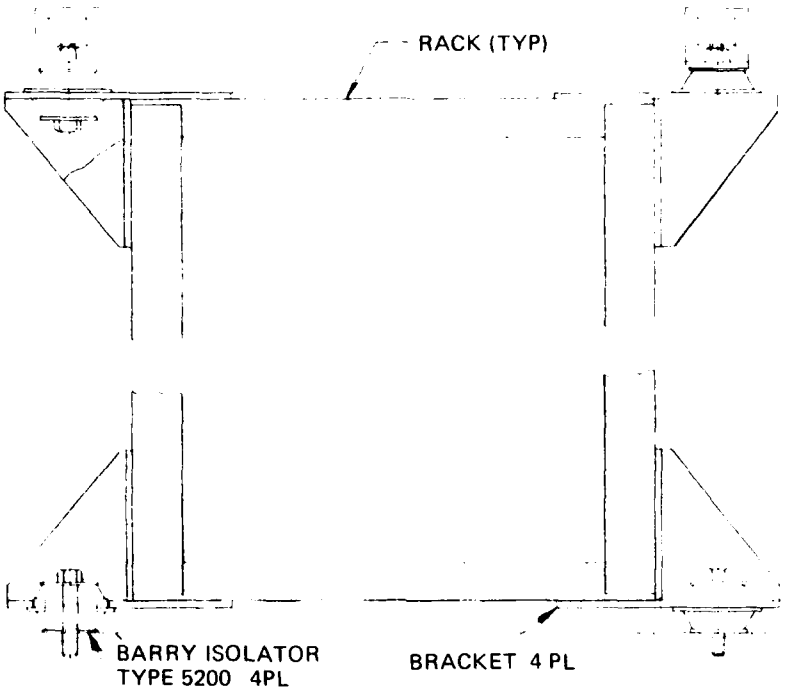

Figure 22 Integrated Rack Isolator Arrangement, Alternate Method

Since the mode of cooling the avionics is strictly by conduction, the liquid-cooled heat exchangers are integral parts of the guide rail. Thermal interface between avionic modules and the guide rails is established by use of IERC spring module retainers. The retainers are made of cadmium plated beryllium copper material to assure intimate contact between the module and the guide rail. Rack isolation from the aircraft structure is accomplished through the use of Barry mount isolators in the same manner as in Candidate A_{21}.

3.2.1.3 Candidate B_{32} - Candidate B_{32} (Figure 17) integrated rack has a conduction cooling system which utilizes air through the guide rails as a heat sink for cooling the ISEM-2A modules. The rack is 10.90 in. wide by 4 in. deep, with a pitch of 6.375 in. for each tier. Each tier accommodates 26 ISEM-2A modules. A typical five tier rack is 36.875 in. high.

The basis structure consists of two extruded aluminum air ducts which form the sides of the rack, and two aluminum channels which form the top and bottom of the rack. The rear cover and the front access door are made of sandwich damping material similar to candidate B_{31}.

The heat exchanger guide rails are secured to the inside of the rack by two vertical angle supports fastened to the air ducts. Thermal interface between avionic modules and the guide rails is established by the use of IERC spring module retainers. The vibration isolation system is the same as candidate B_{31}.

An alternate design concept for candidate B_{32} is to have separate heat exchanger guide rails for each tier of avionic modules as shown by candidate D, Figure 20. The guide rails and the connector plate of the primary backplane become a subassembly which can be removed from the rack as a unit. This improves the modularity aspect of the design and also maintainability. The penalty for this added feature is increased rack height, which is approximately 4 in.

3.2.1.4 Candidate B_{33} - Candidate B_{33} (Figure 18) is an integrated rack with a conduction cooling system which utilizes heatpipe guide rails. The rack is 10.50 in. wide by 4 in. deep, with a pitch of 6.50 in. for each tier. Each tier accommodates 26 ISEM-2A modules. A typical five tier rack is 38 in. high.

The basic structure consists of four extruded aluminum members; two vertical members, one of which is an air duct, and two horizontal members forming the top and bottom of the rack. The rear cover and the front access door are similar to candidate B_{32}.

The heatpipe guide rails are inserted into the rack through openings in the side of the air duct member, and supported on the opposite end by angle supports. A bar on the back side of the guide rail forms a flange to which the connector and primary back plane wiring are fastened. The finned end of the guide rail has a variable conductance flexible heatpipe, which mounts to the aircraft structure to provide a secondary method of cooling. The vibration isolation system used in this candidate rack is similar to candidate B_{32}.

3.2.1.5 Candidate C - Candidate C (Figure 19) is an air-cooled rack with central heat exchanger (a) located at the bottom of the rack. The rack is constructed in four sections; a cap (b) which is 3 in. high, two avionic module sections (c) which are bolted together to form one unit, and a base (d) which

houses the heat exchanger. The four units form the integrated rack assembly which measures 17.76 in. wide by 5 in. deep by 61 in. high. The depth of the rack is controlled by the size of the blowers required to circulate air at both sea level and at its maximum altitude of 45,000 ft. The two module compartments are of identical construction, with each section having an intake and an exhaust duct along the vertical sides. When bolted together, the two adjacent ducts become the intake ducts. A card assembly is formed by two guide rails (e) and the connector panel. This assembly is inserted between the ducts in the module compartment, and is secured to the frame with 1/4-20 bolts. An angle structure inside the module compartments is used to support the secondary backplane (g). The rear cover is constructed of sandwich damping material and is secured permanently to the frame. Two front access doors are used in the rack, one for each compartment. The material for the front doors is the same as that used for the rear cover. Two input/output connectors are located at the top of the frame. Access to primary backplane (h) is achieved by removing the card cage.

The base of the integrated rack houses the heat exchanger assembly, which consists of a liquid-cooled core, two blowers, and a filter assembly. Slots in both the intake and exhaust ducts permit air to flow over the avionic modules and back into the base, where the air is cooled and recirculated through the system. Barry mount vibration isolators are provided to protect the avionics from aircraft induced vibration and shock.

3.2.1.6 Candidate D - Candidate D shown in Figure 20, uses air flow through the avionic modules for cooling the electronic components. The rack for this concept is similar in construction to candidate B_{32}. The difference is in the design of the guide rails which accommodate the hollow core modules. The rack is 14.45 in. wide by 4.00 in. deep. The height is dependent on the number of tiers per rack. A typical five tier rack is 40.5 in. high. Each tier contains 26 hollow core modules spaced at 0.400 in. centers and two i/o connectors located one on each end of the primary backplane.

The basic frame is a rectangular structure with hollow vertical member and horizontal cross members which support the tier assemblies. Four 1/4-20 bolts

secure the tier assemblies to the vertical ducts. The rear cover and the front access door are made of sandwich damping material, similar to candidate B_{31}. The vibration isolation system is similar to candidate B_{31}.

3.2.2 Material Selection

The materials available for the rack's basic structural integrity are similar to those currently used in basic airframe construction. However, additional requirements of low electrical resistance and high thermal conductivity are necessary for a simplified rack design. Table 6 lists the materials and characteristics that were considered.

The nonmetallics graphite epoxy and kevlar epoxy are attractive from a weight and stiffness viewpoint, but in order to negate their adverse characteristics of thermal conductivity and electrical resistance, additional complexity in the rack design would be required. Of the metallic materials considered, the aluminum lithium (AL-3Li) exhibits the most promise for further development. However, since there has not been enough interest in this material only enough has been produced for testing and evaluation. Table 7 shows the ranking system that quantifies the selection of aluminum lithium.

Table 6 Structural Materials Evaluation

MATERIAL	DENSITY ρ (#/IN^3)	SPECIFIC STRENGTH Y/ρ	SPECIFIC STIFFNESS E/ρ	THERMAL CONDUCTIVITY K BTU-FT/HRFT^{20}F	ELECTRICAL RESISTIVITY MICROHM-CM	RAW MATERIAL COST	CORROSION RESISTANCE
AL ALLOY (2024)	0.101	693	104	135	6.3	LOW	GOOD
AL ALLOY (CAST.)	0.097	289	107	135	6.3	LOW	GOOD
AL LITHIUM (Al – 3Li)	0.089	618	135	135*	6.3*	MODERATE	GOOD
TITANIUM	0.164	975	104	9.8	176	MODERATE	EXCELLENT
MAGNESIUM	0.064	328	102	80	17	MODERATE	POOR
ALLOY STEEL	0.28	471	104	38.5	19	LOW	POOR
GRAPHITE EPOXY	0.055	1000	163	2.6	VERY HIGH	HIGH	EXCELLENT **
KEVLAR EPOXY	0.050	1060	90	0.1	INSULATOR	HIGH	EXCELLENT **

*THERMAL CONDUCTIVITY AND ELECTRICAL RESISTIVITY VALUES FOR ALUMINUM LITHIUM (Al – 3Li) ARE NOT AVAILABLE AT THE PRESENT TIME. HOWEVER, BECAUSE OF THE LOW PERCENTAGE OF LITHIUM THESE VALUES ARE BELIEVED TO BE SIMILAR TO 2024 ALUMINUM ALLOY.

**PROTECTIVE COATING MUST BE USED TO PREVENT EPOXY DETERIORATION CAUSED BY PROLONGED EXPOSURE TO ELEMENTS (SUN, WEATHER, ETC)

0009-025W

Table 7 Materials Evaluation Summary

MATERIAL	STRUCTURAL EFFICIENCY (.60)				TECH ADVANCE (0.10)	MATERIAL CHARACTERISTICS (0.30)			TOTAL SCORE	RANK
	WT. (0.15)	MATERIAL COST (0.15)	STIFFNESS (0.18)	INTEGRITY (0.12)		THERMAL COND (0.12)	ELECT. RESIST. (0.09)	CORR. RESIST. (0.09)		
ALUMINUM ALLOY	0.07	0.15	0.11	0.12	0	0.12	0.09	0.045	0.705	2
ALUMINUM (CAST)	0.08	0.15	0.12	0.06	0	0.12	0.09	0.045	0.666	3
AL LITHIUM	0.08	0.075	0.15	0.09	0.10	0.12	0.09	0.045	0.750	1
TITANIUM	0.05	0.075	0.11	0.10	0	0.01	0.003	0.09	0.438	8
MAGNESIUM	0.12	0.075	0.11	0.06	0	0.07	0.03	0.03	0.495	6
ALLOY STEEL	0.03	0.15	0.11	0.10	0	0.03	0.03	0.03	0.48	7
GRAPHITE EPOXY	0.14	0.05	0.18	0.09	0.08	0.002	0	0.09	0.632	4
KEVLAR EPOXY	0.15	0.05	0.10	0.09	0.10	0	0	0.09	0.580	5

0009-026W

The ranking system assigns values to various characteristics of the materials, and rates each material against the others in each category. In this way, since no one material predominates in all categories, a quantitative evaluation is used to determine the overall choice. The best material in each category is given the highest score, with the others receiving a percentage of that value. The relative percentages are based on the characteristics shown in Table 6.

A review of Table 7 indicates that the aluminum materials are clear winners for the basic rack design. The first choice, aluminum lithium, is a relatively new material just appearing on the market place. Its low density, relative to the basic aircraft aluminum alloy series, and assuming sufficient industry interest in further development, makes this alloy a prime candidate for replacement of the 2024 series aluminum that would be used if the rack were built today.

3.2.3 Isolation System

A rack design has been proposed that will incorporate a combination of vibration isolators with a chassis partially constructed from a damped structure, employing constrained layers of a viscoelastic material.

3.2.3.1 Isolators - With regard to the vibration isolators, of the various rack designs proposed in this study, the versatile type 5200 Series Barry mount will meet all the requirements. The specific dimensions are shown in Figure 23.

ISOLATOR

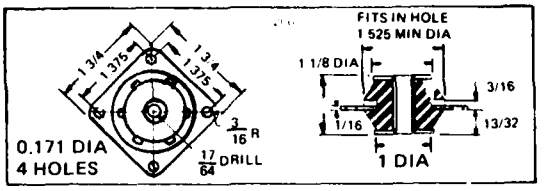

0009-027W **Figure 23 Vibration Isolator**

The Series 5200 isolators are ideal in applications where protection is required from shock, vibration, or noise, or where a combination of these environments are present. The elastomer provides efficient isolation design in any attitude, as well as effective shock protection. The radial to axial stiffness ratio is approximately 0.6. The geometric design incorporates a fail-safe mounting in that even if the elastomer fails the isolator, internal parts are captured.

The isolator with the Barry "Hi-Damp" resilient elements will withstand the required random vibration tests of MIL-STD-810C, with maximum transmissibility of approximately 4.0.

Installation requires no special tools or hardware, and includes options of either a through core or threaded core equipment rack attachment. In addition, the centrally located mounting flange permits the isolator to be partially recessed into the rack, thus reducing the overall package envelope.

The maximum load ranges of the Series 5200 isolator varies from 15 lbs. to 50 lbs. per mount. In this application, the ideal installation is to incorporate two base mounts and two top mounts, thus resulting in a center of gravity mounting. This will minimize the overall motion, thus reducing sway space requirements.

Successful accommodations of all of the above requirements will result in an equipment rack isolation design with a natural frequency of approximately 25 Hz. A 25 Hz resonant isolation system has proven to be the ultimate design frequency consideration, in order to accommodate the rigorous dynamic environmental conditions associated with Naval aircraft carrier suitability operations.

The recommended isolator configurations are shown in Figure 24.

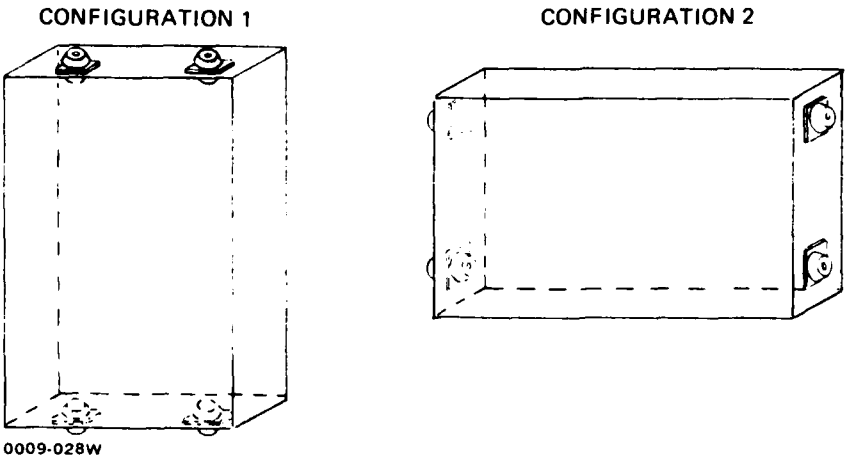

Figure 24 Vibration Isolation Configurations

3.2.3.2 - Damping Materials - The dynamic environment associated with state-of-the-art microminiature components has resulted in unprecedented stresses on every part of the design. Every structural element, regardless of size, material, or geometric shape, will amplify the vibration at certain frequencies. At resonant frequencies, the amplifications are very high because of the small amount of structural damping present in the support structure. As a result, unwanted dynamic stresses are created which transmit high accelerations, consequently producing excessive noise, structural fatigue, or component failure.

A practical solution to this problem has been developed by several isolator manufacturers, who produce a highly damped, sandwich sheet metal construction. In particular, the materials are called "Rigidamp", produced by Barry Controls, and "Dyna Damp", produced by the Lord Manufacturing Company.

The two companies essentially manufacture the same product. The only variation is in the type of elastomer compound utilized.

The basic concept involves damping structural fabrications by the use of viscoelastic damping materials. The structural fabrications may be damped by viscoelastic damping materials employed either as unconstrained layers applied to surfaces of structural members, or as constrained layers interposed between the surfaces of members comprising a structural composite. An unconstrained viscoelastic layer experiences primarily cyclic tension-compression strains when applied to a structural member undergoing flexural vibrations, whereas a con-

strained viscoelastic layer experiences primarily shear strains when incorporated in a structural composite.

Since it generally is necessary to use relatively thick layers of damping material in the unconstrained structural configurations, it is more practical to use a constrained viscoelastic structural configuration which requires only a relatively thin layer of elastomer, i.e., 0.005-0.010 in.

The installation of this material requires no special tools or techniques. Rivets, screws, or bolts can be utilized without any major degradation in damping performance.

For structural load considerations, it is proposed that one sheet of the composite be sized to take the load, with the second sheet of a 0.010 in. thickness, bonded together with a 0.005-0.010 in. thick damping compound.

In addition to the benefits of reducing the structure borne vibrations with the viscoelastic damping materials, tests have also shown an inherent reduction in the problems associated with acoustic noise. A properly designed structural cover can provide proper acoustic transmission loss to reduce the excitation structural resonances, which cause component malfunction.

Therefore, in conclusion, a properly designed integrated rack, utilizing both isolators and structural constrained viscoelastic damping materials, will minimize the vibration shock and noise environmental problems. In particular, the results will be:

- control of amplifications at structural resonances
- increased fatigue life of structures
- improved equipment reliability.

3.2.4 Structural Design of the Critical Rack Configuration

The critical rack configuration selected for a more detailed structural analysis is B_{31} (with liquid cooled guide rails). The rationale for this selection is discussed in the following paragraphs.

The combinations of module and rack locations are diverse, and it is beyond

the scope of this study to do a comprehensive structural analysis of each possible combination. Therefore, only the most promising configurations (A_{21}, B_{31}, B_{32} and B_{33}) were considered as possible candidates for a more detailed structural analysis.

The typical 5 tier rack weights (range 76 - 56 lb) and physical sizes (approximately 4 x 10.5 x 40 in.) are all in the same range, so there is no obvious choice. The configuration that appeared to be the most structurally flexible was B_{31} (with the liquid cooled guide rails), since it uses open channel extruded sections for the end members. Therefore, it was decided to do further strength and deformation analyses on this configuration.

The strength requirements for equipment installations are derived from the MIL-A-8860 series of structural specifications. MIL-STD-810C, environmental test methods, is used for shock and vibration requirements. A summary of design load factors is shown in Table 8.

Table 8 Equipment Design Load Factors

	CRASH(1)	STEADY STATE(2)	SHOCK (2)	
			DESIGN	CRASH
LONGITUDINAL	16 FORE/AFT	4 FWD 6 AFT	20	40
LATERAL	8	4	20	40
VERTICAL	16 DOWN, 8 UP	12.3 DOWN, 7.0 UP	20	40

(1) EQUAL TO OR HIGHER THAN MIL-A-8860 STEADY STATE REQUIREMENTS FOR BOTH A & B V/STOL

(2) MIL-STD-810C REQUIREMENTS

0009-029W

It would be conservative to assume that any specific rack in any location would be designed to sustain the 20g shock environment and be capable of operation. The 40g shock crash load was used to determine an ultimate internal load distribution (material not to fail but be allowed to yield).

3.2.4.1 Structural Description of Candidate B_{31} - Figure 16 describes the five section rack with liquid cooled guide rails. It is mounted on four vibration isolators located in the vertical plane, attaching to the aluminum framing structure near the corners. The basic structural integrity of the rack is supplied by the boundary frames, rigidly attached backplane, and uses the guide rail attachment to the side frames to stiffen the structure. The front access door is assumed

nonstructural, although it would be somewhat effective in the crash condition. The backplane, utilizing "Rigidamp", acts as a shear web between the vertical side frames, thus making the rack act as a deep beam (I_z = 10 in.^{4}) instead of two separate shallow beams (I_z = 0.08 in.^{4}). The guide rails support the open channel side frames, and prevent them from rolling over under eccentric loadings.

The guide rail is considered a primary structural member since it contributes to the rigidity of the overall rack, and also serves to beam the ISEM-2A module loads to the main side frames. It is a simple machined box section with external grooves to support the modules, and an internal cavity for the liquid coolant.

3.2.4.2 Structural Analysis of Candidate B_{31} - A finite element model simulating the basic B_{31} structural arrangement was used to determine the rack deformation characteristics at a loading of 20g in each direction. This model, shown in Figure 25 has 48 nodes and 144 degrees of freedom. The shock isolators are not simulated. The rack weight, 59.18 lbs., is mass distributed among the nodes and the element areas, and gauges are based on Figure 16. Individual inertia 20g loads were applied separately in the x,y, and z direction. The detailed results of the finite element analysis are available in the contractor's file. The resulting deformations are shown in Table 9. For any off-axis loading, these values can be geometrically combined. The maximum deflection of 0.0179 inches relative to the fixed supports is not expected to adversely affect the functioning of the ISEM-2A modules. A survey of the member stresses generated when the rack is subjected to a 40g crash load indicates that the highest stress level (8020 psi, in compression) will occur in the side frames when the crash load is in the y direction. This is well within the materials strength capability. It is obvious that structural optimization could be used to reduce the weight of the rack structure. However, this would be beyond the scope of this study, and would normally occur during the detail design phase.

In summary, the structural configuration of the rack poses no apparent problems that would prevent the successful integration of the avionics into a common rack configuration.

3.2.5 Vibration Analysis

An isolation analysis was performed on the A_{21}, B_{31}, B_{32}, and B_{33} integrated rack candidates. The geometric relationships are shown in Table 10.

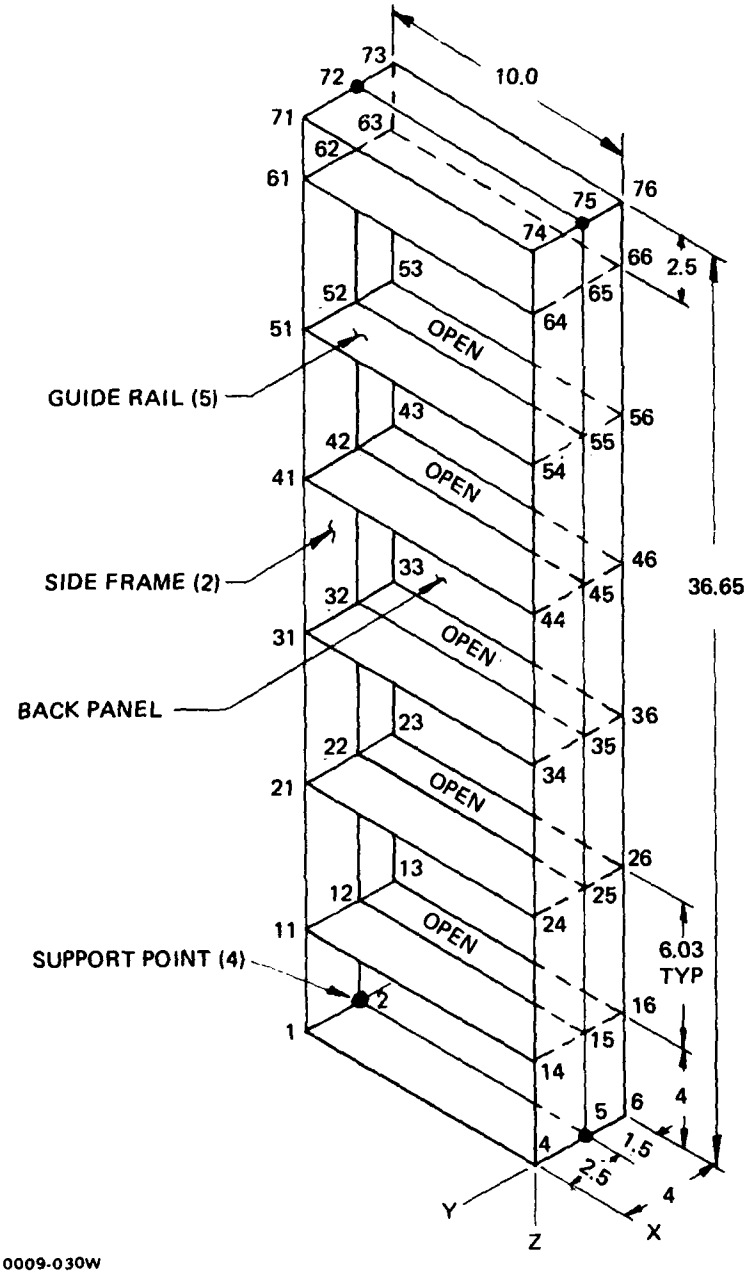

0009-030W

Figure 25 Finite Element Model of Candidate B_{31}

Table 9 Summary of Rack Deformations at 20g[1]

MODE[2]	DEFORMATION MN [3]		
	Δx	Δy	Δz
72	0	0	0
62	0.0062	0.0042	0.00015
52	0.0123	0.0125	0.00030
42	0.0154	0.0176	0.00046
32	0.0157	0.0179	0.00037
22	0.0132	0.0141	0.00032
12	0.0076	0.0064	0.00020
2	0	0	0

(1) RACK WEIGHT = 59.18 LB

(2) REF. FIG. 25

(3) Δx DUE TO Px
Δy DUE TO Py
Δz DUE TO Pz

0009-031W

Table 10 Rack Geometric Relationships

CANDIDATE	WEIGHT (LB)	HEIGHT (IN.)	WIDTH (IN.)	DEPTH (IN.)
A_{21} – AIR-OVER-COMP	76.74	45.96	10.5	4
B_{31} – LIQUID G.R.	59.18	36.65	10.5	4
B_{32} – AIR G.R.	56.01	36.87	10.9	4
B_{33} – HEAT PIPE G.R.	60.89	38.00	10.5	4
C – CENTRAL H. EXCH	142	61	17.7	5
D – HOLLOW CORE	69	40.5	14.5	4

0009-032W

To establish the maximum isolator load variation, the lightest (B_{32}) and the heaviest (A_{21}) rack configurations were examined. In addition, the rack isolator locations will be two on the bottom and two at the top, oriented such that isolator axial plane is parallel to the height dimension. This isolator orientation will essentially result in a center of gravity installation, thus minimizing the contribution of the normally troublesome rocking modes of vibration.

The specific loads in each isolator for the two rack configurations are:

- A_{21}, Weight = 76.74 lb, therefore:
  load/isolator = 76.74 lb/4 = 19.18 lb
- B_{32}, Weight = 56.01 lb/4 = 14.0 lb

An isolator that will encompass the above load requirements is an all elastomeric type isolator manufactured by the Barry Controls Company, and is designated the 5200 Series. The specific isolator that will meet all of the load requirements as well as all of the attitude frequency requirements is the 5220 isolator.

To establish the isolation frequency for the proposed rack configurations, the load/deflection curves indicate that the spring rate for 5220 Series isolator is 1600 lbs./in. Therefore, the A_{21} and B_{32} rack vertical isolation frequencies are:

$$f_{N\,(A_{21})} = 3.13\left(\frac{K}{W}\right)^{\frac{1}{2}}$$

$$= 3.13\left(\frac{1600}{19.18}\right)^{\frac{1}{2}} = 28.58 \text{ Hz}$$

$$f_{N\,(B_{32})} = 3.13\left(\frac{K}{W}\right)^{\frac{1}{2}}$$

$$= 3.13\left(\frac{1600}{14.0}\right)^{\frac{1}{2}} = 33.46 \text{ Hz}$$

The horizontal isolation resonant frequency is determined by the spring rate relationship:

$$\frac{K\ (\text{Horizontal})}{K\ (\text{Vertical})} = 0.6$$

Therefore the maximum spread in frequency for the A_{21} and B_{32} rack configurations are:

$$f_{N\,(A_{21})} = 3.13\left(\frac{1600 \times .6}{19.18}\right)^{\frac{1}{2}} = 22.14 \text{ Hz}$$

$$f_{N\,(B_{32})} = 3.13\left(\frac{1600 \times .6}{14.0}\right)^{\frac{1}{2}} = 25.92 \text{ Hz}$$

In conclusion, the 5220 Series isolators, when subjected to the loads dictated by the various integrated rack configurations will meet the established Grumman isolation criteria for carrier suitable aircraft. Figure 26 defines the frequency and transmissibility ranges which are required to insure that the isolation requirements are met.

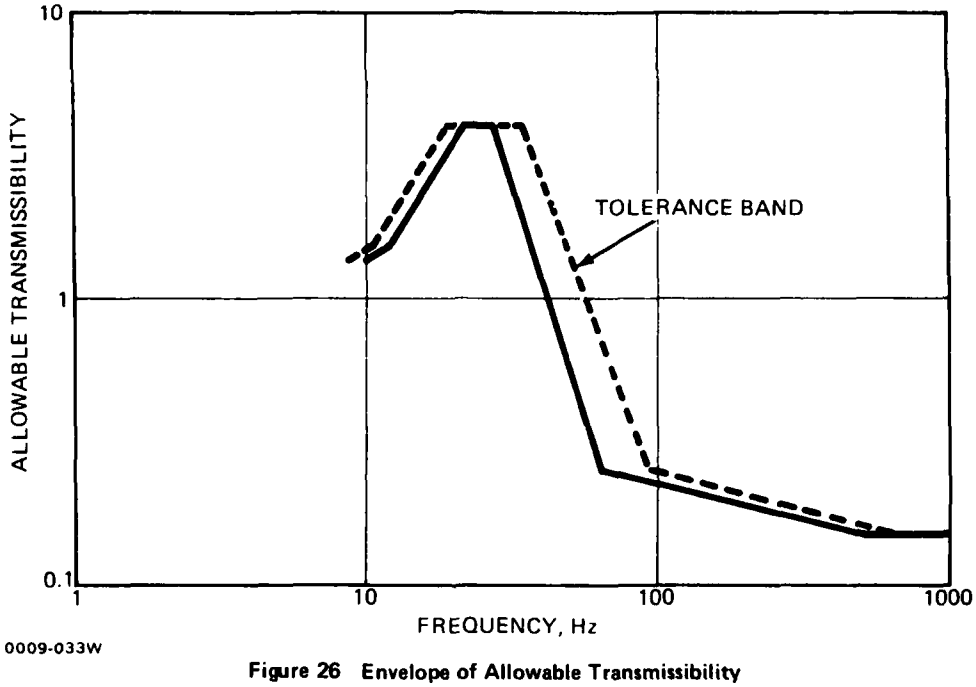

Figure 26 Envelope of Allowable Transmissibility

3.2.6 Aircraft Volume Analysis

In order to fully understand the aircraft impact in the development of an IAR design, both A and B V/STOL design concepts were studied in detail. Types A and B V/STOL aircraft represent significantly different airframe designs, due to their specific mission requirements (sea control ASW/AEW and Fighter/Attack, respectively). In addition to dissimilarity in the airframe, the avionic suit, aircraft installation, and accessibility limitations also diffe signif-icantly. The type A and B V/STOL design concepts represent a good cross-section of future as well as existing military aircraft designs.

Initially, both vehicles were studied to identify all available volume for avionic systems, and to define the accessibility to each proposed equipment area. Preliminary selection of candidate areas for IAR applications were made to identify basic aircraft mechanical sizing requirements (ref. Subsection 2.4). Subsequent detailed studies were performed using the specific IAR candidate designs (A_{21}, B_{31}, B_{32}, B_{33}, C and D) in all candidate equipment areas. The results give a comparison of total capability of each IAR design in both study vehicles. By comparing these numbers, the relative packaging efficiency is indicated (see Table 11).

Table 11 Card Volume Capability

CANDIDATE	A V/STOL	B V/STOL
A21	1924	988
B31	3016	1456
B32	2600	1456
B33	2548	1456
C	520	0
D	1612	910
0009-034W		

To better understand the application of the candidate IAR designs on the study vehicles, additional studies using detailed projected avionic equipment suits were performed. Proposed electronic equipment lists were generated and all subsystem equipment was reviewed for IAR application. Suitable equipment functions were selected and sized to arrive at a required number of card spaces. A detailed partitioning was performed on the selected functions within the specific IAR arrangement for both study vehicles. These were presented in Tables 1 - 3. Using this partitioning and the remaining WRA's, detailed inboard profile drawings were generated from the proposed electronic equipment lists. Figures 27 and 28 highlight the major locations for the IAR or WRA type equipment.

3.2.7 ISEM-2A Hollow Core Configuration

The hollow core module shown in Figure 29 requires that the pitch be increased from the present ISEM-2A which is 0.300 in. to 0.400 in. The method used to determine the pitch requirements is shown in Figure 30 which depicts the present ISEM-2A.

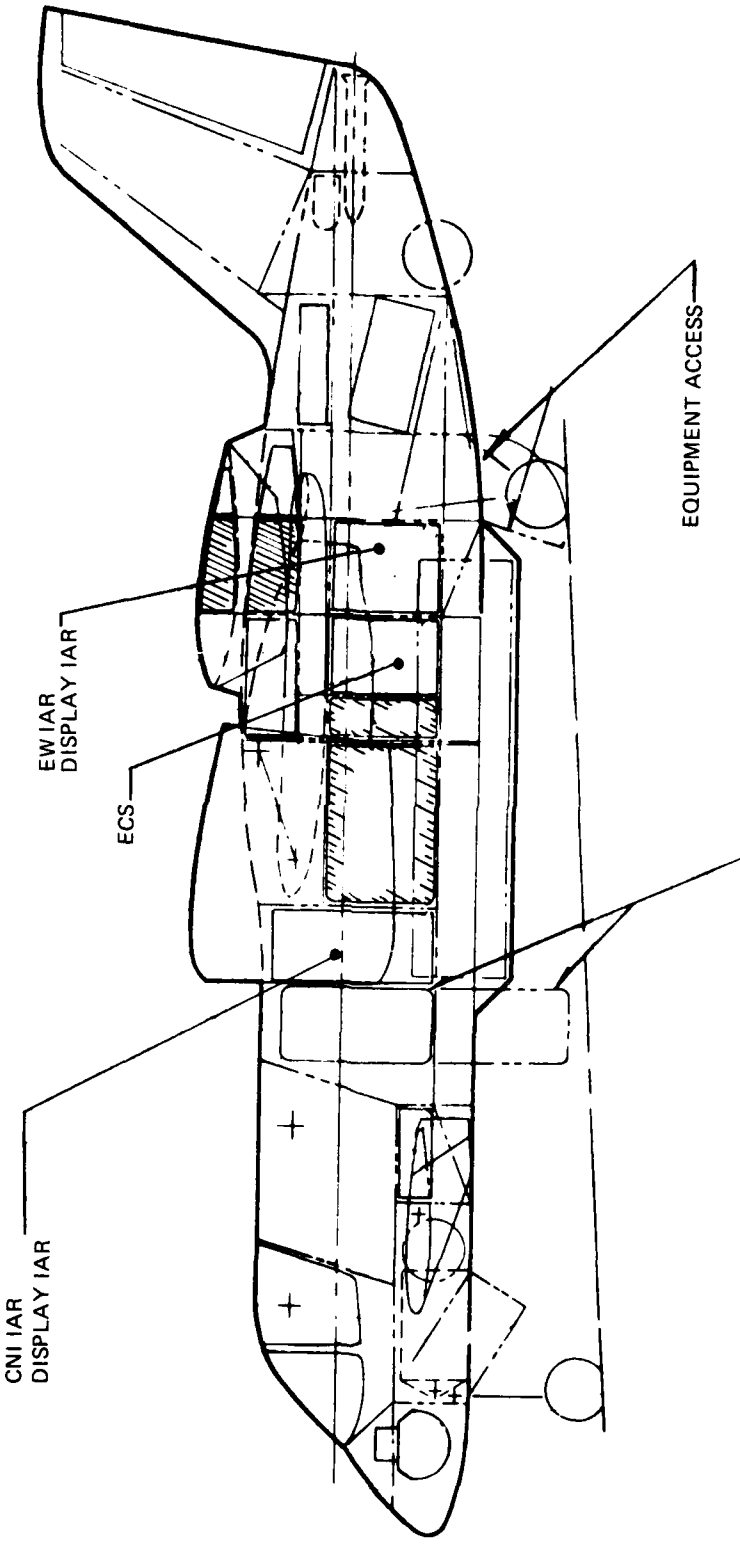

Figure 27 A V/STOL IAR Arrangement

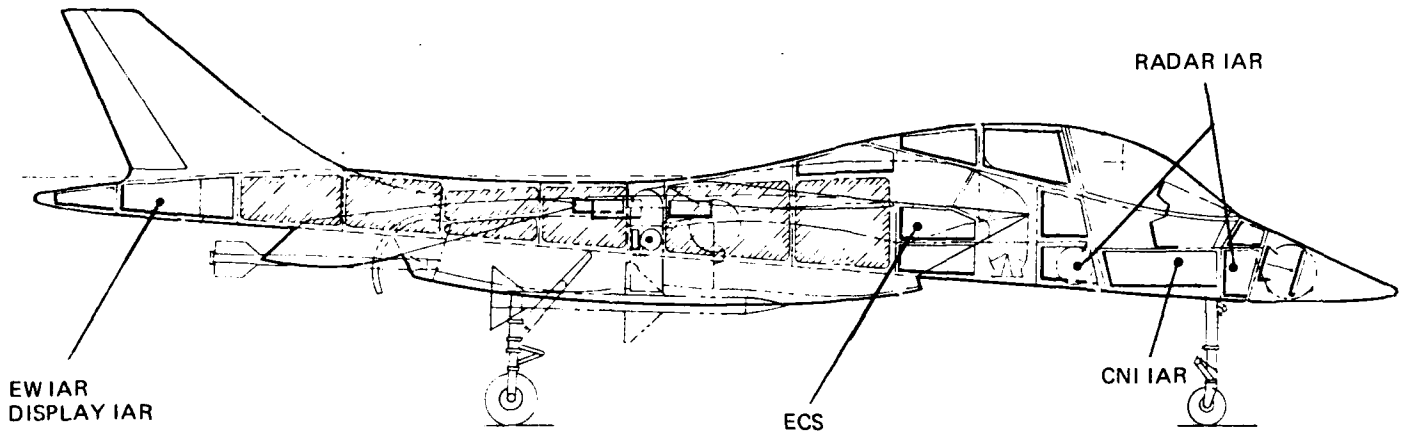

0009-036W

Figure 28 B V/STOL IAR Arrangement

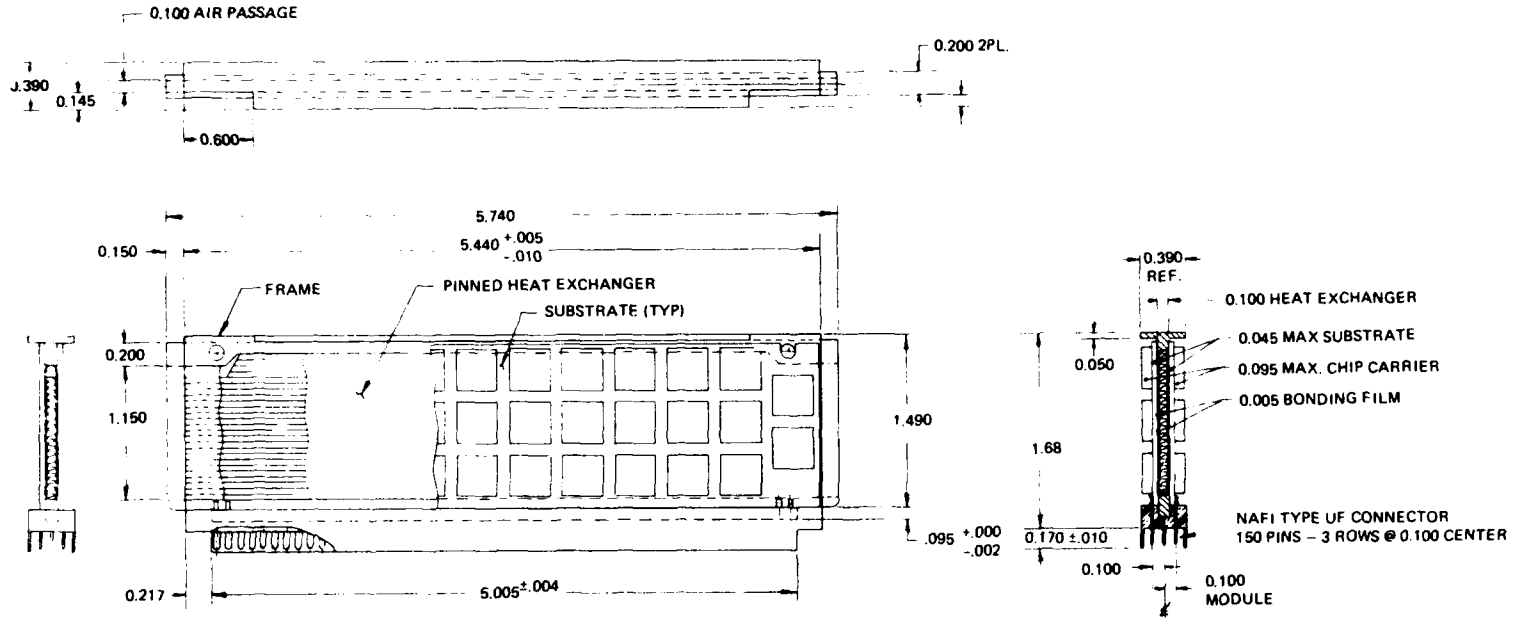

NOTES:

1 – MODULE FRAME MAT'L – G101 ALUM EXTRUSION
2 – HEAT EXCHANGER BONDED TO FRAME
3 – SPECIAL MAFI CONNECTOR REQD.
4 – CHIP CARRIERS 35 PER SIDE (SIZE 0.350 SQ IN.)

ISEM-2A FORM FACTOR WITH
0.400 IN. PITCH REQUIREMENT

0009-037W

Figure 29 Hollow Core Type Module

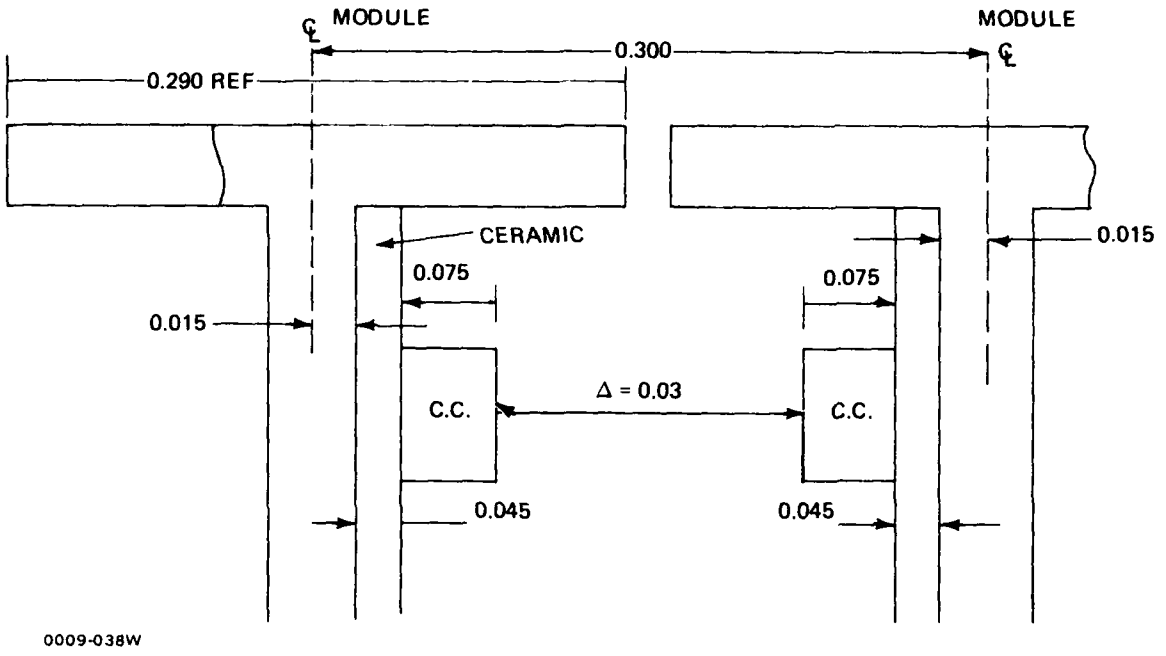

Figure 30 Pitch ISEM-2A Module

In establishing the minimum pitch for the hollow core module with the basic ISEM-2A form factor, a 0.35 in. by 0.35 in. chip carrier with a maximum height of 0.100 in. was used. This height, established by the JEDEC-proposed outlines, can vary from 0.067 to 0.100 in. Based on the minimum dimensions deemed reasonable for the construction of the hollow core module, the minimum acceptable pitch is 0.400 in. This is shown in Figure 31.

With the increased module width requirement for the hollow core, it is now possible to increase the number of interconnecting pins from 100 to 150 as shown in Figure 29, making the hollow core module more versatile. A new 150-pin connector would have to be developed.

3.3 POWER DISTRIBUTION

Several power distribution configurations were developed during the study and are shown in Figures 32 through 35. Figure 32 outlines a nonredundant system utilizing an optical data bus, SOSTEL terminals, and flat wire power lines which are located at a distance from the integrated rack. A SOSTEL terminal, which is located on the main power line, is activated and remains

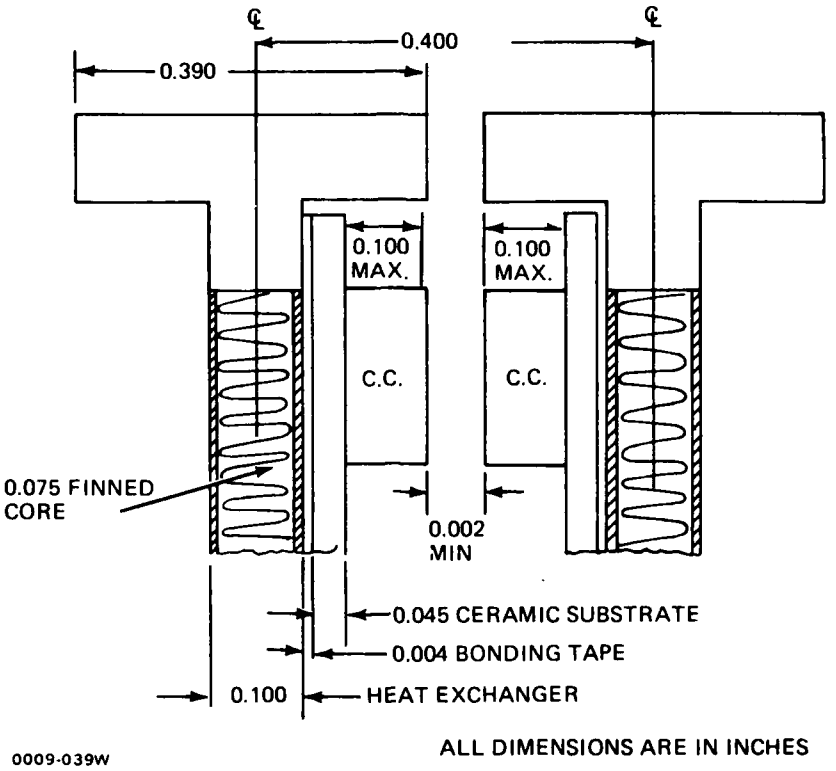

Figure 31 Pitch Establishment, Hollow Core Module

energized upon excitation of the main power line. It controls the flow of power into a secondary power line leading to the integrated rack. The actual power will be switched on and off by a 270V dc power controller, which is in turn controlled by the SOSTEL terminal. A current sensor will provide a signal back to the master processor to confirm proper operation, and will thereby protect the main power line. A 600 micrometer solid single fiber optical data bus line, which provides EMI free operation, is shown tieing the terminal to the Main Processor. If the rack system is located in the benign EMI environment, a twisted shielded pair may be used for the data bus.

The power line feeding to the rack will enter the rack thru a separate power connector, and feed thru a filter to eliminate transients on the power line. Even though the flat cable will be arranged to minimize transient electromagnetic signals (due to characteristics of flat wire configuration - see NADC Task No. F61512001 IED No. 66334), the inductive type filter will pass the dc power

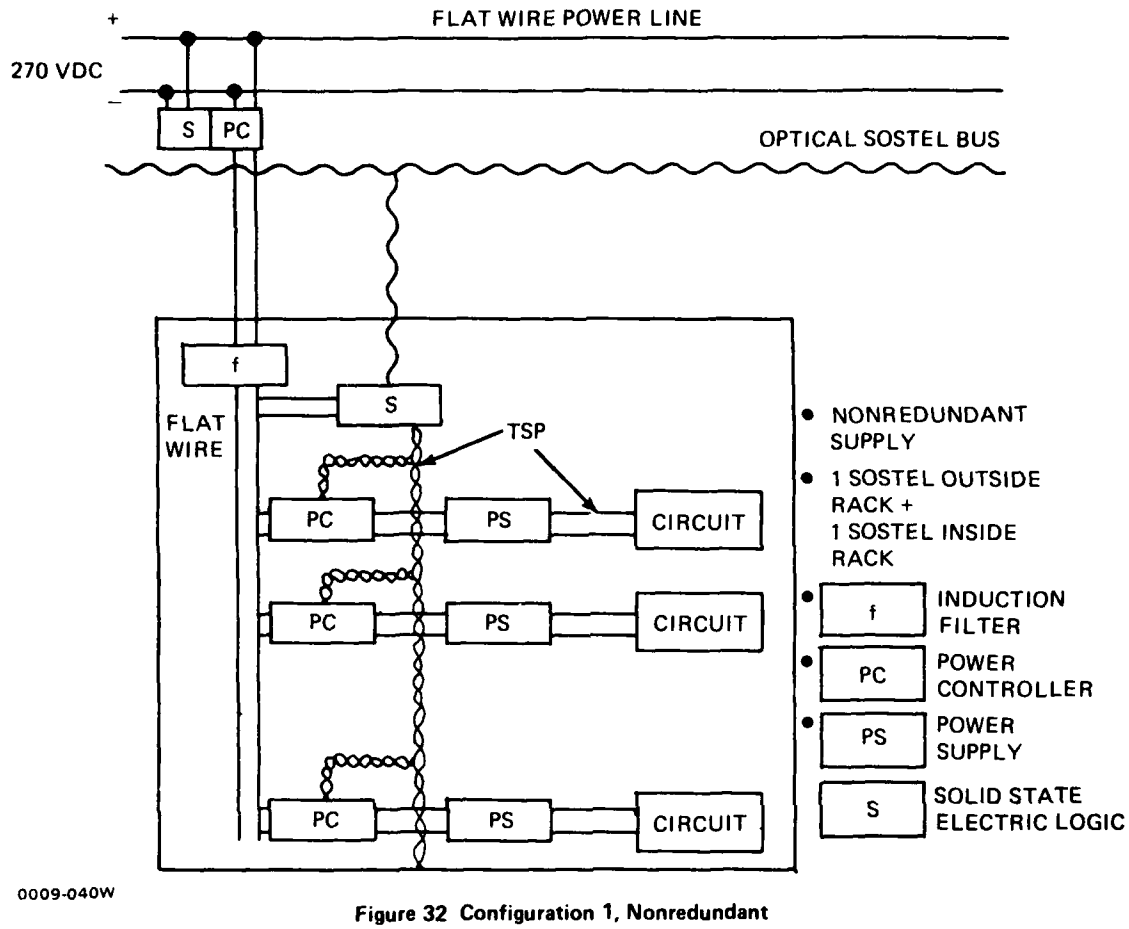

Figure 32 Configuration 1, Nonredundant

and attenuate any remaining transients. Care must be taken in designing the LC characteristics to prevent unwanted oscillations.

A second SOSTEL terminal is located within the integrated rack, which will be energized when the power line to the rack is energized. This terminal will also receive control signals via an optical link to minimize EMI. This SOSTEL will protect the line from shorts in the rack by means of a main controller within the rack. It is assumed that the line to be routed is adjacent to the rack.

A series of power controllers will be installed to control power to individual power supplies which convert 270V dc to 5V dc for use by the subsystem circuits. Up to 64 controller/byte signals can be handled by each SOSTEL Terminal. The number of power controllers is determined by the number of power supplies

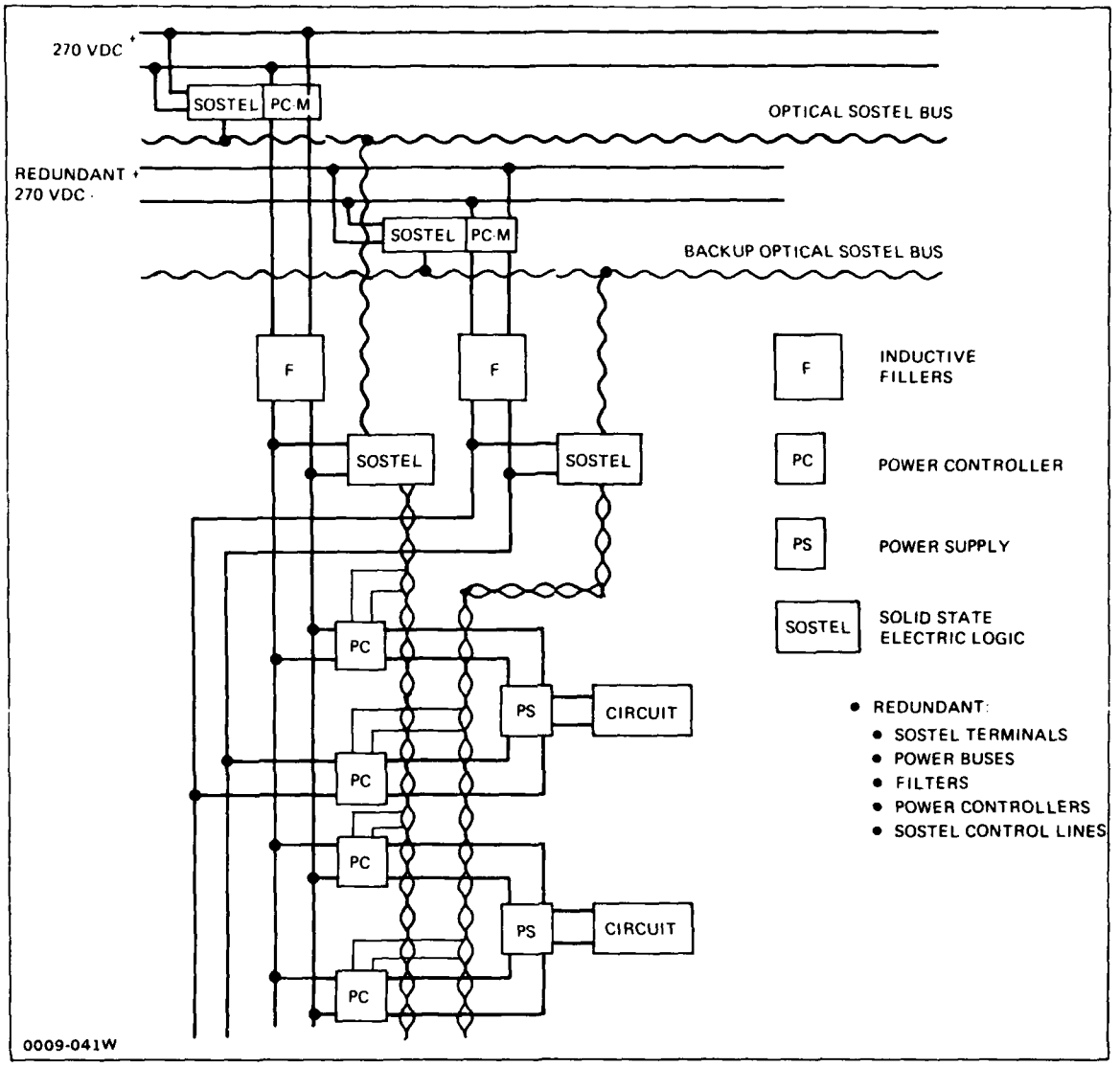

Figure 33 Configuration 2, Partially Redundant

within the rack (one controller per power supply). Two power controllers can be installed on each ISEM-2A card. The power supplies will convert raw 270V dc aircraft power to 5V dc, as required by individual circuits. It became rapidly evident during the study that the power supplies are taking up a substantial part of the rack's available volume. Therefore, work in higher density power supplies is strongly recommended. The study utilized the standard power sup-

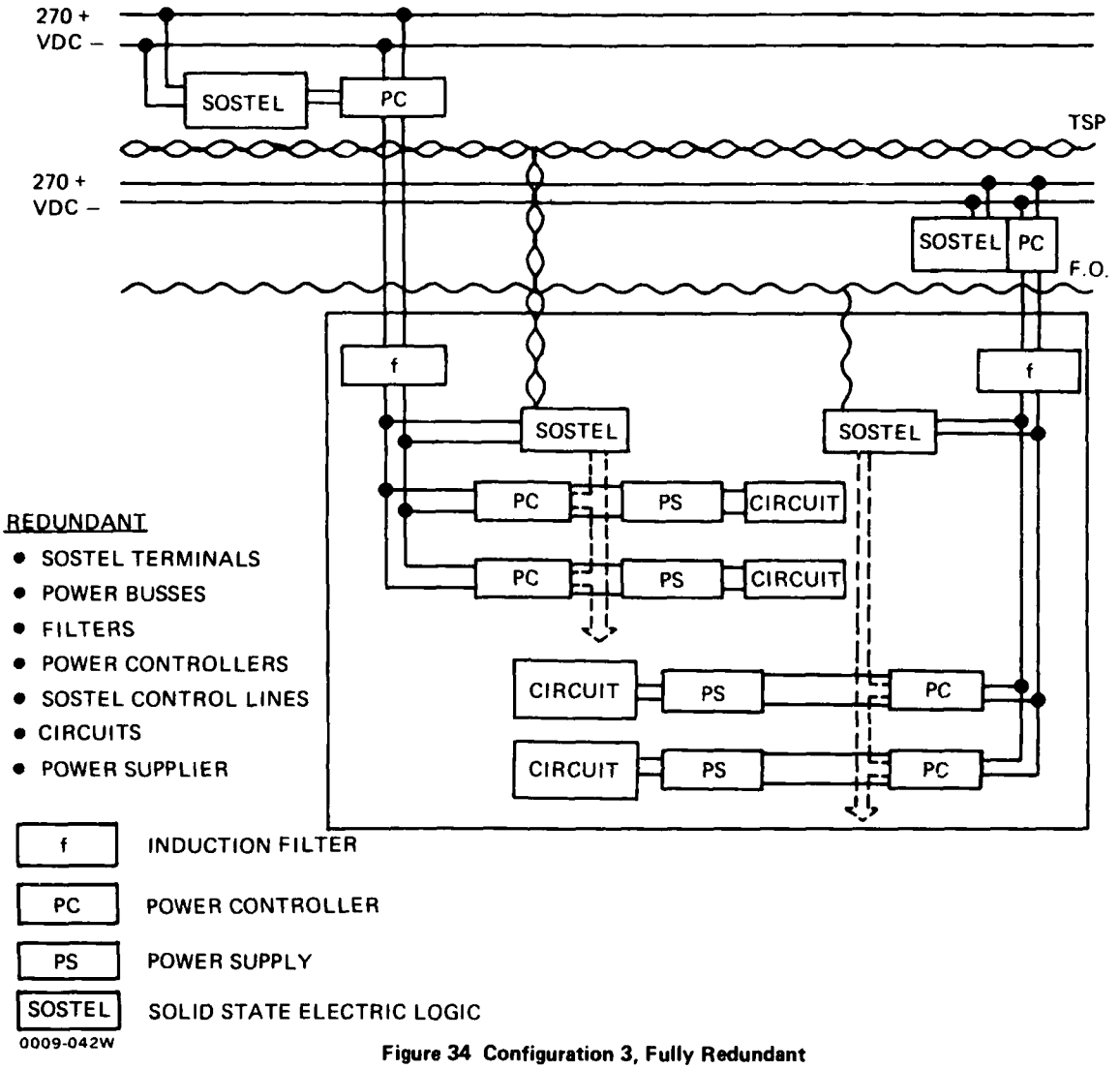

Figure 34 Configuration 3, Fully Redundant

plies under development by Naval Avionic Center as the basis for sizing and partitioning effort.

A power supply configured as seen in Figure 36 will be compatible with the integrated rack design. This (200 watt) power supply configuration is compatible with a full tray of ISEM modules and a 90 watt supply is compatible with a 1/2 tray size. Cooling will be provided in a cold plate mounted in rear of the power supply. This cold plate will in turn be cooled by the same coolant as that which flows thru the guide rails. To ensure flexibility, the rack shall

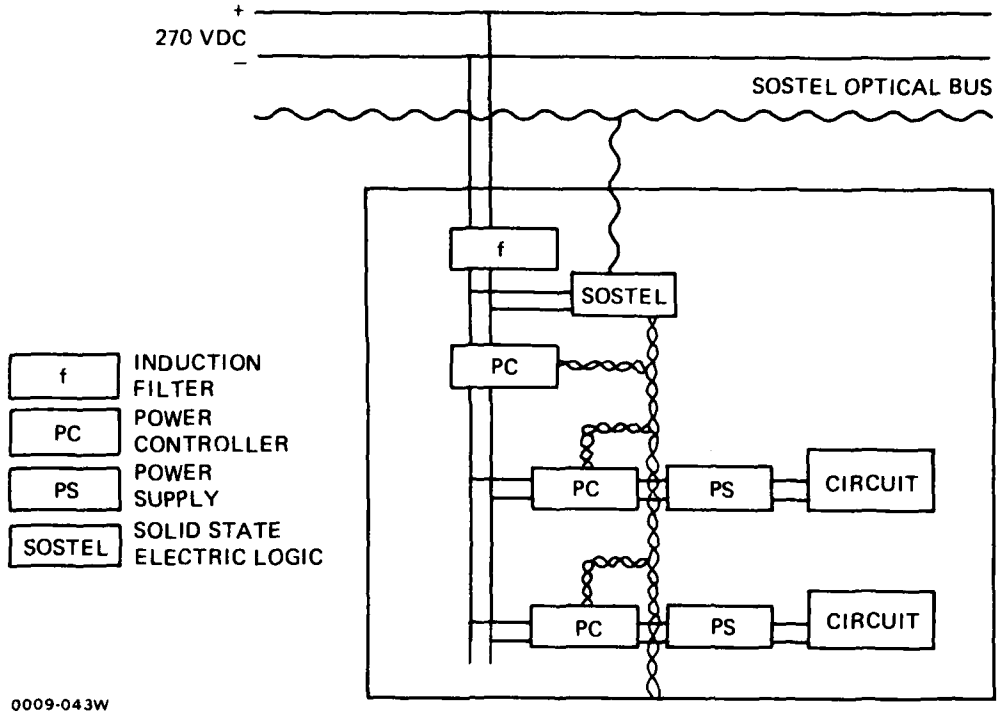

Figure 35 Configuration 4, Nonredundant (Internal SOSTEL Only)

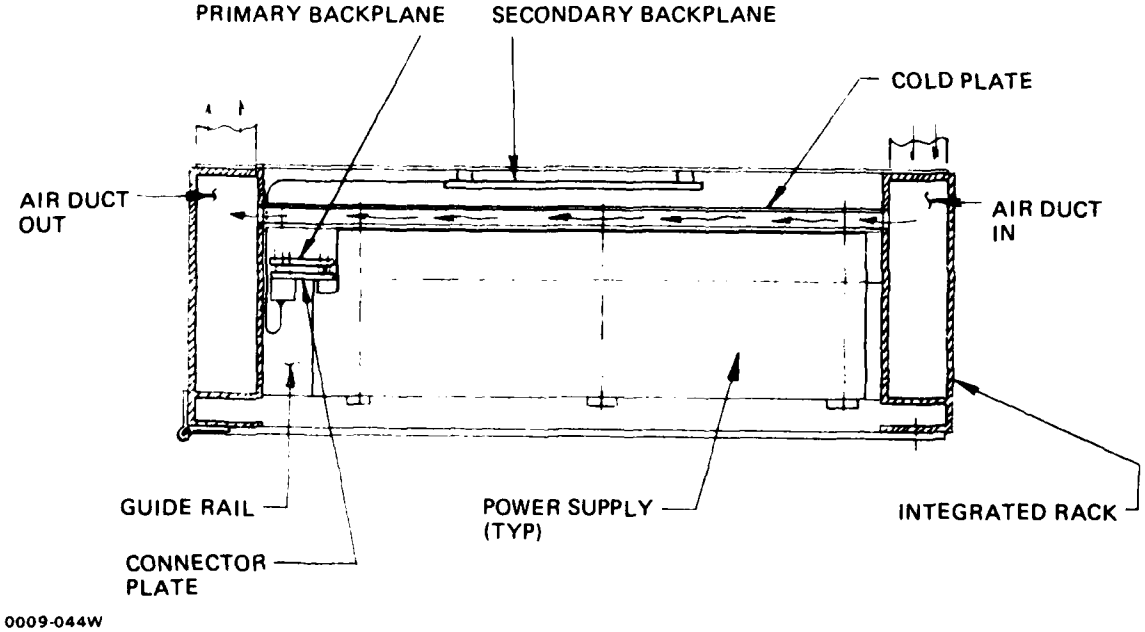

Figure 36 Power Supply Mounting (Typical)

be designed so that the cold plate can be removed and the coolant passages to the side ducts sealed off.

Figure 33 shows the impact of the partially redundant power distribution system. The entire front end of the system has been duplicated, including power lines associated SOSTEL Terminals and Main Power Controller, input filters, racks, internal SOSTEL Terminal, and individual power controllers.

Single power supplies were selected for this configuration, since the power supplies take up so much volume. Figure 34 shows a fully redundant power distribution system. A further variation occurs when only critical circuits are made fully redundant. This is judged to be the optimum design.

Figure 35 shows a nonredundant configuration in which the aircraft power line is routed adjacent to the integrated rack, thereby precluding a separate SOSTEL Terminal at the power line. Instead, a single SOSTEL Terminal located within the rack is utilized. This configuration was judged the cheapest of all configurations, since it had the lowest part count. A drawback to the system is that part of the rack is energized whenever the main power lines are energized. The SOSTEL Terminal must be energized to operate. This can only be achieved by having it constantly on, or else by running a separate power line to the SOSTEL Terminal.

Based on the above studies, a preliminary partitioning of the subsystems for both A V/STOL and B V/STOL, identified in Section 2.1, was made. The power distribution configuration selected for this effort was similar to that shown in Figure 35. However, a redundant SOSTEL Terminal was added to the configuration of Figure 35 to enhance reliability of critical circuits in the sizing study. Since critical circuits have not as yet been identified, only the SOSTEL Terminal was made redundant. Figures 37 and 38 outline preliminary distribution systems for B V/STOL and A V/STOL. Four integrated rack areas are required for B V/STOL and two for A V/STOL. Examination of power requirements for each aircraft rack identified that 10 Amp and 33 Amp power controllers will be required. These units are not currently available, and must be developed (see Figure 39). Based upon these rack requirements, preliminary sizing of power lines was made for each individual rack, and are shown in Table 12.

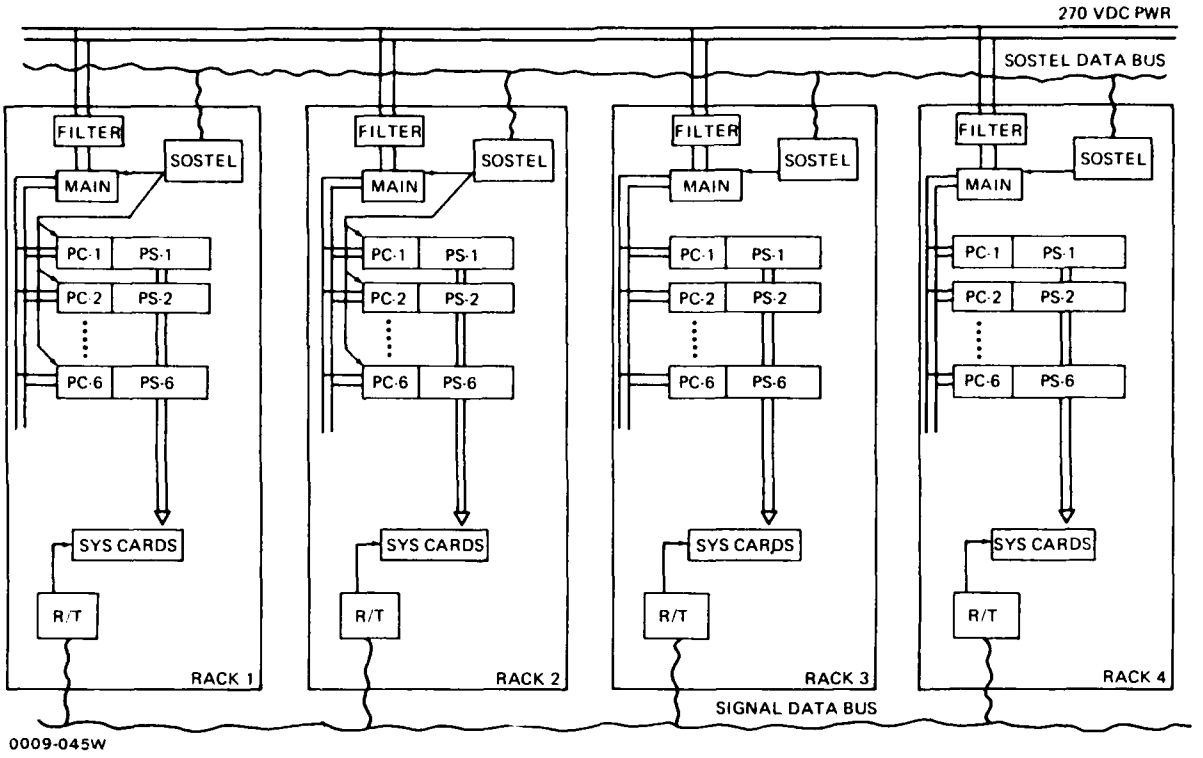

Figure 37 B V/STOL Power Distribution

To convert 270V dc power to desired 5V dc regulated power, the highly efficient switching mode regulator becomes an alternative to the standard series pass regulator currently in use. Preliminary studies indicate that switching mode power regulators may afford a sizeable savings over dissipative supplies, and thereby provide increased watts per cubic inch, i.e., less rack space. (See 270V dc Impact Study, LR28780, Nov. 1978, NADC Contract #N62269-78-C-0007.) The higher efficiency reduces the overall space and weight requirements. With the modulator operating at 25,000 cycles per second on 270V dc, the size of the conversion transformers becomes smaller than current transformers operating on 115V ac power. However, special care must be taken with regards to EMI control (see (1) Switching Mode Power Supply Technology paper by J. Foutz Naval Ocean System Center, Dec. 1978. (2) Limiting EMI from Switching Mode Power Supplies, E. Kamm, Dec. 1978).

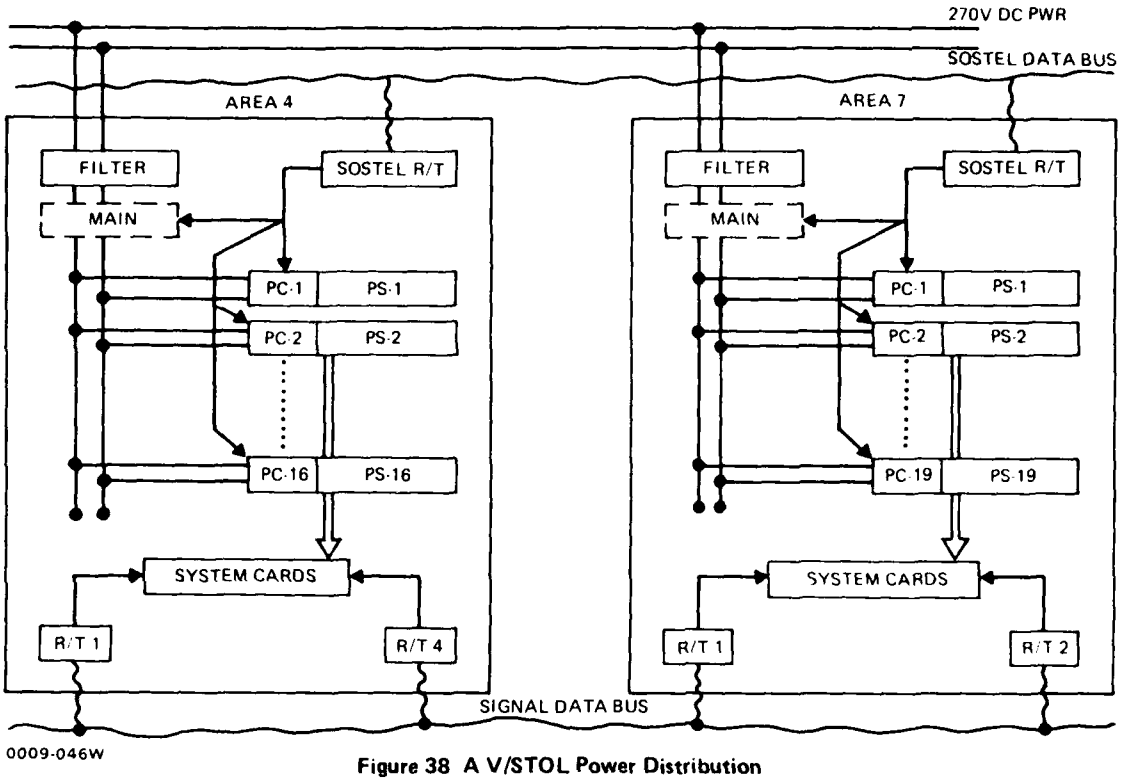

Figure 38 A V/STOL Power Distribution

3.4 EMI CONTROL

Since the integrated rack will contain military digital electronic circuitry, the coupling of electromagnetic interference can upset the proper operation of weapon systems, and thereby destroy the success of a military mission. The general requirement outlined in Subsection 2.3 can impact the design of an integrated rack in several ways, as noted in Figures 40 and 41. The spark gap/Varister design is external to the rack, and therefore was not addressed in this study. Likewise, interconnection wiring external to the rack was not addressed, except as a source of conducted interference voltages and currents. Gamma and neutron radiation, which result from nuclear environments, were partially addressed. Nuclear EMP was addressed as just another form of EMI, which is similar to the lightning-induced interference, but with a higher high-frequency content in the fields (design for higher E, H and planewaves at high frequency, aperture, etc).

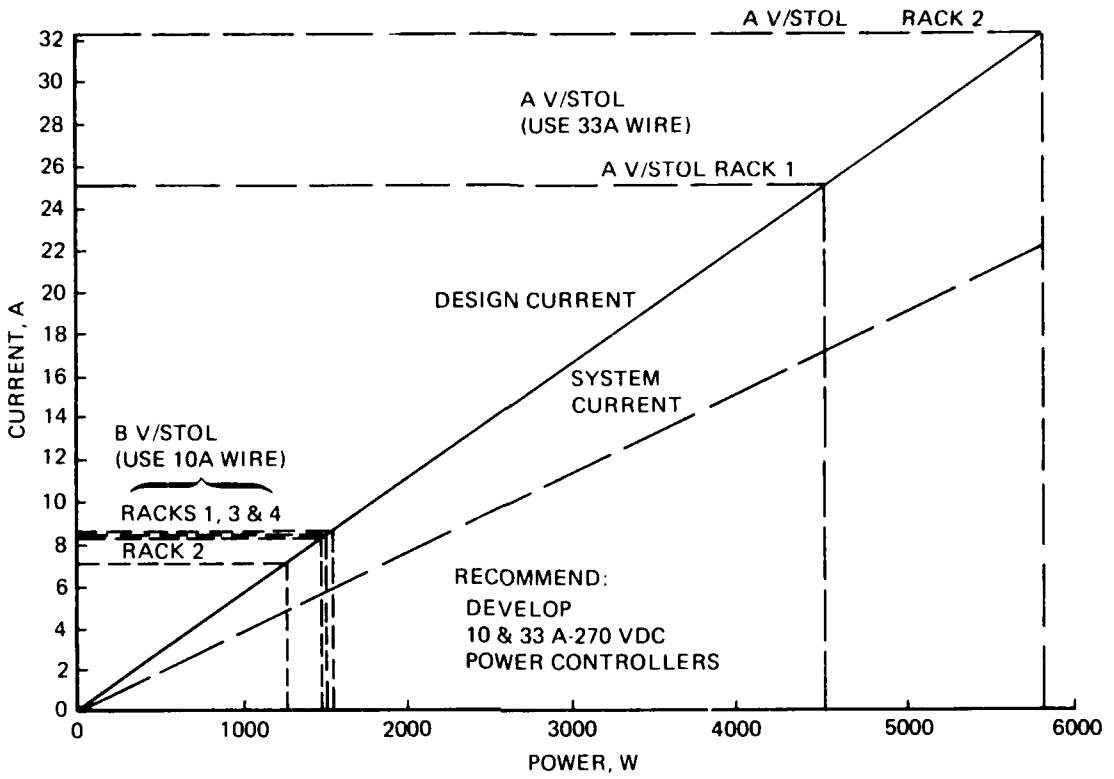

0009-047W

Figure 39 A & B V/STOL Power Requirements for Each Area vs Power Line Current

Table 12 Rack Wire Sizing (@ 30°C Temperature Rise & 20°C Ambient)

RACK AREA	SYSTEM PWR REQMT	COOLING PWR REQMT	TOTAL PWR REQMT	SYSTEM CURRENT	DESIGN CURRENT	RECOMMENDED FLAT WIRE SIZE
A V/STOL						WIDTH x THICKNESS
1	3495	1060	4555	16.9	5.00	0.25 x 0.005
2	4588	1325	5913	21.9	32.85	0.40 x 0.005
B V/STOL						
1	1292	265	1557	6	9	0.30 x 0.0027
2	994	265	1259	5	7.5	0.25 x 0.0027
3	1292	265	1557	6	9	0.30 x 0.0027
4	1259	265	1524	6	9	0.30 x 0.0027

0009-048W

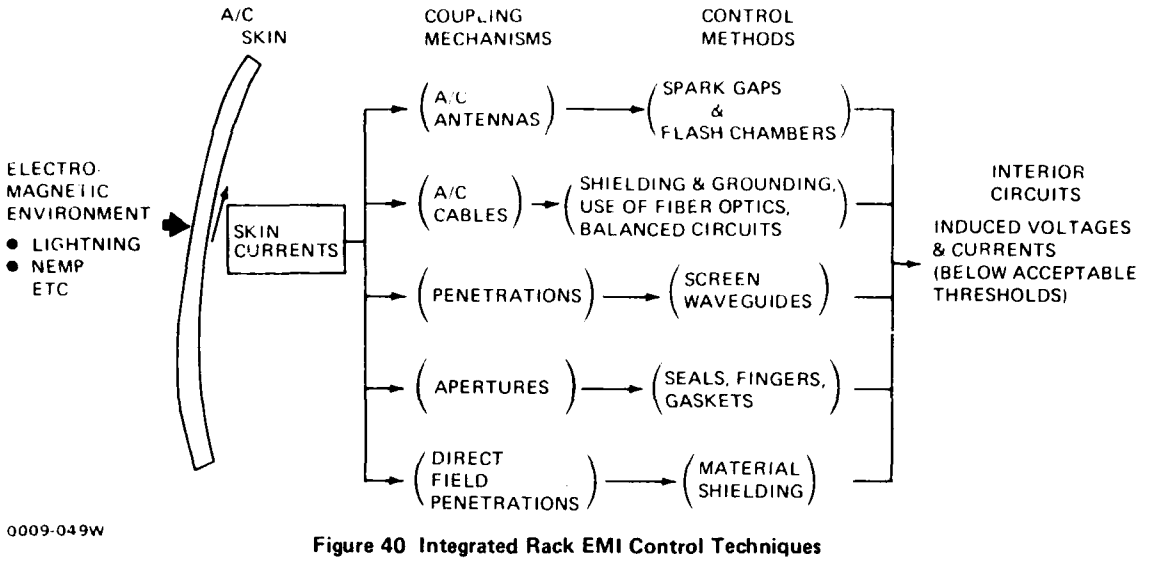

Figure 40 Integrated Rack EMI Control Techniques

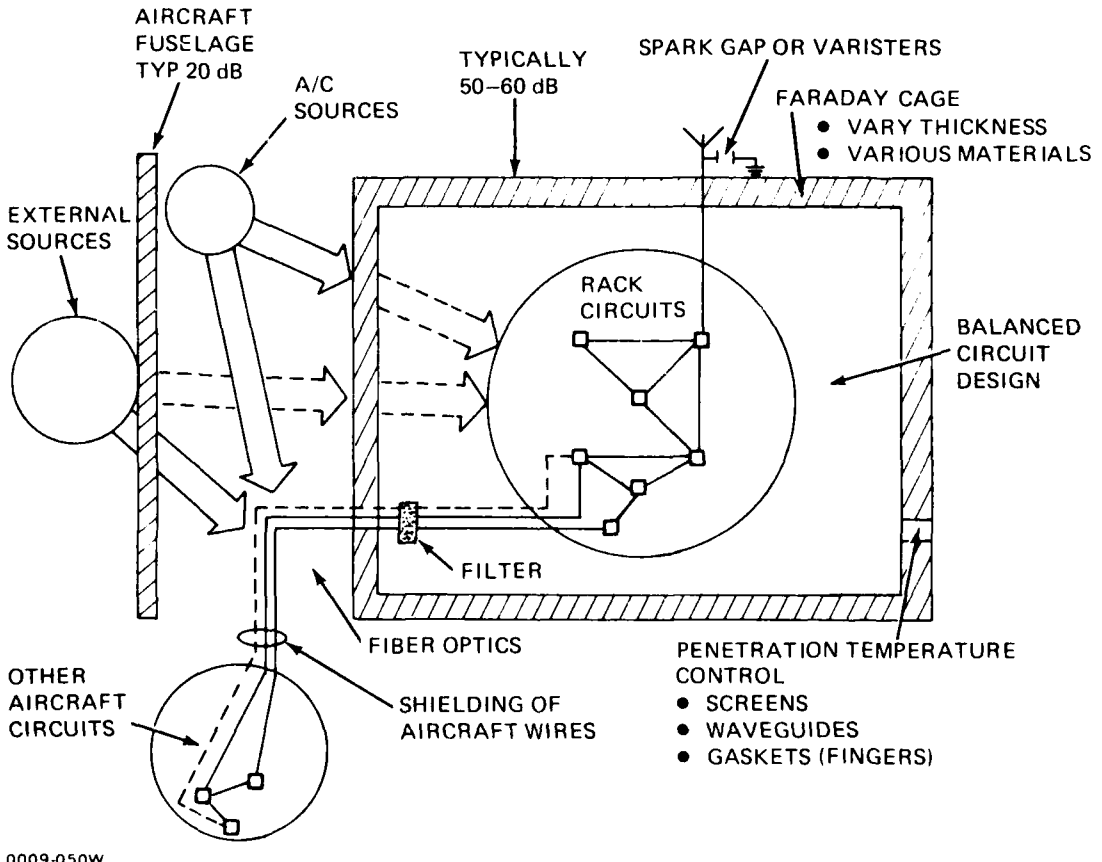

Figure 41 Control Methods

The key to the Grumman integrated rack EMI design is the approach of designing each tray and its associated secondary backplane as an individual Faraday cage.

3.4.1 Faraday Cage Design

The Faraday cage design approach enables the designer to control both radiated and conducted emissions from internal circuits and susceptibility to external interference.

The electromagnetic radiation fields are controlled by:

- Varying the thickness and material of the sides of the Faraday cage
- Controlling circuit loop sizes
- Selecting semiconductor technology with higher upset voltages
- Shielding and controlling the distance between sources and receptors
- Proper aperture design techniques for all seams, openings, etc.

The conduction paths can be controlled by means of:

- Filtering
- Interconnection wire separation and shielding
- Use of fiber optic waveguides which are nonconductive to electric energy.

The Faraday cage controls electromagnetic fields by the mechanisms of absorption and reflection of electromagnetic waves. Equation (1) is used to calulate the absorption loss.

$$A = (3.34)(t)\sqrt{fG\mu} \qquad (1)$$

where

t = thickness of side material in Mils

f = frequency of oscillating field in Hertz

G = conductivity of material relative to copper

μ = permeability of material relative to free space value.

Equation (2) is used to calculate the reflection of Magnetic fields (assuming thick walls and ignoring multiple reflections).

$$R_M = 20 \log \left[0.462/r(\mu/G \times \frac{1}{f})^{0.5} + 0.136\, r(\mu/G \times \frac{1}{f})^{-0.5} + 0.354\right] \qquad (2)$$

where

f, G and μ are as noted above

r = source to shield distance (inches).

NOTE: Equations (1) and (2) from Interference Technology Engineer's Master 1978.

During the study the alternate requirement for lighting was used to determine the effect of a typical lightning strike on a typical circuit within the integrated rack's Faraday cages. Starting with the typical lightning strike (ref. Figure 10, Subsection 2.3.2), an idealized wave form, Figure 42 (SAE Lightning Committee AE-4), was defined for determining indirect effects. Given a 30,000 ampere (peak value) lightning stroke, with a 2μs rise time and 96μs fall time, a Fourier transform of the idealized waveform was obtained. Next, using the absorption and reflection equation (1) and (2), the amplitude versus frequency characteristic on the other side of a 60-mil thick aluminum plate located 1 ft from the source was developed. (This was judged to be similar to an actual field's attenuation from outside to within the rack.) Next, using an inverse Fourier transform, the curve seen in Figure 43 was obtained, which identifies an H (t) inside the rack.

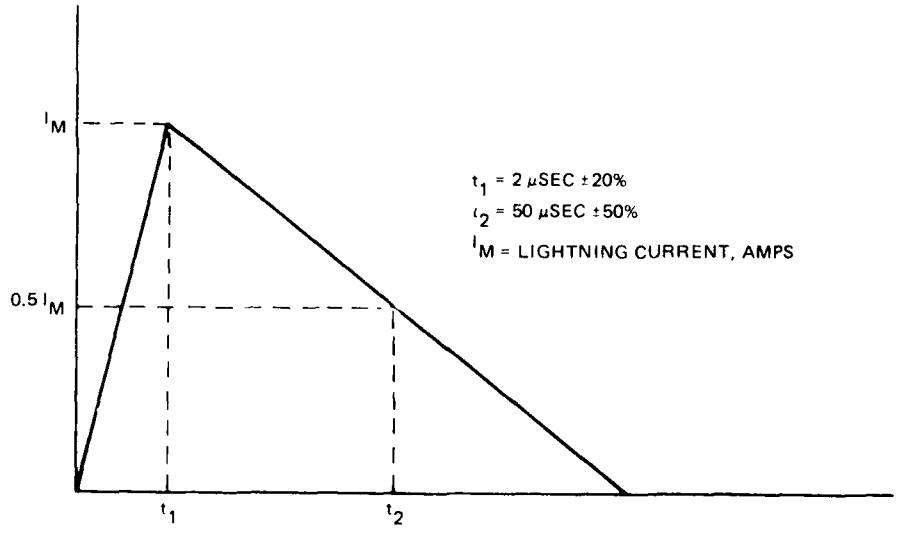

Figure 42 SAE Lightning Test Waveform — Test F — Indirect Effects Evaluation

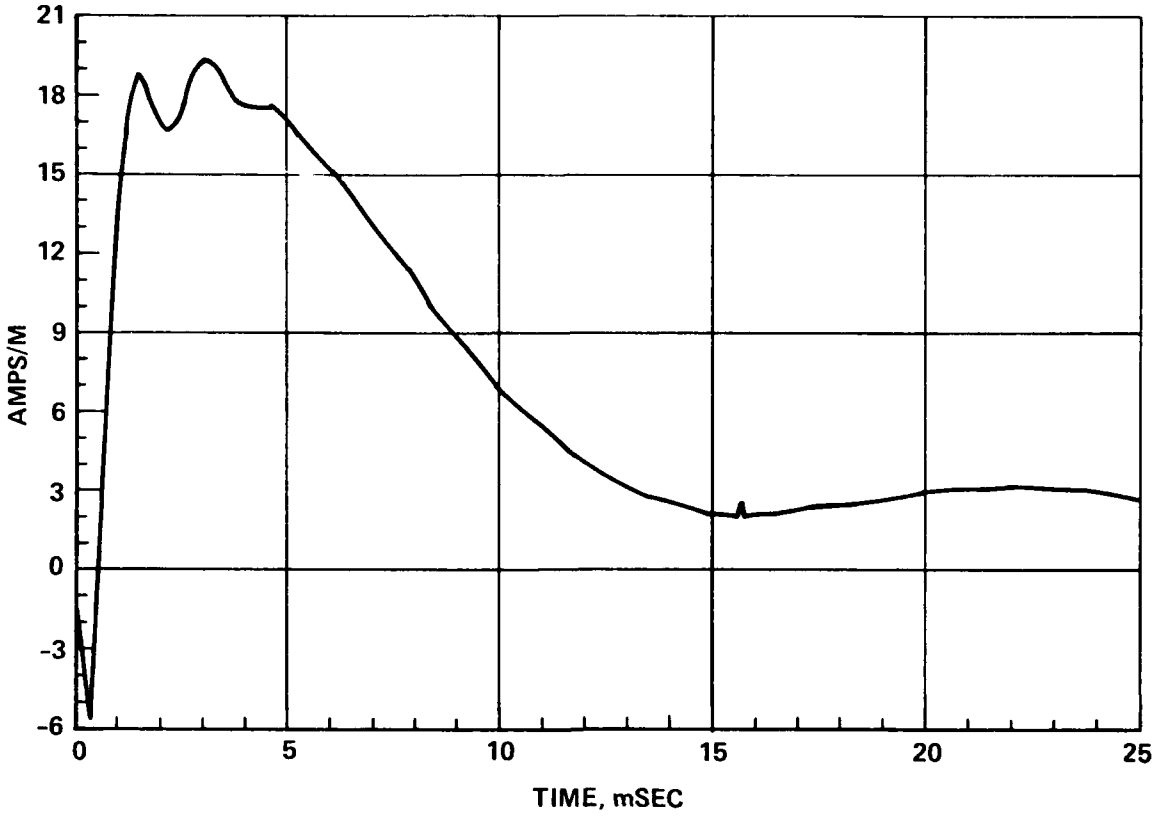

Figure 43 Magnetic Field, H(t) vs Time

A magnetic field's effect on a circuit is a function of the rate of change of field intensity, and of the physical area of the wire loops formed by subsystem circuits. (Multilayer loops must be carefully designed to avoid multiturn multiplying factors.) In a rack, the size of the proposed rack's one square meter loop is the maximum size expected. Naturally, the smaller the loop the less energy coupled into the circuit. The internal changing field causes an unwanted transient voltage in the subsystem circuits. These transient voltages can cause erroneous computations in digital logic circuits, thereby reducing mission effectiveness. The value of allowable upset voltage varies, depending on the type of technology used in the subsystem circuitry. Using Equation (3) and knowing the size of the maximum circuit loops the induced voltage in the circuits is calculated

$$V_{induced} = \frac{d\phi}{dt} = \mu_o A \frac{dH}{dt} n \qquad (3)$$

where

$\mu_o = 12.57 \times 10^{-7}$ H/m

A = area of loop in square meters

n = number of turns in loop

$\frac{dH}{dt} = \frac{\Delta H}{\Delta t}\Big|_{max}$ from resulting H(t)

$$V_I = (12.57 \times 10^{-7})(1)(25 \times 10^3)(1)$$

$$= 31.4 \text{ mV.}$$

This V_I is less than the 100 mV upset voltage. Therefore, the 60 mils of aluminum skin should provide sufficient shielding from a typical lightning strike on the aircraft. (This assumes that amplification from multiple sources doesn't exist.)

The tray-to-tray shielding detailed design can only be addressed when specific circuits are defined using the emission and susceptibility of Mil Std 461/462 (as modified). Likewise, when a complete complement of aircraft on-board sources is defined then the sum total of all field strengths (obtained by superposition) will have to be less than the specified radiated susceptibility values.

The design of apertures and joints, such as door or cover joints, openings for wires, optical fibers, and cooling parts and also corners and seams are important factors in overall shielding effectiveness. As an example, the Faraday cage door with its long, narrow slit gaps provides high loss in shielding effectiveness. However, by means of gasketing, fingers, and door seam designs, the gap length loss can be controlled. For seams, the cost of welding versus the cost of gasketing should be traded during time of detail design (at similar shielding effectiveness values).

Various integrated rack cooling systems were reviewed and all but the air-over-components designs did not cause any openings in the Faraday cages. The air-over-components would require EMI controls such as screening meshes to cut aperture penetration.

The use of fiber optics will eliminate conducted interference coupled to interconnection lines via radiated fields. However, a waveguide (metal sleeving) will be required at each penetration of fiber optics into a Faraday cage. Figure 44 provides values of attentuation in decibels representing attenuation of fields propagating through short waveguides. Use of Mil Std 1553-type of multiplexing of interconnection signals between individual Faraday cages will reduce

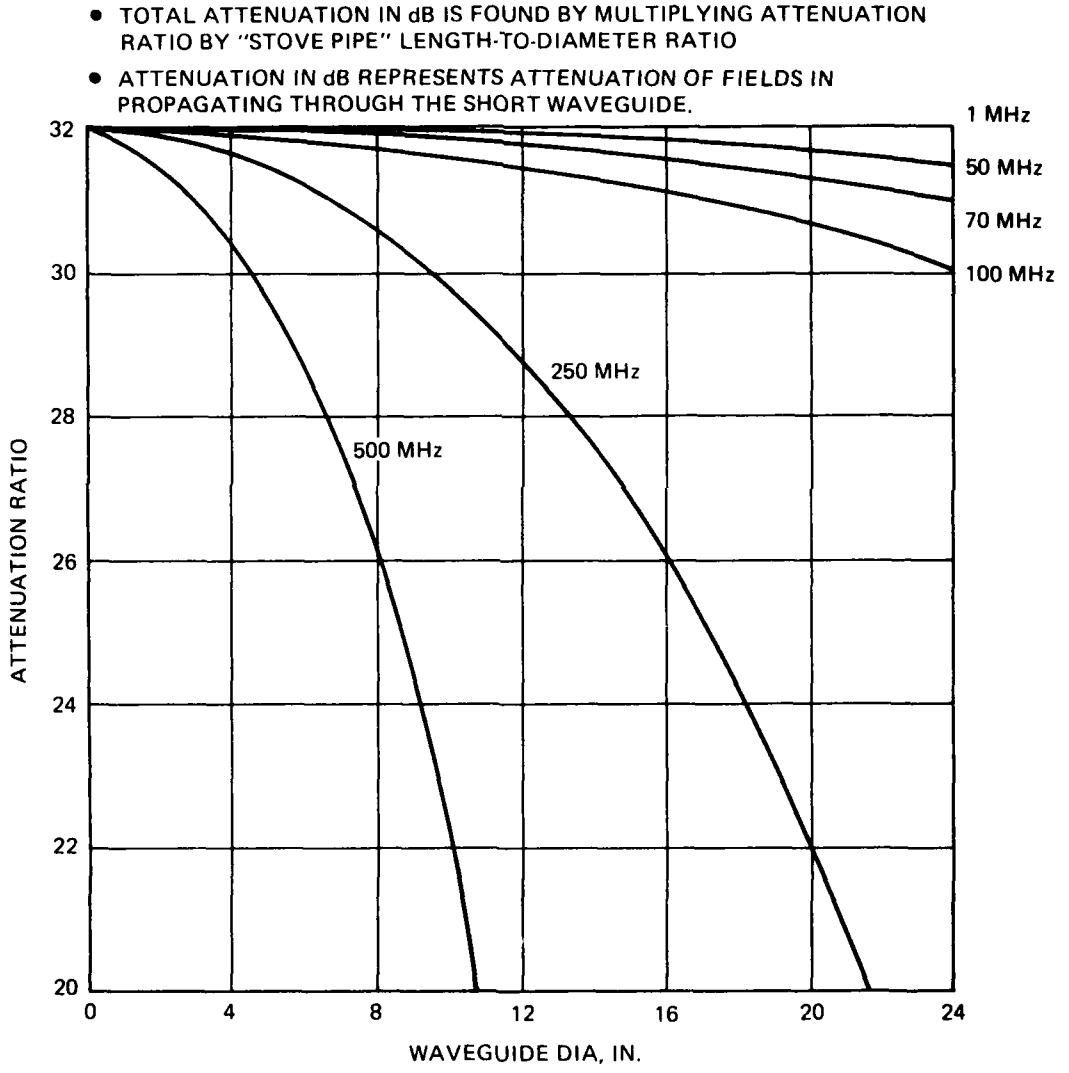

From "Engineering Design Guidelines for EMP Hardening of Naval Missiles and Airplanes" by R.A. Perala, T.F. Ezell, Dec. 1973 – AMRC-R-17

0009-053W

Figure 44 Waveguide Attenuation Ratio at Selected Frequencies vs Waveguide Diameter

the number of conduction paths and thereby ease the conduction control problem. For those interconnections which do not use fiber optics (such as power lines), space has been left for filters to be installed. The only penetration of each tray's Faraday cage is then reduced to the secondary to primary backplane connector. Within each backplane care must be taken during detail to segregate signal lines from power lines. Individual shielding may be required in some backplane wiring. Current use of fiber optics as an EMI control technique is hampered by the current lack of cards with fiber optic connectors (although several vendors are presently introducing card-mounted optical connectors and optical/electrical interface units). Also, the nonavailability of commercial optical backplanes limits the integrated rack's designer to the design and building of his own backplanes. The use of thick 600-μ fibers is expected to ease the design of card-to-motherboard optical fiber connections (see Figure 45).

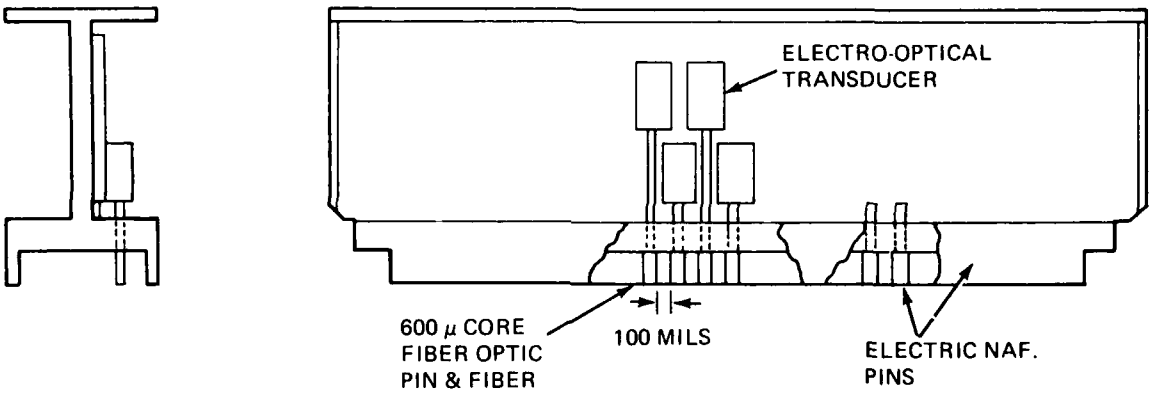

Figure 45 Fiber Optics/Electric Connecting Pins

3.5 THERMAL ANALYSIS

The thermal analysis for the Integrated Rack Concept Study for V/STOL-Type Aircraft was premised on the utilization of ISEM-2A modules in the rack. The basic dimensions of the module used to establish the thermal model is shown in Figure 46.

Since the module is made of aluminum and the thermal conductivity of the aluminum does not vary significantly with temperature, the thermal resistance of the module is essentially constant. In addition, the resistance of the module retainer is also constant for all given configurations. The net result is that the

cumulative thermal resistance between the component junction and the rail heat sink wall is constant.

Figures 47 and 48 illustrate three basic module rack installations for two basic cooling concepts: air over components and conduction cooling.

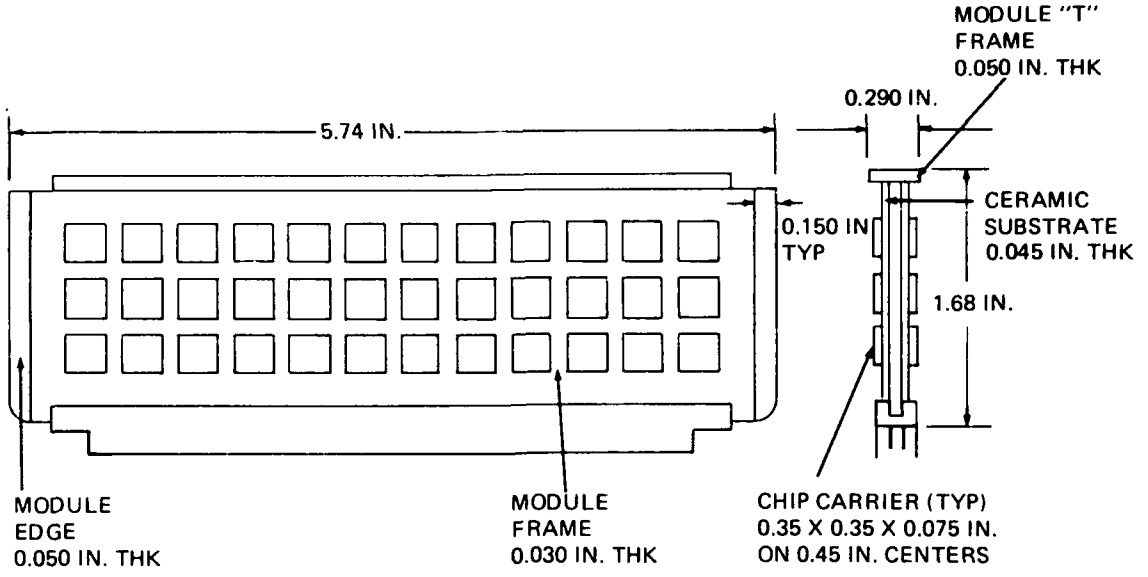

0009-055W

Figure 46 ISEM-2A 36 Chip Carriers per Side

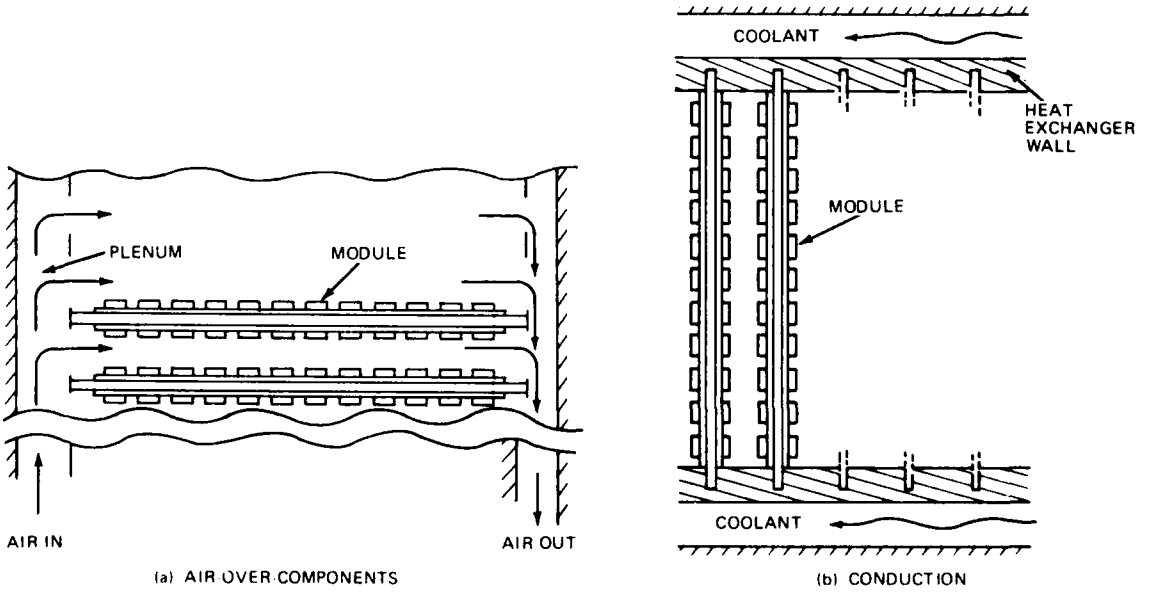

0009-056W

Figure 47 Typical Module Installation

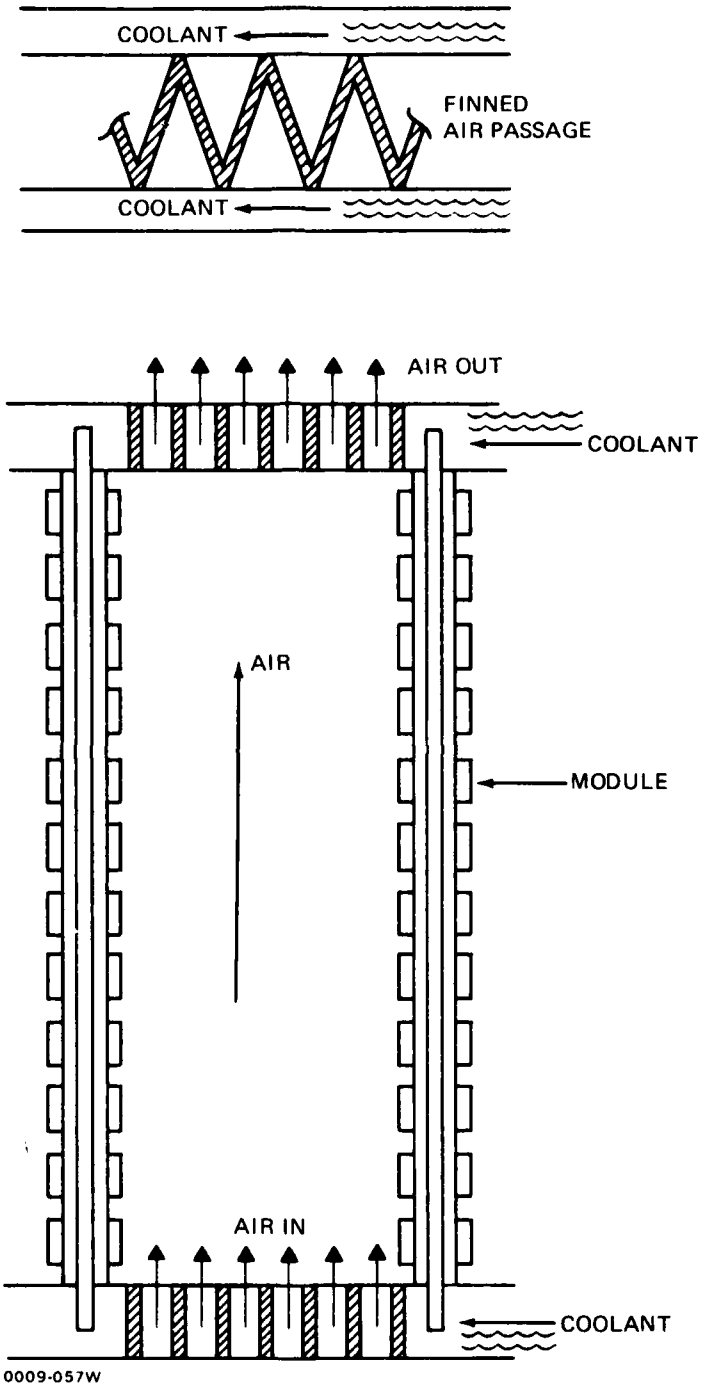

Figure 48 Air Flow for Typical Air-Over-Components Concept

For the conduction cooling concept (Figure 47 (b)), the temperature difference from the heat exchanger wall to the junction of the chip carrier (c.c.) located at the center of the module is strictly a function of the module power dissipation. For the air over component concept (Figures 47 (a) and 48), the thermal path from the junction to an ultimate heat sink has two parallel paths to follow, and can be shown schematically as shown in Figure 49.

The thermal resistance from a component junction to the rail coolant, nodes 1 to 4, is significantly higher than the thermal resistance from a component junction to the airflow over the module, nodes 1 to 6. The thermal resistance from nodes 1 to 6 is a function of the airflow rate between adjacent modules. The resistance is the same for all configurations evaluated.

In order to approach the thermal study in a rational and logical manner, it was assumed that all the components mounted on a module were of the same size, and that the heat dissipated on the module was uniformly distributed amongst 72 chip carriers (36 per side).

3.5.1 Conduction Cooling

Figure 50 reflects the thermal network used for the conduction model. Since the model is symmetrical, only ¼ of the module had to be defined. This model reflects 69 nodal temperatures, and the nodal identification is as follows:

Component Case:	1-3, 7-9, 13-15, 19-21, 25-27, 31-33
Component Junction:	52-69
"T" Frame:	37-42
Module Frame:	4-6, 10-12, 16-18, 22-24, 28-30, 34-36
Module Edge:	43-45
Heat Exchanger Wall:	46-48
Coolant:	49-51

Figure 51 is included to illustrate the physical location of the nodal points on an actual module.

In the case of the conduction module, the thermal resistance between the hottest component (node 54) and the wall of the heat sink (node 48) is fixed, and the temperature rise depends only on the power dissipated. The thermal resis-

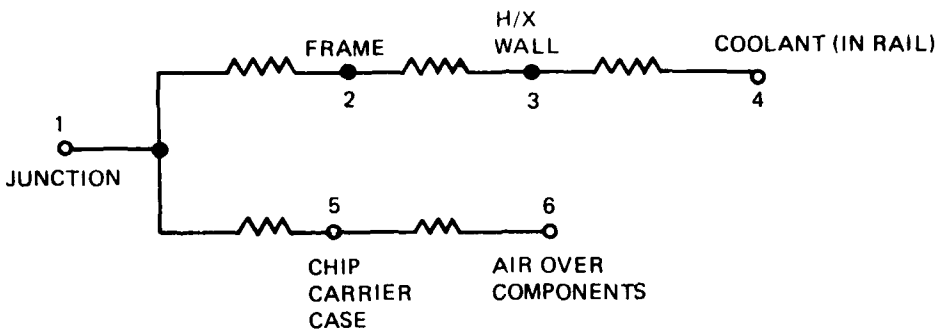

0009-058W

Figure 49 Resistance Network

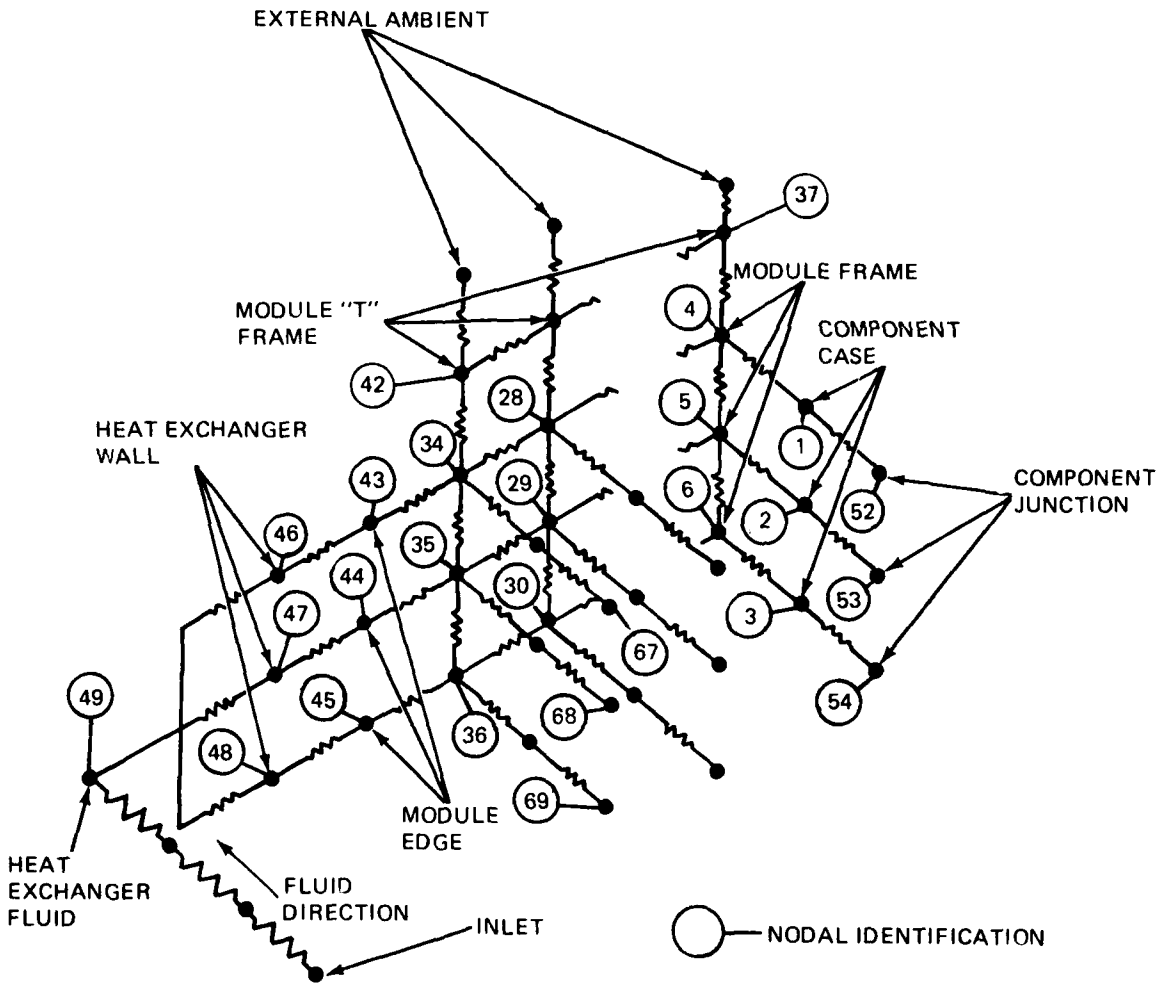

0009-059W

Figure 50 ISEM-2A Typical Conduction Thermal Model

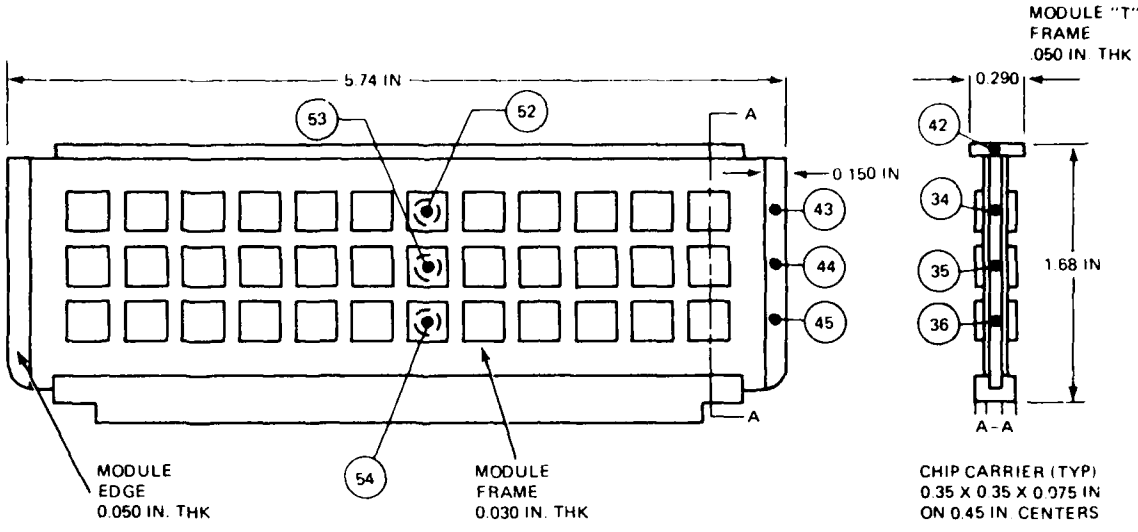

NOTE: NODES 52, 53, 54 ARE JUNCTION NODES FOR CENTERBOARD COMPONENTS

0009-060W

Figure 51 ISEM-2A-NODAL Point Location

tance between those two nodes was 6.89°C/W (based on total module heat dissipation) for a 0.030 in. module frame thickness.

It should be noted at this point that the available module real estate and connector capability result in a module configuration which requires module heat to flow out thru a highly resistive path. On the other hand, if the heat flow were shunted to the "T" frame, the thermal resistance could be reduced for the center component (node 54) from 6.89°C/W to approximately 3.55°C/W. However, obtaining an effective thermal interface with the "T" frame is difficult due to tolerance accumulation.

In addition, for the conduction module configuration, the coolant temperature rise must be taken into consideration. As the coolant passes thru the rail heat exchanger it is absorbing the module heat. Therefore, the coolant temperature at the last module in a tier is higher than it was for the first module, since this system is effectively a series arrangement. Figure 52 illustrates this point.

3.5.2 Air Over Components

Figure 53 represents the thermal model used for the air over components concept. This model is also symmetrical, however, half of the module must be utilized to maintain the symmetry created with the airflow pattern. This network

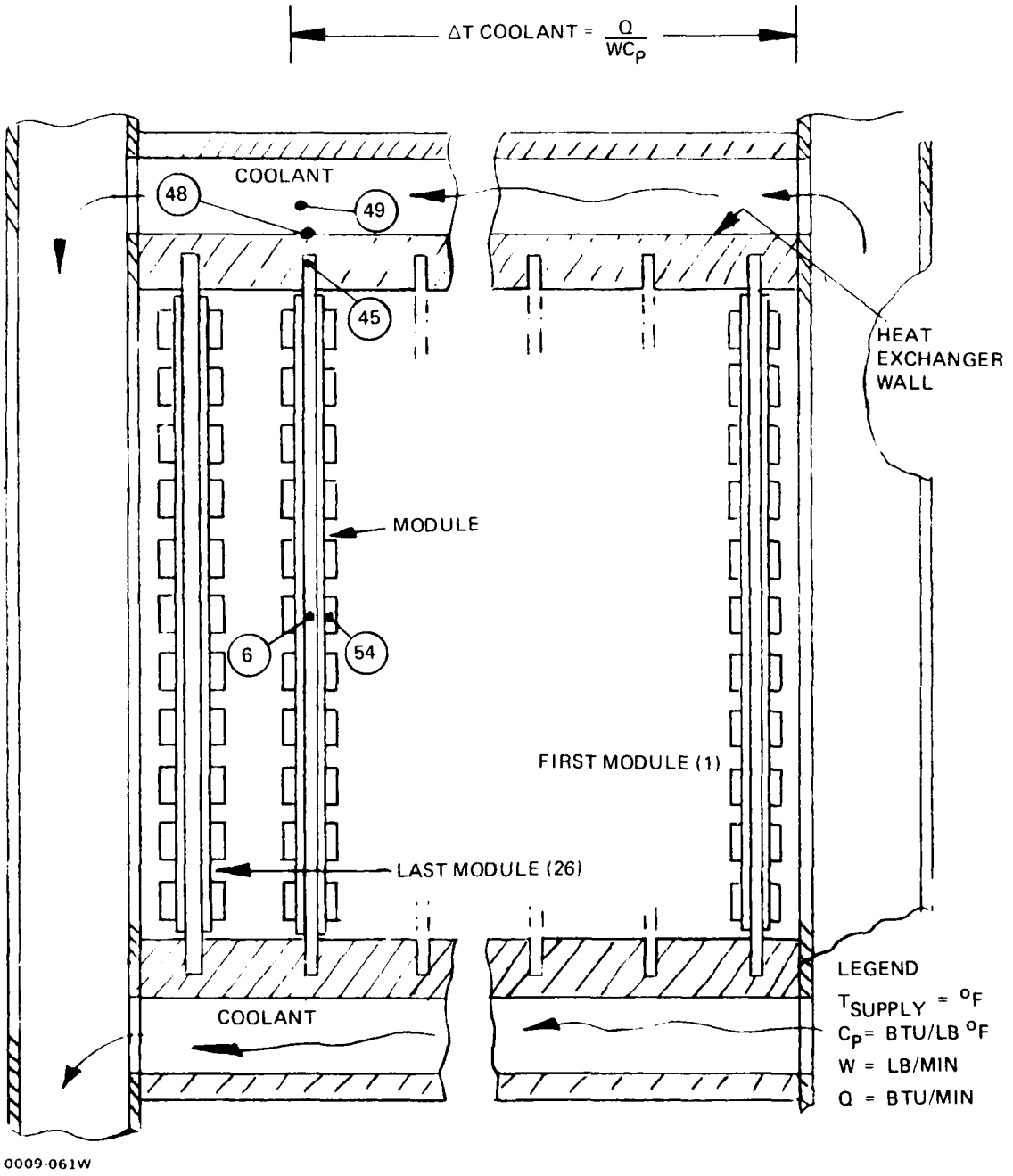

Figure 52 Typical Conduction Installation, Candidate B

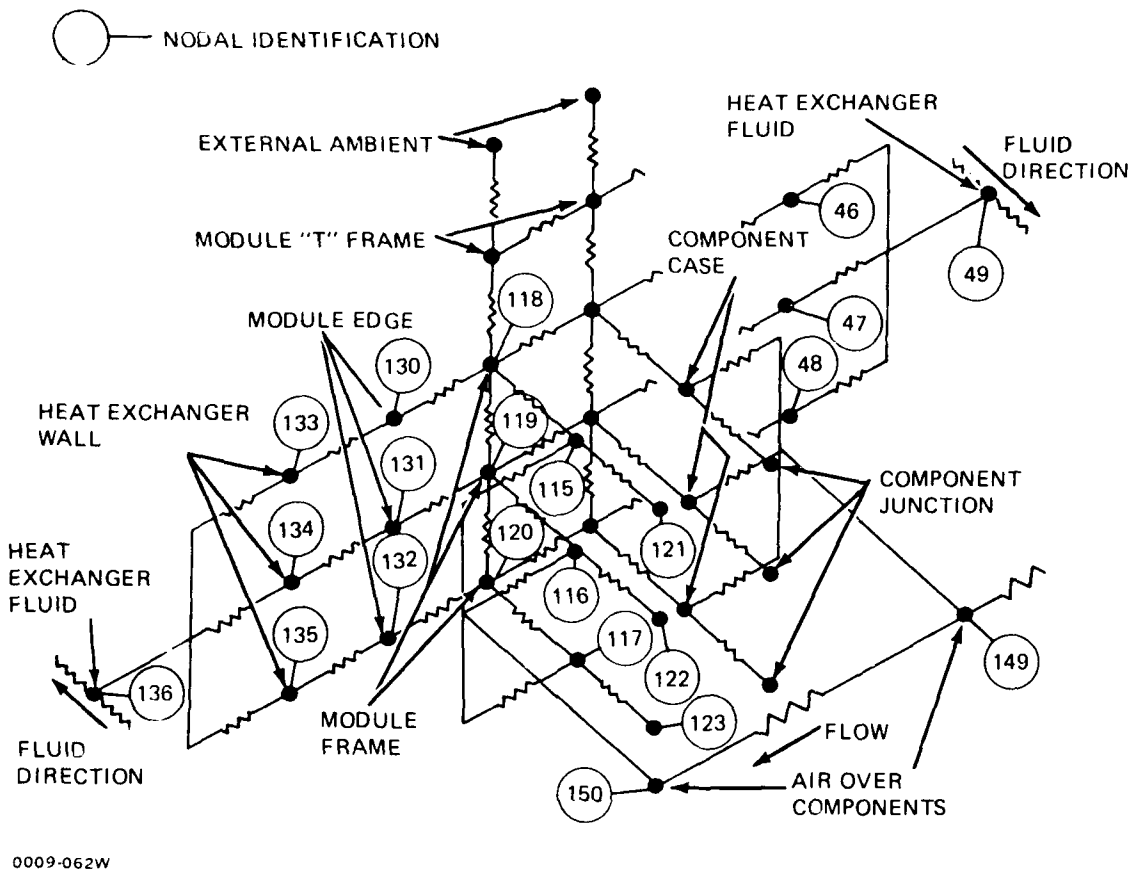

Figure 53 ISEM-2A Air-Over-Components Thermal Model

contains 150 nodal temperatures, and the nodal identification is as follows:

Component Case:	1-3, 7-9, 13-15, 19-21, 25-27, 31-33, 70-72, 79-81, 88-90, 97-99, 106-108, 115-117
Component Junction:	52-69, 76-78, 85-87, 94-96, 103-105, 112-114, 121-123
"T" Frame:	37-42, 124-129
Module Frame:	4-6, 10-12, 16-18, 22-24, 28-30, 73-75, 82-84, 91-93, 100-102, 109-111, 118-120
Module Edge:	43-45, 130-132
Heat Exchanger Wall:	46-48, 133-135
Coolant:	49 & 136
Air Over Component:	
Inlet:	203 (inlet boundary node-constant temperature)
Air Nodes:	139-150

The conduction effect is still present in this model; however, the thermal resistance between the component junction and the heat sink is shunted by the airflow over the component. The thermal resistance for this model is primarily a function of the mass flow rate between the modules.

In order to correlate the analytical thermal model to an actual physical system, Figures 54 and 55 are presented to correlate the model with physical locations.

3.5.3 Surface Conductance Between Heat Exchanger Wall & Coolant

For the conduction module the thermal resistance of the module/interface/heat exchanger wall is constant. The only thermal resistance that is subject to variation is the resistance between the heat exchanger wall and the coolant. This resistance is primarily a function of two major parameters; the coolant mass flow rate, and the core of the heat exchanger thru which the coolant is flowing.

Independent of the exact design details, it was mandatory to define the variation in the heat exchanger wall temperature as a function of thermal conductance (reciprocal of thermal resistance). Figure 56 illustrates that variation.

In Figure 56, we can clearly see the effect of the conductance between the heat exchanger wall and the coolant on the heat exchanger wall temperature. This change is directly translated to the junction temperature of the chip carrier (c.c.) which is located at the center of the board in the conduction model.

From a practical point of view, if we could design a rail heat exchanger with a conductance of 3 Btu/hr°F/module we would be designing a system that could tolerate some variation of flow rate without a catastrophic impact on junction temperature. Since it was necessary to establish design criteria so that a point design could be developed, it was assumed that it would be possible to achieve a conductance of 3 Btu/hr/°F/module. In doing this, it was recognized that this assumption had to be iterated for a point design.

It is now possible to qualitatively compare the thermal characteristics of the ISEM-2A module integrated in a rack for two cooling concepts, conduction and air over components, as a function of module power and coolant supply temperature.

AD-A081 864 GRUMMAN AEROSPACE CORP BETHPAGE NY F/G 1/3
INTEGRATED RACK CONCEPT STUDY FOR V/STOL TYPE AIRCRAFT.(U)
JAN 80 E V RAMIREZ, B BORGENSON, A CASERTA N62269-78-R-0294
UNCLASSIFIED NADC-78-11360 NL

2 OF 3
AD
A081 864

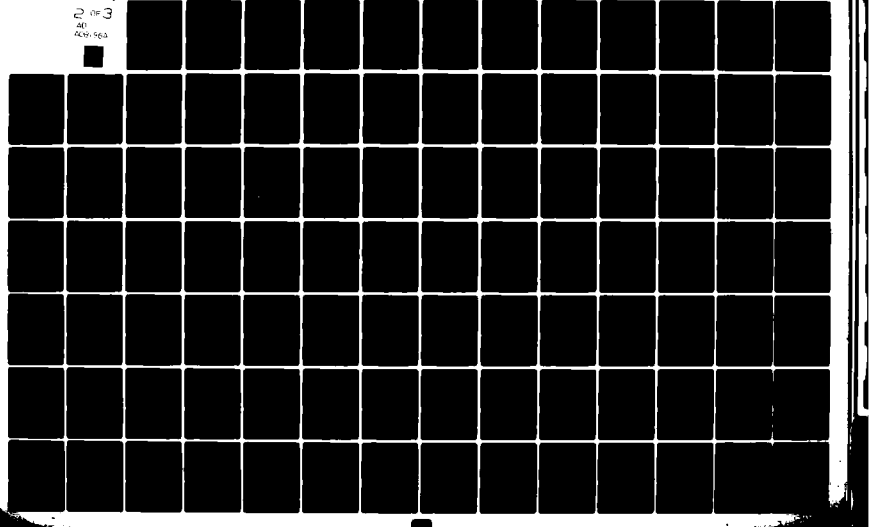

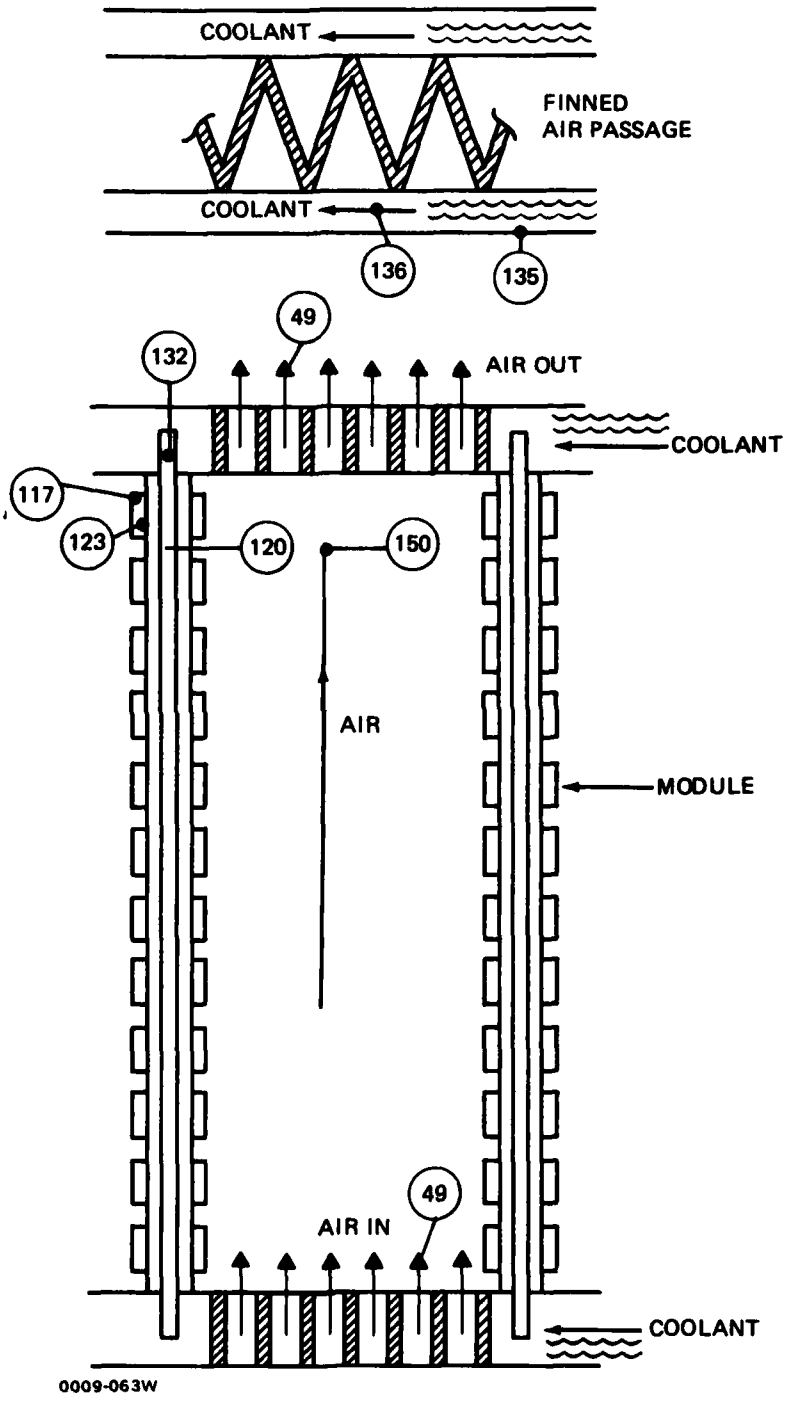

Figure 54 Typical Component Location for Air-Over-Components Concept

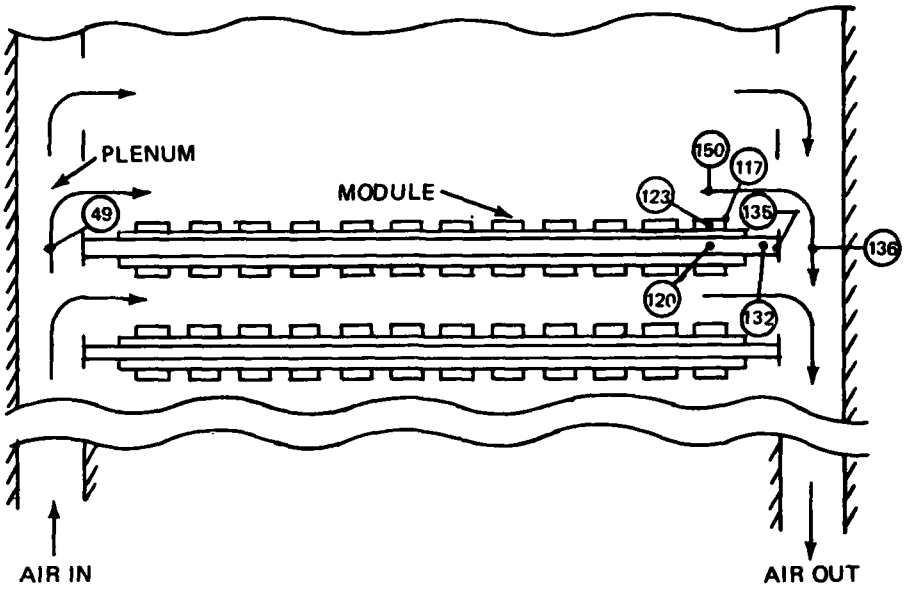

0009-064W

Figure 55 Typical Airflow for Air-Over-Components, Candidate C

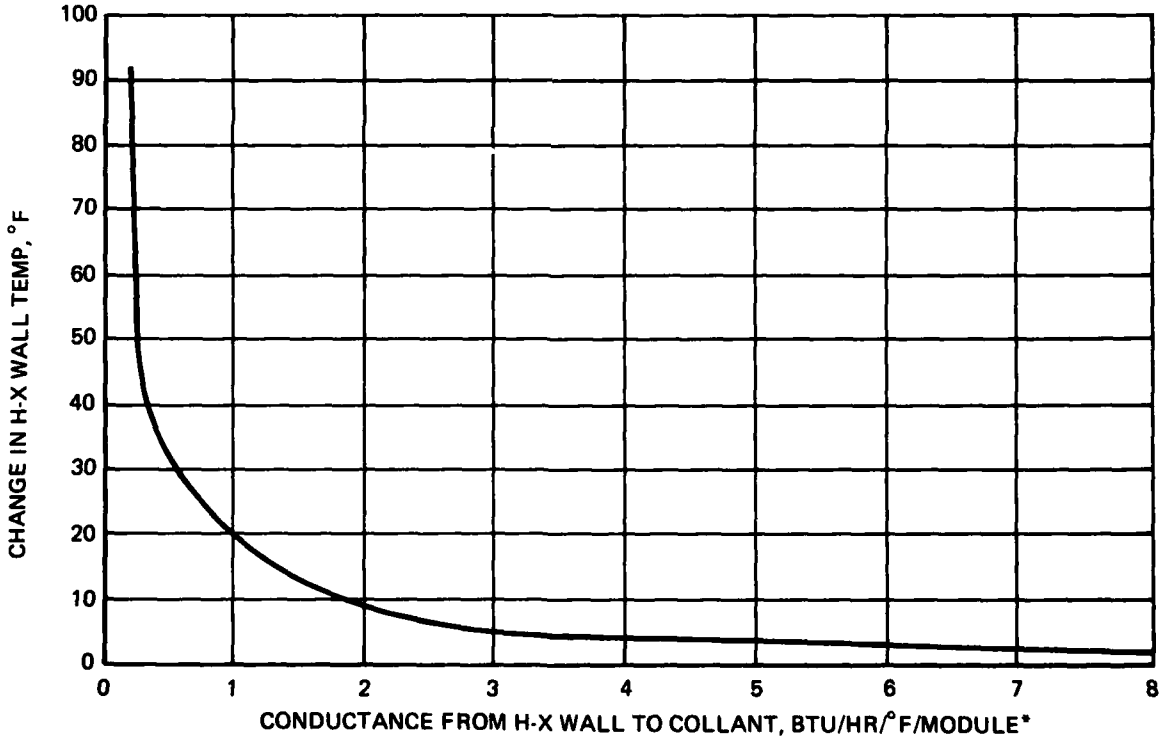

*BASED ON 20 WATTS/MODULE

0009-065W

Figure 56 Heat Exchanger Wall Temperature vs Overall Conductance to Fluid

3.5.4 ISEM-2A Cooling Requirements

Figure 57 thru 60 represent a composite summary of the thermal characteristics of the ISEM-2A module for two modes of cooling conduction and air over components as a function of module power and coolant supply temperature at the inlet to the rail heat exchanger. The plots cover a range of power dissipation from 5 to 20 watts per module. At each power level, module maximum junction temperatures in the range of 60°C to 125°C is shown as a function of coolant supply temperature and coolant flow rate at inlet to the rail heat exchanger. For the conduction module, it was assumed that the coolant in the rail heat exchanger was air. It is recognized that the coolant could be something other than air such, as Coolanol-25 or a heatpipe. For a point design this will be evaluated in Subsection 3.5.5, and the net effect on ECS airflow rate per KW will be defined as a function of ECS supply temperature for each rack cooling concept.

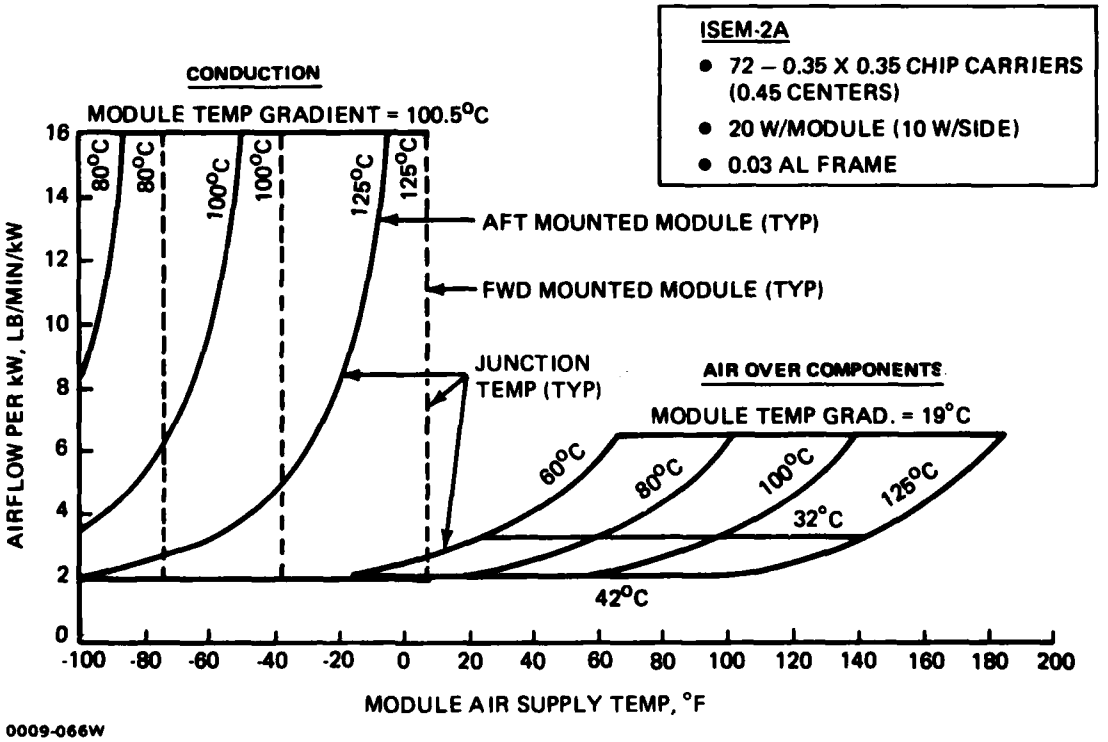

Figure 57 ISEM-2A Cooling Requirements, 20 W/Module

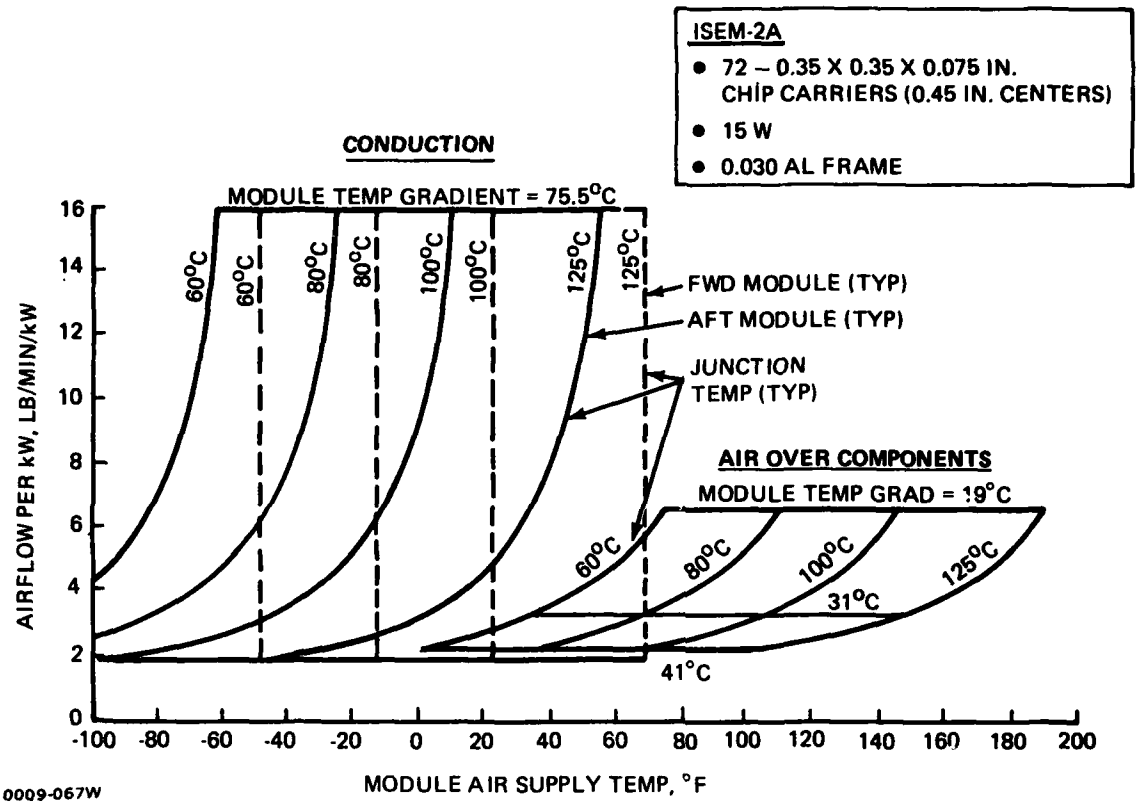

Figure 58 ISEM-2A Cooling Requirements, 15 W/Module

In addressing the results in Figures 57 through 60, there are two key factors to observe: module temperature gradient, and the required coolant supply temperature for a specific component junction temperature at a given airflow rate.

Temperature gradient is defined as the temperature difference between the hottest and coldest points on the module frame. For the conduction model it would be node 6 minus node 45 and for the air-over-components model it would be node 120 minus node 45.

In reviewing these parameters, it must be remembered that at this point these parameters do not reflect a system point design, and can only be treated in a qualitative fashion. For the air over component design approach, the module temperature gradient is a function of the airflow rate. For the range of airflows

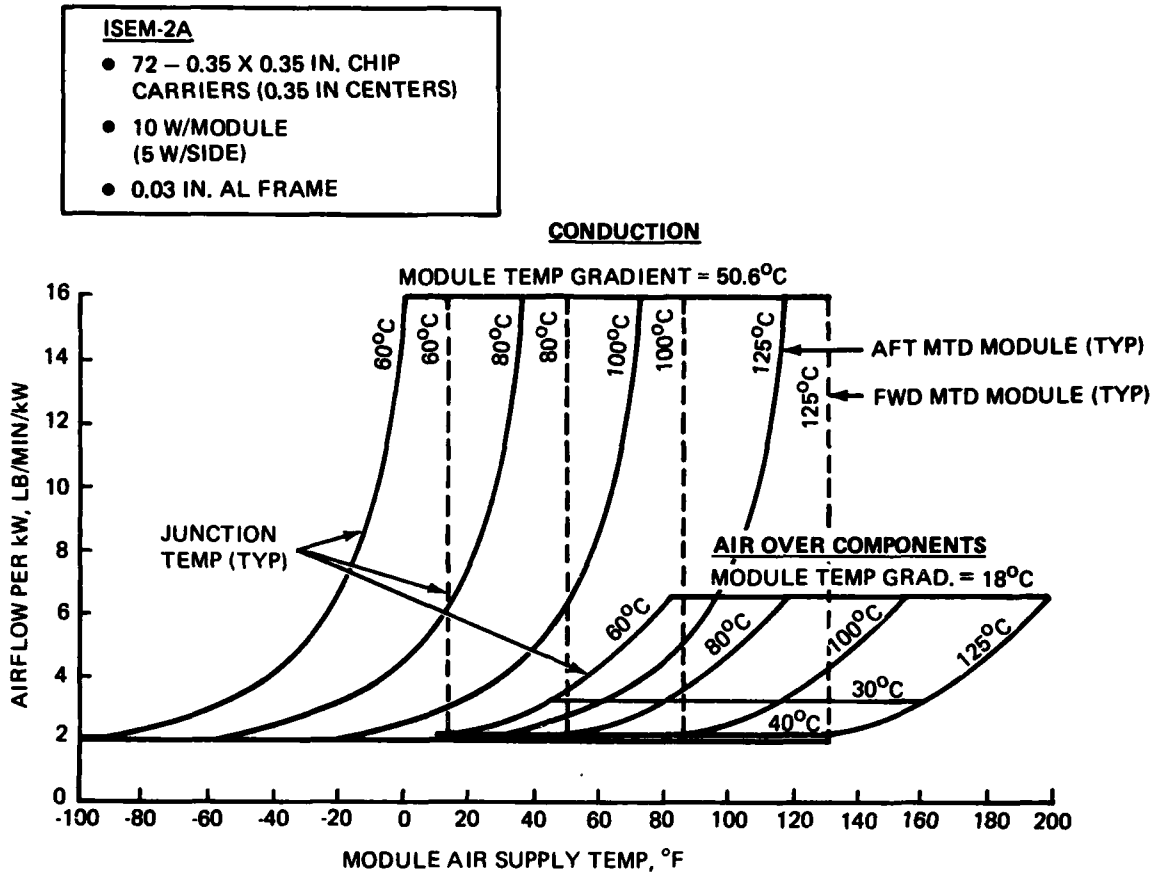

Figure 59 ISEM-2A Cooling Requirements, 10 W/Module

considered, the module temperature gradient varies between 19°C and 42°C, regardless of the total module power.

It is apparent that the airflow supply temperature for the air over component concept does not vary significantly for the increase of the module power from 5 to 20 watts.

With regard to the air over components concept, the only deceptive point brought out in a point design is sizing the fan to be compatible with the system desired.

For the conduction module, since the thermal resistance is essentially constant the module temperature gradient is a function of module power, and varies from 100.5°C for a 20 watt module to 24.6°C for a 5 watt module.

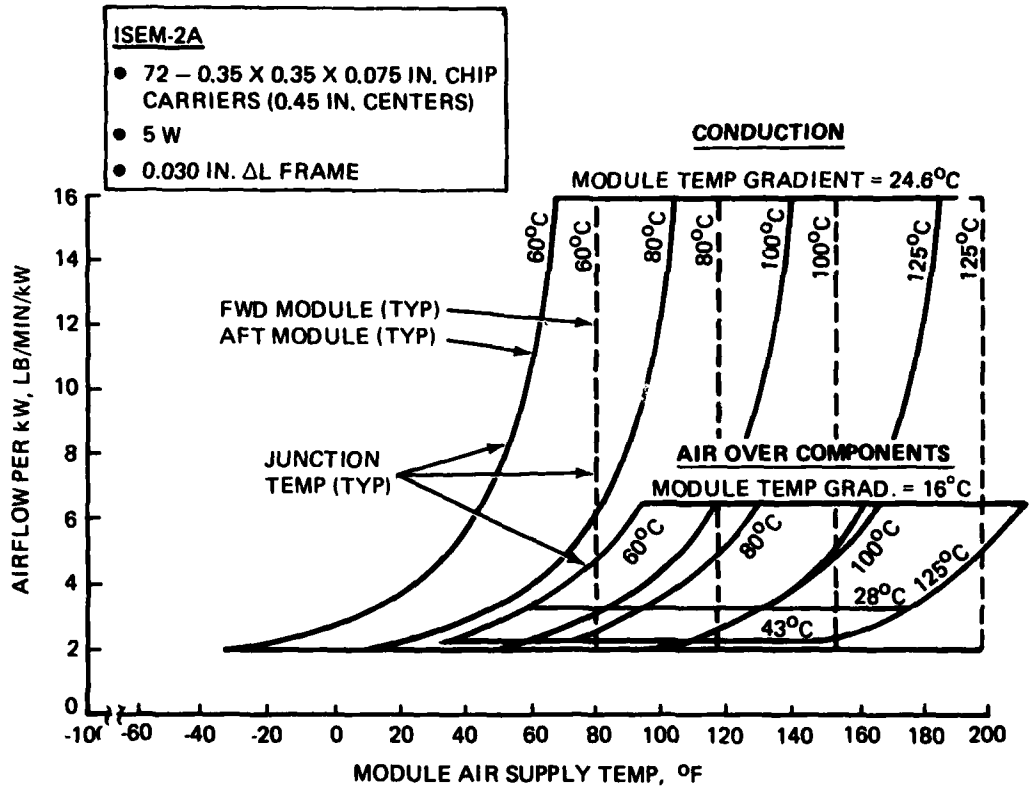

Figure 60 ISEM-2A Cooling Requirements, 5 W/Module

As the module power varies from 20 to 5 watts, you pass through two extremes. At 20 watts you cannot build an ECS to satisfy the conduction cooling requirements and at 5 watts you can build a system that can be competitive and possibly cheaper than the air over components. It is apparent in Figures 57 through 60 that both the air over component and conduction cooling concepts for an ISEM-2A module are feasible for the same ECS requirements when the module power is limited to 5 watts of heat dissipation.

3.5.5 Integrated Rack Point Design

As a result of the avionic equipment partitioning for A and B type V/STOL aircraft, it was concluded that the ISEM-2A module nominal power requirement would be 5 watts except for the core board design (10 watts). Based on that definition, four integrated rack rail cooling concepts were evaluated (air rail, liquid rail, heatpipe rail and core board) for each configuration.

Based on the power requirements of the module, an integrated rack/ECS system was designed for each concept. The purpose of this was to relate the average module junction temperature to an ECS interface requirement of flow rate and supply temperature.

3.5.5.1 Air Rail - In the air guide rail concept, the ISEM-2A modules are cooled by conduction. The rail consists of the internal cooling passages and the external module guides in one integral unit. The internal passages have been provided with a double layer of fins to improve the heat transfer between the flowing air and the wall of the rail. In this configuration, the air in the rail is entirely isolated from the modules. As such, the rail can be fed conditioned ECS cooling air directly, without concern for module contamination by entrained moisture or other possible bleed air contaminants. Figures 61 and 62 reflect maximum junction temperature as a function of ECS airflow and air supply temperature. For the conduction module, the difference between module maximum junction temperature and module average junction temperature is a function of the module heat dissipation. This variation is given for the ISEM-2A module in Figure 63.

Since we are concerned with a specific rack configuration (26 modules per tier), for discussion it is convenient to relate ECS requirements to the average junction temperatures in a tier. Figure 64 provides that interpretation for the air rail configuration.

3.5.5.2 Liquid Rail - For the liquid rail concept, two heat exchangers are involved in the system cooling concept. The first is a liquid rail heat exchanger used to cool the modules in the rack, and the second is a liquid/air heat exchanger that interfaces with the ECS conditioned air. The rail liquid heat exchanger was optimized with a liquid flow rate of 15.4 lb/min/kW. This resulted in an 8°F (4.5°C) liquid temperature rise in the rail heat exchanger.

The impact of integrating the liquid system with the ECS interface is defined in Figure 65, and the average junction temperature profile as a function of ECS flow rate and supply temperature is presented in Figure 66.

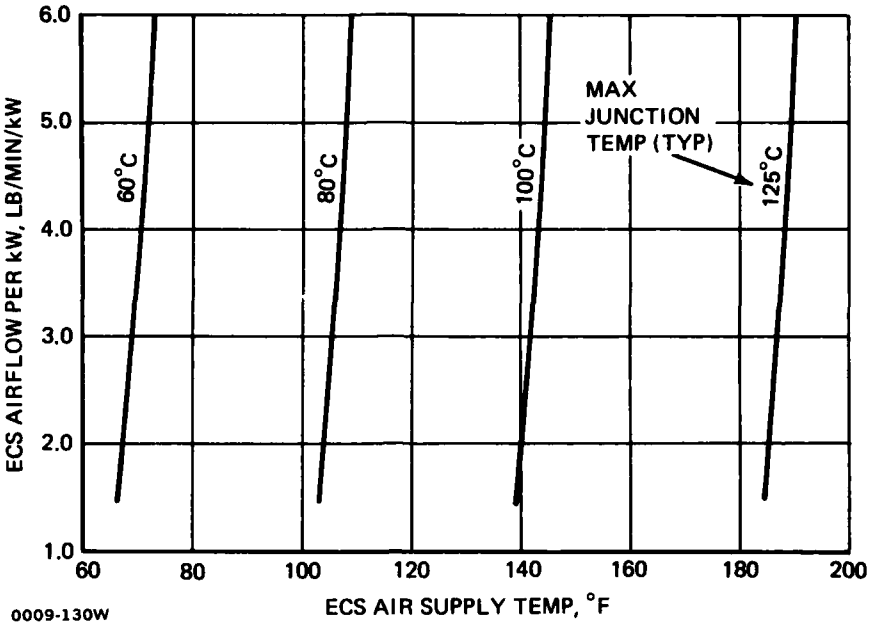

Figure 61 Five Watt Conduction Module With An Air Rail, Forward Module

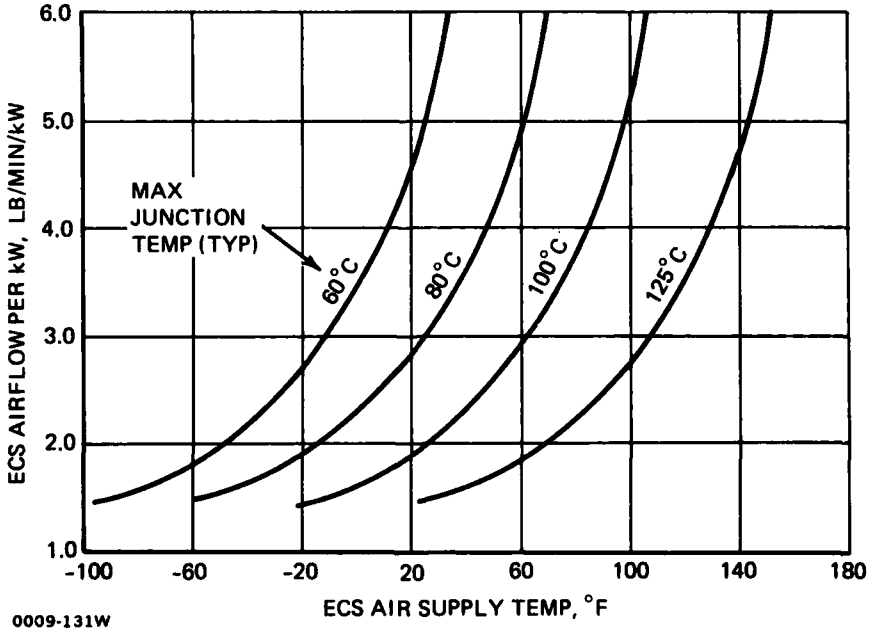

Figure 62 Five Watt Conduction Module with an Air Rail, Aft Module

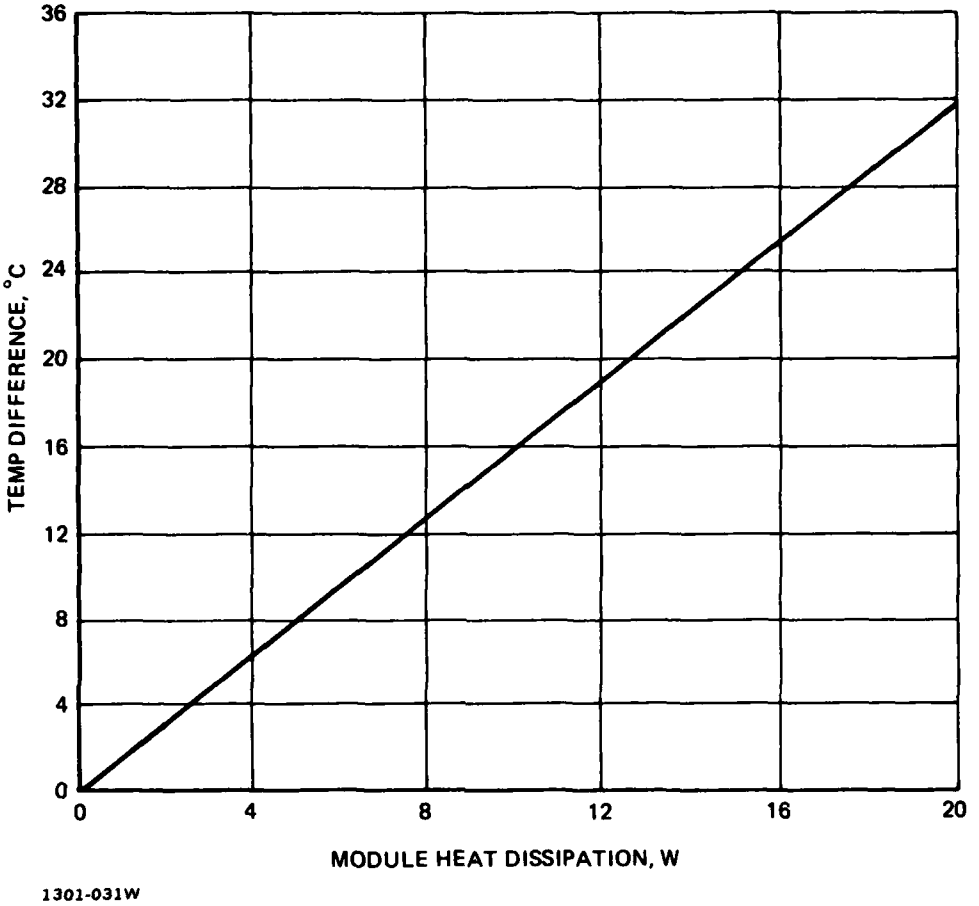

Figure 63 Maximum Junction Temperature minus Average Junction Temperature

3.5.5.3 Air Over Components -

Heat Transfer Model

The third cooling scheme to be considered a viable candidate for fulfilling the rack cooling requirement is the air over component scheme. In order to understand this concept and relate the system requirements back to the ECS, refer to the diagram given in Figure 67.

In this approach, the liquid rail heat exchanger is used to remove the heat from the fan air. All the liquid is returned to the Liquid/ECS air heat exchanger, where the heat transported by liquid is removed by the ECS air.

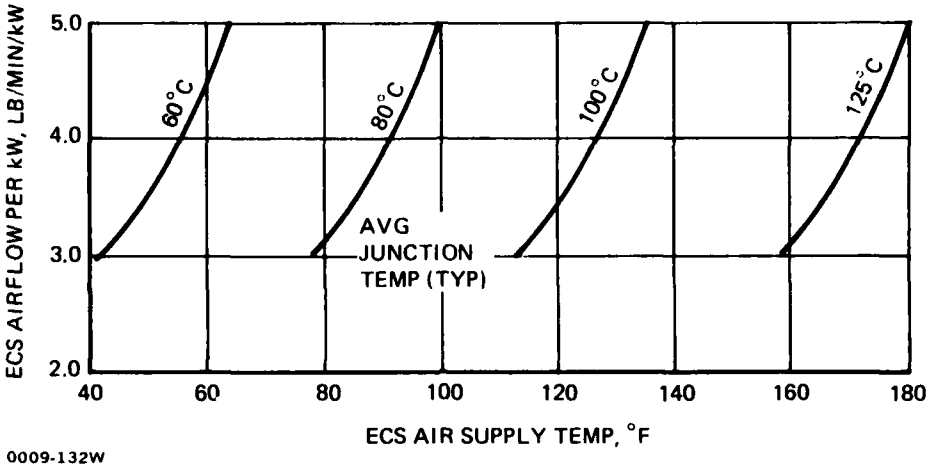

Figure 64 ISEM-2A Cooling Requirements, Conduction to Air Rail, 5 W/Module

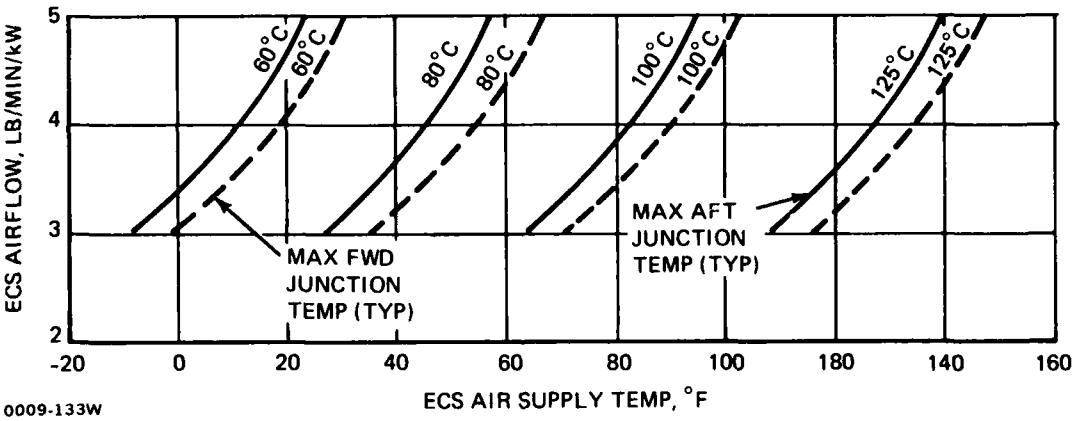

Figure 65 ISEM-2A Cooling Requirements, Conduction to Liquid Rail, 5w/Module

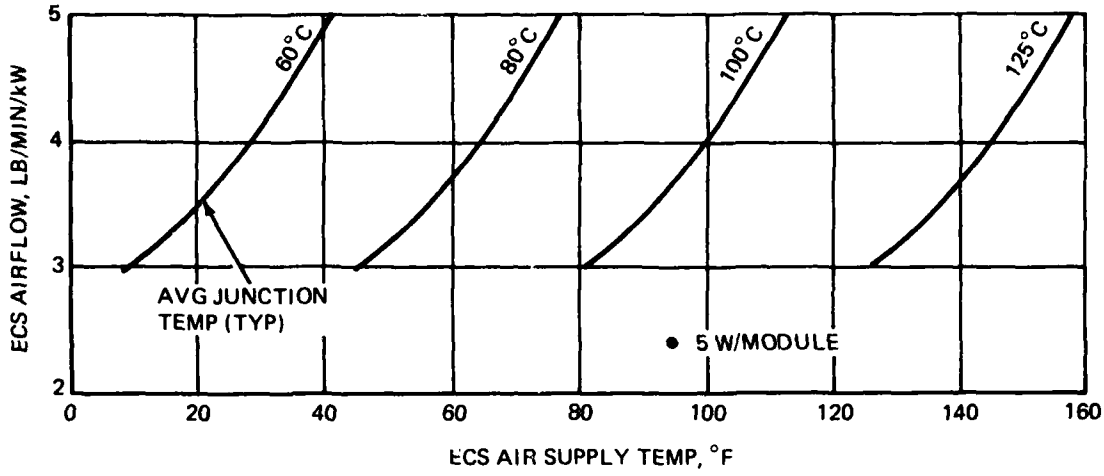

0028-134W

Figure 66 ISEM-2A Cooling Requirements, Conduction to Liquid Rail 5w/Module

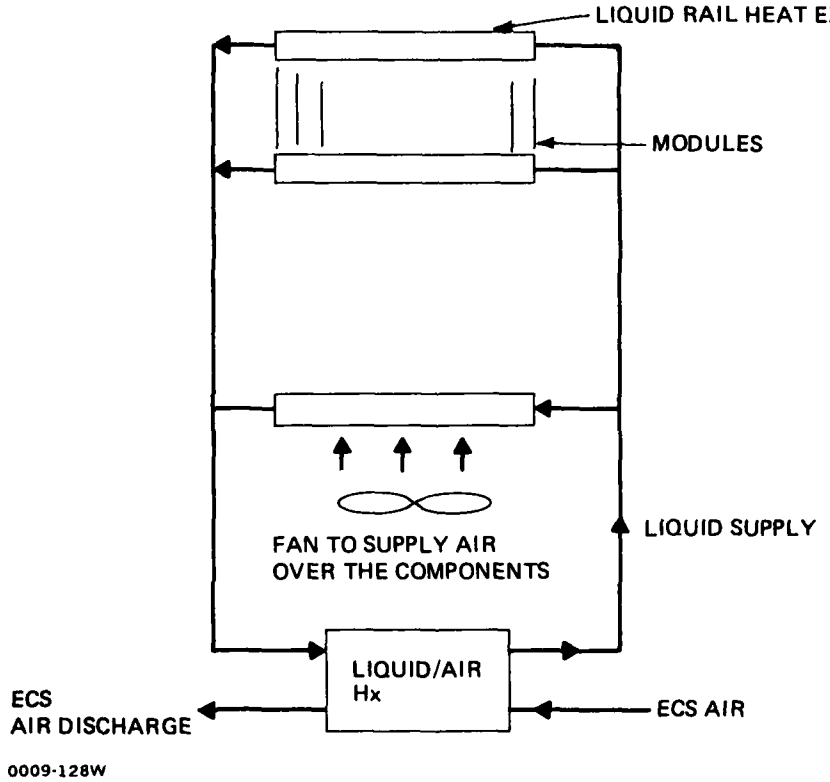

0009-128W

Figure 67 Air-Over-Components, Heat Transfer Diagram

Figure 68 describes the ECS airflow requirement as a function of the ECS supply temperature for various maximum junction temperatures.

The optimized rail heat exchanger liquid flow rate is 15.4 lb/min/kW. Since the average temperature is again desired, the variation of the average junction temperature from the maximum junction temperature is given as a function of the airflow over the components (Figure 69).

Utilizing the design curves defined in Figure 60 for a 5 watt module with air over components, and the results of Figure 68 and 69, the average component junction temperature as a function of ECS airflow rate and supply temperature is presented in Figure 70.

Pressure Drop

In order to properly select a fan for this cooling concept, the module pressure drop had to be defined. Figure 71 defines the analytical pressure drop characteristic for the ISEM-2A module on a 0.300 pitch, and the construction is defined in Figure 40.

This pressure drop, coupled with the airside pressure drop for the heat exchanger rail and maximum rack height, provides the total pressure drop requirement for the rack fan. This aspect of the design is described in more detail in the ECS section of this report.

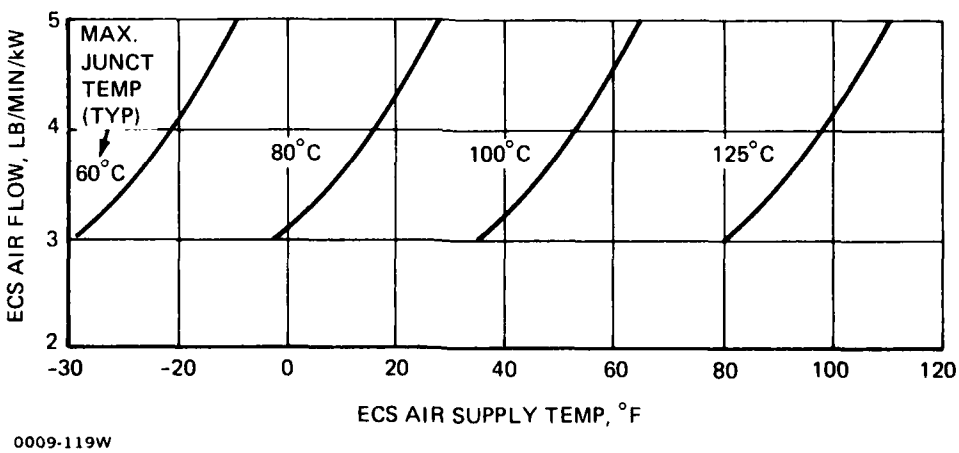

Figure 68 ISEM-2A Cooling Requirements, Air-Over-Components, Maximum Junction Temperature 5 W/Module

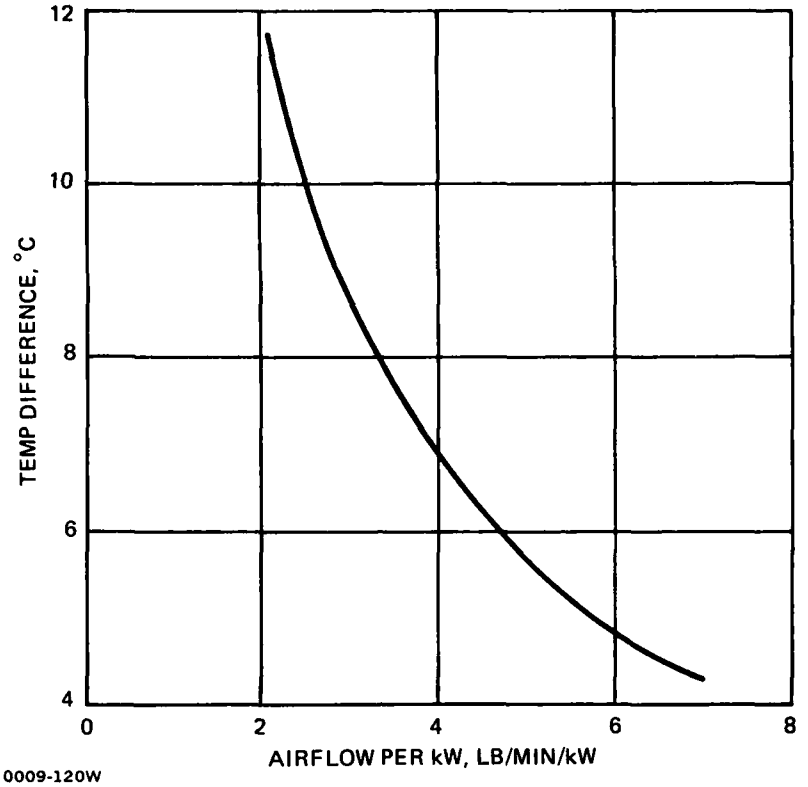

Figure 69 Air-Over-Components Maximum Junction Temperature minus Average Junction Temperature

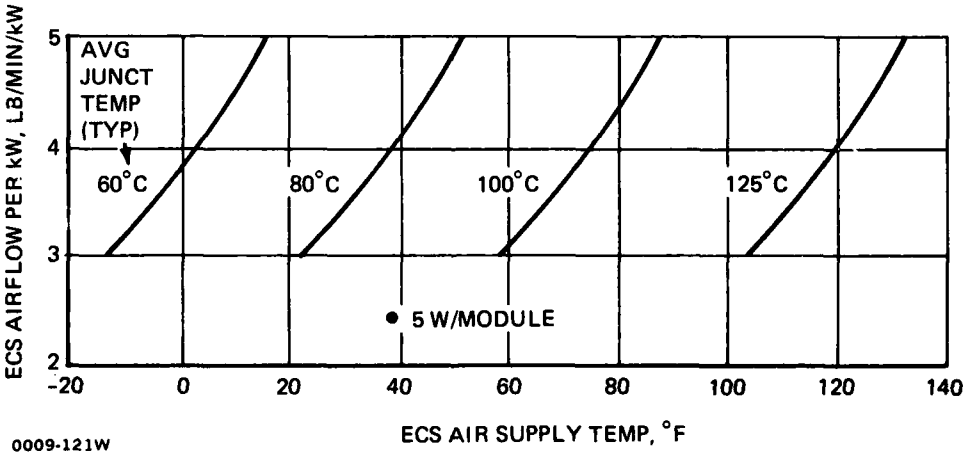

Figure 70 ISEM-2A Cooling Requirements, Air-Over-Components

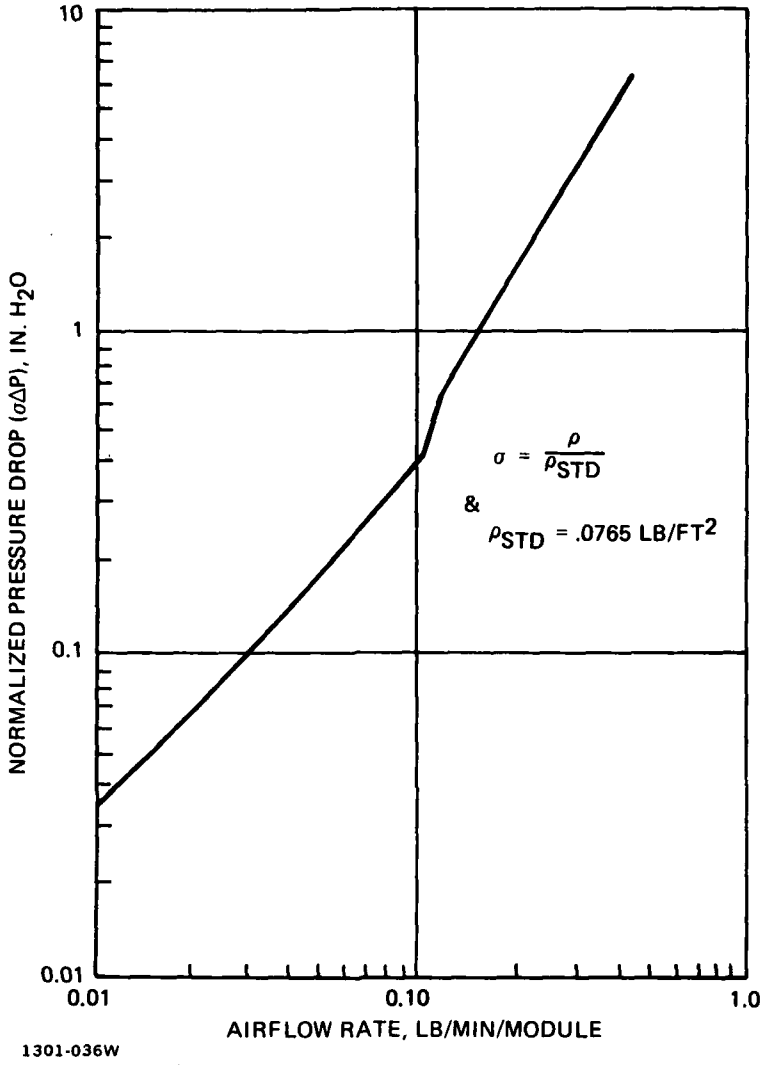

Figure 71 ISEM-2A Module Pressure Drop Without Rails

3.5.5.4 Heatpipe Rail - Another guide rail cooling concept was evaluated for the rack. This approach necessitated that the rail be used as an evaporator, and that the condenser be designed external to the rail. Since space provisions would not permit parallel cooling of the condensers, a series system had to be utilized. Figure 72 shows that the ECS penalty for a given junction temperature is more severe with this approach than for any of the other schemes previously described. As a result, it was eliminated.

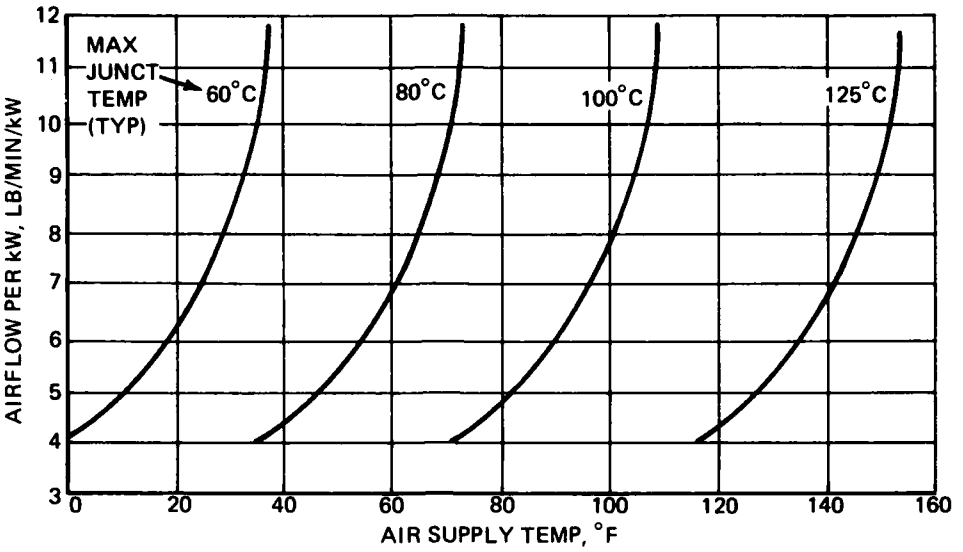

0009-074W

Figure 72 Conduction Module With Heatpipe Rail

3.5.5.5 ISEM-2A Core Board Thermal Analysis - The results of the thermal analysis performed for the core board configuration (Figure 29) is presented in Figures 73 through 76, for power ranging from 5 to 20 watts. The figures represent the variation of air flow vs supply temperature. These results are predicated by utilizing an off-the-shelf fin configuration in the core. The thermal and pressure drop characteristics are presented in Figure 77. In order to make a valid evaluation with previously presented designs, Table 13 compares the conduction air rail and liquid air rail concepts for 10 watt module designs to the core board design.

From a thermal point of view, the results presented in Table 13 are very revealing. When the attainable component junction temperatures for the air rail, liquid rail, and core board concepts are compared, it can be concluded that:

- The core board concept can reduce maximum junction temperatures from 20 to 35°C for the ECS flow range and supply the selected temperature range
- The core board concept provides a more uniform temperature profile on the module when compared to the other two concepts. This point can be qualified as shown in Table 14.

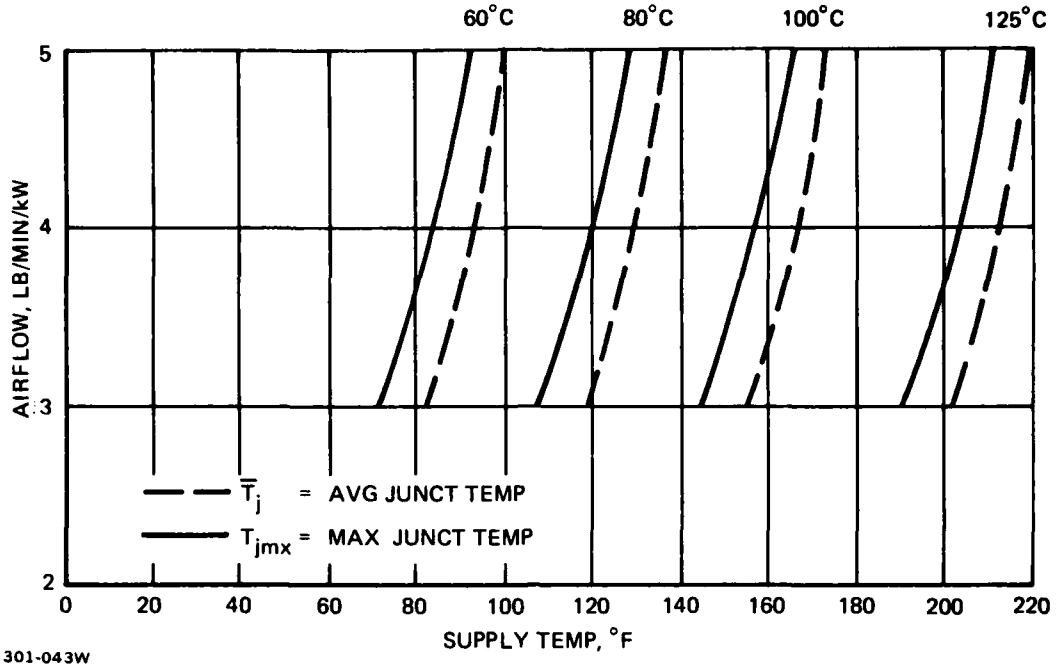

Figure 73 Core Board, 5 W/Module

Qualitatively speaking, the more uniform the module temperature distribution, the more reliable the module will be. However, to quantify that improvement would require testing. The one factor that must be emphasized with the core board design is that it definitely indicates that ISEM-2A modules can be designed with maximum power levels of 20 watts.

We know that designing a 20W conduction module with an air rail sink requires an ECS supply temperature of -40°F (See Figure 57) for a 125°C maximum junction temperature at an airflow rate of 3 lb/min/kW. This would indicate that it is impossible to design that system, whereas with the core board concept, the ECS supply temperature can be 147°F for the same maximum junction temperature.

3.6 ENVIRONMENTAL CONTROL SYSTEMS

This portion of the study addressed the Environmental Control System (ECS) required in Integrated Avionic Racks to provide ISEM-2A module cooling. The three distinct modes of cooling, air over components, conduction, and hollow core modules, each required different rack designs with unique ECS components. Two rack designs were considered for the air-over-components concept, A21

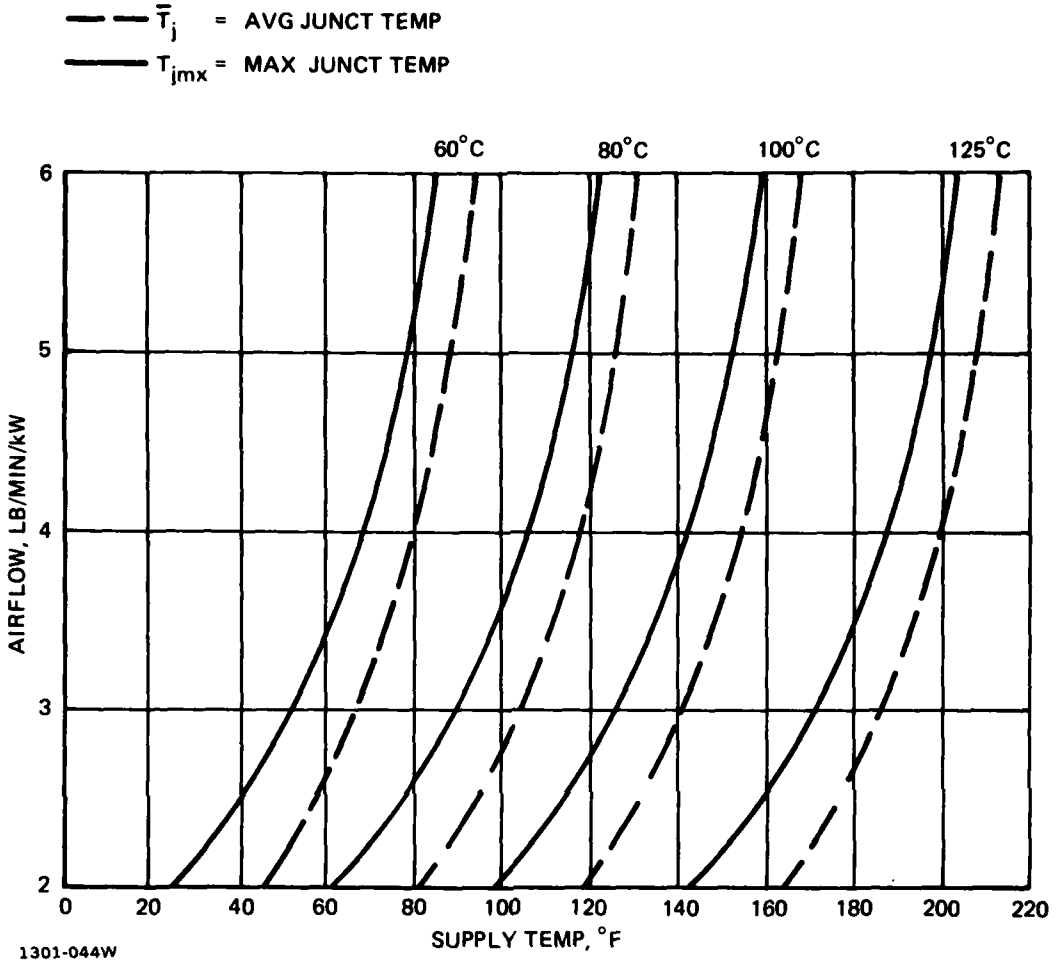

Figure 74 Core Board, 10 W/Module

and C. The conduction concept also considered two different designs, B31 and B32. A single design, D, was studied for the hollow core module cooling concept.

It was considered beyond the scope of this study to investigate the various V/STOL aircraft ECS systems which would ultimately become the heat sinks for rack avionics. In this effort, where rack performance was the single topic of investigation, a fixed input of aircraft cooling air was considered for all the rack designs. The performance of each rack has been presented in terms of ISEM-2A module maximum and average component junction temperature, based on the aircraft ECS providing 3 to 5 lb/min/kW of cooling air over a temperature range of 40° to 80°F.

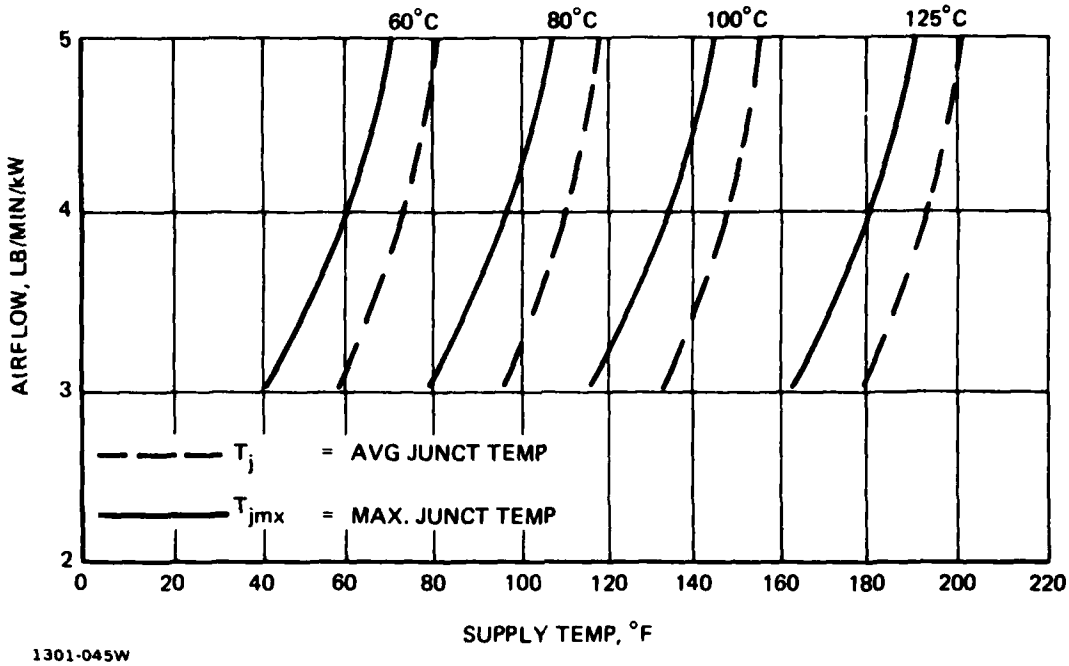

1301-045W

Figure 75 Core Board, 15 W/Module

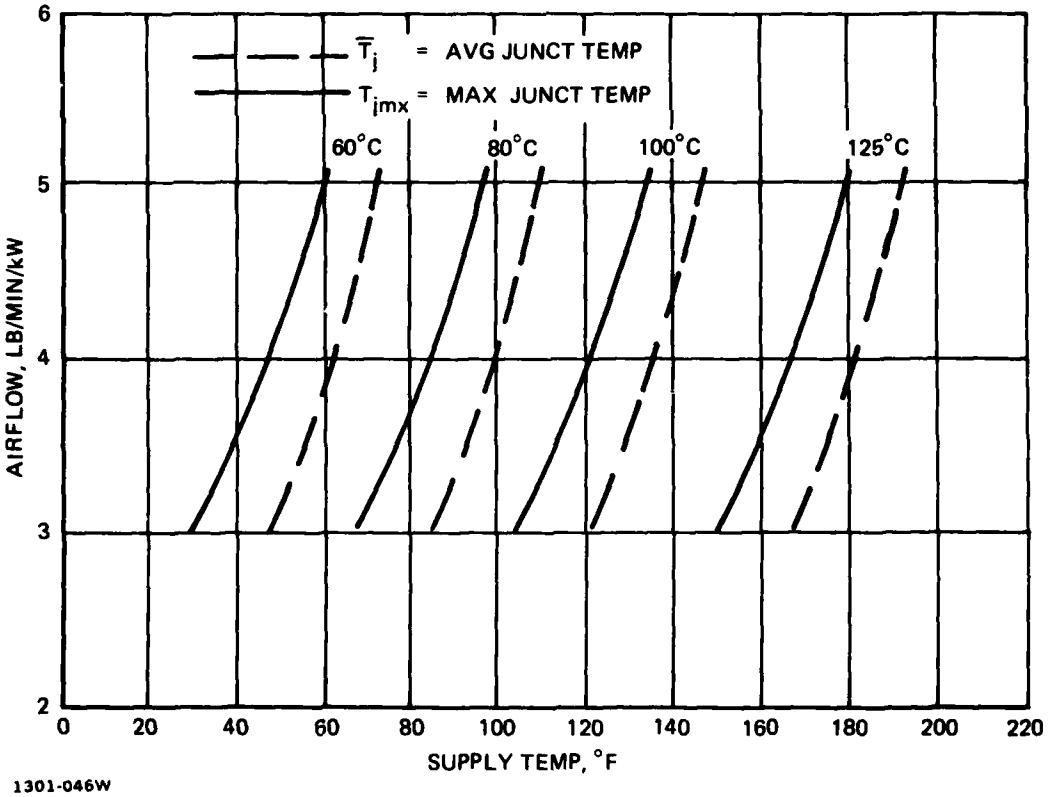

1301-046W

Figure 76 Core Board, 20 W/Module

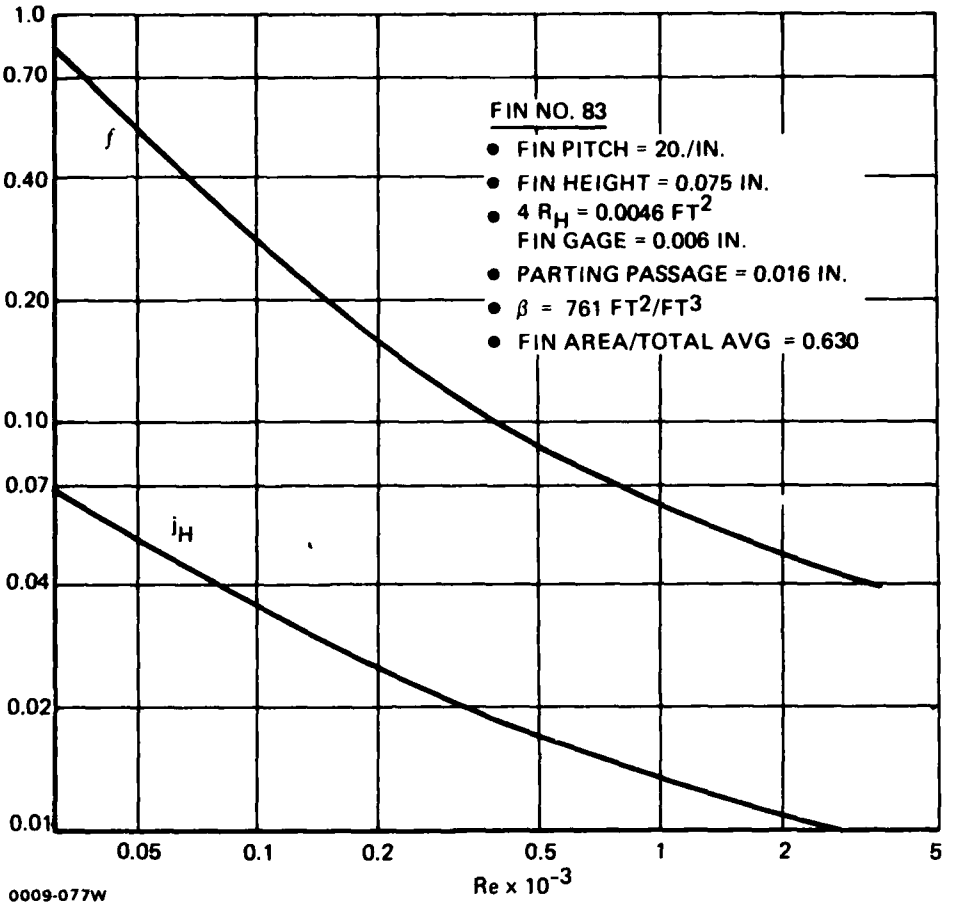

Figure 77 Fin Configurations

The power dissipated by each ISEM-2A module is of course crucial to the sizing of a rack ECS system. In this study, rack designs A_{21}, B_{31} and B_{32} were investigated at power dissipation levels of both 5 and 10 watts per module. Design C was studied at 5 watts, and design D was considered at 10 watts only. In each case, the ECS components were selected and sized to best suit the heat load, and yet minimize space and weight requirements.

3.6.1 Candidate A_{21} - Air-Over-Components

3.6.1.1 System Description & Operation - The concept developed in rack design A_{21} for cooling the ISEM-2A modules consists of circulating conditioned internal rack air over the module mounted components. A set of rack mounted

Table 13 – Thermal Analysis Comparison for 10 W Module

FLOWRATE W/Q LB/MIN/KW	ECS SUPPLY TEMP °F	AIR RAIL		LIQUID RAIL		CORE BOARDS	
		* T_{jmax}-°C	T_{jave}-°C	* T_{jmax}-°C	T_{jave}-°C	* T_{jmax}-°C	T_{jave}-°C
3	40	126	88	125	107	52	45
	60	137	99	136	118	63	56
	80	148	110	147	129	74	67
4	40	113	81	114	96	44	38
	60	124	92	125	107	55	49
	80	135	103	136	118	66	60
5	40	106	76	107	89	39	34
	60	117	88	119	100	50	45
	80	128	99	130	112	61	56

*MAXIMUM JUNCTION TEMPERATURE FOR AIR AND LIQUID RAIL IS DEPENDENT ON THE CARD LOCATION WITHIN THE TRAY AS SHOWN IN FIGURE 52. FOR THE CORE BOARD DESIGN, THE MAXIMUM JUNCTION TEMPERATURE IS INDEPENDENT OF CARD LOCATION WITHIN A TRAY AND IS SIMILAR TO FIGURE 54.

0009-075W

Table 14 Component Junction Temperature Variation for 10 W Modules

CONCEPT	MODULE POWER	W/Q LB/MIN/KW	COMPONENT JUNCTION TEMPERATURE VARIATION – °C
AIR RAIL	10	3	126 TO 50
LIQ RAIL	10	3	125 TO 89
CORE BOARD	10	3	52 TO 38

0009-076W

heat exchangers serve as the heat sink for the circulating air. An intermediate thermal transport loop supplies liquid coolant to each of the rack mounted exchangers from a single aircraft mounted heat exchanger. This exchanger provides the interface with the cooling air of the aircraft ECS system. ECS cooling air, as mentioned above is considered to be the ultimate sink for the heat dissipated by the modules. Figure 78 is a schematic of the design A_{21} cooling systems. The major components of the rack ECS are shown as well as the elements of the liquid transport system and the aircraft interface.

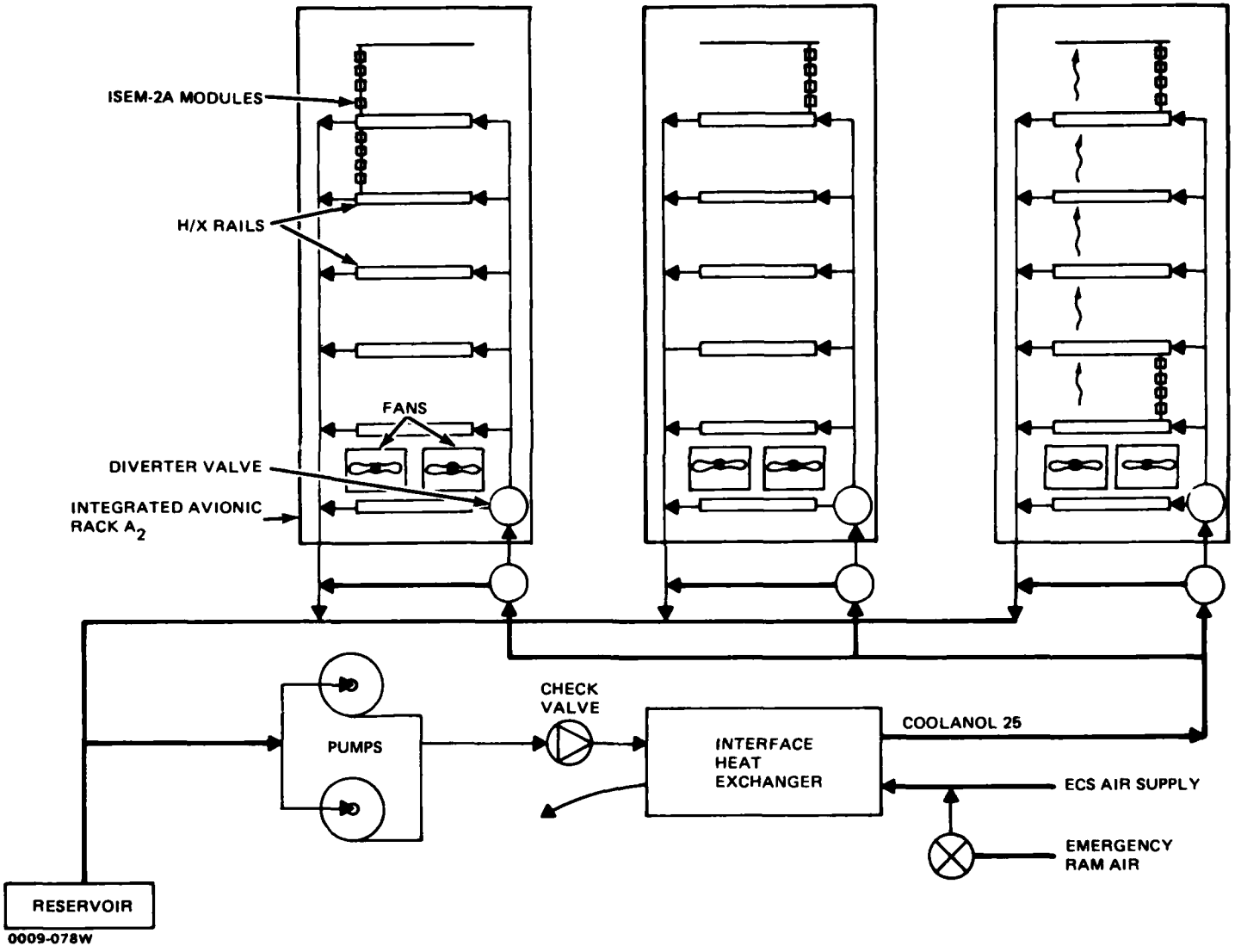

Figure 78 ECS Components & Flow Paths, Candidate A_{21} – Air-Over-Components

Liquid coolant is fed in parallel to the various racks making up an aircraft installation. Coolant circulation through the interface heat exchanger and the racks is provided by a redundant set of pumps. This assures that a single pump failure will not interrupt rack cooling. Redundancy of the ultimate heat sink is also available. In the event of primary ECS failure, emergency ram air supplied to the interface heat exchanger can be used to maintain module cooling.

The rack A_{21} ECS components are shown in Figure 79. A redundant set of centrifugal fans are provided to circulate internal rack air over the modules. Air leaving the fan is forced through an integral rail heat exchanger, where it is cooled by the flow of liquid coolant. The air then passes over the modules and absorbs the dissipated heat. It passes through another integral rail heat exchanger, where the heat acquired over the first set of modules is removed. This cooling and heating process continues until the last row of modules in the rack is cooled. The warm air is then forced down the back of the rack, behind the modules and the secondary backplane. It passes over the fan motors and is cooled in another heat exchanger, before being ducted to the inlet scroll of the centrifugal fans for re-circulation.

3.6.1.2 Heat Exchanger Core - The heat exchanger rail between each row of cards is a cross-flow plate-fin design. Air flows upward through three finned passages, while liquid flows across in two finned passages. This has been shown in Figure 18. The narrow width of the racks and the close proximity of the primary backplane to the H/X rails limited the volume available for the rails and the associated liquid headers. It was therefore necessary to flow the liquid coolant across the rack and provide headers on each end. The air side slots which are parallel to the liquid coolant passages must also extend across the rack. The module slots in the guide rail are oriented at right angles to this. While this results in some blockage of the air side fins by the guide rail, adequate flow area is maintained.

Two factors dictate the air side design of the heat exchanger rail. The first is a requirement to minimize air side pressure loss, because this ultimately affects the fan size required. The second is a minimum air side flow length, so that the least possible amount of rack volume is used. However, these goals do

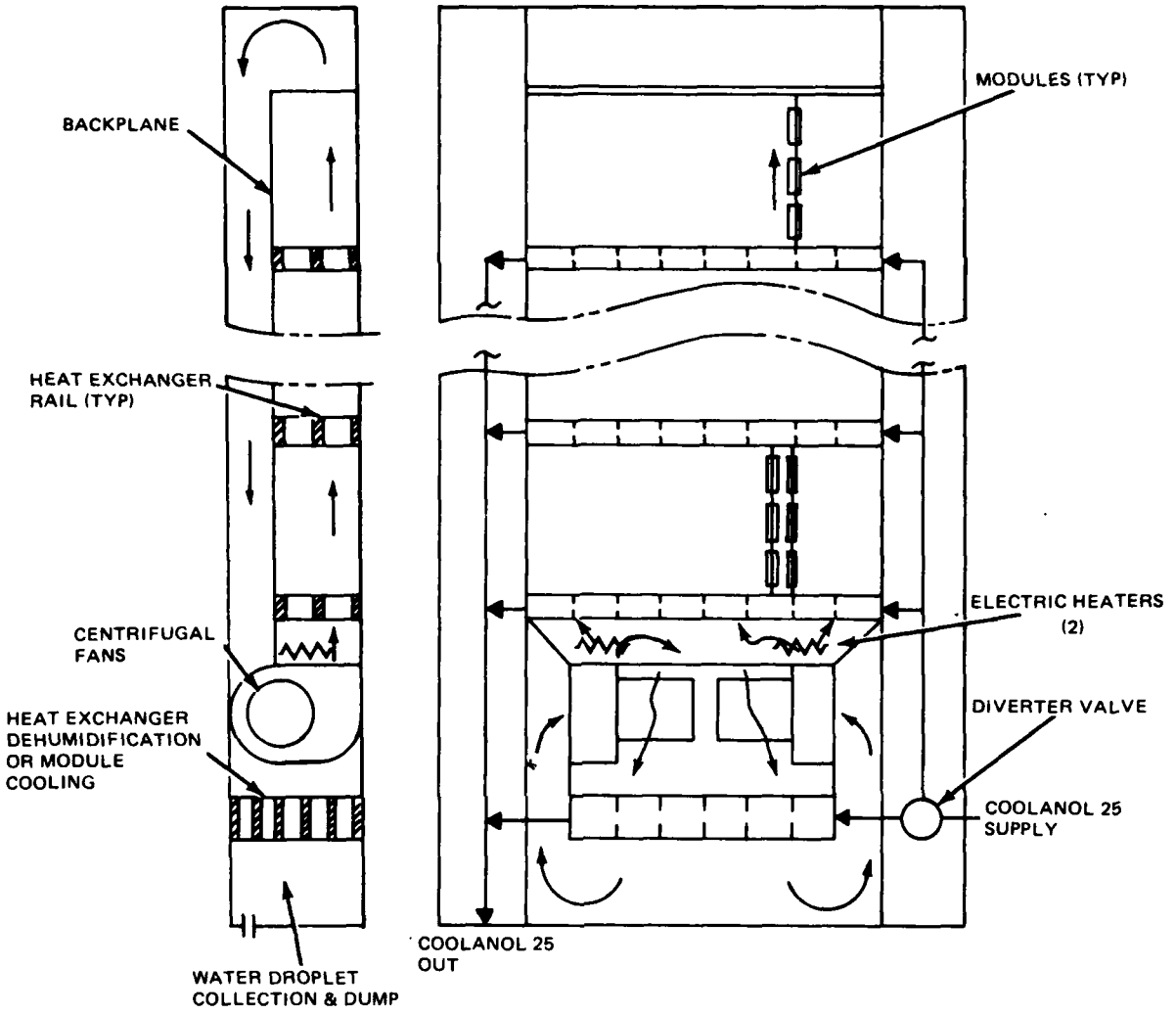

0009-079W

Figure 79 ECS Components & Flow Paths, Candidate A_{21}

not necessarily coincide when selecting an air side fin. Consequently, many fin designs were studied before selecting the final core size. On the liquid side, fin selection and coolant flow rate are important in assuring good overall performance and minimum core size.

The liquid cooling loop for the A_{21} rack has been evaluated using Coolanol 25 as the heat transfer fluid. Grumman has had favorable experience using Coolanol 25 for electronic equipment cooling on the F-14A aircraft. While Coolanol is more viscous and does not have as high a heat capacity as an

ethylene glycol/water mixture, it does have other advantages. Coolanol is a dielectric, and glycol is not. Furthermore, Coolanol is noncorrosive, unlike water/glycol mixtures. Since the modules contain exposed connector pins, this is a critical consideration.

A typical air over components rack is considered to have five rows of twenty-six modules, with an average power dissipation of five watts per module. The cooling requirements of air flow and supply temperature for this rack design have been shown in Figure 60. Initial heat exchanger core sizing calculations were conducted at each maximum junction temperature of 60°, 80°, 100° and 125°C, for air flow rates of 3.0, 4.0, and 5.0 lb/min/kW. In each case, it was initially assumed that the coolant supplied to each rail was 10°F colder than the air supply temperature required to maintain a specific junction temperature in Figure 60. A core with a 1.25 in. air flow length, a 7.80 in. liquid coolant flow length, and a stack height of 1.40 in. was shown to be effective over this spectrum of air flows and required supply temperatures. This core size was later verified at the actual air flows available from the fans, and at the actual liquid coolant supply temperatures provided by the interface heat exchanger.

Figure 80 shows the performance of the core in the form of an effectiveness map, for a range of air and Coolanol 25 flow rates. The map was constructed at an air inlet temperature of 167°F and a Coolanol inlet temperature of 77°F, which is the design point for an 80°C maximum junction temperature on the module. Off design point performance of the unit can be evaluated with this effectiveness map.

Coolanol flow rate is also a variable affecting heat exchanger rail size. The capacitance ratio of the air to Coolanol is defined as:

$$\frac{C_{AIR}}{C_{COOLANOL}} = \frac{(WC_P)_{AIR}}{(WC_P)_{COOLANOL}}$$

It was found that maintaining this ratio at about 0.10 for a range of air and Coolanol flows helped minimize the core air flow length.

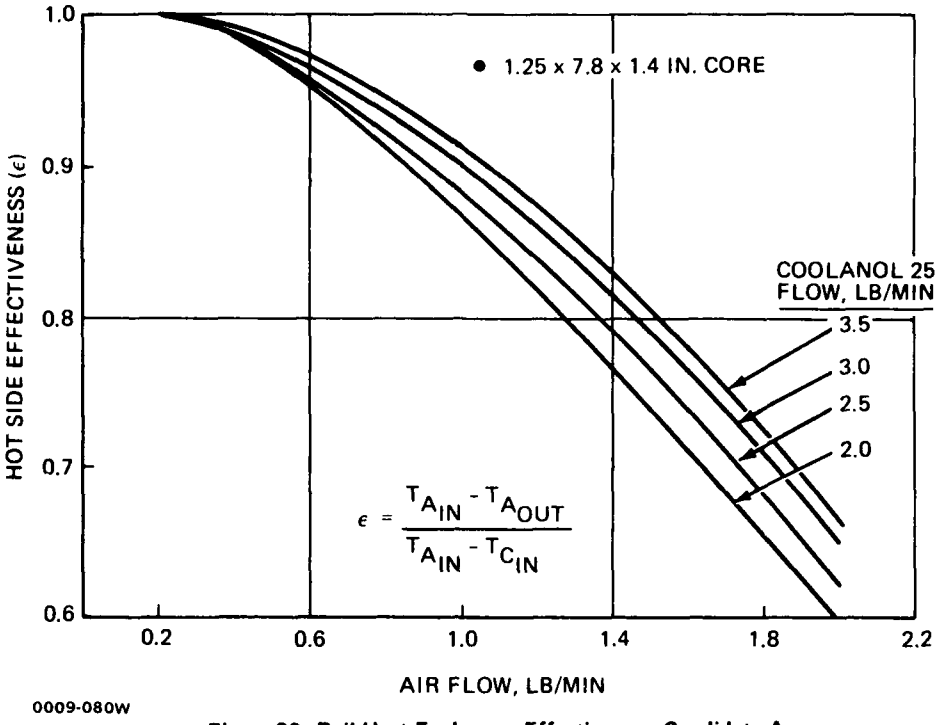

Figure 80 Rail Heat Exchanger Effectiveness, Candidate A_{21}

Figures 81 and 82 are plots of the air side and liquid side pressure losses for the 1.25 x 7.80 x 1.40 in. core size. This data, along with rack ducting losses, will be the basis for fan and pump sizing.

Coolanol 25 pressure losses for racks of 3, 4, and 5 tiers are shown in Figure 83. These losses include the heat exchanger rail losses and the coolant distribution duct losses inside the rack.

3.6.1.3 Fan Selection - The air over components cooling mode requires a fan to circulate the cooled air. Some of the factors affecting the selection of the device are the required cooling air flow, the pressure rise required to overcome system resistance, the available volume, the available power source, the power consumption, and the fan weight.

Air side losses for the rack include flow through the heat exchanger rails and the ISEM-2A modules, as well as turning and friction losses. Module losses are shown in Figure 71, and are the most significant losses in this rack. Depending on air flow rate, they are forty to one-hundred percent higher than

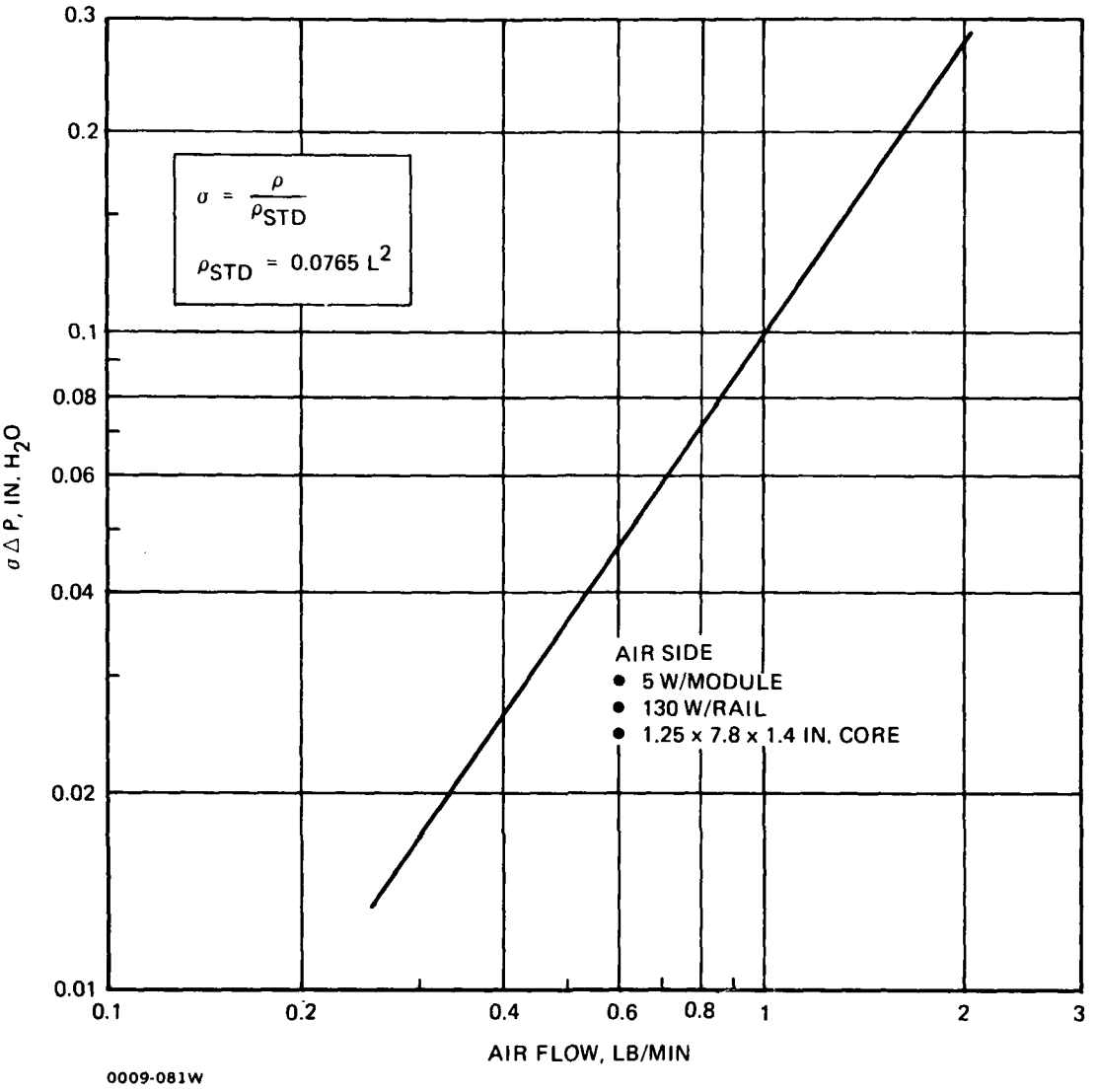

Figure 81 Heat Exchanger Air Side Pressure Loss, Candidate A_{21}

the losses of the heat exchanger rails. The rails and the modules together represent the most significant portion of rack losses. Since the rails are arranged in a series manner, with respect to airflow, the number of module-rows (or tiers in the rack), significantly affects the total pressure loss of the system. Figure 84 shows the normalized pressure loss $\sigma\Delta P$ for a range of flows and rack sizes.

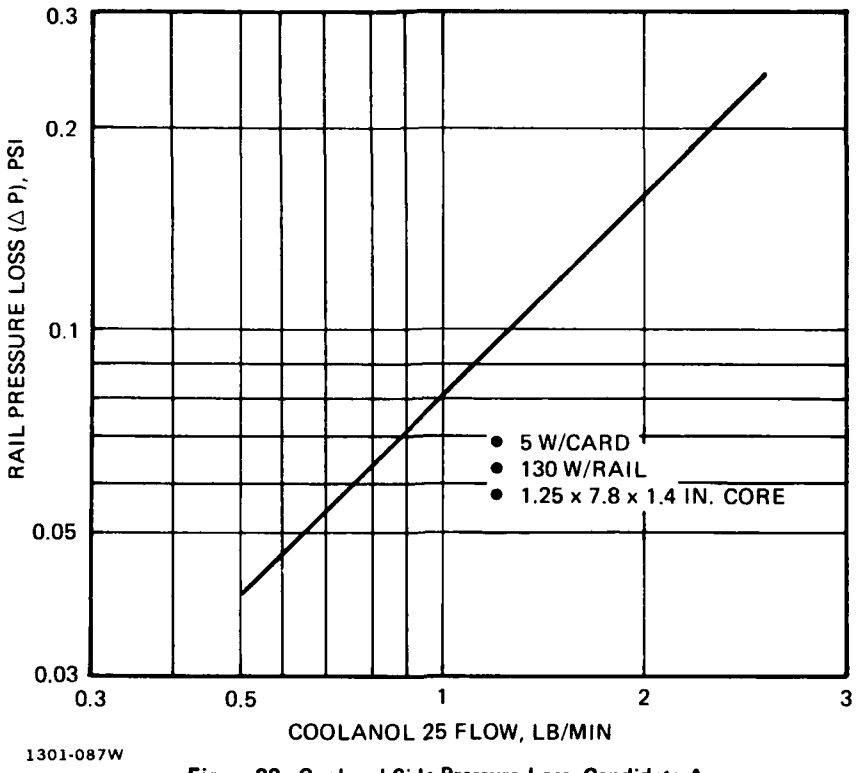

Figure 82 Coolanol Side Pressure Loss, Candidate A_{21}

In both A and B V/STOL aircraft, the racks are expected to operate in unpressurized compartments. The service ceiling of both aircraft is considered to be about 45,000 ft. In order to maintain a given module junction temperature, a constant weight flow of air is required. Fans, being basically constant volume flow devices, will be sized at the 45,000 ft. point to provide the required cooling weight flow with the low density air available. For single speed fan designs, this would result in over-cooling and high power consumption at lower altitude and sea-level operation. For this reason, altitude varying fans and infinitely variable speed 270 volt D.C. fans have been considered. The altitude varying fan increases RPM as the density decreases. However, these fans are not available with a static pressure rise in the range required to cool multi-tier racks. The 270 Volt D.C. fans appear to be available in the size range required. They have an associated electronic box which varies their speed over the range required. Fans of this type are currently being investigated and

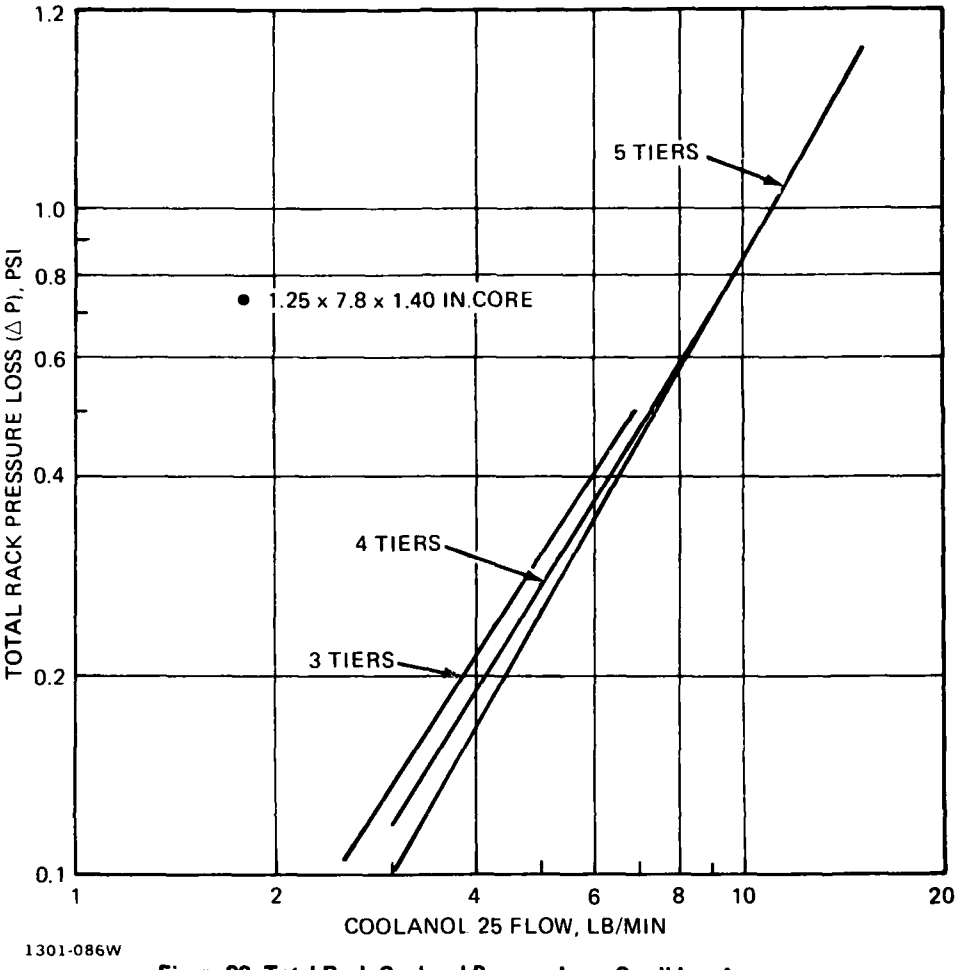

Figure 83 Total Rack Coolanol Pressure Loss, Candidate A_{21}

developed by fan manufacturers. Table 15 is a summary of data on variable speed 270 Volt D.C. fans, obtained from AiResearch Corporation. Fan 1 is applicable to rack design A_{21}.

The system resistances for various rack sizes have been plotted against volume flow in cubic feet per minute in Figure 85. Fan curves for a particular JOY/TASK axivane fan have been superimposed on the system resistance curves. A single fan, two fans placed in series, and a set of series fans placed in parallel are shown. The resultant idealized curve is representative of what is required to cool multi-tier racks, although four fans are not recommended. The design point of the AiResearch Fan No. 1 is also shown. Its performance curve is

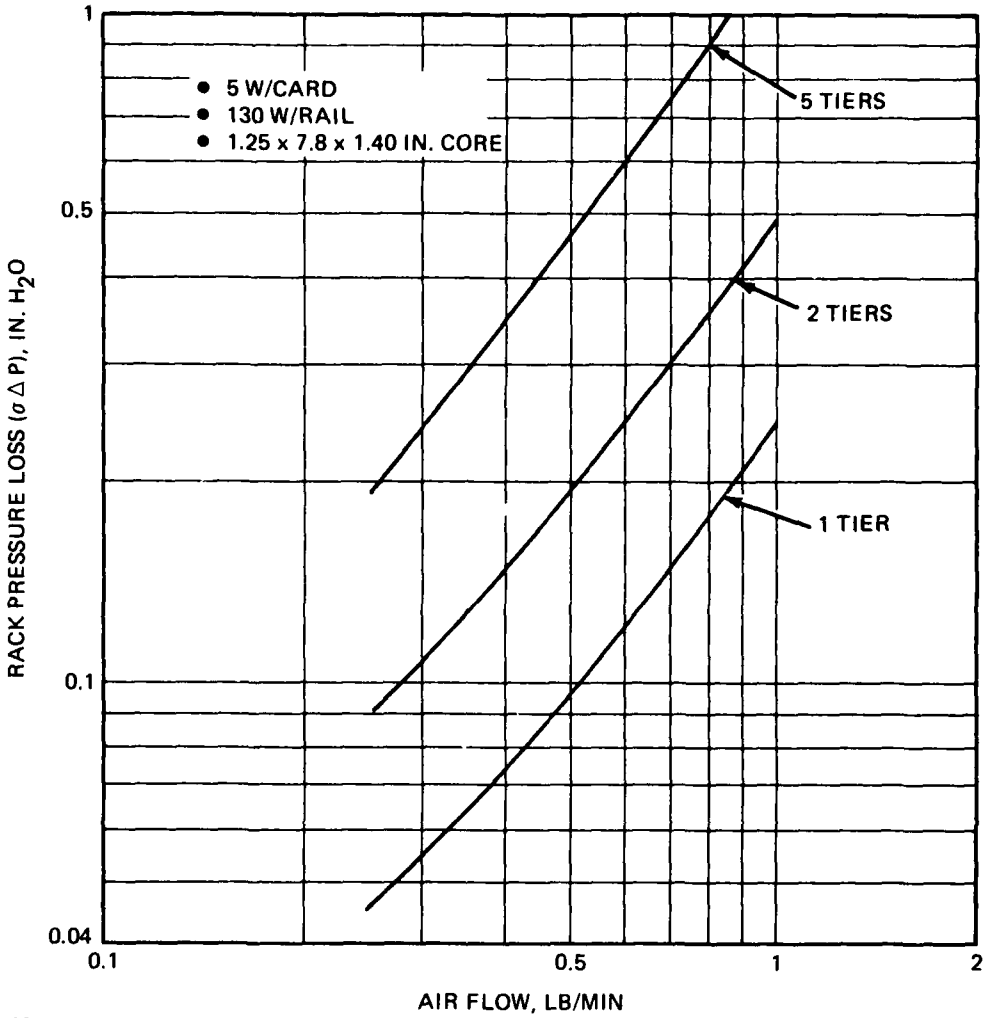

Figure 84 Total Rack Air Pressure Loss, Candidate A_{21}

expected to be somewhat similar to the idealized curve shown. The intersection of the system resistance curves and the fan curve represents the operating point of the fan. For the variable speed designs however, this intersection represents 45,000 ft. only. Decreased fan speeds may be used as air density increases to maintain the same cooling air weight flow. Thus, the fan operating point will drop along the system resistance line for operation at lower altitudes. Fan power consumption will be correspondingly reduced.

For a five tier rack design, a maximum weight flow of about 2.90 lb/min/kW will be available for rack cooling at 45,000 ft. This flow limitation is considered

Table 15 AiResearch 270 Volt Variable Speed Fan Data

FAN NUMBER		1	2	3	4
RACK		A	C	C	C
TYPE		2-STAGE CENT.	AXIAL	AXIAL	AXIAL
DESIGN POINT 45,000 FT	FLOW, CFM	28	196	388	1039
	$\frac{\Delta P}{\sigma}$, IN H_2O	18.4	3.18	12.6	30.0
SIZE, IN.		4.0 OD. x 7.0	3.5 OD x 4.0	3.75 OD x 4.5	5.5 OD x 6.5
WEIGHT, LB		4.2	2.5	3.7	5.6
POWER, W	45 K FT	46	48	254	1050
	S.L.	30	31	127	315
SPEED, RPM	45 K FT	23,000	15,280	25,400	30,000
	S.L.	3,400	2,275	3,780	4,620
ELECTRONIC CONTROLLER	SIZE, IN.	1 x 4 x 6	1 x 4 x 6	3 x 4 x 6	–
	WT, LB	1.25	1.25	2.5	10

0009-083W

realistic, since system resistance increases sharply with increasing flow. The AiResearch Fan No. 1 is a two stage centrifugal design, and its ultimate capability is not expected to be much higher than the stated design point. Larger fans are of course available, but they will exceed the 4 in. width dimension of the rack, and will require significant increases in input power.

3.6.1.4 Intermediate Coolanol Loop & Interface Heat Exchanger - Air, as provided by the aircraft ECS, has been established as the ultimate sink for the module heat load in each rack concept. This provides a common basis for comparison of the thermal performance of the various rack designs. Maximum and average component junction temperatures are the criteria used to judge performance, based on fixed inputs of flow rate and temperature from the aircraft ECS system.

In the case of design A_{21}, the liquid coolant acts as a transport medium to the aircraft ECS for the heat rejected by the fan circulated rack air. The coolant system, with its associated ducting, valving, redundant set of pumps, and heat exchanger, must be considered as a weight and power penalty to rack design A_{21} when comparing it with the other candidates.

The interface heat exchanger was sized using the Coolanol flow rate of 15.4 lb/min/kW. This corresponds to a capacitance ratio $C_{AIR}/C_{COOLANOL} = 0.1$,

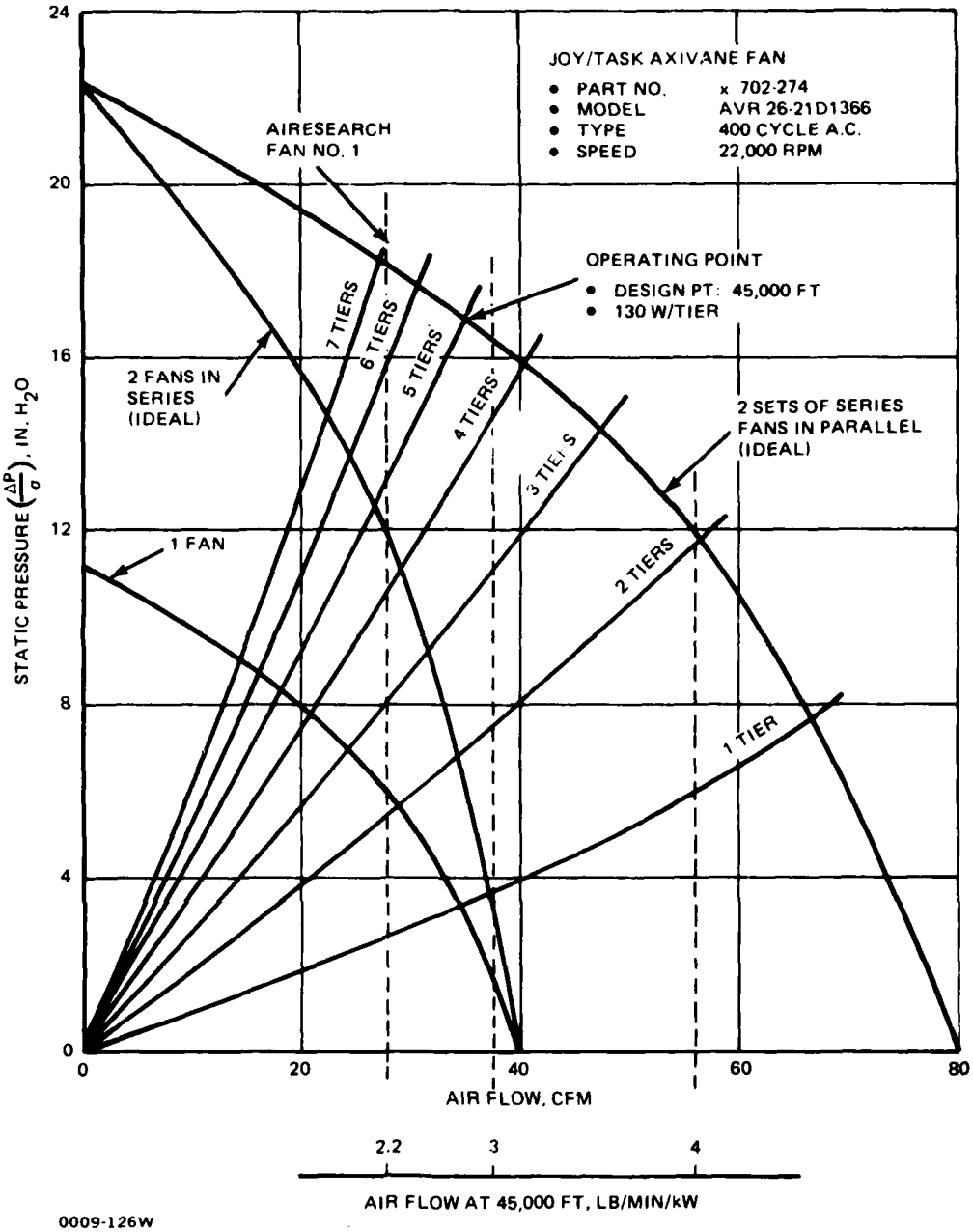

Figure 85 Fan Sizing Requirements, Candidate A_{21}

for a fan circulated air flow rate of 2.9 lb/min/kW. This Coolanol flow rate was selected, based on the minimum core volume requirements of the rack mounted air Coolanol heat exchangers. For the core size selected (1.25 x 7.8 x 1.4 in.), a rapid loss of heat exchanger rail performance would result at lower Coolanol flow rates. Thus, the interface heat exchanger core was designed to accommodate the Coolanol flow rates required by the racks. Interface heat exchanger performance was evaluated considering a range of ECS cooling air flow rates from 3 to 5 lb/min/kW, at supply temperatures of 40°F to 80°F.

Figure 86 illustrates the entire cooling system for an air over components rack, and shows the different flows and temperatures involved. The table in the lower portion of the figure illustrates the temperatures available throughout the system, from the ECS sink to the fan airflow supplied to the modules. The air supply temperature to the module can be used in conjunction with Figure 60 to determine component junction temperatures for a 5 watt module. The first portion of Table 16 summarizes the performance of the air over components concept for the 5 watt module, in terms of maximum and average component junction temperatures.

3.6.2 Candidate B_{31}

3.6.2.1 System Description & Operation - The ISEM-2A modules in rack B_{31} are cooled by conduction. The top and bottom of each module is fitted into a liquid cooled guide rail. The liquid coolant is ultimately sinked to the aircraft ECS through an air-liquid heat exchanger. As above, the aircraft is assumed to provide air to this interface heat exchanger at a temperature of 40° to 80° F, and at flow rates of 3 to 5 lb/min/kW. Figure 87 schematically illustrates the B_{31} conduction cooled racks and their associated aircraft interface.

The modules in the conduction racks are arranged in rows of twenty-six each. The number of tiers stacked together is not limited by cooling considerations, as in the A_{21} design. Each guide rail in the conduction design is fed in a parallel mode from the coolant supply. Along a given rail though, the modules are series cooled. This cooling mode then results in a family of maximum junction temperatures along a rail. The guide rail and Coolanol distribution ducts are the only ECS equipment required for basic module cooling.

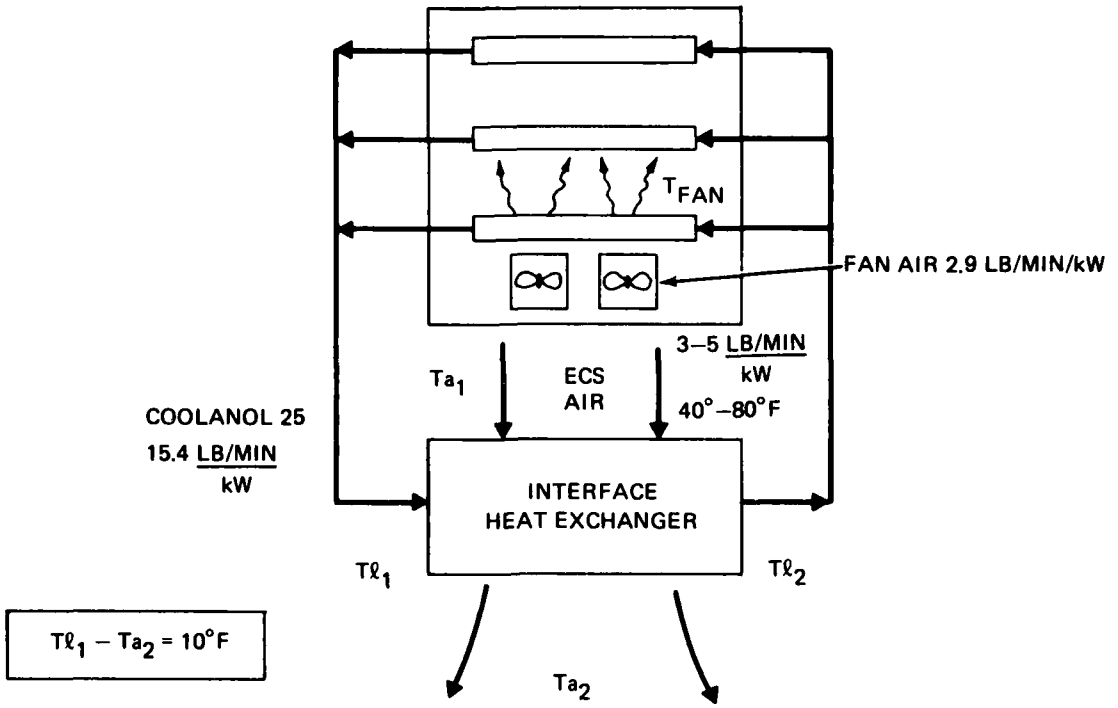

@ ECS AIR SUPPLY TEMPERATURE $Ta_1 = 40°F$

	INTERFACE H/X			COOLANOL LOOP				FAN LOOP		
	W/Q_a LB/MIN / kW	ΔTa °F	Ta_2 °F	W/Q_{LIQ} LB/MIN / kW	W_{LIQ} LB/MIN	$T\ell_1$ °F	$T\ell_2$ °F	W/Q_{FAN} LB/MIN / kW	W_{FAN} LB/MIN	T_{FAN} °F
5W	3	79	119	15.4	2.0	129	121	2.9	0.39	131
	4	59	99	15.4	2.0	109	101	2.9	0.39	111
	5	47	87	15.4	2.0	97	89	2.9	0.39	99
10W	3	79	119	11.4	3.0	129	118	3.0	0.78	125
	4	59	99	11.4	3.0	109	98	3.0	0.78	105
	5	47	87	11.4	3.0	97	86	3.0	0.78	91

0009-082W

Figure 86 Cooling System Performance (Air-Over-Components)

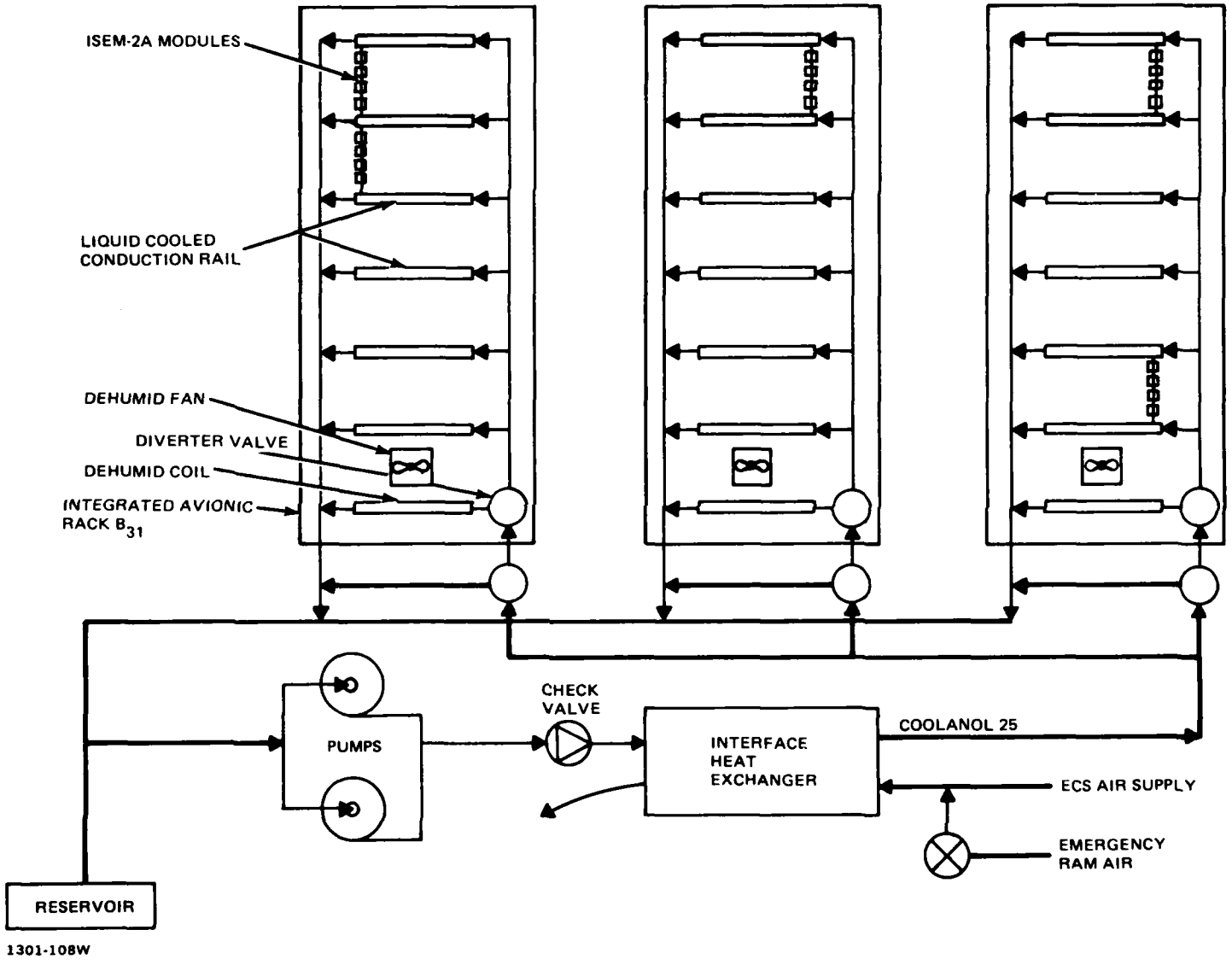

Figure 87 ECS Components & Flow Paths, Candidate B_{31} – Liquid Rail Conduction

When installed in an aircraft, the various racks will be parallel fed liquid coolant from the interface heat exchanger. Coolant circulation through the interface heat exchanger and the racks is provided by two pumps operating in parallel. This assures that a single pump failure will not interrupt rack cooling. Redundancy of the primary heat sink can be provided by ram air, as in the air over components design A_{21}.

3.6.2.2 Liquid Rail Design - The liquid cooling rail consists of the card guide with an enclosed finned coolant passage. Liquid flows across the rack through a 0.072 x 1.45 in. cross section, effectively removing half the heat load of the fifty-two modules that fit into the 26 upper and 26 lower card guides. As mentioned in Subsection 3.4, the temperature difference between a component junction and the wall of the coolant passage is dependent only on module power. However, the temperature difference between the passage wall and the coolant is a function of fin configuration and coolant flow rate. The fin design was selected for the 5 watt rail minimized the wall to fluid temperature difference while maintaining low Coolanol flow rates. Figure 88 shows the expected performance of this rail, in terms of module maximum junction temperatures, with respect to Coolanol 25 supply conditions. The actual operating point of the rail in terms of maximum junction temperatures is dependent on the supply temperatures of the Coolanol available from the interface heat exchanger. Figure 89 shows the Coolanol pressure loss of this rail and associated distribution ducts for several different rack sizes.

3.6.2.3 Interface Heat Exchanger - The heat load carried by the Coolanol from the modules is absorbed by the aircraft ECS cooling air in the interface heat exchanger. As in the air over components scheme, the liquid transport system, with its associated ducting, valving, pumps, heat exchanger and controls, must be considered as a weight and power penalty to the B_{31} rack concept.

The interface heat exchanger was designed with a Coolanol flow rate of 15.4 lb/min/kW. This flow rate was selected at the point of optimum rail performance with a 5 watt heat load, and represents the lowest practical flow rate that could be supplied. The rail performance in terms of component maximum and average junction temperature was evaluated at this point. Figure 90 shows the components of the liquid rail and interface heat exchanger system.

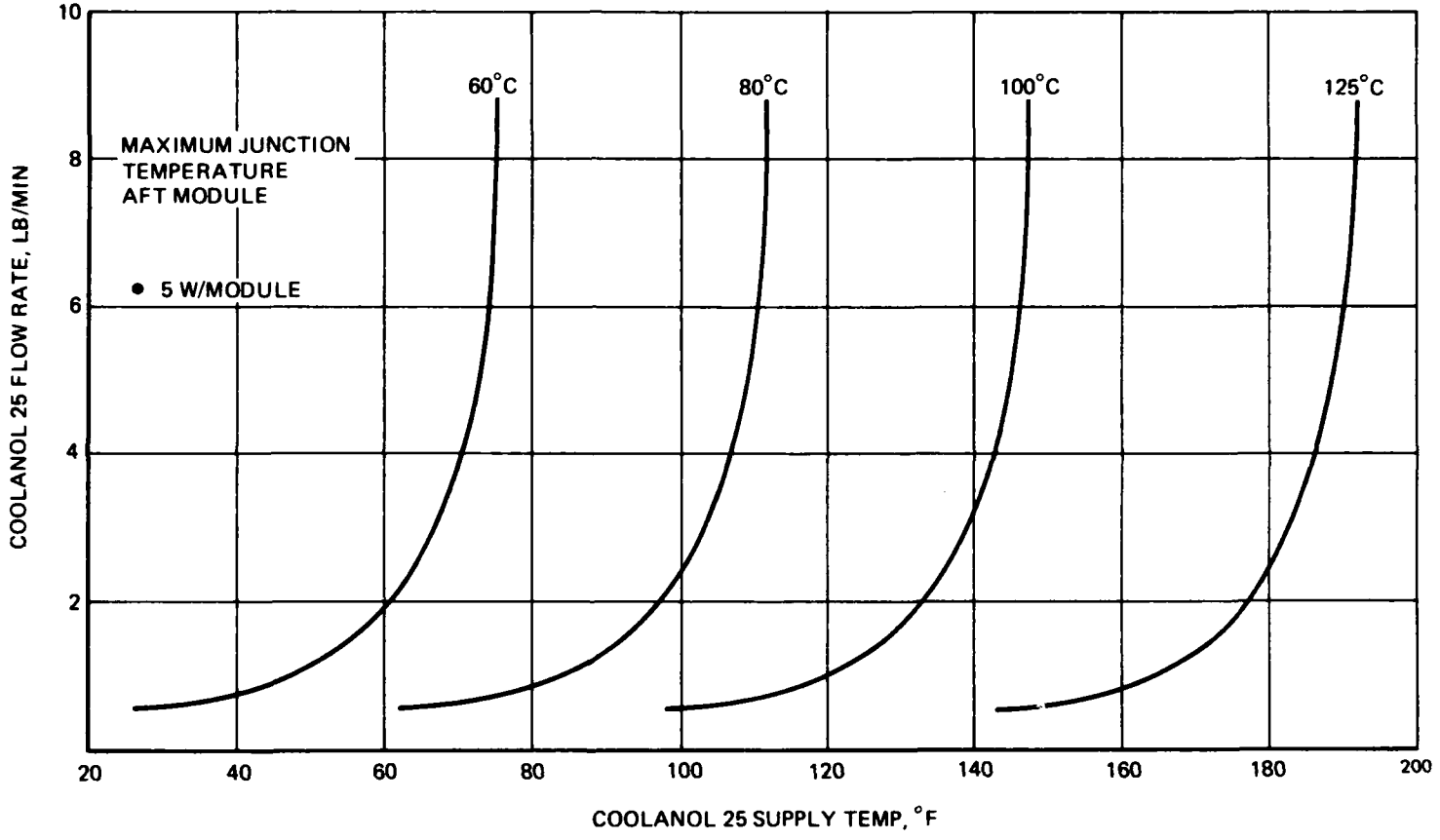

0009-135W

Figure 88 Candidate B_{31} Liquid Rail Performance

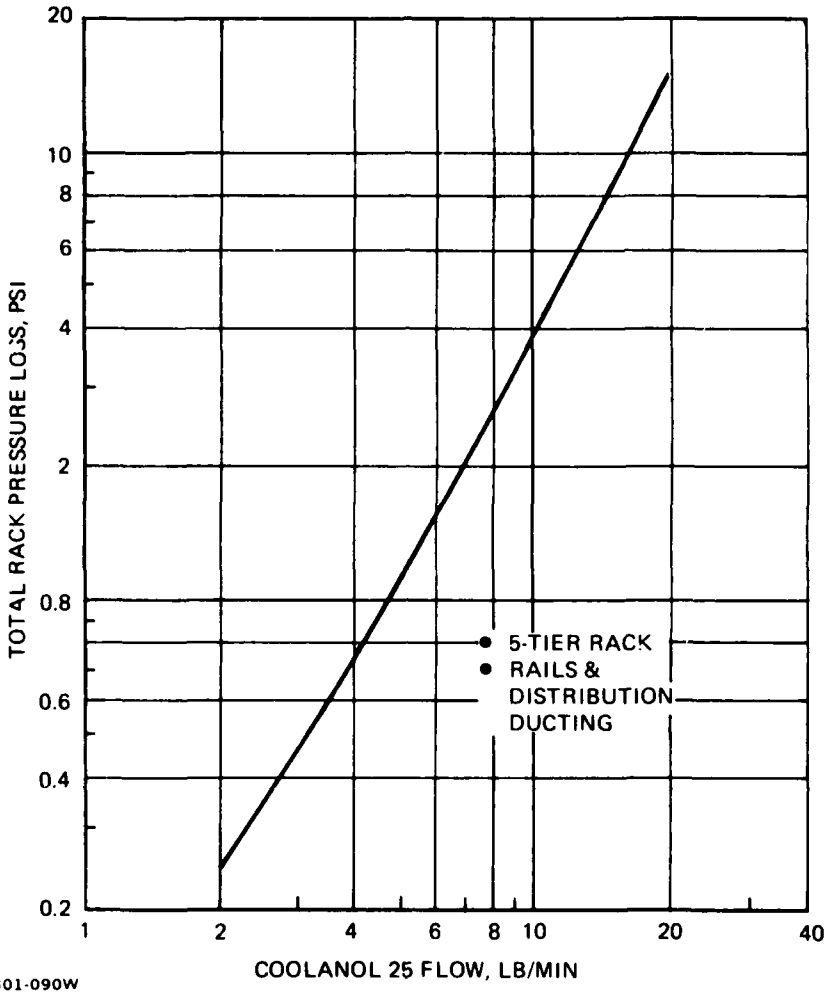

Figure 89 Total Coolanol Pressure Loss, Candidate B_{31}

The flows and temperatures available at each point of the system are shown in the table for a 40°F ECS air supply temperature. The temperature exiting the interface heat exchanger (Tl_2), which is the rail supply temperature, can be used in conjunction with Figure 88 to determine component junction temperatures. Table 16 summarizes the performance of the 5 watt liquid rail in terms of maximum and average junction temperature for ECS air supply temperatures of 40° to 80°F and flow rates of 3 to 5 lb/min/kW.

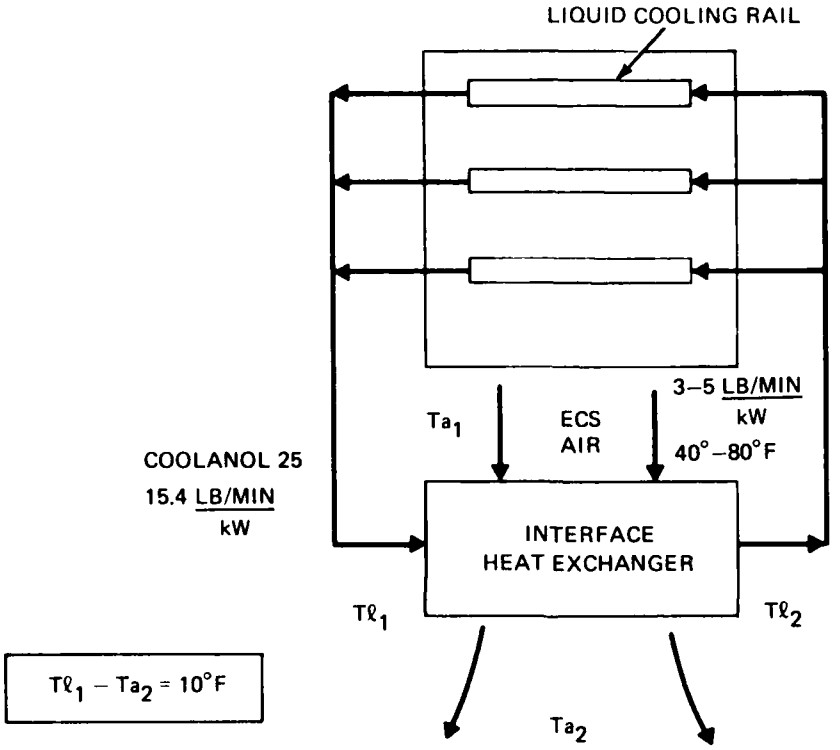

	INTERFACE HEAT EXCHANGER				COOLANOL LOOP			
	W/Q_{AIR} LB/MIN / kW	Ta_1 °F	ΔTa °F	Ta_2 °F	W/Q_{LIQ} LB/MIN/kW	ΔTℓ °F	$Tℓ_1$ °F	$Tℓ_2$ °F
5W	3	40	79	119	15.4	8	129	121
	4	40	59	99	15.4	8	109	101
	5	40	47	87	15.4	8	97	89

0009-086W

Figure 90 Cooling System Performance (Liquid Rail)

Table 16 Air-Over-Components Cooling Data, A_{21}

FLOW RATE (W/Q) LB/MIN/kW	ECS SUPPLY TEMP, °F	5 W		10 W					
		FAN 2.9 LB/MIN/kW FLOW: 0.38 LB/MIN		FAN 3.0 LB/MIN/kW FLOW: 0.78 LB/MIN		FAN 4.0 LB/MIN/kW FLOW: 1.04 LB/MIN		FAN 5.0 LB/MIN/kW FLOW: 1.3 LB/MIN	
		T_j MAX., °C	T_j AVG, °C	T_j MAX., °C	T_j AVG, °C	T_j MAX., °C	T_j AVG, °C	T_j MAX., °C	T_j AVG, °C
3	40	103	94	106	97	96	89	91	85
	60	115	106	117	108	107	100	102	96
	80	126	117	128	119	118	111	113	107
4	40	96	87	95	86	86	79	81	75
	60	108	99	106	97	96	89	91	85
	80	119	110	117	108	107	100	102	96
5	40	84	75	88	79	79	79	74	68
	60	92	83	79	70	90	83	85	79
0009-085W	80	107	98	74	65	101	94	96	90

3.6.3 Candidate B_{32}

3.6.3.1 System Description & Operation - ISEM-2A modules in rack design B_{32} are again cooled by heat conduction through the top and bottom of each module. The cooling medium in this rack design however is air. The source of this coolant could be either ram air or conditioned ECS air, depending on the aircraft and flight conditions. The inlet plenums and enclosed guide rails provide complete isolation of the modules from the cooling air. An interface heat exchanger with the aircraft systems is not required, unlike the designs with intermediate liquid cooling loops. The system is shown schematically in Figure 91.

The modules are again arranged in rows of twenty six each. The air is introduced to the rail at one end and cools each module in succession. The air temperature, however, increases as it absorbs module heat. This results in a profile of increasing component maximum junction temperatures from the air inlet to the end of the rail. Cooling air is fed in parallel from a distribution plenum to each rail. The pressure loss, $\sigma\Delta P$, for the distribution plenums and the guide rails, is shown in Figure 92. Rack sizes up to eight tiers high appear to be possible before rack pressure loss exceeds aircraft supply capability.

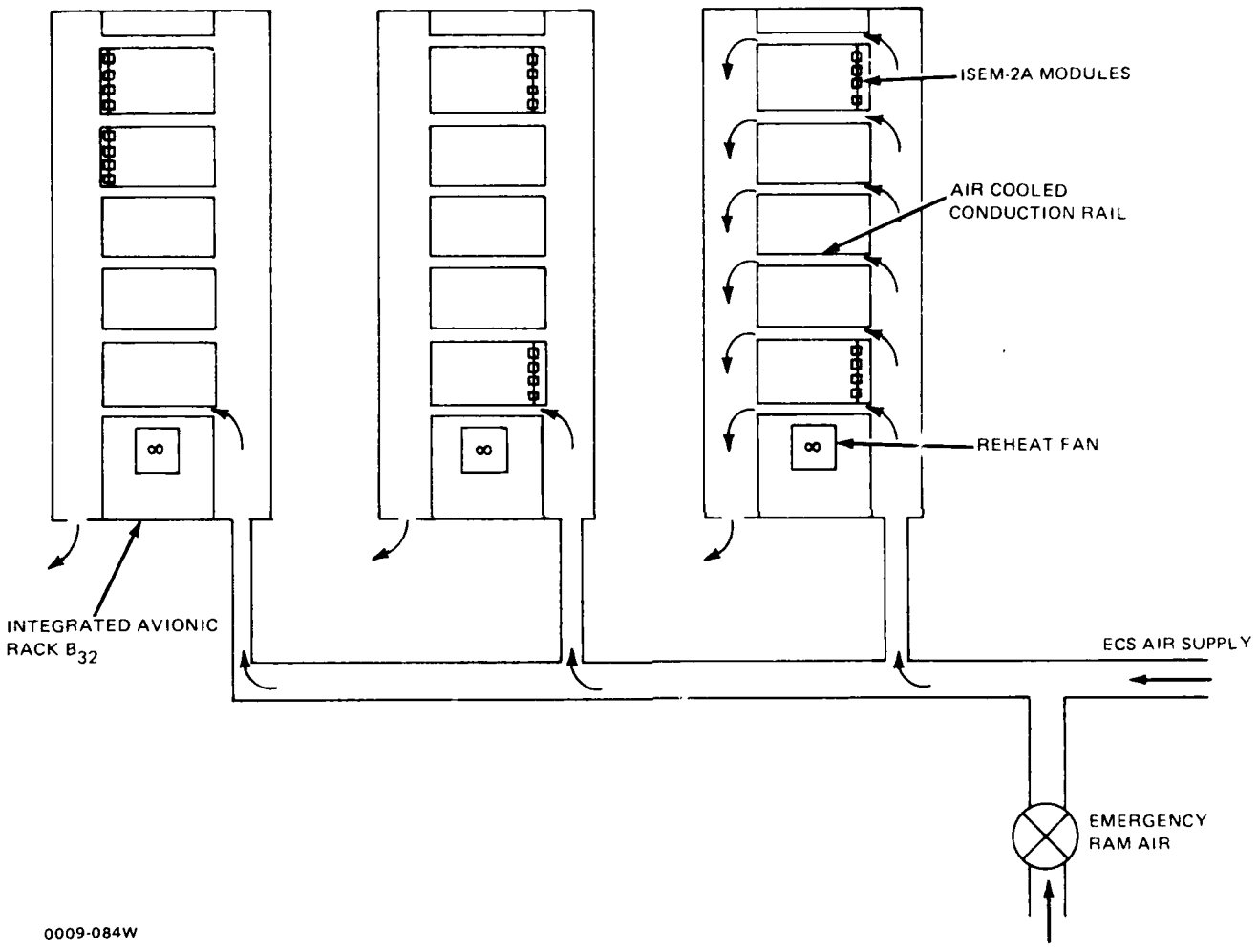

Figure 91 ECS Components & Flow Paths, Candidate B_{32}, Air Rail Conduction

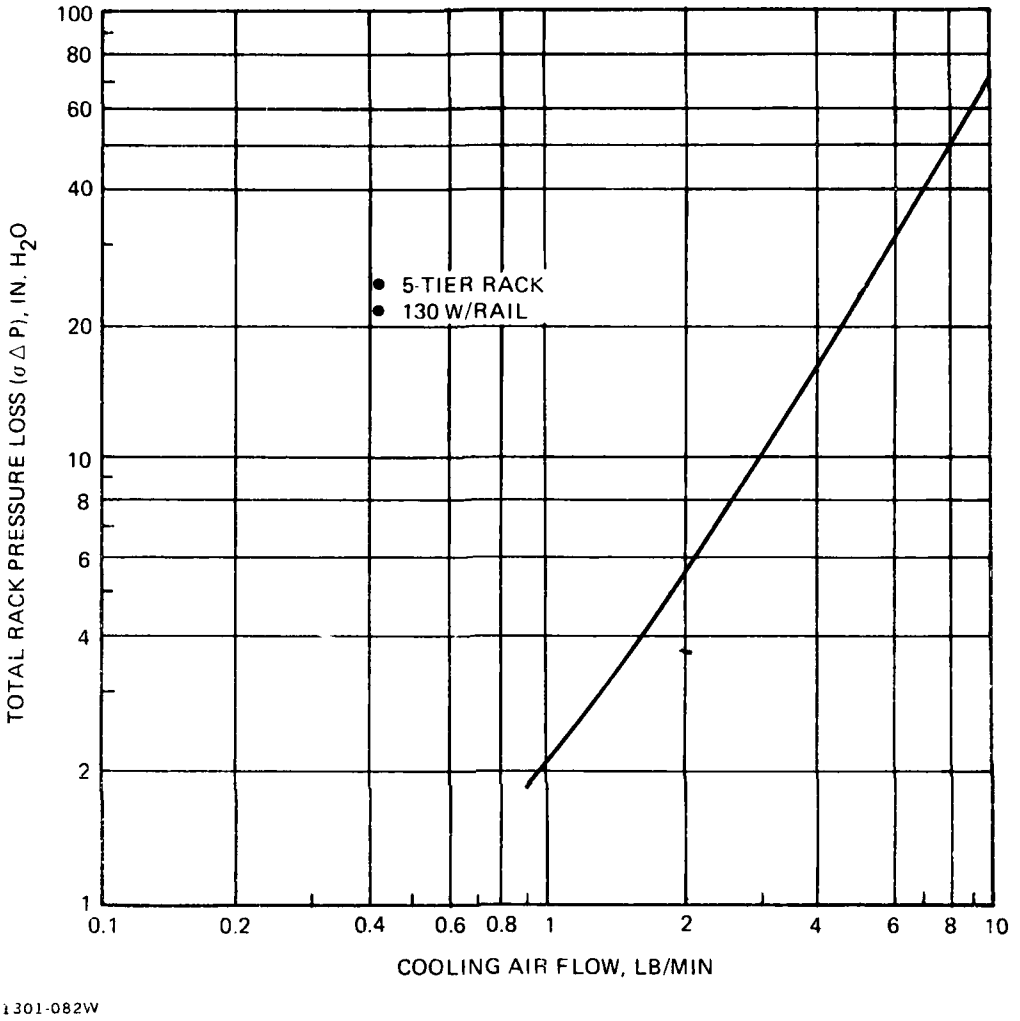

1301-082W

Figure 92 Total Rack Air Pressure Loss, Candidate B_{32}

3.6.3.2 Air Rail Design - The air guide rail consists of the hollow guide rail with two rows of fins inside. The flow cross section is about 1.45 in. wide by about 0.41 in. deep. In selecting the fin configuration, the conductance from the heat exchanger wall to the cooling air was maximized while keeping pressure loss at a reasonable level. The resulting rail performance has been previously presented in Figures 61 and 62. For air flow rates of 3 to 5 lb/min/kW at supply temperatures of 40° to 80°F, the rail performance in terms of maximum and average junction temperatures for the five watt module is shown in the first part of Table 17.

Table 17 Rail Cooling Data, Conduction

FLOW RATE (W/Q) LB/MIN/kW	ECS SUPPLY TEMP, °F	AIR RAIL, B_{32}				LIQUID RAIL, B_{31}			
		5 W		10 W		5 W		10 W	
		T_j MAX, °C	T_j AVG, °C	T_j MAX, °C	T_j AVG, °C	T_j MAX, °C	T_j AVG, °C	T_j MAX, °C	T_j AVG, °C
3	40	89	59	126	88	88	77	125	107
	60	100	70	137	99	99	88	136	118
	80	112	82	148	110	110	100	147	129
4	40	76	52	113	81	76	66	114	96
	60	87	63	124	92	88	77	125	107
	80	98	74	135	103	99	88	136	118
5	40	68	47	106	76	70	60	107	89
	60	79	58	117	88	81	71	119	100
	80	90	69	128	99	92	82	130	112

0009-088W

3.6.4 Candidate C

3.6.4.1 System Description & Operation - The ISEM-2A modules in this rack design are cooled by the circulation of conditioned rack air. A rack mounted central heat exchanger is provided as the cooling sink for the air. An intermediate Coolanol 25 thermal transport loop supplies coolant to the central heat exchanger in each individual rack, as shown in Figure 93. The racks are parallel fed Coolanol 25 by a redundant set of pumps. A single air/liquid heat exchanger is provided to interface the Coolanol 25 System with the aircraft ECS. In the case of primary ECS failure, emergency ram air cooling can be supplied at this interface. The modules, however, are always isolated from either ram air or the conditioned air of the primary ECS by the intermediate Coolanol 25 loop.

Internal rack components and operations are illustrated in Figure 17. A redundant set of axial fans, located just above the central heat exchanger, provide circulation of internal rack air. The air leaving the fans is ducted up a central plenum and parallel fed to the modules mounted on both sides. Plenums on each side of the rack collect the warmed air exiting the modules. The two streams are ducted downward and converge at the bottom of the rack. The air

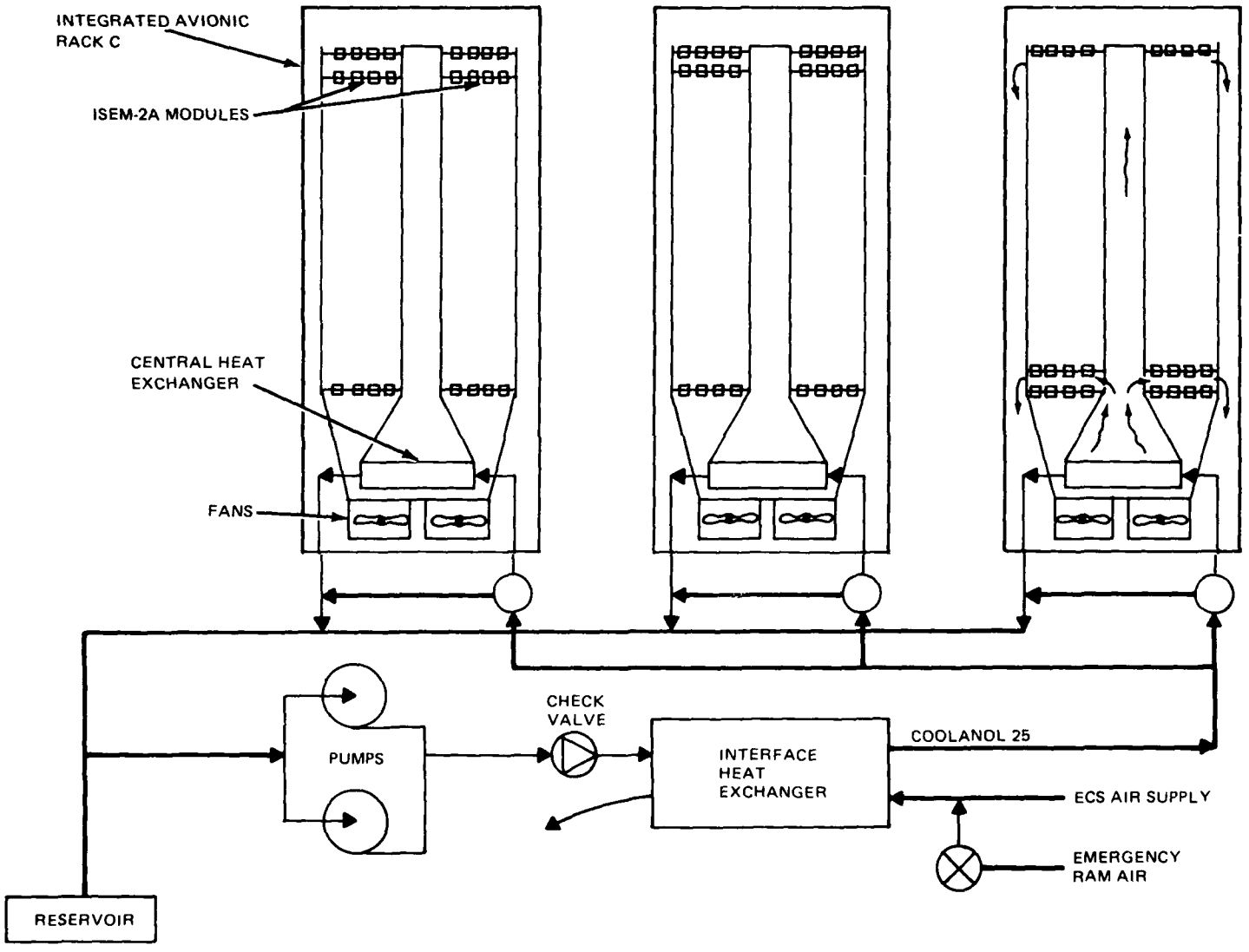

0009-122W

Figure 93 ECS Components & Flow Paths Candidate C, Air-Over-Components

is turned upward through the air/liquid heat exchanger. The heat load from the modules and fan motors is dumped into the Coolanol 25. After being filtered, the cooled air enters the fan to be again circulated over the modules.

Designs A_{21} and C both cool the ISEM-2A by providing air over the module components. Rack C differs from A in that all the cooling air is provided from one central heat exchanger. All the cards in rack C are fed air in parallel with each other. In rack design A_{21} however, each row of twenty-six modules is arranged in series. A small amount of air is repeatedly heated and cooled as it passes over each tier. The configuration difference means that the fans in rack C must circulate more air at a given density than rack A_{21} requires to cool the same number of modules. For instance, a C rack requires twice the airflow required for a two tier A_{21} design, and five times the airflow required for a five tier A_{21} design. This difference highlights one disadvantage of the C design; fan input power will be higher than required by design A_{21} to cool the same number of modules.

The baseline rack design considered for this study contains 260 modules. They are arranged in banks of 130 with a pitch of 0.3 in. This rack size contains twice the number of modules as the baseline A_2 design. The average power of each module has been considered to be five watts.

3.6.4.2 Central Heat Exchanger - The central heat exchanger selected for this rack design is a single pass, cross-flow, plate-fin type. The internal rack air is cooled as it flows upward through eight finned passages. The Coolanol 25 absorbs the heat of the air as it flows across the rack in nine finned passages. Domed headers are provided on each side for the Coolanol inlet and outlet.

The chief considerations in selecting a core size for the rack are minimum volume and minimum air side pressure loss. Various air side and liquid side fins were traded off before arriving at a final core size. The airflow requirements are shown in Figure 60. A range of Coolanol 25 flows was considered. The Coolanol was considered to be supplied to the core 10°F colder than the air-side outlet temperature required by Figure 60. The final core size selected shown in Figure 94, was 1.0 in. on the air side, 10.0 in. on the Coolanol side, with a 4.0 inch stack. The performance of this core for various hot and cold flow rates is shown in Figure 95. This core size is considered reasonable for

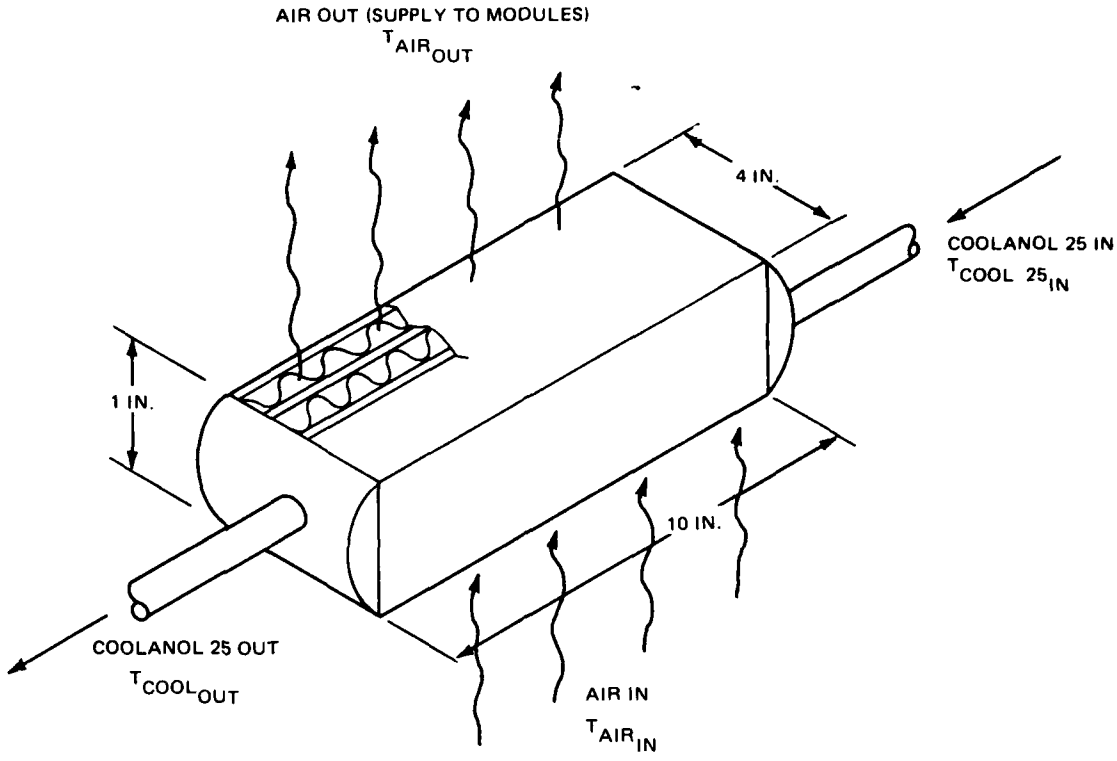

0009-087W

Figure 94 Candidate C Cross-Flow Heat Exchanger

fan air flows of 3 to 5 lb/min/kW and any supply temperature required to maintain maximum junction temperatures of 60°C to 125°C assuming the proper Coolanol temperature can be supplied by the aircraft ECS.

Referring back to Figure 95, the "design point" used as the starting point for pressure drop calculations is: AIR, 5.72 lb/min, 164°F; Coolanol 25, 15.6 lb/min, 100°F, and corresponds to 4.4 lb/min/kW @ 80°C maximum junction temperature. If, however, the Coolanol flow rate is cut in half, to 7.8 lb/min, the performance suffers only slightly, yielding maximum function temperatures only about 3°C higher than predicted by Figure 60. Flow rates lower than about 7.8 lb/min ($C_{min}/C_{max} = 0.4$) show large losses in performance, however.

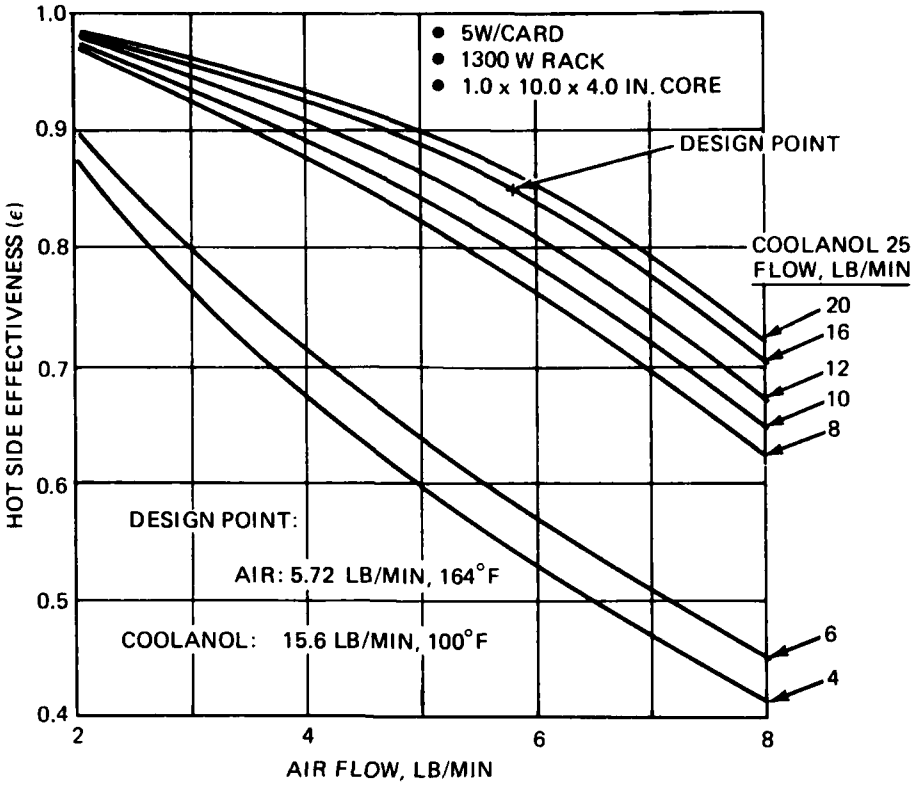

1301-064W

Figure 95 Heat Exchanger Effectiveness, Candidate C

The Coolanol side pressure drop performance of the heat exchanger core is shown for a range of flow rates in Figure 96. The rack ducting losses are considered minimal.

On the air side, pressure loss calculations were begun at the "design point", but were then normalized to a range of flow and air temperatures. Losses considered include the plenum supply duct, the ISEM-2A modules, the collection plenums, the flow turning and converging losses, the filter losses and the heat exchanger core losses. Figure 97 shows the normalized pressure losses, $\sigma\Delta\rho$, for a range of air flow rates. These data formed the basis for the fan sizing calculations.

3.6.4.3 Fan Selection - The same factors that affected the selection of the fan for the A rack design apply for the C rack. They are: the selected flow; the required static pressure rise; the available volume; the power source; the power consumption; and the fan weight. Again, the fan design point is considered to

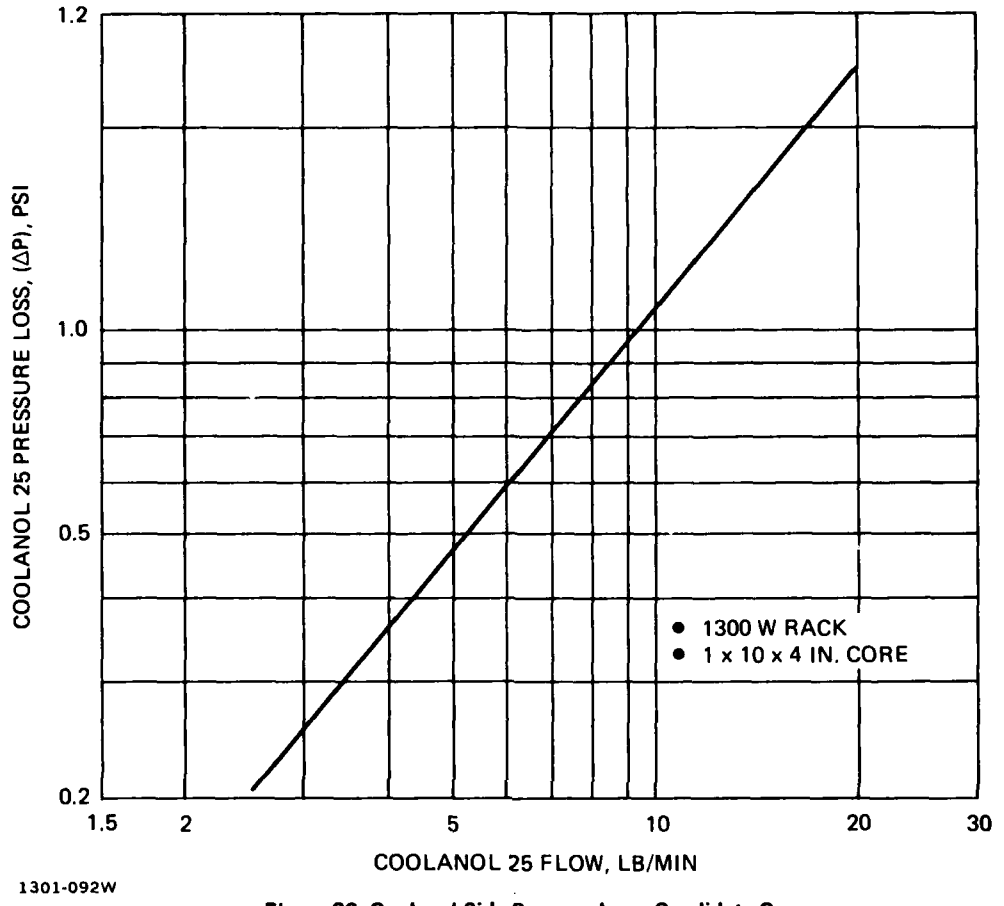

Figure 96 Coolanol Side Pressure Loss, Candidate C

be 45,000 ft. so that adequate weight flow of air is delivered at altitude. Variable speed, 270 volt D.C. devices were again considered because of the advantages they demonstrated for the A_{21} design. Referring to Table 15 AiResearch Fans 2, 3 and 4 were considered for rack C.

The AiResearch Fan No. 4 is unusable as presented, because its diameter exceeds that of the rack. Using the fan laws, the fan was scaled down in diameter at a constant RPM. The resulting static pressure rise $\Delta p/\sigma$, and input power, at 45,000 ft., are plotted in Figure 98. Each point along these curves represent different, discreet fans, at their design point. A fan diameter of 4.0 inches is considered maximum for this rack. As illustrated in Figure 98, the fan design point at 45,000 ft. is now specified in terms of maximum weight flow, static pressure rise and input power.

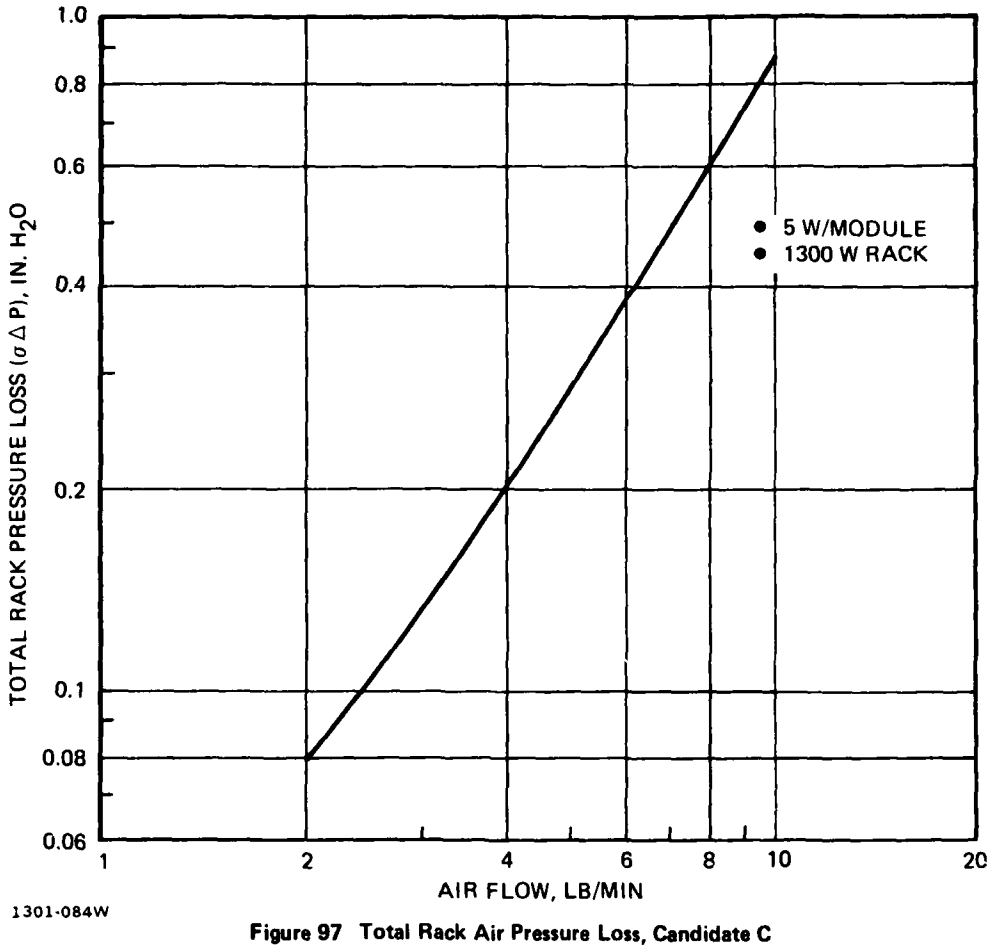

Figure 97 Total Rack Air Pressure Loss, Candidate C

The rack system resistance curve has been plotted as $\Delta\rho/\sigma$ for varying CFM in Figure 99. The design points for the AiResearch Fans No. 2, No. 3 and the scaling curve for No. 4 are also shown. A second scale on the bottom, weight flow at 45,000 ft, is also shown. Fan No. 2 is undersize for this wattage rack. Fan No. 3 will provide flow to the modules at a rate of over 3 lb/min/kW, but it will not provide much more than this. Fan No. 4 of course could provide higher flows if allowed to exceed the 4.0 in. diameter limit. Flows of about 4.0 lb/min/kW are possible if the diameter is increased to about 4.5 in. The point is that rack width can be a limitation to the amount of cooling air provided to the modules, since fan sizes may be affected. This point is very significant when one considers rack designs with more than 260 - 5 watt modules, or racks with modules of average power greater than 5 watts.

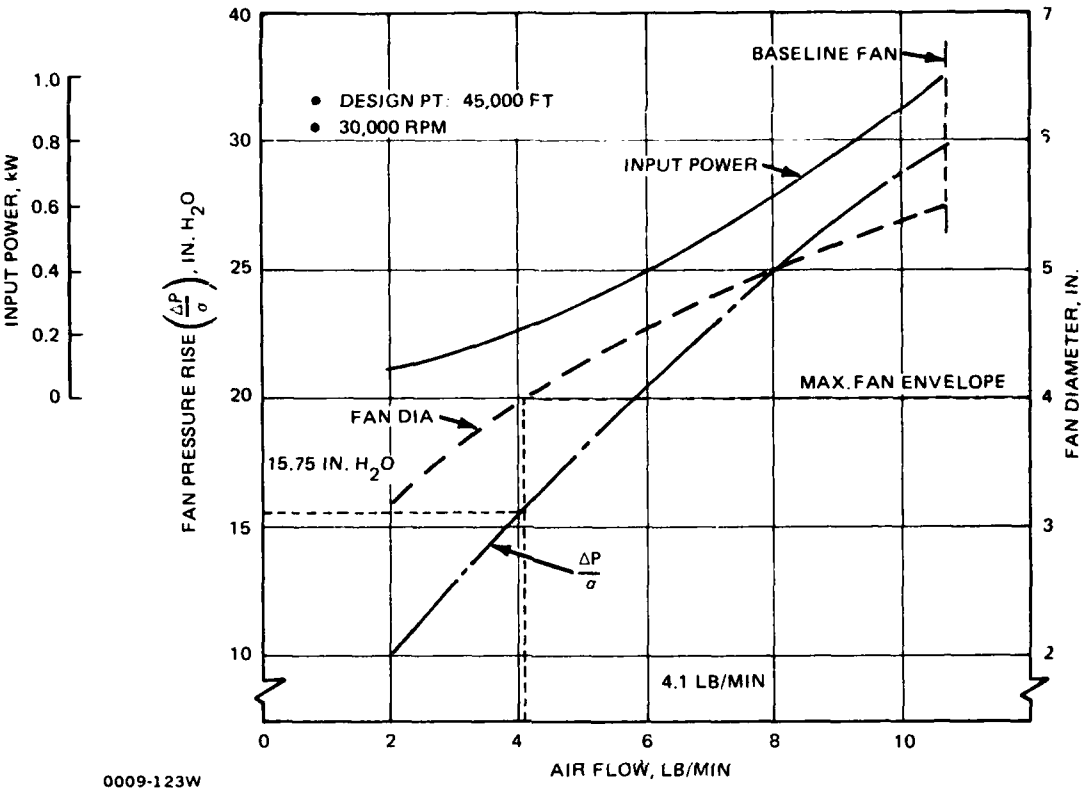

Figure 98 Fan Scaling Curves for AiResearch Fan 4, Candidate C

3.6.4.4 Rack Design C - Limitations - Rack design C has been found to be of limited value because of its size. It does not fit into the B V/STOL, and fits in only a few locations in A V/STOL. For this reason, the design has been screened from further considerations. While rack design C has some ECS limitations, it is not an unfeasible design from a cooling standpoint.

3.6.5 Integrated Avionic Rack - Humidity & Condensation Control

The configurations of both A and B V/STOL indicate that any avionic racks be located in unpressurized compartments. Since it would be impractical to seal the racks, all rack components are subject to the environment of the unconditioned equipment bays. For design purposes, it has been considered that the racks will be subject to air with a maximum moisture content of 180 grains per pound of dry air. The dew point at sea level corresponding to this absolute

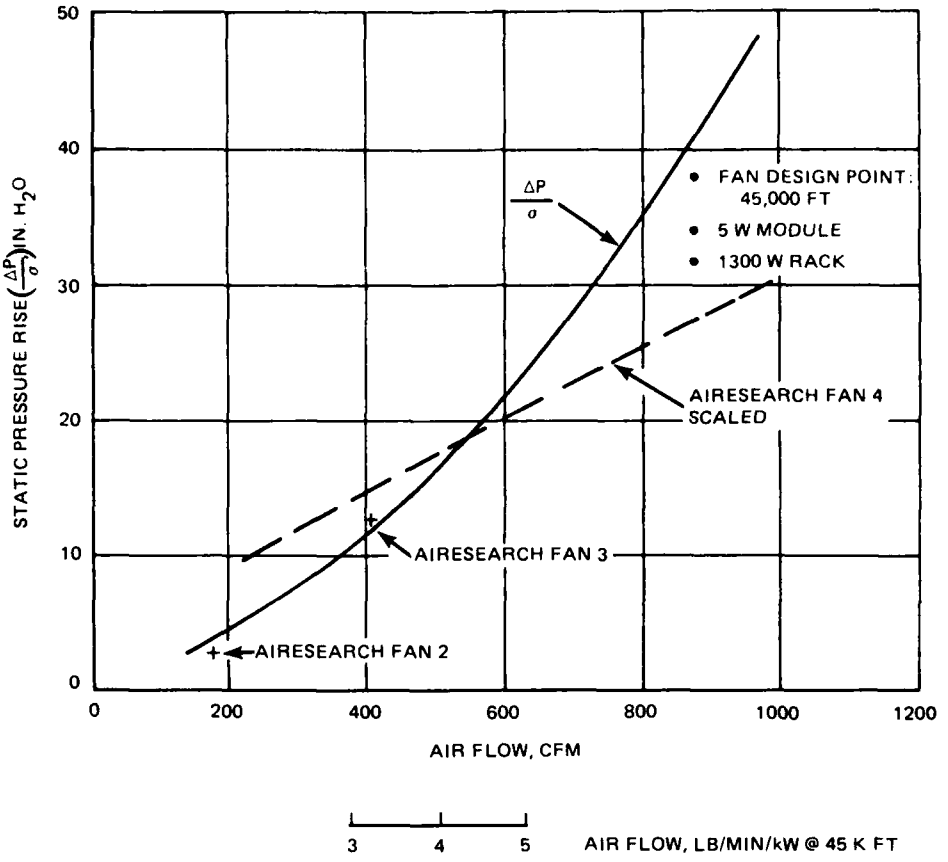

Figure 99 Fan Selection Data for Candidate C

humidity is 84.5°F. Both aircraft will operate at pressure altitudes up to 45,000 ft.

There are several conditions under which internal rack components may be subject to condensation. The potential for condensation exists when: 1) the relative humidity of the circulating cooling air is near the saturation point, 2) the circulating cooling air contains entrained moisture, 3) the heat exchanger rail temperature is below the dew point temperature of the internal rack air, 4) equipment allowed to cold soak at altitude is below the dew point temperature of air entering the rack as the aircraft descends, 5) in parked aircraft, racks containing air at high relative humidities cool overnight to temperatures below the dew point of the air.

The above indicate a spectrum of possibilities for condensation. Not all the rack designs, however, are subject to all of these condensation modes. Table 17 is a summary of these modes and the rack designs that are affected.

None of the rack designs that have been developed allow air from the aircraft ECS to be circulated over the electronic components. This air is always isolated, either by the heat exchanger rail, or by the intermediate Coolanol loop. Thus, the only source of moisture for the racks is internal air. Changes in internal air occur when the racks are opened or when changes in pressure altitude cause the racks to breathe. The exchange of internal rack air with the ambient should be small. The rack can be considered as a semi-closed system. The total amount of moisture available to be condensed is thus somewhat limited.

3.6.5.1 Dehumidification Process - One method of reducing the potential for condensation in a particular rack involves lowering the absolute humidity, and thus the dew point, of circulating internal rack air. This concept is illustrated on a psychrometric chart in Figure 100. Internal rack air enters a heat exchanger at some dry bulb temperature and relative humidity, as represented by point A on Figure 100. The air is first cooled to its saturation temperature, point B. As cooling continues, moisture condenses from the air on the heat exchanger surface. The air exits the heat exchanger at point C in a saturated condition, but

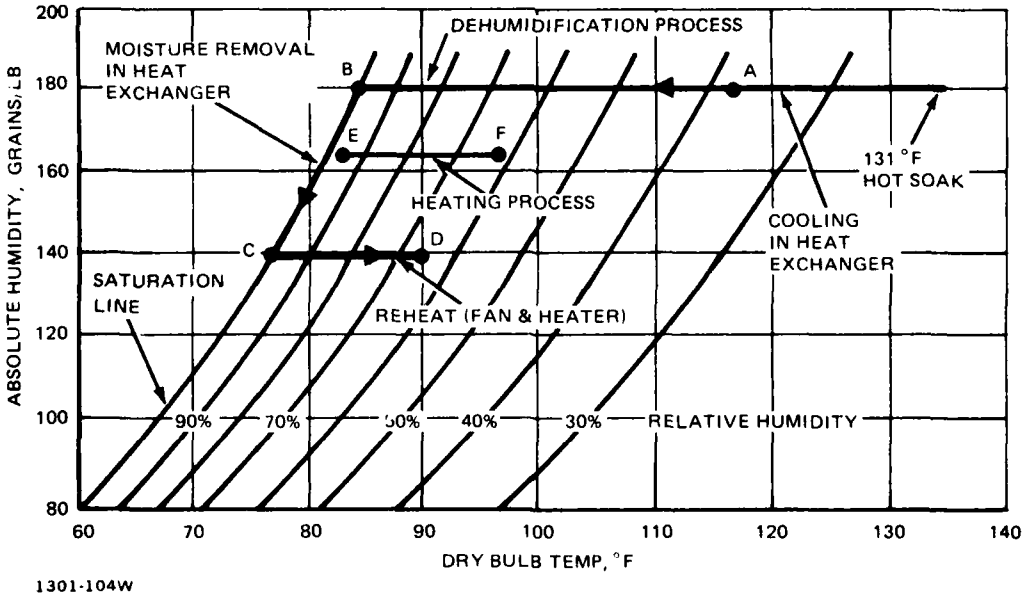

1301-104W

Figure 100 Dehumidification/Heating Processes Plotted on Psychrometric Chart

with a lower absolute humidity than at point A. Heat is added to the air by the fan and a heater, until the air is at 90°F, which is above the dew point of 84.5°F for air containing 180 gr/lb absolute humidity at Sea Level. This 'dried' air is circulated over the rack equipment to warm the components, and to absorb any condensed moisture. It is then routed back to the heat exchanger.

This method is effective in preventing condensation from any of the sources summarized in Table 18. It provides air to circulate over the components with a positive reduction in absolute humidity, as required by items 1 thru 3. It also provides dry warm air for warming cold soaked components as in items 4 and 5. This assures that the equipment is totally free of any condensed moisture prior to electrical operation. When the system is electrically turned on, the electric heater is shut off. The cycle can also be used after electrical shut down.

3.6.5.2 Heating Process - A second method for reducing condensation potential is a simple heating process. This is illustrated by path E-F in Figure 100. Before electronic start-up, a fan and heater are turned on. The circulating air is heated so as to reduce its relative humidity ratio. The warmed air can be used to eliminate cold spots on the equipment, due to altitude or over-night cold-soaks. Moisture absorbtion and heat transfer to the cold components will cool the air before it is recirculated thru the heater. This process, however, will

Table 18 Sources of Condensation

ITEM	SOURCES OF CONDENSATION	A_{21} AIR/COMP	B_{31} LIQUID RAIL	B_{32} AIR RAIL
1	R.H. OF COOLING AIR NEAR SATURATION TEMP	*	N/A	COMPONENTS ISOLATED
2	COOLING AIR CONTAINS ENTRAINED MOISTURE	NO SOURCE	NO SOURCE	COMPONENTS ISOLATED
3	H/X RAIL TEMP BELOW 84.5°F DEW POINT (A/C SUPPLY: 40° – 80°F; 3 – 5 LB/MIN/kW)	* 60°C MAX JUNCT	* 60° – 80°C MAX JUNCT	*
4	ALTITUDE COLD SOAK; DESCEND TO S.L.	*	*	*
5	OVERNIGHT COLD SOAK; RACK IN HUMID ENVIRONMENT	*	*	*
0009-089W	*CONDENSATION MAY OCCUR			

have a limited moisture absorbtion capability. Since there is no coil, the absolute humidity of the air cannot be reduced, and the total amount of moisture contained in the rack will be constant. Racks that have, for some reason, accumulated a moderate amount of condensate cannot be effectively dried out. This method will only work in reducing cold spots and high relative humidities either before electronic turn on or after shut down.

Candidate A_{21} - Dehumidification

The equipment required for cooling rack design A_2 can easily be arranged to include a dehumidification mode. The arrangement has been shown in Figure 79. The only additional components required are a Coolanol diverter valve and a heater, as shown in Table 19.

The dehumidification mode can be used to dry out the electronics before flight. The fans and the Coolanol supply will be turned on. The diverter valve will provide Coolanol from the interface heat exchanger to only the bottom rail of the rack. The fans will circulate air over the components in the normal manner. Moisture will be removed as the air is cooled in the heat exchanger. Reheat will be provided by the fan and heater to reduce the relative humidity of the air before it again circulates over the modules.

At sea level, the fan in a 5 tier rack will be circulating air at 0.38 lb/min. With all the Coolanol diverted to the bottom rail, it will be flowing at 5.9 lb/min. The temperatures and flow rates of the air provided at the interface heat exchanger will determine Coolanol temperature and ultimately rack internal air temperature as it leaves the lower rail. Figure 101 shows the resultant internal rack air supply temperature as a function of heat load at the interface heat exchanger for ECS flows of 3 to 5 lb/min/kW and temperatures of 40° to 80°F. Once rack air is cooled, it will be reheated only to 90°F, so as to be above the dew point of 84.5°F for air at sea level containing 180 grains/lb of moisture. Additional information provided in Figure 101 shows the heat load of the cooling air for a Sensible Heat Ratio of 0.80. It is cooled from 90°F to some lower supply temperature. The crossover points show the different air supply temperatures where the cooling capability of the system matches the heat load of the air.

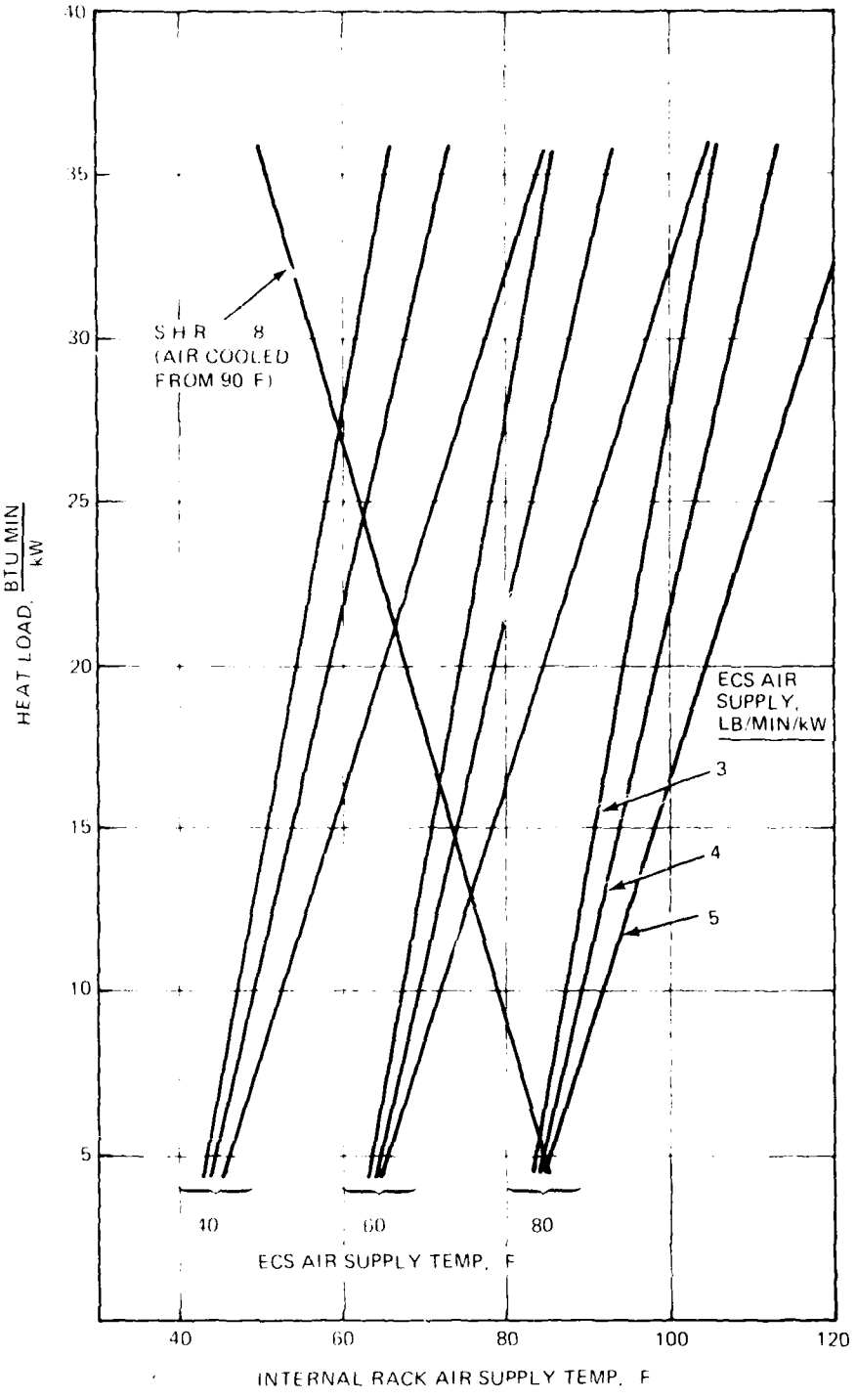

1301-066W

Figure 101 Dehumidification, Candidate A_{21}

Table 19 Rack Dehumidification & Heating Impact on Basic Rack Cooling Modes

COMPONENT	AIR OVER COMPONENTS A_2	CONDUCTION	
		B_{31} LIQUID RAIL	B_{32} AIR RAIL
DEHUMIDIFICATION MODE			
• DEHUMIDIFICATION COIL	INTEGRAL	ADD	ADD
• FAN	INTEGRAL	ADD	ADD
• HEATER	ADD	ADD	ADD
• COOLANOL 25 SUPPLY	INTEGRAL	INTEGRAL	N/A*
• COOLANT DIVERTER VALVE	ADD	ADD	ADD
• TEMPERATURE SENSORS	ADD	ADD	ADD
• RACK WEIGHT INCREASE	1.5 LB	2.9 LB	–
• RACK HEIGHT INCREASE	SAME	2 IN.	–
HEATING MODE			
• FAN	–	ADD	ADD
• HEATER	–	ADD	ADD
• TEMPERATURE SENSORS	–	ADD	ADD
• RACK ECS WEIGHT	–	0.8 LB	0.8 LB
• RACK VOLUME	–	1.0 IN.	1.0 IN.

*NO COOLANOL 25 SYSTEM IN A/C AIR COOLED COIL WILL NOT FIT IN RACK

0009-090W

Candidate B_{31} - Dehumidification

The basic cooling mode of design B_{31} is conduction to liquid cooled guide rails. Referring again to Table 19, the only component required for dehumidification that is integral to the basic cooling system is the Coolanol 25 supply. A heat exchanger, fan, heater and diverter valve will all have to be added to provide for moisture removal. It should be noted that air circulation is critical to any dehumidification scheme. The conduction rail is designed such that no provision for air flow thru the rail is available, as in the air/liquid heat exchanger design of rack A_{21}.

An alternate path for air flow has been found, and is shown in Figure 102. A 0.6 x 0.9 in. opening exists at the top and bottom of each ISEM-2A module. Air can be ducted up the front of the rack between the door and the module. Midway up each module, a gasket on the door, used to hold the modules in position will also serve as a block to the airflow. This will force the air to enter the

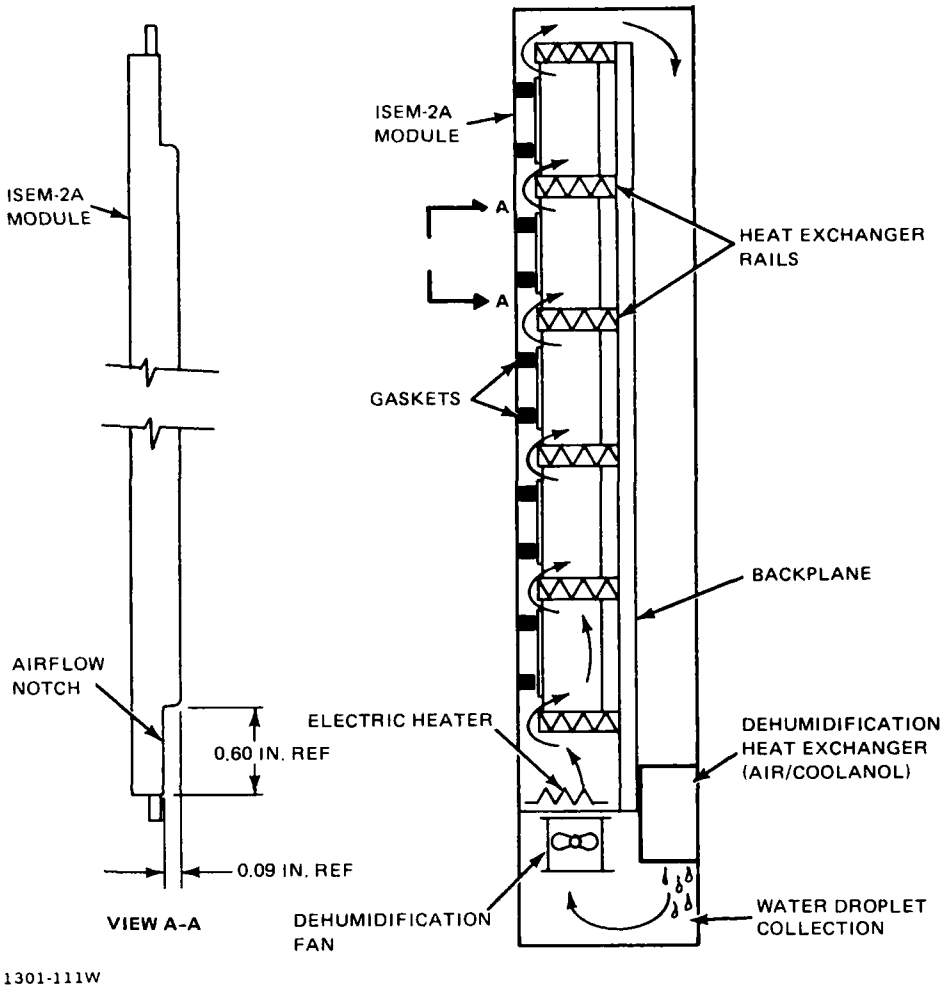

Figure 102 ECS Components & Flow Paths, Candidate B_{31}

modules through the 0.6 x 0.09 in. opening, and flow over the components. It will exit at the upper opening. This process will be repeated for each tier of modules. At the top of the rack, the air will be ducted down behind the backplane to an air liquid heat exchanger. Here the cooling process will remove moisture, which can be collected at the bottom of the rack. The air then is turned upward and passes thru the fan and heater, which lowers the relative humidity, before being recirculated over the cards.

The dehumidification process is expected to be used at low altitudes or sea level. The normal flow of Coolanol will be diverted from the cooling rails to the dehumidification coil. The fan and heater will be energized only during the dry-

out process. Figure 103 shows the pressure loss for the dehumidifying air flow. A fan size on the order of Rotron's Aximax 2E will provide a circulation flow of about 18 CFM. This fan, however, is configured with a 400 Hz. ac motor. A dc motor would be required to be compatible with rack power supplies. The Coolanol heat exchanger has been sized as a crossflow plate-fin design. Its dimensions are 2.0 in. air side, 8.0 in. Coolanol side with a 1.60 in. stack. Its effectiveness map for a range of air and coolanol flows is presented in Figure 104.

The dehumidification heat exchanger will be supplied Coolanol at 2.64 lb/min for a 5 tier rack design. The temperature and flow rates of the ECS air supplied at the interface heat exchanger will, however, determine the coolanol supply temperature, and ultimately the temperature to which internal rack air

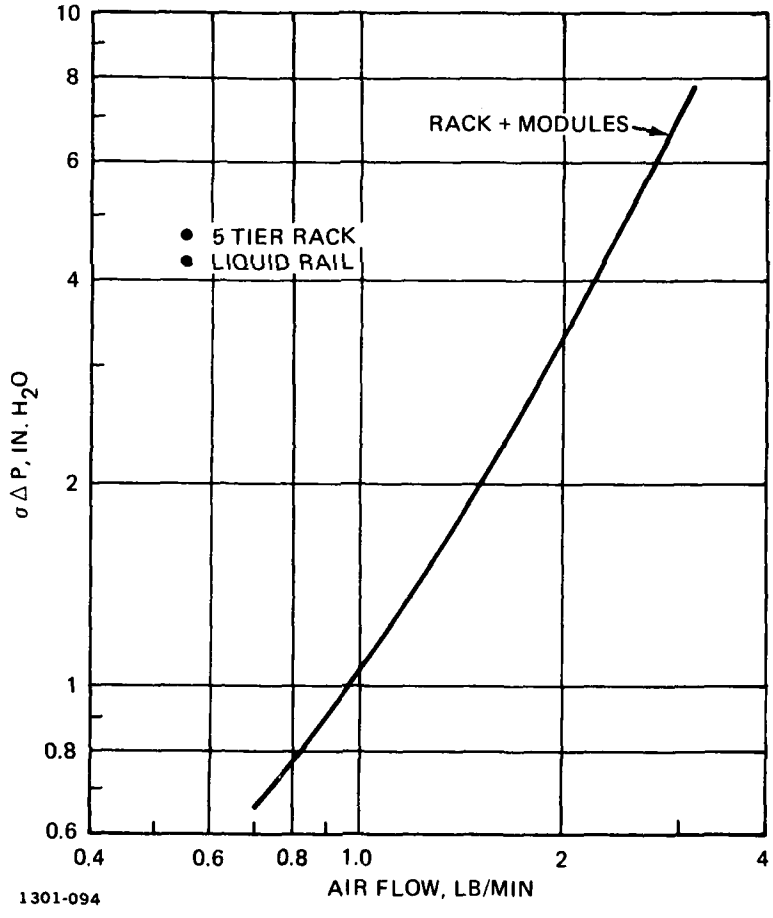

Figure 103 Total Rack Pressure Loss, Candidate B_{31}, Dehumidification Air

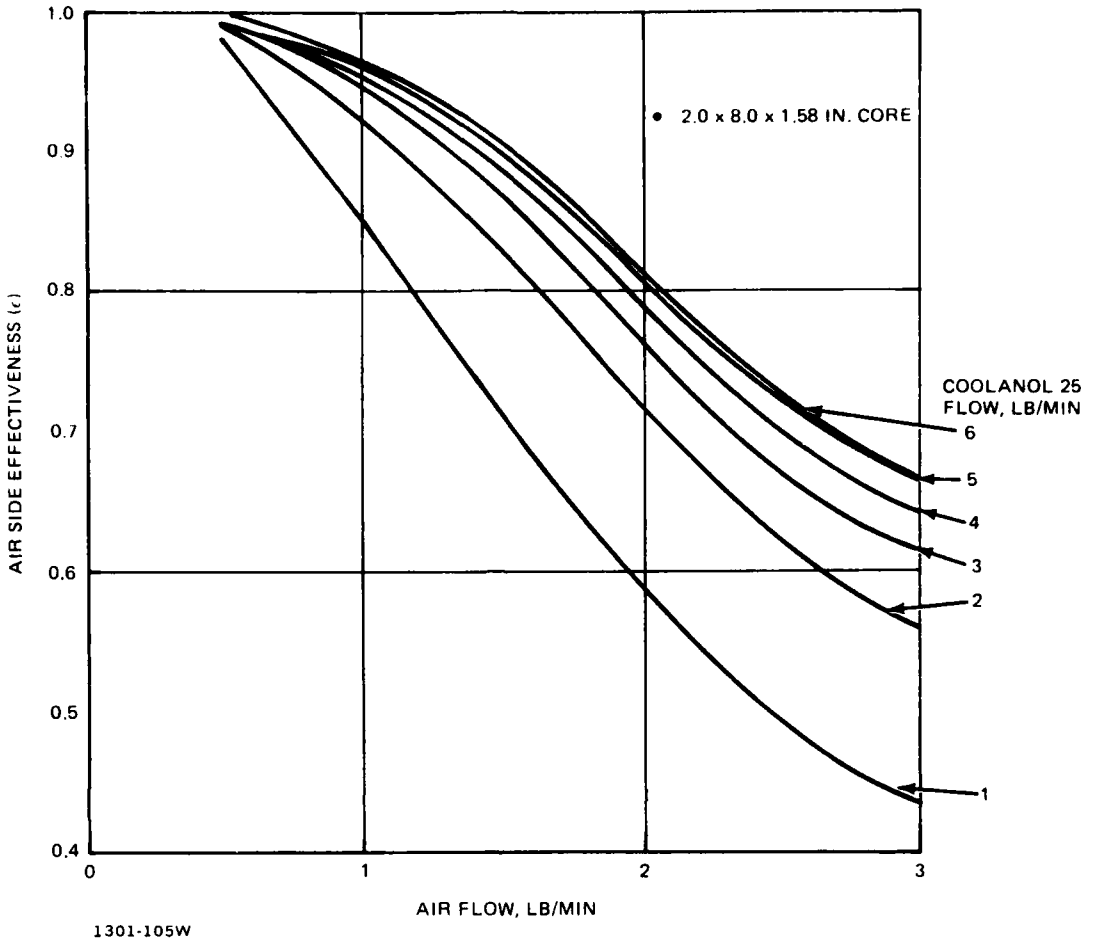

Figure 104 Dehumidification Heat Exchanger Performance, Candidate B_{31}

can be cooled to. Figure 105 shows the resultant rack air supply temperatures as a function heat load for ECS supply temperatures of 40° to 80°F and ECS supply flows of 3.0 to 5.0 lb/min/kW. Cooled rack air will be reheated to 90°F prior to circulation over the components, where it absorbs moisture. The moist air entering the heat exchanger will have to be cooled from 90° to a temperature near the coolanol supply temperature. Figure 105 also shows the heat load that must be removed from this air as it is cooled from 90°F to a given supply temperature, for a Sensible Heat Ratio of .80. The crossover points illustrate where system cooling capability matches the system heat load requirements.

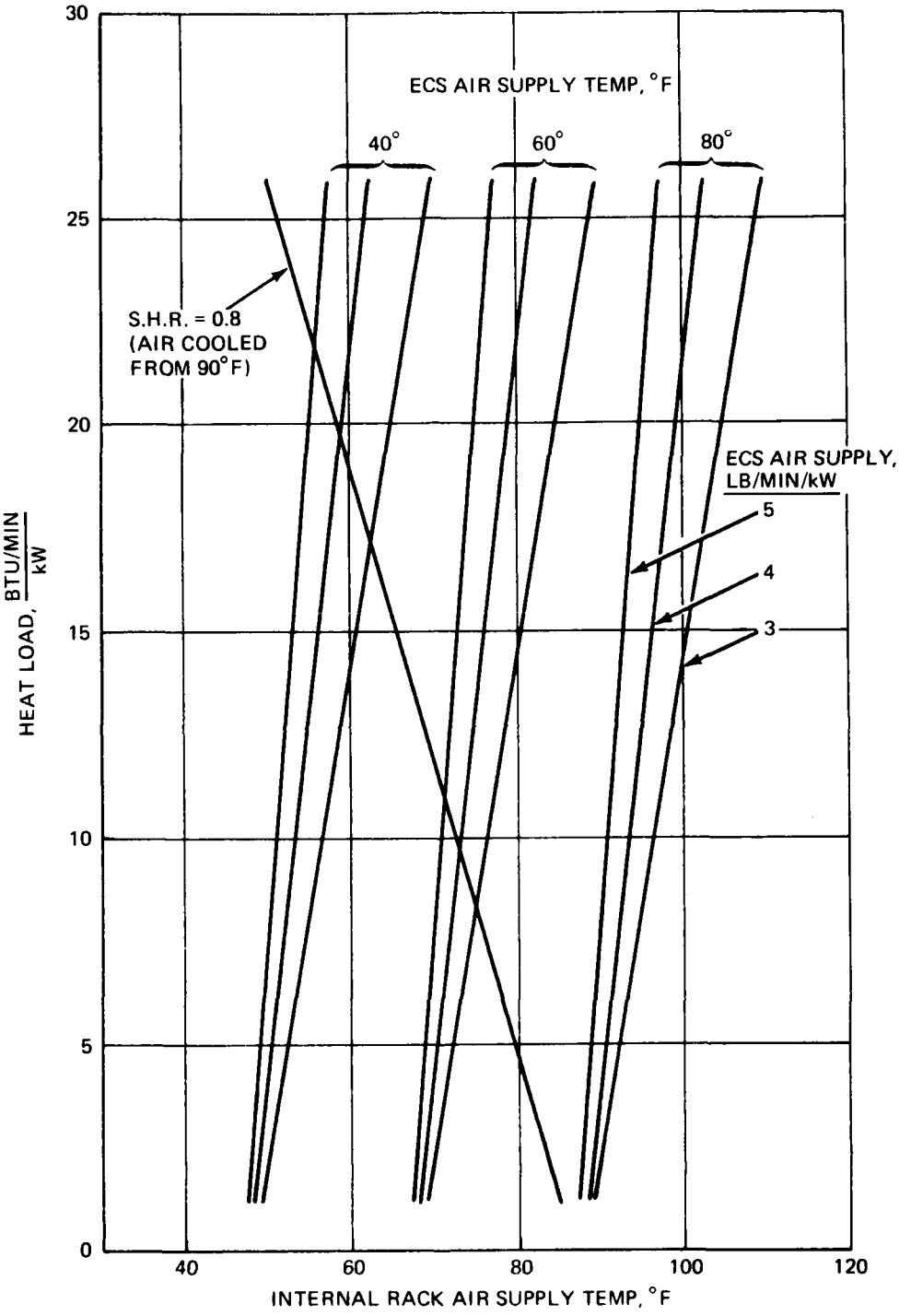

1301-067W

Figure 105 Dehumidification, Candidate B_{31}

Candidate B_{32} - Heating

This rack design utilizes the conduction mode with an air cooled guide rail. Since Coolanol is not used for basic cooling, it is not available for a dehumidification coil. The volume required for an air to air heat exchanger appears to be prohibitive. Preliminary calculations place the core size at 5.0 in. recirculating air side, 8.0 in. ECS air side, and 2.0 stack height. A core of this size will not fit in the rack B_{32} without a major modification.

For this rack design, a fan and a heater can be provided to lower the relative humidity of the internal rack air or to warm cold spots, prior to electrical turn on. Once the rack electronics is turned on, the fan and heater are shut down. The fan would be the same as sized for design B_{31}. The heater would be thermostatically controlled to 90 or 100°F, a temperature above the dew point of 84.5° for air containing 180 gr/lb of moisture at sea level.

3.6.6 Rack Designs for ISEM-2A Modules Dissipating 10 Watts

In the first portion of the study, racks containing ISEM-2A modules dissipating 5 watts each were considered. The three most favorable designs resulting from this effort have been reconsidered for modules which dissipate 10 watts of power. The candidates are: A_{21} AIR OVER COMPONENTS; B_{31} LIQUID COOLED CONDUCTION; and B_{32} AIR COOLED CONDUCTION. Both conduction designs require only minor modifications to accommodate the higher heat load. The AIR OVER COMPONENTS design A_{21}, however, becomes unfeasible with the higher power dissipation requirement. System pressure losses are so high under some flight conditions that it becomes impossible for reasonably sized fans to deliver the required cooling airflow. This will be discussed more fully in the following section.

3.6.6.1 Candidate A_{21} - Air Over Components - 10 Watt Module - The basic configuration of the 5 tier rack designed for the 5 watt module is unchanged when considering a 10 watt module. The fan heat exchanger rail sizing though, had to be reevaluated for the higher power. However, no functional changes to the operation of the rack or to the intermediate liquid cooling system were considered. Figures 78 and 79 apply equally in picturing the operation of the 5 and 10 watt A_{21} concepts.

Heat Exchanger Rail

The core configuration and dimensions of the rail heat exchanger did not require revision for the 10 watt per module heat load. The increased heat transfer was accomplished strictly by a revision of air and Coolanol 25 flow rates. The weight flow of the cooling air supplied by the fans, considered over the range of 3 to 5 lb/min/kW, was simply assumed to be doubled in going from racks with 5 watts per module to racks with 10 watts per module. Thus, the air flows at the heat exchanger rails for a 10 watt module were 0.78 to 1.30 lb/min, compared to 0.39 to 0.65 lb/min for the 5 watt module. The Coolanol 25 flow rate however, only required a 50% increase, from 2.0 lb/min at 5 watts to 3.0 lb/min at 10 watts to provide good heat exchanger rail performance. This represents a decrease in flow rate per kilowatt from 15.4 lb/min/kW at 5 watts to 11.4 lb/min/kW at 10 watts. This relative reduction in flow rate per kilowatt is due to the rapid increases in the convective heat transfer coefficient between the Coolanol and the fin surfaces, which occur when the Coolanol 25 flow is increased from 2.0 to 3.0 lb/in. The performance increase is significant enough to preclude the need to double the Coolanol 25 flow rate and maintain the higher weight flow rate per kilowatt of 15.4 lb/min/kW. The air side effectiveness curves, presented in Figure 80 remain valid for the 10 watt module rack design.

The heat exchanger rail performance, in terms of air side and liquid side pressure losses are the same curves as presented for 5 watts per module, Figures 81 and 82.

Interface Heat Exchanger

As in the 5 watt rack design, the interface heat exchanger was sized to accommodate a Coolanol flow which was optimized for the rack mounted heat exchanger rail. As mentioned this flow was 11.5 lb/min/kW. Again, ECS cooling air was supplied at 3 to 5 lb/min/kW at 40° to 80°C. The lower table in Figure 86 illustrates the temperatures available at different points in a 10 watt rack system for an ECS air supply of 40°F. The air supply temperature to the module (last column) can be used in conjunction with Figure 59 to determine the component junction temperatures. Figure 106 however, nicely summarizes the

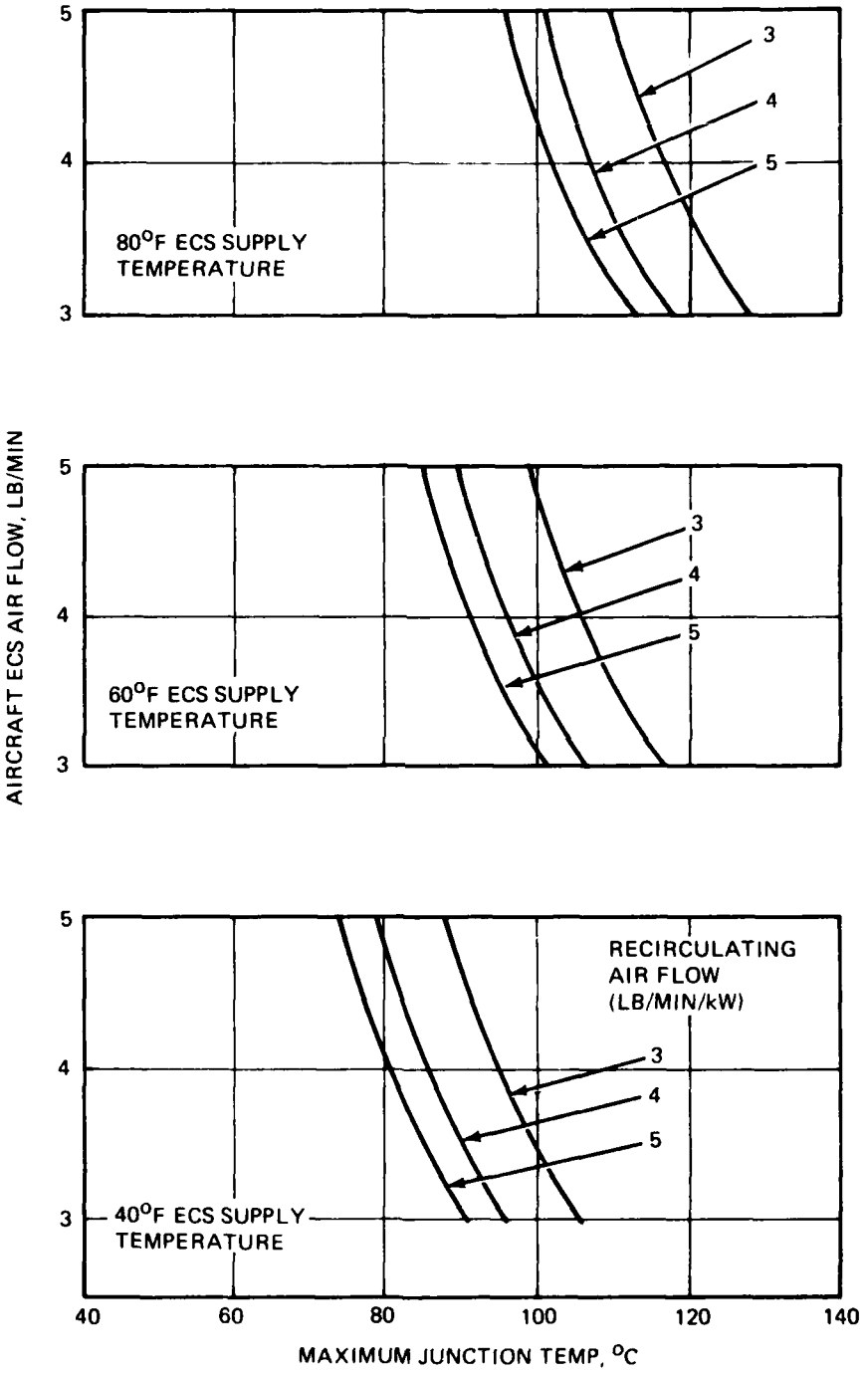

0009-091W

Figure 106 Candidate A_{21} Performance, 10 W/Module

expected 10 watt rack performance in terms of maximum module junction temperature for the range of ECS flow rates and temperatures considered, and for fan supplied flow rates of 3 to 5 lb/min/kW. Further, a comparison of 5 and 10 watt rack design performance, in terms of module maximum and average junction temperature, can be made by referring back to Table 16. The performance in both cases looks good, until one considers the fan requirements to deliver these flows.

Fan Sizing

As Figure 84 shows, rack size, in terms of the number of tiers, and increasing airflow both serve to increase the pressure losses experienced by the recirculating air. In order to maintain the same air flow per kilowatt (lb/min/kW) as the 5 watt design, the weight flow (lb/min) of air supplied to the modules must be doubled for the 10 watt case. This requirement, along with the necessity to operate the racks at altitude in unpressurized compartments, combine to make severe demands on the sizing of a recirculation fan. Figure 107 illustrates this problem. The airflow per kilowatt is plotted against normalized static pressure losses ($\Delta P/\sigma$) for rack sizes of 3, 4 and 5 tiers, at pressure altitudes of 35,000, 40,000 and 45,000 ft. A normalized static pressure loss ($\Delta P/\sigma$) of 20 in. H_2O is considered to be about the upper limit for fans designs that do not exceed the 4.0 in. width of the rack. Under these restrictions, as Figure 105 shows, even a 3 tier rack cannot operate at 45,000 ft, the service ceiling for both the A and B V/STOL. Further, 4 and 5 tier racks cannot be operated even at 35,000 ft. The inability of the 4 and 5 tier rack designs to operate at altitude preclude their use in the unpressurized compartments of A and B V/STOL aircraft. While a 3 tier rack is not as severely limited by aircraft altitude, the large volume and weight devoted to fans in each rack (see Figure 11) make this design A_{21} for 10 watts per module noncompetitive with other rack designs considered in this study.

3.6.6.2 Candidate B_{31} - Conduction, Liquid Rail - 10 Watt Module - As in the A_{21} air-over-components design, no functional changes to the B_{31} rack were considered necessary for the 10 watt per module design. The temperature difference between a component junction and the wall of the coolant passage has been fixed by the selection of a module power of 10 watts, and is unalterable by

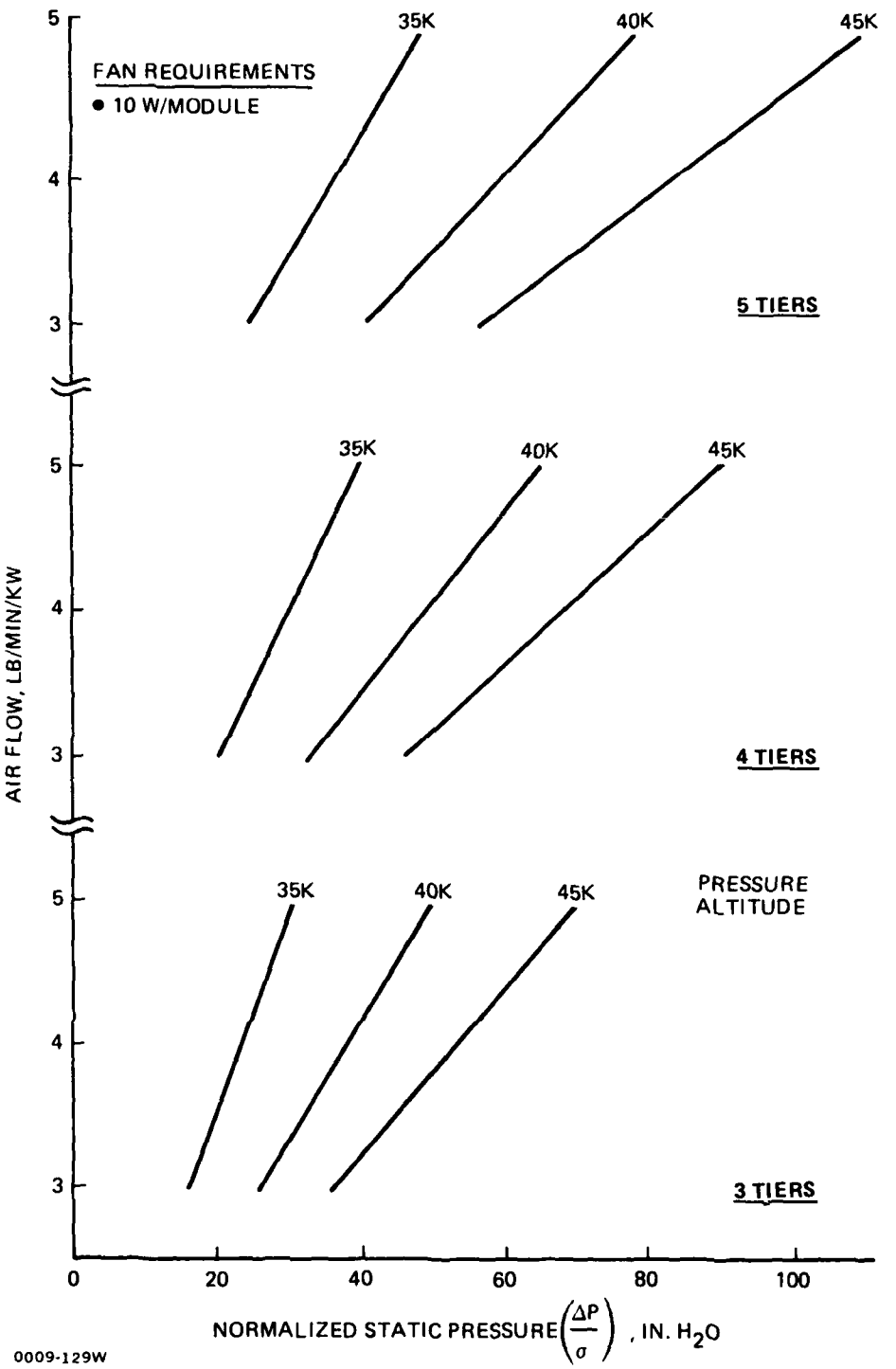

Figure 107 Candidate A_{21} Fan Requirements, 10 W/Module

ECS considerations. The temperature difference between the passage wall and the coolant, however, is affected by the fin configuration selected and flow rate of the coolant supplied. These two items constitute the areas investigated for the 10 watt Liquid Conduction rail design.

For the 5 watt design, many fin configurations were analyzed and their performance compared. The two fins best suited for the job were fins 52 and 58, standard designs from the Grumman Raves System E10 Computer Program Library. Their performance was very similar at the 5 watt power. At 10 watts however, the performance difference became magnified, with fin 58 being the best performer. Figure 108 is a plot of the temperature difference from an aft module maximum junction temperature to the coolant supply temperature, as a function of Coolanol 25 flow rate. In the flow range of 2 to 4 lb/min, the temperature difference T_{j-s} is 12°F less for fin 58 than for fin 52. Thus, using fin 58 results in an almost a 7°C lower maximum component junction temperature than would result with fin 52 at the same Coolanol in flow and temperature conditions.

The performance of the interface heat exchanger must be considered when selecting a flow rate to be supplied to the rails. The range of air temperature and flow rates provided by the aircraft ECS to the interface heat exchanger has been fixed to enable comparison of one rack design to another. In addition, the hot side Coolanol inlet temperature has been established to be 10°F above the exit temperature of the ECS air. This ground rule assures that the interface heat exchanger will be of reasonable size and weight. Under these conditions, the temperature reduction experienced by the liquid in the interface heat exchanger is strictly a function of flow rate. This can be understood by considering the following equation:

$$Q = W\ Cp\ \Delta T$$

where

Q = BTU/min

W = lbs/min

Cp = BTU/lb-°F

ΔT = °F

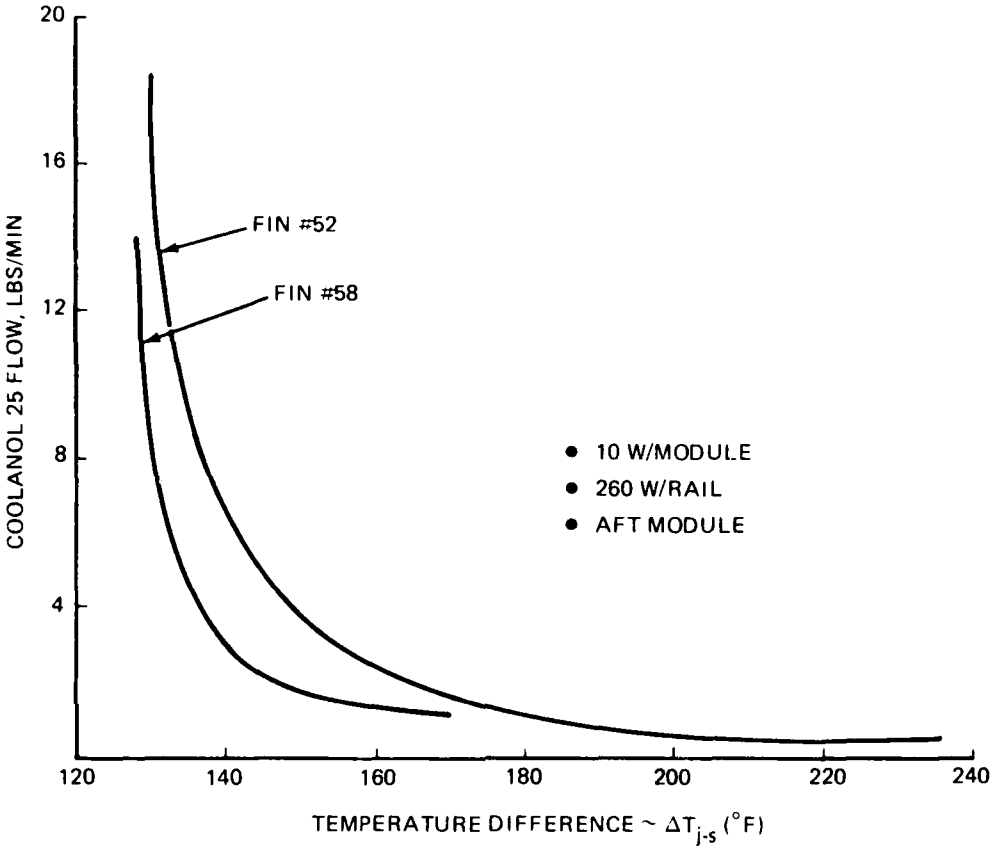

0009-136W

Figure 108 Module Junction to Coolanol Supply Temperature, Candidate B_{31}

which can be rearranged as follows:

$$\Delta T = \frac{Q}{WCp}$$

For a given heat transfer rate, the temperature reduction experienced by the Coolanol 25 in the interface heat exchanger is an inverse function of the Coolanol flow rate. That is, if the Coolanol flow rate is increased, the temperature reduction (ΔT) is decreased. A Coolanol flow rate of 2 lb/min has a ΔT in the interface heat exchanger of 16°F while a flow of 4 lb/min has a ΔT of 8°F. In

other words, for the same inlet temperature at the interface heat exchanger, Coolanol can be supplied to the modules 8°F colder if the flow rate is 2 lb/min than if 4.0 lb/min were supplied.

Referring back to Figure 108 and fin 58, the temperature difference from the module component junction to the coolant supply temperature can be reduced 10°F by increasing the Coolanol 25 flow rate from 2 to 4 lb/min. Thus, at 2 lb/min the Coolanol is provided 8°F colder than at 4 lb/min, but the difference between the Coolanol supply temperature and the module maximum junction temperature is just 10°F higher than at 4 lb/min. In effect, the same module maximum junction temperature is delivered whether the Coolanol 25 is supplied at 2 lb/min or at 4 lb/min. The lower flow rate was selected to minimize pressure losses and therefore pump input power.

The performance of the liquid guide rail for 10 watts per module is presented in Figure 109. The aft module maximum junction temperature of 60°, 80°, 100° and 125°C are plotted for ECS air flow rates of 3 to 5 lb/min/kW as a function of ECS air supply temperature. In addition, the performance of the 5 and 10 watt configurations can be compared on the basis of maximum and average junction temperature in Table 17. This figure also presents data from the B_{32} Air-Cooled Conduction rail so that the two configurations B_{31} and B_{32} can be compared.

The pressure loss of the individual heat exchanger rails and the losses for a typical 5 tier rack are presented in Figure 110. The total rack losses include friction losses, turning losses and extraction losses for the entire system of Coolanol distribution and collection ducts which are inside the racks.

3.6.6.3 Candidate B_{32} - Conduction, Air Rail - 10 Watt Module - The redesign of the B_{32} rack for a module power of watts followed a procedure very similar to that used for the redesign of B_{31} Liquid Conduction rail. That is, the fin configuration for the guide rail and the coolant flow rate were the principal areas of investigation. It is important to note, though, that the temperature difference between a module component junction and the wall of the coolant passage (ΔT_{j-w}) has been fixed by the selection of a module power of 10 watts. This temperature difference is by far the most significant portion of the total temperature difference between a module component junction and the coolant supply

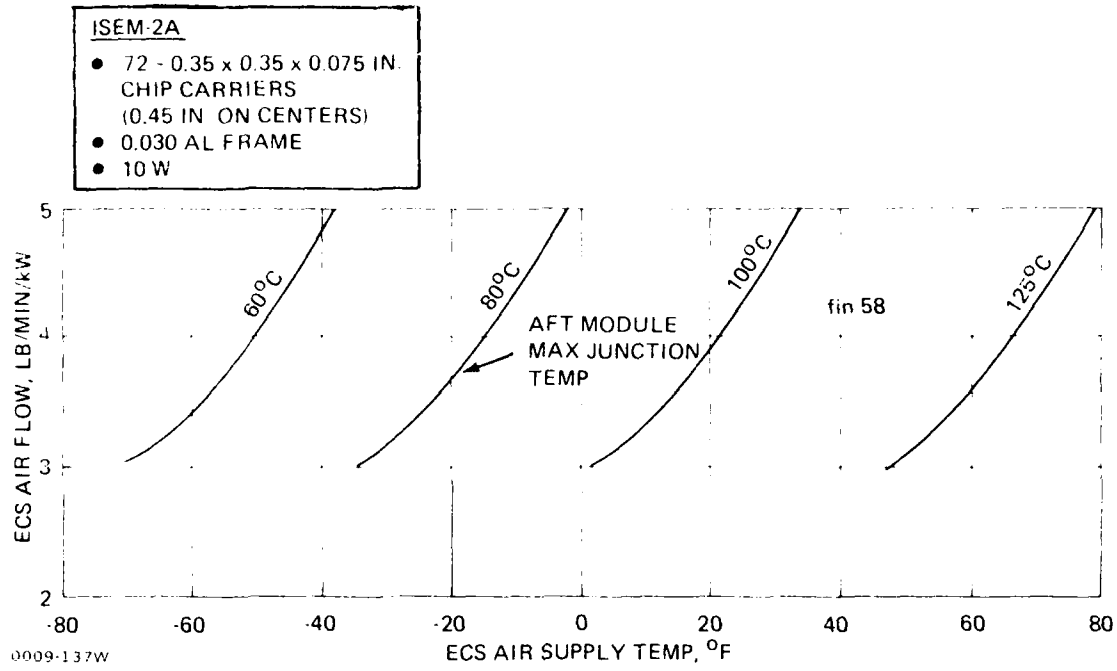

Figure 109 ECS Performance of Candidate B_{31}

temperature (ΔT_{j-s}). No matter how good the cooling system performance, this difference (ΔT_{j-w}) cannot be reduced.

The fin design selected for the 5 watt module was reinvestigated for the 10 watt design along with other additional candidates. The fin used at 5 watts was fin 10-60 from Kays and London's text, Compact Heat Exchangers. At 10 watts a comparable fin M2, was identified from the Grumman Raves E10 Computer Program Library. The performance of the two fin configurations were almost identical at 10 watts. It was found, however, that fin M2 exhibited a significantly lower pressure drop than fin 10-60 at comparable flow rates. Figure 111 illustrates the performance of a 10 watt conduction air rail with fin M2 for the aft module maximum junction temperatures of 60°, 80°, 100° and 125°C, as a function of ECS air flow and ECS air supply temperatures. Table 17 presents the performance in tabular form so that the air rail may be compared to the liquid rail performance at 5 and 10 watts. Figure 112 shows the performance improvement in terms of pressure drop gained by using fin M2 over fin 10-60.

The results presented in Table 17 require the 10 watt conduction module to be cooled at an ECS flow rate of 5 lb/min/kW. This would be consistent with Grumman's derating policy which would not permit maximum junction tempera-

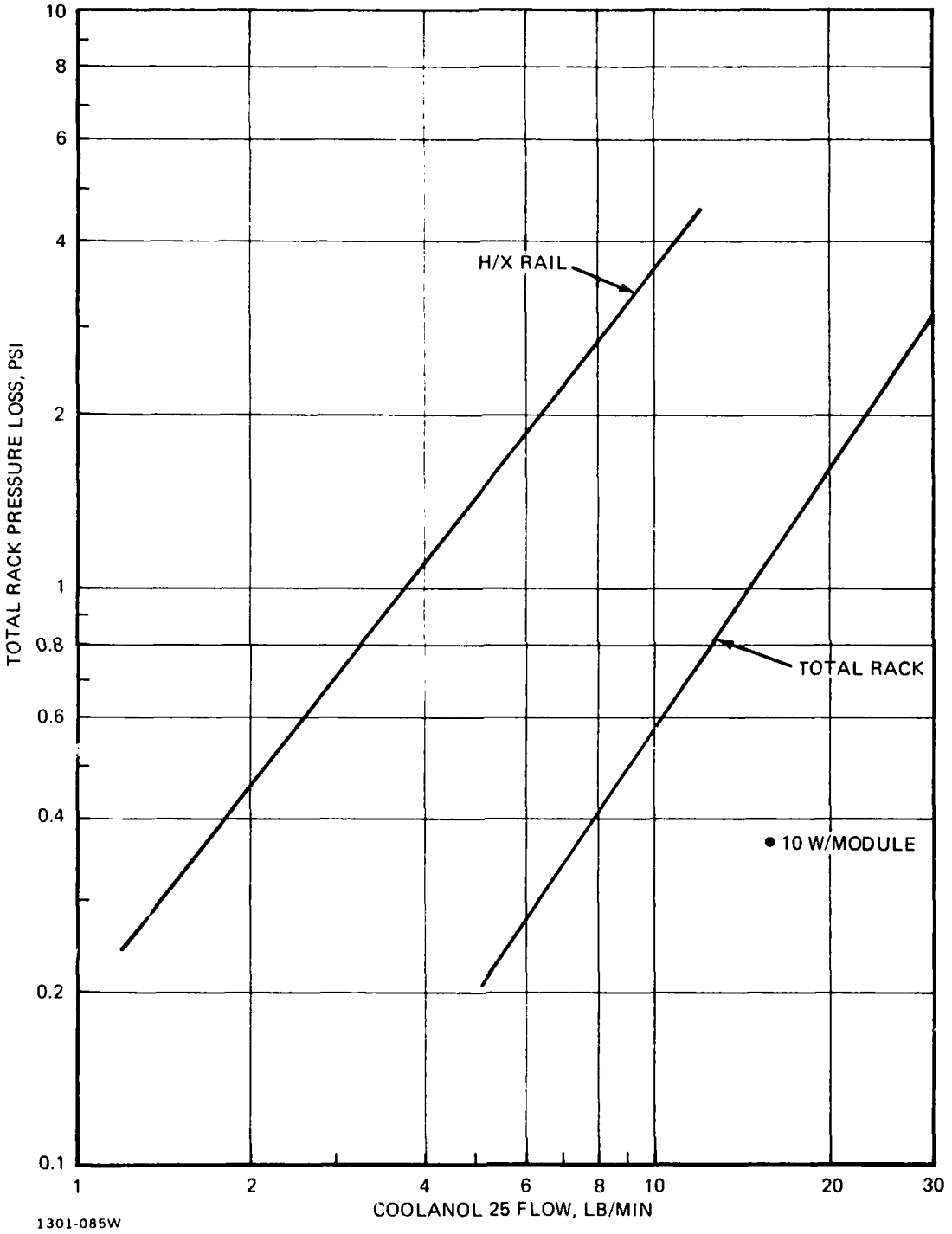

Figure 110 Total Rack Pressure Loss, Candidate B_{31}

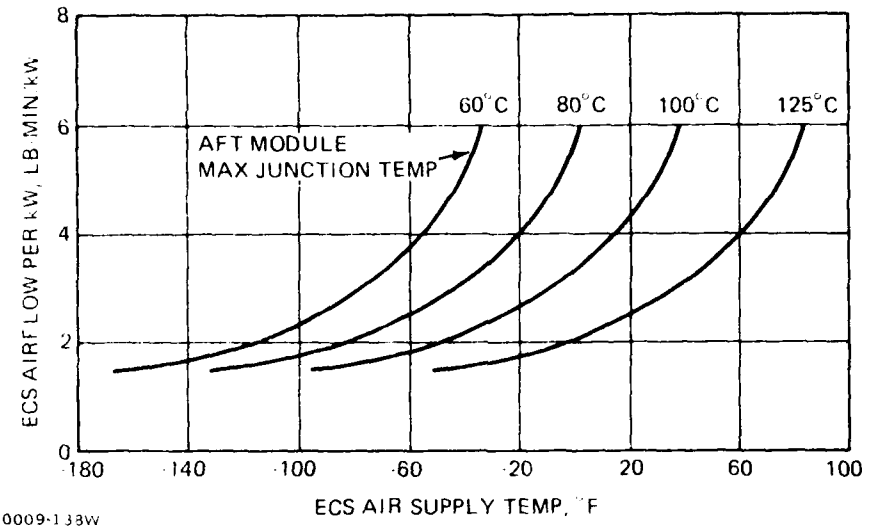

Figure 111 Candidate B_{32}, 10 W/Module

ture to be greater than 110°C.

The primary reason for the good performance shown by the B_{32} air rail is that the ECS air can be used directly in the rail. Both A_{21} air-over-components and B_{31} liquid cooled rails require an interface ECS air to Coolanol 25 heat exchanger, before coolant can be supplied to the rails. The net effect due to the inevitable inefficiencies of the liquid/air heat exchanger is that coolant cannot be supplied to the heat exchanger rails in the racks A_{21} and B_{31} as cold as would be possible if ECS air could be supplied directly.

3.6.7 Candidate D - Hollow Core ISEM-2A Modules

3.6.7.1 System Description & Operation - In the discussion of the previous rack designs, two separate and distinct modes of cooling ISEM-2A modules have been considered. The first method consists of passing cooling air along the long dimension of the module directly over the component surface. The second method considered conducting the component heat to the aluminum frame of the module, and then along the long dimension of the frame to cold-plate heat sinks. Both methods have their limitations, which have been discussed. The hollow core ISEM-2A module cooling concept has been proposed as a way of overcoming limitations of the previous two concepts.

The basic configuration of the core board module has been shown in Figure 29. The module itself is constructed around an internally finned air passage. Airflow through the module is along the long dimension. The heat of the compo-

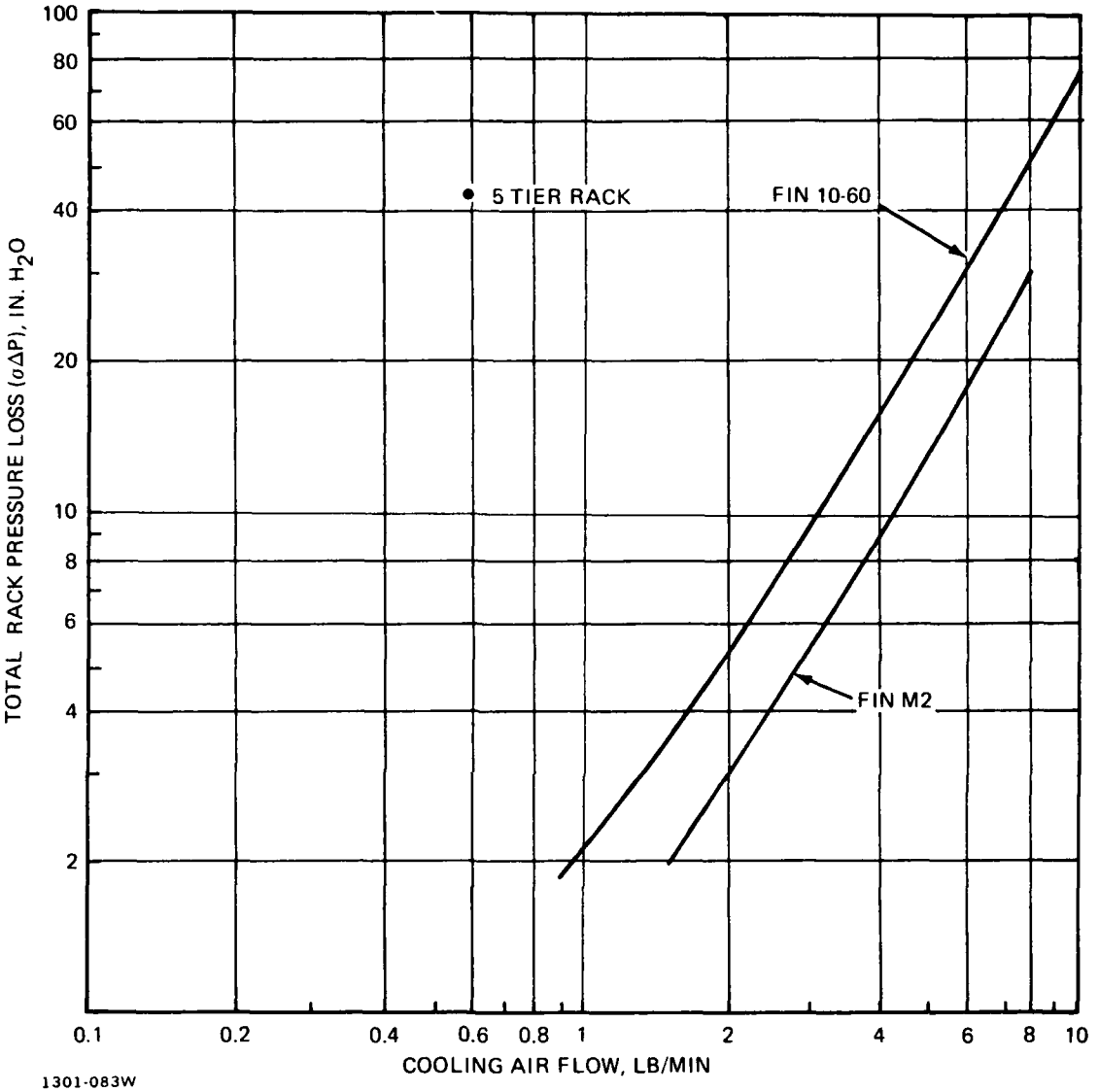

Figure 112 Total Rack Air Pressure Loss, Candidate B_{32}

nents is conducted to the air passage wall and is then convected to the flowing air.

The rack designed for the hollow core module has been shown in Figure 20. The baseline configuration has 5 tiers of 26 modules each. Air inlet and exhaust plenums are provided along the full length of each side of the rack. The core of each card is supplied a flow of cooling air from a distribution manifold attached to the inlet plenum. The airflow from each row of modules is collected by an exhaust manifold and ducted to the side exhaust plenum. From here the warmed

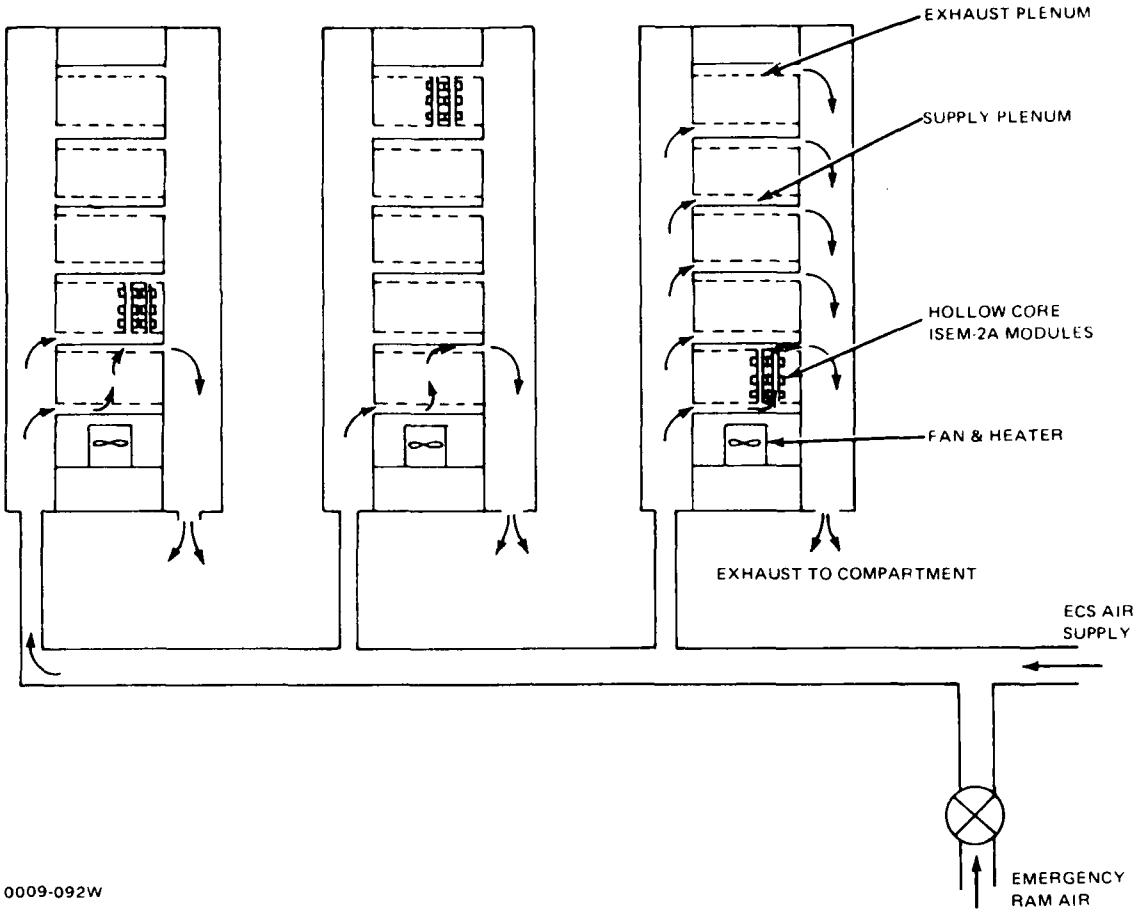

Figure 113 ECS Components & Flow Paths, Candidate D, Hollow Core ISEM-2A

air is dumped into the aircraft compartment. The rack air supply system, and the internal rack flow paths are shown in Figure 113.

The hollow core rack is similar to rack B_{32} conduction air rail in that the module components are completely isolated from the flow of cooling air. Therefore, the use of moist cooling air directly from the aircraft ECS or ram air, in an emergency, will not contaminate the components. As a result, an interface system between the aircraft ECS and the racks is not required, thereby saving weight and cost. In addition, the use of aircraft ECS air directly will yield the lowest component maximum junction temperatures attainable, because the coolant supply temperature is the lowest available. The inefficiencies of an intermediate thermal loop between the rack and the aircraft ECS can only result in coolant supply temperatures to the modules that are higher than a direct feed approach.

3.6.7.2 Hollow Core ISEM-2A - The hollow core ISEM-2A was originally considered with no internal fin. However, it quickly became obvious that the use of a finned core had large advantages. For one thing, the thin flat walls of the card require stiffening to support the internal pressures exerted by the flow of cooling air. Internal fins will provide that support. More important, however, they provide a significant reduction in module maximum junction temperature by improving the heat transfer between the module wall and the flowing cooling air. The fin configuration selected for the module has been presented in Figure 77. The penalty that must be paid for the performance improvement is an order of magnitude increase in the module airflow pressure loss. Figure 114 shows the pressure loss for the internally finned core board module. It is important to note, however, that aircraft ECS air supply usually has the capability of a pressure head of several pounds per square inch (PSI) if required. It will be shown that the r ck D losses are not nearly that large.

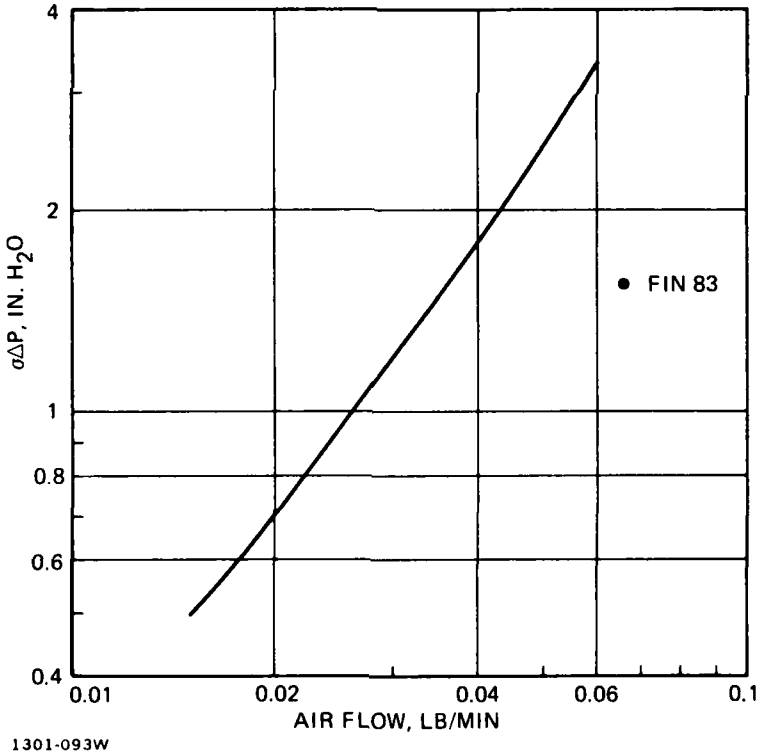

Figure 114 Hollow Core ISEM-2A Module Air Pressure Loss, Candidate D

3.6.7.3 Module Air Distribution Manifold - The modules, in each row of 26, are fed cooling air in a parallel fashion. Ideally, the duct supplying the modules should be designed as an infinite reservior, where the total pressure is constant throughout. However, it was estimated that for this rack, at flows of 3 to 5 lb/min/kW, the supply duct would have to be 1.4 in. wide by 1.0 to 1.7 in. deep. The width is not a problem, but the depth is excessive. A single row of modules 5.75 in. high would require 2 to 3 inches total for the depth dimension of inlet and exhaust plenums. The supply duct was therefore designed as a manifold, where the air distribution to the modules was the variable. It was felt that this approach was the only viable one because metering the air flow to each module would be a nearly impossible task.

A flow cross section of 1.4 by 0.40 in. was selected for the supply duct. The resultant module airflow distribution is shown in Figure 115 for total rack flow rates of 3 to 5 lb/min/kW. It shows that each module along the rail operates with a different cooling airflow rate, and consequently a different maximum component junction temperature.

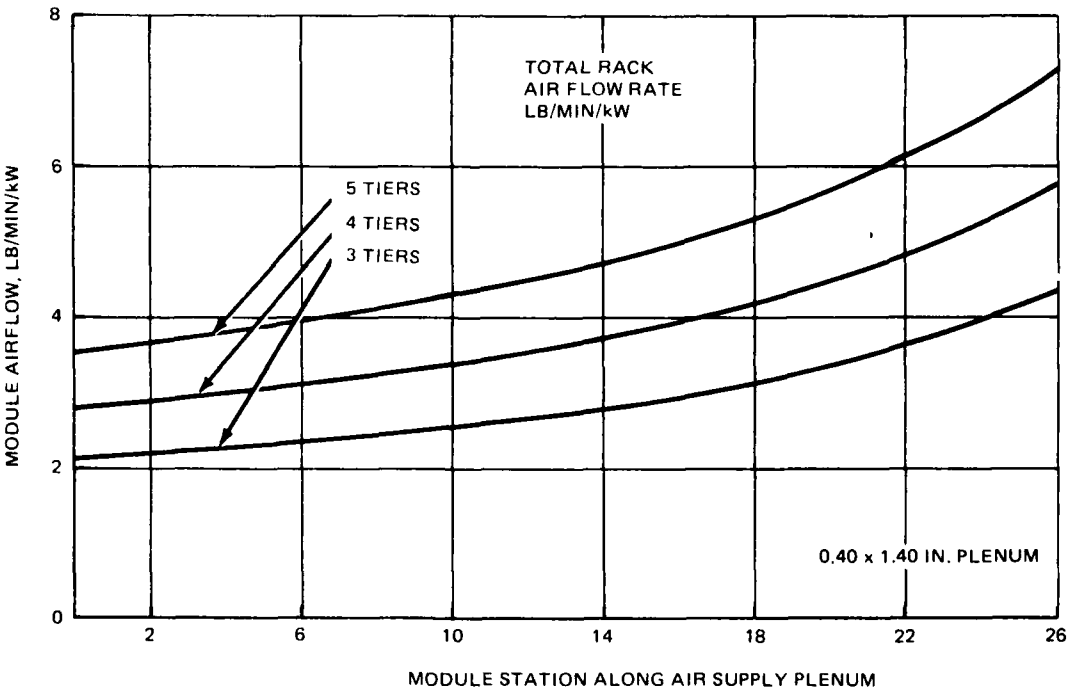

1301-106W

Figure 115 Hollow Core ISEM-2A Air Flow Distribution, Candidate D

The total pressure loss curve for a 5 tier rack with 10 watt core board ISEM-2A modules is shown in Figure 116. This curve summarizes the losses of the inlet plenum, the distribution duct, the modules, the exhaust duct and the exhaust plenum. A 5 tier rack supplied at 5 lb/min/kW has a total pressure loss of about 4.9 in. H_2O, which is well within the capability of the aircraft ECS supply.

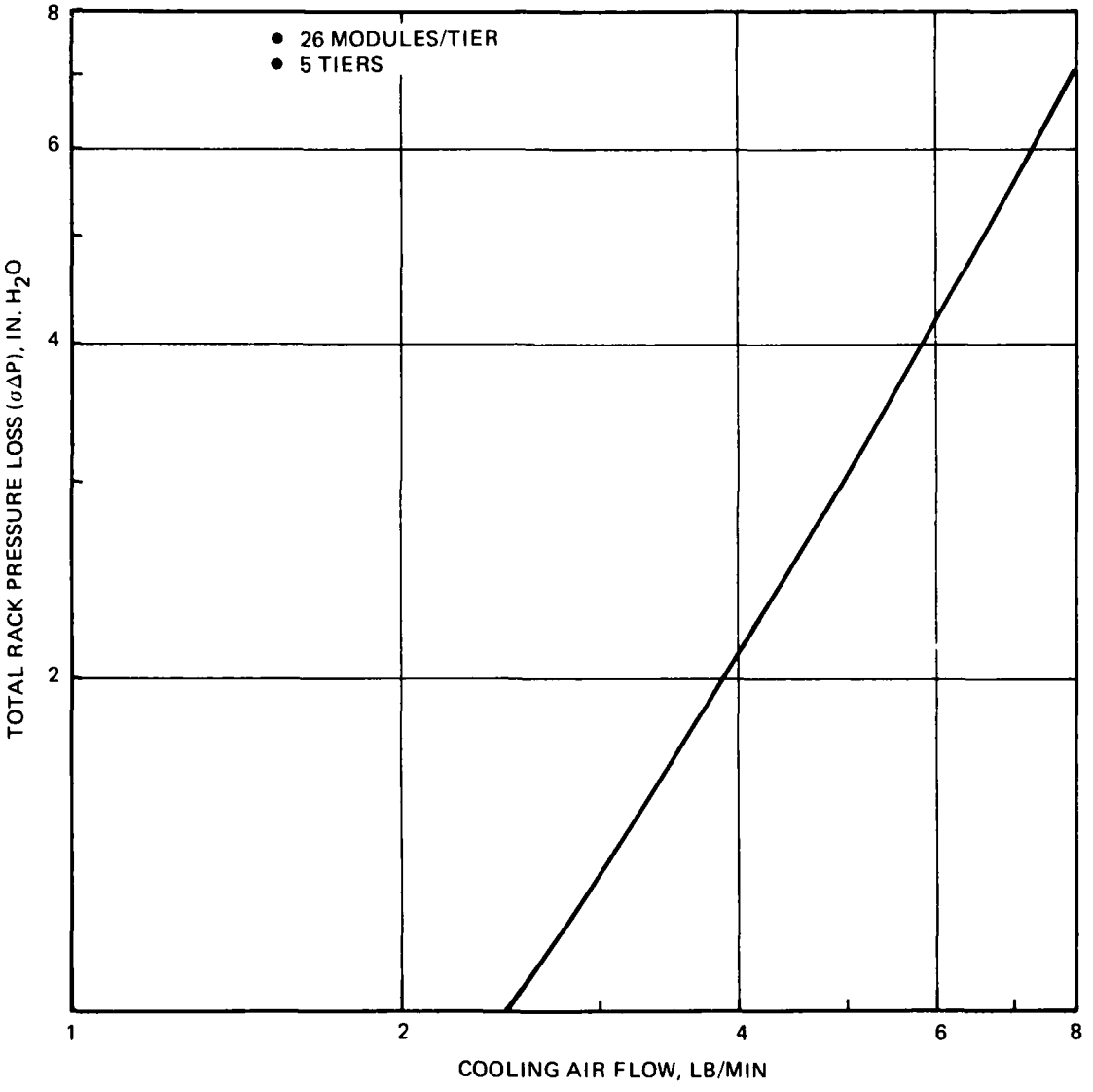

Figure 116 Rack Total Pressure Loss, Candidate D

The performance of the 10 watt Core Board module in terms of component maximum and average junction temperatures is presented in Table 20. This table, when compared to the idealized performance previously presented in Table 12, illustrates the effect of increased junction temperatures due to the unequal distribution of flow to the module. The Core Board, however, yields the lowest maximum and average junction temperatures of any of the rack designs considered with a 10 watt module. In addition, for the concepts considered in this report, the Core Board appears to be the only feasible approach for modules dissipating power greater than 10 watts.

3.6.7.4 Candidate D - Dehumidification - Rack candidate D is very similar to design B_{32} when modes of dehumidification are considered. The electronic components on the module are isolated from the flow of cooling air, and thus a major source of moisture, by the plenums and the finned passages internal to the module. For the same reasons as enumerated for B_{32}, a coil for dehumidification represents a significant weight and volume increase for the system. Thus, like B_{32}, a reheat system consisting of a fan and a heater would be provided to reduce some of the potential moisture effects.

3.7 RELIABILITY & MAINTAINABILITY (R & M)

A primary objective of the Modular Avionics Packaging (MAP) Program is the improvement of reliability and maintainability of aircraft avionics through the use of modular packaging concepts employing standard avionic modules. By providing a benign, low temperature environment the integrated rack can decrease the failure rate of electronic components, particularly semiconductor devices. In

Table 20 Rack Mounted Hollow Core ISEM-2A Performance, Candidate D, 10 W/Module

FLOW RATE (W/Q) LB/MIN/kW	ECS SUPPLY TEMP °F	$T_{j_{MAX.}}$ °C	$T_{j_{AVG}}$ °C
3	40	64	47
	60	75	58
	80	86	69
4	40	54	40
	60	65	51
	80	76	62
5	40	47	35
	60	58	46
	80	69	57

0009-094W

addition, the rack concept will permit easy removal and replacement of avionic modules thereby reducing aircraft downtime and lowering support costs.

All rack concepts were designed around the ISEM-2A avionic module with identical accessibility and remove/replace features. R & M design parameters were maximized as part of the trade-off process necessary to select the most satisfactory design and each rack concept was assessed independent of avionic modules. Failure rates for standard electrical and electronic components were obtained from Mil-HDBK-217 and for mechanical and electromechanical components from RADC-TR-75-22. Failure rates for heatpipes used in rack configuration B_{33} were engineering estimates based upon Grumman in-house heatpipe programs which include OAO spacecraft (8 years without failure) and consultation with Lloyd A. Nelson, project engineer for Hughes/Navy heatpipe programs and a recognized heatpipe expert. A table of rack component failure rates and configurations in which the components are used is presented in Table 21.

For the purpose of life cycle cost evaluation four representative functional avionic modules were postulated: memory, digital, analog and power supply. Each module type was given a component mix representative of its function, and its failure rate calculated at 125°C, 100°C, 80°C and 60°C average junction temperatures. Module failure rates were normalized to one card per rack slot, i.e.,

Table 21 Rack Component Failure Rates

ELEMENT	FAILURE RATE (FAILURES PER 10^6 HRS)	RACK CONFIGURATION				
		A_{21}	B_{32}	B_{31}	B_{33}	D
PRIMARY BACKPLANE	15.25	X	X	X	X	X
SECONDARY BACKPLANE	1.54	X	X	X	X	X
RACK & COOLING LOOP	70			X		
BLOWER	107	X				
FILTER	27	X				
GUIDE RAIL	0	X	X	X	X	X
HEAT PIPE	50				X	
HUMIDITY CONTROL (10% DUTY CYCLE)	50	X		X		

0009-095W

some modules may occupy two or more card spaces because of component height or partitioning efficiency but the module failure rates presented result from the full module failure rate divided by the number of card slots it occupies. For example, the power supply module is expected to occupy one full tier (26 slots) or one-half tier (13 slots). Thus, the normalized module failure rate will be 1/26 or 1/13 of the full power supply module failure rate. Normalized failure rates of the four module types versus junction temperature are presented in Figure 117.

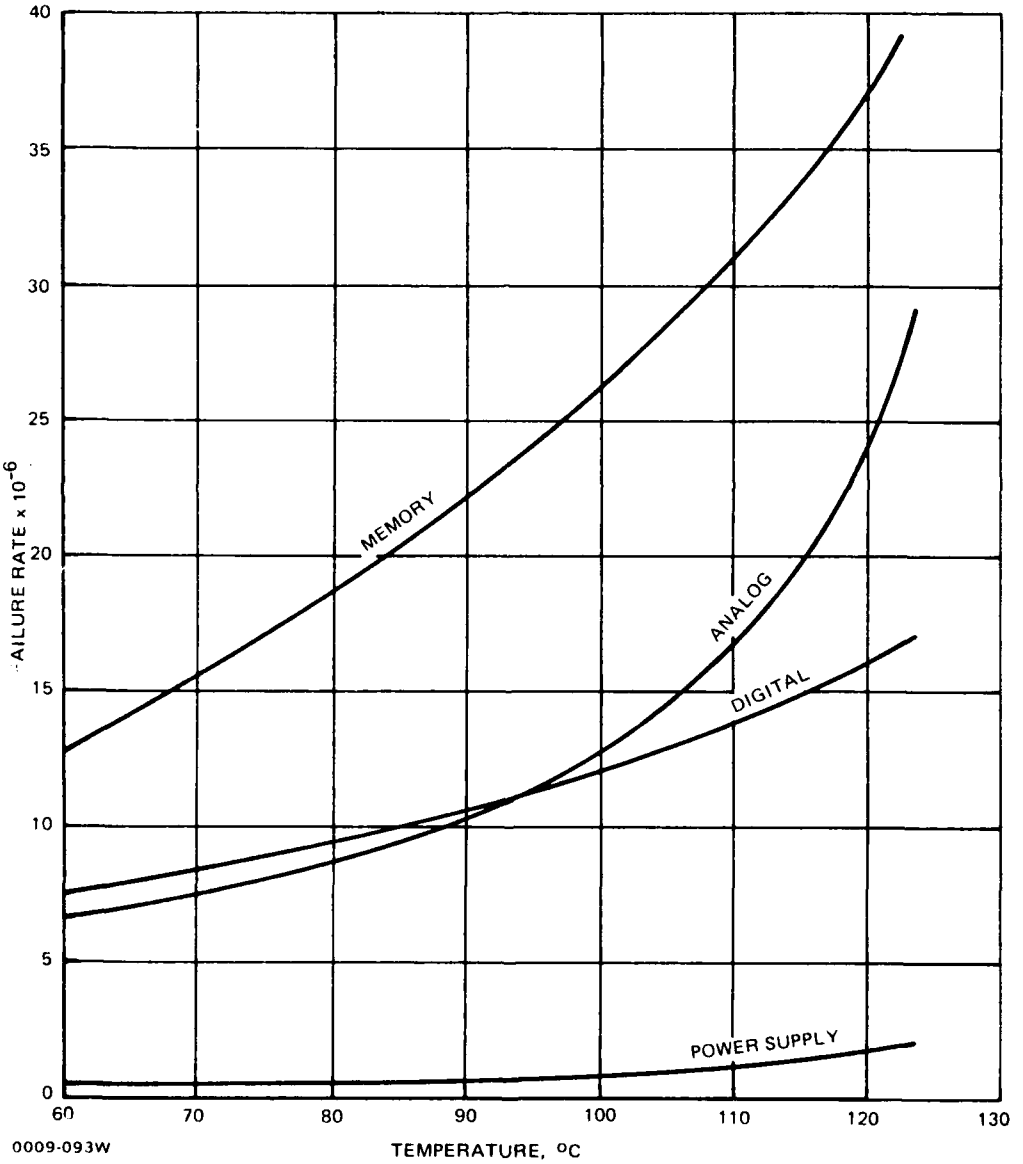

Figure 117 Module Failure Rate (per Slot) vs Temperature, 2 x 6 In. Module

Avionics reliability at the different junction temperatures for B V/STOL (Ref. 1) is shown in Table 22. To obtain these numbers, the following equipments were incorporated into the B V/STOL avionics racks and partitioned into the four module functional types

- Tactical Fighter TIDS Terminal
- IFF KIT-1A/TSEC
- IFF KIR-1A/TSEC
- CNI Processor
- Electronic Warfare Processors
- Display Generators
- Bulk Memory
- Display Processors
- Radar Signal Processor.

The predicted rack avionics MTBFs were converted to realistic operational MFHBFs based upon Grumman's study of predicted equipment reliability versus actual field data (Ref. 2). The study indicates that a ratio of 3:1 (MTBF:MFHBF) is appropriate for this type of avionics. The table indicates that the 1990 rack avionics is expected to show a 4 to 7 times reliability improvement over the equivalent current WRAs. The MTBFs and MTTRs of the individual racks were calculated as shown in a typical R & M estimate work sheet (Table 23). The conceptual nature of the rack design did not lend itself to a rigorous analysis of mean repair time employing methodology described in Mil-HDBK-472 "Maintainability Prediction". A more appropriate "consensus" (Ref. 3) method was employed which involves working with the designer and asking specific questions about troubleshooting and repair until repair times were obtained. This method has two advantages:

- The design engineer is reminded of the need to consider maintainability as a design factor
- Since the design exists only on paper the design engineer is the preferred source for an accurate estimate.

Table 22 B V/STOL Rack Avionics Reliability

MODULE TYPE	RELIABILITY AT AVERAGE JUNCTION TEMPERATURE				
	60°C	80°C	100°C	125°C	
MEMORY	0.0014097	0.0021534	0.0028749	0.0045399	PREDICTED FAILURE RATE
DIGITAL	0.001785	0.0021896	0.002856	0.004165	
ANALOG	0.0003264	0.0003984	0.000600	0.0016752	
POWER	0.0001335	0.0001602	0.0002403	0.0064881	
TOTAL FAIL RATE	0.0036546	0.0049016	0.0065712	0.0168	
TOTAL RACK AVIONICS MTBF	273	204	152	59	1990 PREDICTED MTBF
*PERCENT IMPROVEMENT IN MTBF FROM HIGHER TEMP	33	34	158	–	
RACK AVIONICS MFHBF (1/3)	91	68	51	20	1990 OPERATIONAL MTBF

0009-096W

*EXAMPLE – % IMPROVEMENT IN MTBF FROM 125°C TO 100°C = $\frac{152-59}{152}$ = 158%

Table 23 Typical Reliability/Maintainability Estimate (Air-Over-Components, A_{21})

REPLACEABLE COMPONENT/ASSEMBLY	N	λ $\times 10^{-6}$	N λ $\times 10^{-6}$	MAINTENANCE TASK TIME (MIN)					
				LOCATE	ISOLATE	R & R	CHECK	TIME	N λ x TIME
PRIMARY BACKPLANE	5	15.25	76.25	5	5	20	5	35	2668.75
SECONDARY BACKPLANE	1	1.5	1.5	5	5	35	5	50	75
RACK (INCL. COOLING LOOP)	1	70	70	1	1	120	1	123	8610
BLOWER VAR SPEED	2	107	2.4	1	1	10	1	13	2782
FILTER	1	22	27	1	1	2	1	5	135
TOTAL			388.75						14281 14270.75

MTTR $\frac{14281}{388}$ 36.58 MIN

MTBF $\frac{1}{388} \times 10^6$ 2556 HR

0009-097W

Table 24 presents the R&M characteristics of a standard tier rack for each of the cooling configurations.

Redundancy and backup provisions were also considered in the overall evaluation of the five rack systems, and are presented in Table 25. Those concepts with liquid loops, i.e., A_{21} and B_{31}, employ redundant coolant pumps to insure a reliable heat sink for the racks. The air-side rail concepts, B_{32} and B_{33}, receive cooling air directly from the ECS, and thus require no intermediate heat exchanges, making it less complex than the liquid loop. Overall, configuration D, Air Cooled, Hollow Core module provides the highest reliability with the lowest redundancy/backup complexity.

References - (Section 3.7)

1. Advanced V/STOL Fighter Attack Aircraft, Grumman Aerospace Corp., Study Project AIR-03PA-056, April 1978

2. Evaluation of Environmental Profiles For Reliability Demonstration RADC Report Na. TR-75-242, Grumman Aerospace Corp.

3. Maintainability Parameters Using the Consensus Method, L. T. Jones, Proceedings 1978 Annual Reliability and Maintainability Symposium

Table 24 Individual Rack R&M Characteristics for a Standard 5 Tier Rack

TIERS	AIR OVER COMPONENT A_{21}		CONDUCTION LIQUID B_{31}		CONDUCTION AIR B_{32}		CONDUCTION HEAT PIPE – AIR SIDEWALL B_{33}		HOLLOW CORE MODULE	
	MTBF (HOURS)	MTTR (MINUTES)	MTBF (HOURS)	MTTR (MINUTES)	MTBF (HOURS)	MTTR (MINUTES)	MTBF (HOURS)	MTTR (MINUTES)	MTBF (HOURS)	MTTR (MINUTES)
5	2556	36 6	6770	76.8	12855	35.3	2650	170	12855	35.3

0009-098W

3.8 LCC MODEL DESCRIPTION

The Grumman Total Life Cycle Cost (LCC) Model can be defined simply as a computer program that sums RDT&E and Acquisition Costs (Production plus Initial Support) using accounting equations and Operations and Support costs. The Initial Support and Operation and Support (O&S) costs have been added using the Grumman-modified USAF AFLC Logistic Support Cost (LSC) Model.

Table 25 Redundancy & Backup Considerations

INTEGRATED RACK CONFIGURATION	PRIMARY COOLING MODE			REDUNDANT/BACKUP COOLING MODE		
	RACK	INTERMEDIATE COOLING RACK	HEAT SINK	RACK	INTERMEDIATE COOLING RACK	HEAT SINK
AIR OVER COMPONENTS A_{21}	AIR SUPPLIED BY FANS	LIQUID COOLANT SUPPLIED BY 2 PUMPS	ECS	REDUNDANT FANS	REDUNDANT PUMPS	RAM AIR
CONDUCTION LIQUID RAIL B_{31}	LIQUID COOLANT	LIQUID COOLANT SUPPLIED BY 2 PUMPS	ECS	NONE	REDUNDANT PUMPS	RAM AIR
CONDUCTION AIR RAIL B_{32}	AIR THRU GUIDE RAILS	NOT REQUIRED	ECS	NONE REQUIRED	NOT REQUIRED	RAM AIR
CONDUCTION HEAT PIPE AIR SIDEWALL B_{33}	AIR THRU SIDE RAILS	NOT REQUIRED	ECS	HEAT PIPE TO A C STRUCTURE	NOT REQUIRED	A C STRUCTURE
HOLLOW CORE AIR D 0009-099W	AIR THRU MODULES	NOT REQUIRED	ECS	NONE	NOT REQUIRED	RAM AIR

The final result, the total LCC, is a summation of the individual cost elements across all aircraft systems for the specified life cycle. Prior application to both in-house and AF-funded LCC studies has proved the models accuracy and value in tradeoffs of alternate systems, subsystems and lower-level equipment designs.

An additional program was used to format the LCC into the cost elements of OPNAV-90P-02, "Navy Program Factors Manual". This program has proved extremely valuable in calibrating and validating the model with historical Navy operation and support cost data.

3.8.1 LCC Ground Rules & Assumptions

The first step in setting up the LCC study was to establish ground rules and a scenario for A and B V/STOL. The scenario used was based on Grumman's design in which the aircraft were deployed to three classes of sites: large ships (carriers), small ships, and shore sites with the following complement of aircraft:

A V/STOL

Large Ships

4 CV's with 18 aircraft each

Small Ships

20 DD-963's with 2 aircraft each

Shore Sites

6 Shore Sites with 42 aircraft each

B V/STOL

Large Ships

5 CV's with 12 aircraft each

6 VSS's with 8 aircraft each

Small Ships

10 DD-963's with 4 aircraft each

6 LHA's with 4 aircraft each

12 SWATH's with 4 aircraft each

Shore Sites

3 Shore Sites with 48 aircraft each.

The total of 364 operational aircraft was used in the LCC model in each case for the A and B V/STOL's. This total was escalated to 473 production aircraft to account for Standard Depot Level Maintenance (SDLM) and attrition aircraft requirements.

Additional assumptions and ground rules included in the analysis were:

- 15 years life cycle
- 25 flight hours per month per aircraft during normal operation
- 35 flight hours per month per aircraft during wartime
- 10% expected backorder level for spares (90% probability of no stockout at O-level)
- Two level maintenance - O and D-level
- Remove and replace (R&R) only maintenance at O level, all other repair at D-level

- R&R manhours and failure rates determined by the R&M study (see Section 3.7)
- Depot consumable materials used at a rate of $5.19 per hour of repair (typical of past observed depot consumable material costs)
- Depot turn-around time for repair of avionics is 1.8 months
- One percent of all repair actions result in an item condemnation (except for fans which have a 10% condemnation rate and filters which are a throwaway item)
- All costs in 1979 dollars
- No scheduled maintenance is required for the rack and the rack avionics.

3.8.2 Rack Hardware LCC Study

The objective of the rack hardware LCC study was to determine the sensitivity and document the LCC (Production plus Initial Support, and O&S) for each alternative rack configuration (A_{21}, B_{31}, B_{32}, B_{33} and D). RDT&E costs, the non-recurring engineering costs, and the rack avionic costs were all assumed to be constant, and therefore excluded. Production unit costs for each configuration were estimated by Grumman manufacturing and subcontractors. Each rack configuration was broken down into its major components to model Initial Support and O&S costs. Each component accumulated all respective repair material and labor costs over the life cycle. To these costs the additional costs of the stockage and repair for lower level assemblies were accounted for by adding 1% of the major unit costs to each repair action.

The results of the rack hardware LCC study are tabulated in Table 26 and graphed in Figures 118 and 119. Production costs are clearly the drivers accounting for better than 90% of the LCC in each concept. The Initial Support and O&S costs are relatively low, due to the high reliability of each concept. The most cost effective design concept - conduction with air guide rails (B_{32}) has a highly reliable and relatively simple design. On the other extreme the air over components with liquid guide rails concept (A_{21}), is the most complex and costly over the life cycle. For this design, the fans are the cost drivers accounting for approximately 80% of the LCC. The cost driver for the conduction type concepts

Table 26 Life Cycle Cost Summary for Rack Hardware (Thousands of Dollars)

V/STOL TYPE	RACK CONCEPT	RDT&E	PRODUCTION	INITIAL SUPPORT COSTS	OPERATIONS & SUPPORT COSTS	TOTAL	NO OF RACKS	COST/ RACK
A	A_{21} AIR OVER COMPONENTS LIQUID RAIL		107,100	858	4,186	112,144	8514	13,172
A	B_{31} CONDUCTION LIQUID GUIDE RAILS		44,731	165	963	45,859	6622	6,925
A	B_{32} CONDUCTION AIR GUIDE RAILS		38,084	48	394	38,526	7568	5,091
A	B_{33} CONDUCTION HEAT PIPE		42,449	316	1,717	44,482	7568	5,878
B	A_{21} AIR OVER COMPONENTS LIQUID RAIL		68,959	671	2,791	72,421	5676	12,759
B	B_{31} CONDUCTION LIQUID GUIDE RAILS		26,590	121	650	27,361	4730	5,785
B	B_{32} CONDUCTION AIR GUIDE RAILS		21,523	32	225	21,780	4730	4,605
B	B_{33} CONDUCTION HEAT PIPE		26,258	186	861	27,305	4730	5,773
B	D HOLLOW CORE	–	25,366	42	259	25,667	5676	5,425

0009-100W

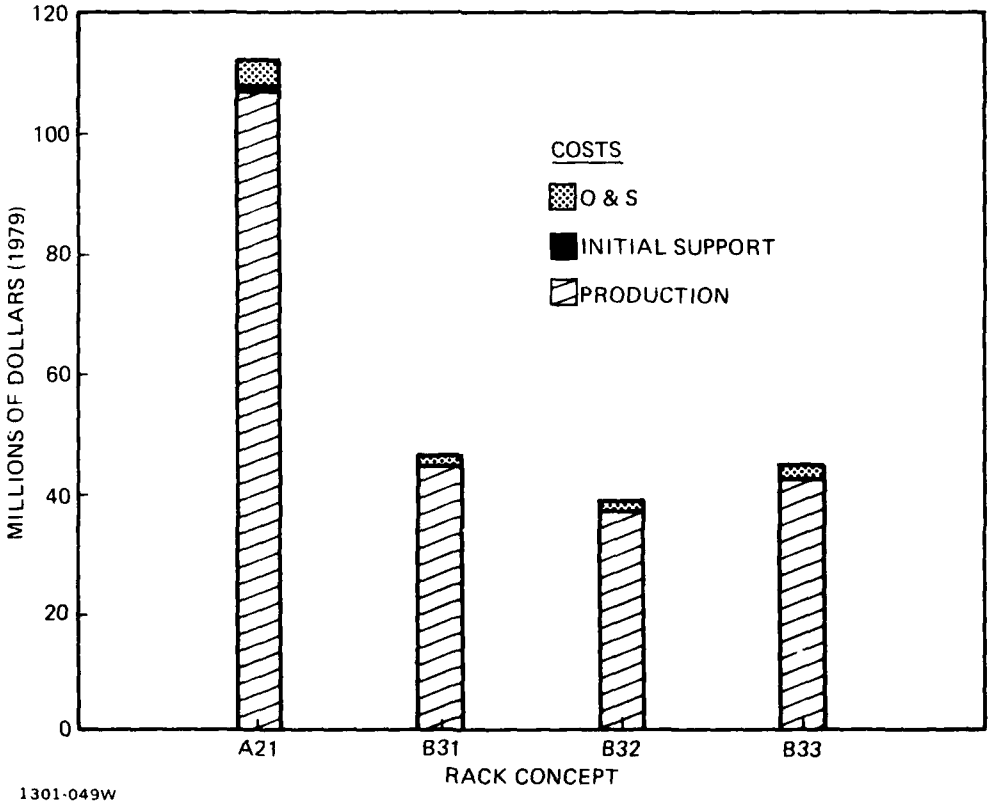

1301-049W

Figure 118 LCC Summary For Rack Hardware of A V/STOL

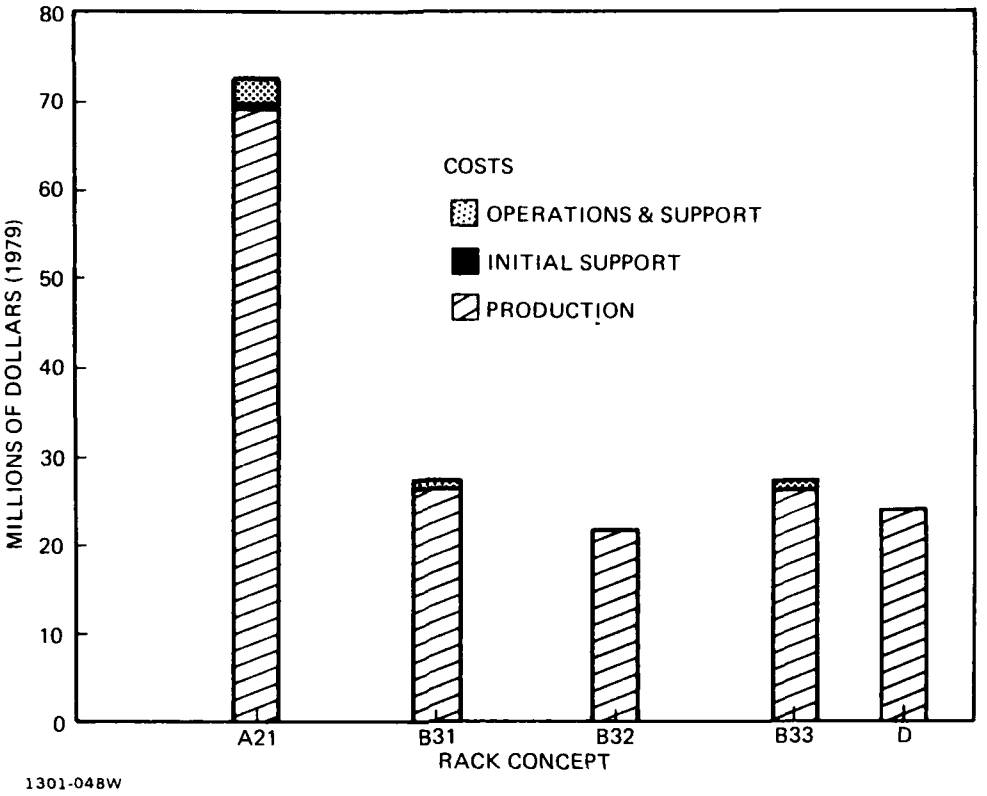

Figure 119 LCC Summary For Rack Hardware of B V/STOL

(B_{31}, B_{32}, B_{33}) is the rack structure itself, accounting for 50-75% of the LCC.

3.8.3 Rack Avionic LCC Sensitivity

The objective of this study was to evaluate the life cycle cost saving and/or penalty due to operating the rack avionics modules at different junction temperatures. As expected the analysis showed there is an inverse relationship of MTBF to junction temperature. The results are shown in Figure 117. The curves, generated by R&M analysis, show the impact of the junction temperature change on MTBF. As shown, there are four generic module types: memory, digital, analog and power supply. Based on the observed power supplies' relative insensitivity to temperature change, it was excluded from any detailed analysis. The number of individual generic type modules in each category was determined from the postulated system architecture. For initial sparing, a minimum of one contingency O-level spare per module per site was assumed with additional spare requirements

based on the individual predicted MTBF and depot pipeline turnaround times. The additional cost of stockage and repair for lower level assemblies were accounted for by adding 0.1% of the total unit cost of each generic module type to each repair action.

The results of this portion of the study are tabulated in Table 27 and Figure 120. Production costs were included and held constant to give a relative magnitude and weight to the support costs. Production costs are clearly shown to be the drivers accounting for over 85% of the LCC at an 80°C junction temperature (or MTBF x 1.00). This temperature corresponds to a system MTBF of 69.9 hours which also accounts for a low Initial Support and O&S cost.

To analyze MTBF sensitivity, MTBF values which were even lower than that corresponding to 125°C (see Table 27) were utilized. The study based on predicted reliability data therefore indicates as shown in Figure 120 that costs are relatively insensitive to junction temperatures below 125°C which includes all temperatures used in the thermal sensitivity study. This is primarily due to the anticipated high reliability of the rack modules and the ease of maintenance of the rack configuration. The initial spare costs are insensitive to the high MTBF policy of one minimum spare for each module. Only at very low MTBF values do O&S costs

Table 27 Rack Avionics LCC Sensitivity to Junction Temperature (MTBF)

			M$				
JUNCTION TEMP °C	SYSTEM MTBF	RDT&E	PRODUCTION COST	INITIAL SUPPORT COSTS	OPERATION & SUPPORT COST	TOTAL LCC	MTBF MULTIPLIER
60°C	97.1	–	217.816	25.872	5.116	248.804	1.390
80°C	69.9	–	217.816	26.037	7.106	250.959	1.000
100°C	52.4	–	217.816	26.335	9.472	253.623	0.750
115°C	42.6	–	217.816	26.523	11.646	255.985	0.610
125°C	37.0	–	217.816	26.753	13.400	257.969	0.530
	18.5	–	217.816	28.133	26.797	272.746	0.265
	3.7	–	217.816	38.621	133.968	390.405	0.053

0009-101W

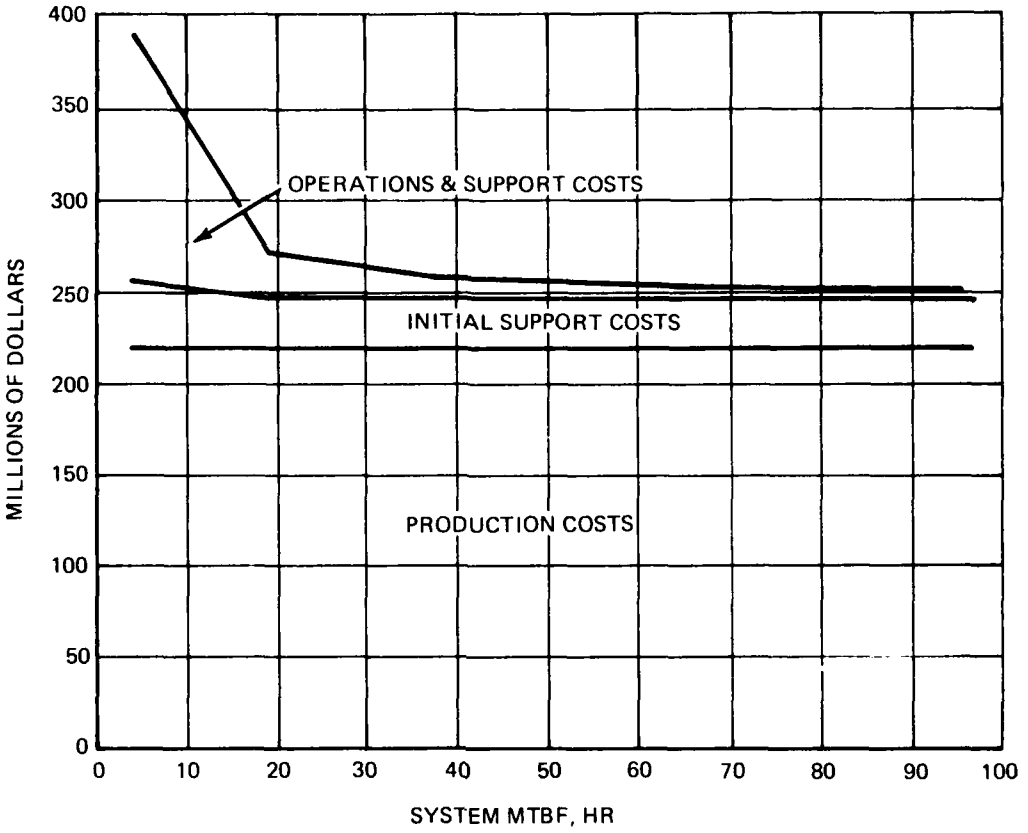

NOTES: (1) RELIABILITY (MTBF) IS PREDICTED UPON THE INHERENT CAPABILITY OF THE SYSTEM FOR A GIVEN JUNCTION TEMPERATURE.

(2) PRODUCTION COSTS WERE KEPT CONSTANT TO SIMPLIFY THE LCC MODEL.

(3) FOR PARAMETRIC COMPARISONS JUNCTION TEMPERATURES IN EXCESS OF 110°C WERE CONSIDERED. HOWEVER, GOOD DESIGN PRACTICE DICTATES THAT THE JUNCTION TEMPERATURE ALWAYS BE LESS THAN 110°C. THE INTEGRATED RACK WAS DESIGNED FOR AN 80°C JUNCTION TEMPERATURE.

0009-102W

Figure 120 Rack Avionics LCC Sensitivity to MTBF

begin to rapidly increase. This highlights the optimality of the proposed systems at their expected operating junction temperatures and MTBF's.

It should be noted that temperatures above 110°C were considered only for parametric comparisons. However, good design practice dictates that junction temperature always be less than 110°C. The Integrated Rack was designed for an 80°C junction temperature.

4 - SELECTION OF THE PREFERRED DESIGN

4.1 ASSESSMENTS OF CONCEPTS

The Integrated Rack designs which have been developed for the study are evaluated in this section. To perform the evaluation a program was developed which assesses the concepts. The results of the program in conjunction with the results of life cycle costs, risk and performance data are used to select the most promising concepts which should be pursued in future studies.

4.2 SENSITIVITY EVALUATION PROGRAM

The Sensitivity Evaluation Program (SEP) consists of utilizing and evaluating all the technology disciplines associated with the Integrated Rack design. As some disciplines are considered more vital to the design of the rack than others, their importance are reflected by the use of weighting factors. For example, in evaluating a design of the rack, the evaluation of efficient thermal management for any specific rack design is considered more important than the card volume capability evaluation. Thus as shown in Table 28, the thermal discipline is assigned a weighted factor of 1.0 while the volume evaluation receives a weighted factor of 0.7. Each evaluation discipline uses values from 0 to 10 to denote performance. A 10 in any one area signifies that the rack concept has extremely good characteristics for that discipline being considered. Note that the weighted result is the product of the weighted factor and the performance value. The weighted results for the rack designs which use 5 watts/module are shown in Table 29. Since some racks have different performance at 10 watts and the D, Hollow Board Core Design was only considered at 10 watts, a separate SEP was conducted. Table 30 contains the results of the SEP when 10 watts/module are used.

The input to the SEP was performed as objectively as possible. Summary rationales were developed from each of the disciplines involved in the SEP. Missing from providing an input was the power discipline which by virtue of the

Table 28 Weighting Factors

RELIABILITY	1.0
THERMAL	1.0
ENVIRONMENTAL CONTROL	1.0
HUMIDITY CONTROL	1.0
EMI PROTECT	1.0
MAINTAINABILITY	0.9
MECHANICAL	0.8
CARD VOLUME CAPABILITY	0.7

0009-103W

Table 29 Result of SEP at 5 W/Module

DISCIPLINE	INTEGRATED RACK CONFIGURATIONS			
	A_{21}	B_{31}	B_{32}	B_{33}
THERMAL	6.0	8.0	10.0	0
ENVIRONMENTAL CONTROL	6.0	8.0	10.0	0
HUMIDITY CONTROL	10.0	8.0	6.0	8.0
RELIABILITY	4.0	8.0	10.0	4.0
MAINTAINABILITY	7.2	3.6	9.0	1.8
MECHANICAL RACK PACKAGING EFFICIENCY	2.4	7.2	8.0	6.4
EMI PROTECT	6.0	10.0	10.0	10.0
CARD VOLUME CAPABILITY	4.2	7.0	7.0	7.0
TOTAL	45.8	59.8	69.3	35.8

0009-104W

rack designs being very similar, no significant differences resulted between the concepts being evaluated.

4.2.1 Thermo ECS & Humidity Control Summary

Three distinct modes of cooling the ISEM-2A modules have been considered in this study. Rack designs A_{21} and C were developed to evaluate the air over components concept. Racks B_{31} and B_{32} were designed to use conduction to

Table 30 Results of SEP at 10 W/Module

DISCIPLINE	INTEGRATED RACK CONFIGURATIONS			
	A21	B31	B32	D
THERMAL	0	7.0	9.0	10.0
ENVIRONMENTAL CONTROL	0	8.0	10.0	10.0
HUMIDITY CONTROL	10.0	8.0	6.0	6.0
RELIABILITY	2.0	5.0	10.0	10.0
MAINTAINABILITY	8.1	4.5	9.0	9.0
MECHANICAL RACK PACKAGING EFFICIENCY	2.4	7.2	8.0	3.2
CARD VOLUME CAPABILITY	4.2	7.0	6.3	2.8
EMI PROTECT	8.0	9.0	9.0	10.0
	34.7	55.7	67.3	61

0009-105W

liquid and air heat sinks. The final rack design considered, concept D, used an air cooled module incorporating a hollow core with the ISEM-2A form factor. Racks A_{21}, B_{31}, B_{32} and C were developed for a module power dissipation of 5 watts. In addition, a power dissipation of 10 watts per module was considered for concepts A_{21}, B_{31}, B_{32} and D.

ECS airflow from the aircraft has been established as the ultimate heat sink for all the designs in order to provide for a common basis of performance comparison. The performance of each of the rack designs can be compared by using the following tables: Table 16, for air over components; Table 15 for conduction air and liquid rails; and Table 20 for hollow core ISEM-2A.

At the 5 watt per module power, the B_{32} air-conduction design yields the lowest component average junction temperature of the three racks considered, A_{21}, B_{31}, and B_{32}. However, the maximum component junction temperature is about the same as the B_{31} liquid-conduction design. The air over components design A_{21} performs significantly worse at 5 watts per module than either conduction design. One reason for this is the low air flow rate available from the fan. Other problems with this design will be addressed below.

At 10 watts per module, the hollow core ISEM-2A exhibits the lowest component maximum and average junction temperatures of the four designs considered. The max. junction temperatures are at least 60°C lower than those of the nearest rival, the B_{32} air-conduction design. In addition the Hollow Core design has a much smaller and uniform band of junction temperatures, and lower module temperature gradients than the air-conduction design. The Hollow Core also appears to have the capability to be used at higher module powers. Both conduction designs will be hampered at higher module powers due to the high thermal resistance between a module component and the coolant passage wall. Low ECS coolant supply temperatures are required to overcome this resistance and yield reasonable junction temperatures. These low ECS supply temperatures, however, soon become impossible to supply.

The B_{31} liquid-conduction design has component maximum junction temperatures about the same as the B_{32} air-conduction at 10 watts per module. Its average component junction temperatures, however, are 20°C higher than concept B_{32}. The principal reason for this relatively poor performance is the temperature at which coolant is available to the modules. In both designs B_{32} and D, the ECS air is provided directly to the racks. In design B_{31}, the Coolanol must be cooled in the interface heat exchanger by the ECS air before being pumped to the racks. Within the range of ECS air flows considered, 3 to 5 lb/min/kW, the Coolanol temperature supplied to the racks will be significantly higher than that of aircraft ECS air itself.

Air over components, A_{21}, at 10 watts does not perform well even if the required air flows from the fans could be supplied. The component maximum and average junction temperatures are significantly higher than the other three rack designs. An important reason is the number of interfaces across which the module heat must be transferred. Heat from a component must first be transferred to the fan circulated air. This air dumps its heat load into the Coolanol, which in turn, finally transfers it to the ECS air at the interface heat exchanger. The

number of transfers and the inefficiencies of each result in the poor performance of air over components with respect to the other concepts. Even if the racks were placed in pressurized compartments, so that the full cooling air flows can be supplied by the fans, air over components cannot outperform the two conduction designs or the hollow core ISEM-2A. Comparing the 10 watt performance of A_{21} in Table 16 with the other design illustrates this fact.

In addition to evaluating performance in terms of maximum and average component junction temperature, the penalties of weight and input power required by the different cooling modes must be considered. Tables 31 and 32 present an assessment of these penalties for the A and B V/STOL vehicles. The extremes of the module maximum and average junction temperatures attainable by each design

Table 31 Penalties for Basic Rack Cooling Modes, A V/STOL

	A_{21} AIR/COMPONENTS		B_{31} LIQUID RAIL		B_{32} AIR RAIL		D HOLLOW CORE ISEM-2A
MODULE POWER, W	5	10	5	10	5	10	10
TOTAL RACK ELECTRONIC LOAD, kW	11	22	11	22	11	22	22
TOTAL A/C ECS AIR FLOW, LB/MIN	33–55	66–110	33–55	66–110	33–55	66–110	66–110
A/C ECS AIR SUPPLY TEMP, °F	40°–80°	40°–80°	40°–80°	40°–80°	40°–80°	40°–80°	40°–80°
MODULE AVG JUNCTION TEMP, °C	117°–75°	–	100°–60°	129°–89°	82°–47°	110°–76°	69°–35°
MODULE MAX JUNCTION TEMP, °C	126°–84°	–	110°–70°	147°–107°	112°–68°	148°–106°	86°–47°
COOLANOL 25 FLOW, LB/MIN/kW	15.4	11.5	15.4	7.7	–	–	–
COOLANOL 25 FLOW RATE, LB/MIN	170	254.0	44.7	170	–	–	–
FAN FLOW, LB/MIN/kW	2.9	3–5					
FAN INPUT POWER, kW (PRIMARY COOLING)	1.6	NOT PRACTICAL	–	–	–	–	–
PUMP INPUT POWER, kW	3.5	5.2	3.5	3.5	–	–	–
WEIGHT, A/C INTERFACE ECS SYSTEM, LB	186	199	166	166	35	38	46
TOTAL WEIGHT OF RACKS INSTALLED IN A/C, LB	1281	1281	940	940	879	879	1110
TOTAL WEIGHT OF RACKS + INTERFACE SYSTEM, LB	1467	1480	1106	1106	914	917	1156

0009-106W

Table 32 Penalties for Basic Rack Cooling Modes, B V/STOL

	A_{21} AIR/COMPONENTS		B_{31} LIQUID RAIL		B_{32} AIR RAIL		D HOLLOW CORE ISEM-2A
MODULE POWER, W	5	10	5	10	5	10	10
TOTAL RACK ELECTRONIC LOAD, kW	6	12	6	12	6	12	12
TOTAL A/C ECS AIR FLOW, LB/MIN	18–30	36–60	18–30	36–60	18–30	36–60	36°–60°
A/C ECS AIR SUPPLY TEMP, °F	40°–80°	40°–80°	40°–80°	40°–80°	40°–80°	40°–80°	40°–80°
MODULE AVG JUNCTION TEMP, °C	117°–75°	–	100°–60°	129°–89°	82°–47°	110°–76°	69°–35°
MODULE MAX. JUNCTION TEMP, °C	126°–84°	–	110°–70°	147°–107°	112°–68°	148°–106°	86°–47°
COOLANOL 25 FLOW, LB/MIN/kW	15.4	11.5	15.4	7.7	–	–	–
COOLANOL 25 FLOW RATE, LB/MIN	92.4	138.5	92.4	92.4	–	–	–
FAN FLOW, LB/MIN/kW	2.9	3–5					
FAN INPUT POWER, kW	0.90	NOT PRACTICAL	–	–	–	–	–
PUMP INPUT POWER, kW	1.9	2.8	1.9	1.9	–	–	–
WEIGHT, A/C INTERFACE ECS SYSTEM, LB	138	157	130	130	59	64	64
TOTAL WEIGHT OF RACKS INSTALLED IN A/C, LB	680	680	443	443	409	409	563
TOTAL WEIGHT OF RACKS + INTERFACE SYSTEM, LB	818	837	573	573	468	473	627

0009-107W

for the standard ECS air flow inputs are shown. Total aircraft requirements for Coolanol flow and pump input power and fan air flow rates and input powers have also been shown.

In racks where there is a Coolanol loop, its weight has been presented as the A/C Interface System Weight. It includes weights of the following items: interface heat exchanger, Coolanol 25, pumps, tanks, ducting, couplings, valves, controls and supports. For the racks using air cooling, the Interface System is considered to be the weights of the ducting, couplings, valves, controls and supports required to supply the racks with air.

In addition, for each rack design, the weight of the entire compliment of racks in an aircraft is presented. The total of the ECS Interface System weight and the weight of the aircraft compliment is also shown. In both A and B VSTOLs, the trends are the same. Design B_{32} air-conduction imparts the lowest overall weight penalty to the aircraft. The hardware required by the B_{31} liquid-conduction design, the closest rival, is about 100 lbs heavier in the B V/STOL and about 200 lbs heavier in the A V/STOL. Designs D, hollow core ISEM, and A_{21}, air over components, are even heavier than this.

From an ECS standpoint, the A_{21} air over components design is clearly the poorest performer of the various concepts presented, at both 5 and 10 watt module powers. While the B_{31} liquid conduction does not offer as good junction temperature performance as the B_{32} or D designs, at 10 watts it is more easily provided with a complete dehumidification system. The addition of a liquid dehumidification loop to either the B_{32} or D designs would add a significant weight and complexity factor to these systems. In terms of simplicity of rack design and cooling system design, however, the B_{32} air conduction design is clearly the most favorable.

Thermally, the relative merits of the 5 watt conduction modules are evaluated by use of the thermal resistance summary shown in Table 33. The figure illustrates that the ECS airflow requirement for the heatpipe rail is significantly greater than for the other two designs and hence should not be a viable integrated rack candidate. Present state of the art Environmental Control Systems can be defined which provide 3 to 5 pounds/min/kw of ECS conditioned airflow and nominally 40 to 80°F air supply temperatures. Table 34 summarizes the resulting average and maximum junction temperatures for the various rack design concepts. The table shows that for a given ECS output, the air rail concept consistently produces lower average junction temperatures.

4.2.2 Reliability & Maintainability Evaluation of the Candidate Systems

The R&M characteristics of the individual racks configuration are combined into A and B V/STOL racks systems to yield the overall Reliability and Maintainability estimates and assessments presented in Table 35. The power

Table 33 Thermal Resistance Summary

MODULE DESCRIPTION CONDUCTION	COOLANT	COOLANT FLOW RATE LB/MIN/kW	ECS AIRFLOW LB/MIN/kW	THERMAL RESISTANCE °C/W	COMMENTS
LIQUID RAIL 5W MODULE	COOLANOL 25	4.06 13.54 67.69 155.38	3.0 – – –	9.26 7.89 6.89 6.65	ΔT JUNCT – COOLANT USE 1/2 MODULE DISSIPATION TO GET ΔT ABOVE COOLANT TEMPERATURE
AIR RAIL 5W MODULE	AIR	1.46 3.00 6.00 12.00	1.46 3.00 6.00 12.00	7.95 7.79 7.26 6.91	SAME AS ABOVE
HEAT PIPE RAIL 5W MODULE 130W CONDENSER	EVAP FREON-12	–	–	7.80	ΔT= JUNCT – EVAP USE 1/2 MODULE DISSIP TO GET ΔT ABOVE EVAP
	COND. FREON-12	–	4.0 6.0 12.0 16.0	19.30 18.63 18.60 18.46	ΔT= JUNCT – MEAN AIR SUPPLY USE 1/2 MODULE DISSIP TO GET ΔT ABOVE MEAN AIR TEMP.

0009-108W

Table 34 Five-Watt Module

FLOW RATE W/Q LB/MIN/kW	ECS SUPPLY TEMP °F	AIR RAIL		LIQUID RAIL		AIR OVER COMPONENTS	
		T_{jmax} °C	T_{javg} °C	T_{jmax} °C	T_{javg} °C	T_{jmax} °C	T_{javg} °C
3.0	40 60 80	89 100 112	59 70 82	88 99 110	77 88 100	98 109 121	90 101 112
4.0	40 60 80	76 87 98	52 63 74	76 88 99	66 77 88	89 100 111	80 91 102
5.0	40 60 80	68 79 90	47 58 69	70 81 92	60 71 82	82 93 104	73 84 96

0009-109W

AD-A081 864 GRUMMAN AEROSPACE CORP BETHPAGE NY F/G 1/3
INTEGRATED RACK CONCEPT STUDY FOR V/STOL TYPE AIRCRAFT.(U)
JAN 80 E V RAMIREZ, B BORGENSON, A CASERTA N62269-78-R-0294
UNCLASSIFIED NADC-78-11360 NL

3 OF 3
AD
A081864

END
DATE FILMED
4-80
DTIC

Table 35 R&M Estimate & Assessment, Total Rack System

INTEGRATED RACK CONFIGURATION	A V/STOL		B V/STOL		FEATURES
	MTBF	MTTR	MTBF	MTTR	
AIR OVER COMPONENTS A_{21}	150	38.6	284	38.0	MOST COMPLEX LOWEST RELIABILITY
CONDUCTION – LIQUID RAIL B_{31}	398	71.6	752	77.0	SUBJECT TO COOLANT LEAKS POOR MAINTAINABILITY
CONDUCTION – AIR RAIL B_{32}	756	35.4	1428	35.4	LOW COMPLEXITY NO COOLANT LEAKAGE PROBLEMS SHARES BEST OVERALL R & M WITH D
CONDUCTION – HEAT-PIPE, AIR SIDEWALL B_{33}	156	170	294	170	HEAT PIPES CAUSE OF POOR R & M
AIR HOLLOW CORE D	756	35.4	1428	35.4	LOW COMPLEXITY NO COOLANT LEAKAGE PROBLEMS SHARES BEST R & M CHARACTERISTIC WITH B_{32}

0009-110W

dissipation per board (either five or ten watts) was not a consideration in the R&M estimates. The ECS was assumed to have the capability of providing the same component environment for both power dissipation levels. The analysis shows that rack concepts B_{32} - Conduction Cooling/Air-Cooled Guide Rails and D - Air Cooling/Hollow Core Module have the best R&M characteristics from the total rack system and individual rack viewpoint.

4.2.3 Mechanical Evaluation

An important consideration in evaluating the Integrated Rack concepts is the packaging efficiency of the rack designs. A comparison was performed for a typical 5 tier (26 modules/tier) rack. The volume and weight of the rack designs were independently used to determine packaging efficiency. Packaging efficiency can be described by the last two columns of Table 36. In one case, the volume was used to determine the number of modules per cubic inch of the

Table 36 Rack Packaging Efficiency

CANDIDATE	AREA (SQ IN)	VOLUME (CU IN)	WEIGHT (LB)	MODULES PER RACK	MODULES	
					PER IN.^{3}	PER LB
A1 AIR OVER COMP.	482.58	1930.32	76.74	130	0.0673	1.694
B31 LIQUID G. R.	384.82	1539.30	58.18	130	0.0844	2.234
B32 AIR G. R.	401.88	1607.53	56.01	130	0.0808	2.321
B33 HEAT PIPE G.R.	399.00	1596	60.89	130	0.0814	2.135
*C CENTRAL H. E.	1083.36	5416.8	142.0	260	0.0479	1.831
D	585.22	2340.9	69.0	130	0.056	1.884
0009-111W						

rack space. Obviously this value should be as large as possible. Weight can also be used as a Figure of Merit in determining packaging efficiency. The weight of each rack is applied to the basic 130 modules/rack to derive the number of modules per pound. Overall, the conduction air and liquid guide rail designs prove to be the most efficient. Although the liquid guide rail design B_{31} has slightly better volume capability, it is heavier than the air rail design. Consequently the air rail rack B_{32} was chosen as the best. A summary of the weight analyses for the six rack designs is shown in Table 37.

4.2.4 Card Volume Capability Summary

The rack designs with the exception of concept C, were developed to be suitable for use in both A and B V/STOL aircraft. From a volume viewpoint, the need exists for the rack designs to satisfy both configurations. The sum of the card volume capability for both V/STOL aircraft is therefore compared to the total card volume requirements in Table 38. The results indicate that the conduction cooled racks were the only designs capable of meeting the card volume requirements. The hollow board concept for example, although attractive

Table 37 Summary of Weight Analysis (lb)

(TYPICAL FIVE TIER RACK – 130 ISEM-2A MODULES EXCEPT AS NOTED BY *)						
CANDIDATES	A21	B31	B32	B33	C*	D
FRAME ASSY	14.64	13.42	13.13	12.34	48.94	21.18
GUIDE RAILS/HE		5.04	5.68	10.91		8.81
GUIDE RAILS	4.04				8.00	–
HEAT EXCHANGER	11.34				1.50	–
CONNECTOR PLATE	2.02	2.02	1.95	1.75	3.54	3.26
PRIMARY BACK PLANE	1.50	1.50	1.50	1.50	3.60	1.75
SECONDARY BACK PLANE	1.25	1.25	1.25	1.25	2.50	1.50
ISEM-2A MODULE	32.50	32.50	32.50	32.50	65.00	32.50
FANS	6.00	0.50	–		7.40	–
DEHUMIDIFIER	1.20	1.20	–			–
COOLANT	0.75	0.75			0.50	–
VARIABLE CONDUCTANCE HP				0.64		–
DIVERTER VALVE	1.00	1.00				–
FILTERS	0.50				0.75	–
TOTAL	76.74	59.19	56.01	60.89	141.73	69.00

*CANDIDATE C ACCOMMODATE TWO TIMES THE NUMBER OF ISEM-2A AS ALL OTHER CANDIDATES.

0009-112W

Table 38 Total Card Volume Capability

CANDIDATE	TOTAL CARD CAPABILITY*
A_{21}	2912
B_{31}	4472
B_{32}	4056
B_{33}	4004
C	520
D	2522
COMBINED V/STOL REQUIREMENT 3179	
*TOTAL COMBINES A AND B V/STOL CAPABILITY	

0009-113W

by its higher thermal capability does not result in an attractive choice when considering volume. The increase in pitch of the cards is directly responsible for the penalizing effect it has in volume capability.

4.2.5 EMI Control For Candidate Configurations

An evaluation of the five prime Integrated Rack Configurations (A_{21}, B_{31}, B_{32}, B_{33}, D) has identified that the four conduction designs are better than the air over components designs from an EMI standpoint. The air over components design is judged to be poor since openings in the Faraday cage for the air will require special EMI waveguide control techniques which are not required for both the liquid and air cooled guide rail configurations. Air over components cooling of power supplies is especially poor since power supplies have transformer couplings operating from 400 cycles per second to 25,000 cycles per second and typically dissipate 25% of the power that they provide. Therefore, these power supplies require large ports for air cooling. The hollow core design D is judged to be better than the others since the cards are further apart and wire-to-wire coupling is minimized. For each application a different set of EMI standards governs. Typically, depending on the type of IC technology used (CMOS, I^2L, or T^2L, etc) for the specific application, a variation in protective measures is required. The 60-mil thickness of the skin of the rack cabinet will be sufficient for the integrated rack to be used on the type V/STOL aircraft.

Internal generated fields can be controlled with groundplane cards which fit snugly into the rack slots and separate various parts of the circuits. Proper separation of wires for EMI control can be used in the design process once signal characteristics including frequency, voltages, current, impedance, rise time, etc. are quantized. The advent of Fiber Optics backplanes and card connectors will tend to simplify the EMI control problems to a great degree.

4.3 EVALUATION SUMMARY

Two separate evaluations at 5 and 10 watts were performed to arrive at the preferred rack configurations. The SEP results shown in Tables 29 and 30 indicate that the conduction air guide rail configuration B_{32} was the most viable. The results of SEP when combined with the life cycle costs, development risks

and performance criteria then determined the final selected designs. Table 39 shows the five candidates and their ratings relative to the criteria that was used. The summary indicates that the conduction cooled air guide rail B_{32} is judged to be the most efficient conceptual design (see Figure 121). When only 5 watts per card are utilized, the liquid guide rail configuration B_{31} was judged to be the second best. If the average power dissipation is 10 watts per card then the hollow board design D would be the alternate (second choice) to the air guide rail design. When the average power per card is increased beyond 10 watts, then the only viable approach to use is the hollow board design.

4.4 OTHER APPLICATIONS

The Integrated Rack concepts as they are described in this report are not limited to use in just V/STOL type aircraft. The modularization concept of incremental size racks widens their application. The use of the rack in the B V/STOL aircraft proves that from a mechanical design, they can be made applicable to other aircraft such as F-14's E-2C's and A-6's. In these aircraft, some racks must be supported on movable structures to provide accessability to the avionics.

In both applications, all the WRAs from existing avionic areas were removed and totally replaced with IAR configurations which fit into the area. The results shown in the table of Figures 122 and 123 indicate that the two conduction racks makes best use of the available volume.

Table 39 Evaluation Summary

	A21 AIR OVER COMPONENTS	B31 LIQUID GR	B32 AIR GB	B33 HEAT PIPE GR	D HOLLOW CORE
SENS EVAL PROGRAM	THIRD	SECOND	FIRST	FOURTH	SECOND
LIFE CYCLE COST	FOURTH	SECOND	FIRST	THIRD	SECOND
DEVELOPMENT RISK	SMALL	NONE	NONE	SMALL	NONE
PERFORMANCE	SENSITIVE TO PRESSURE DROPS	ACCEPT.	ACCEPT.	UNACCEPTABLE	ACCEPTABLE
SUMMARY		SECOND *	FIRST		SECOND +
0009-114W					

* FOR 5 WATT MODULE
+ FOR 10 WATT MODULE

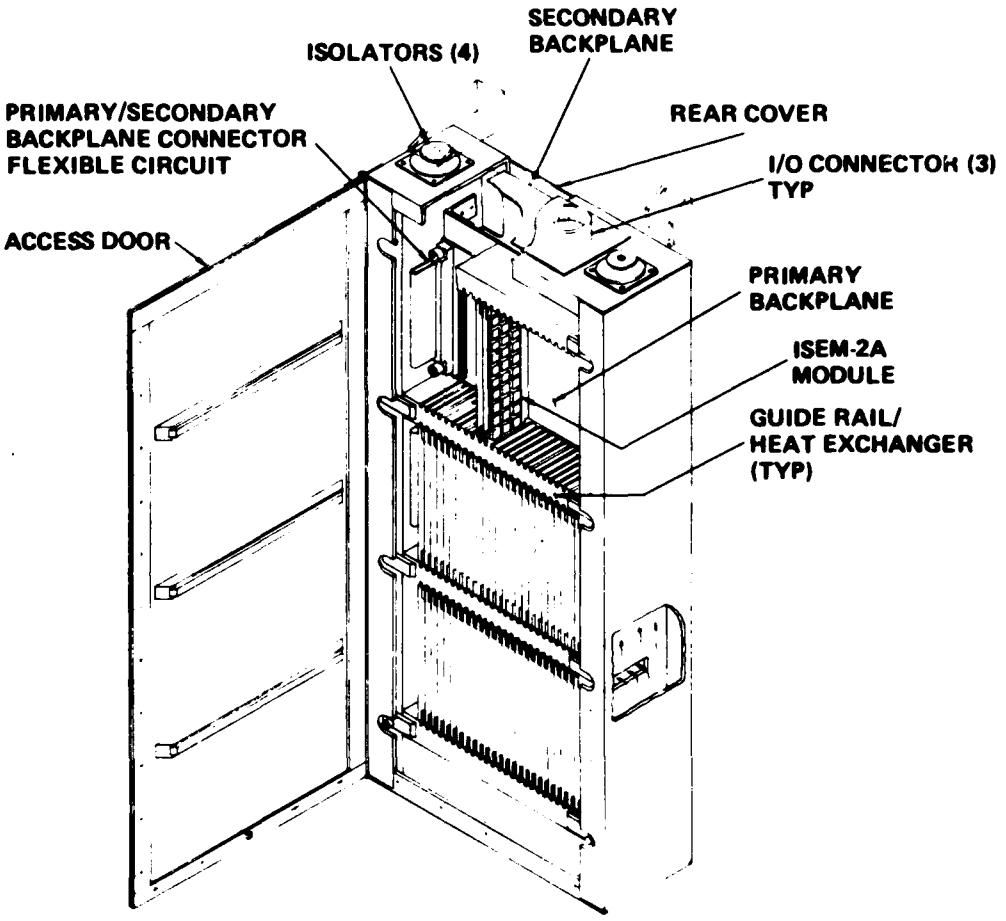

Figure 121 Conduction Integrated Rack, Air-Cooled Guide Rails

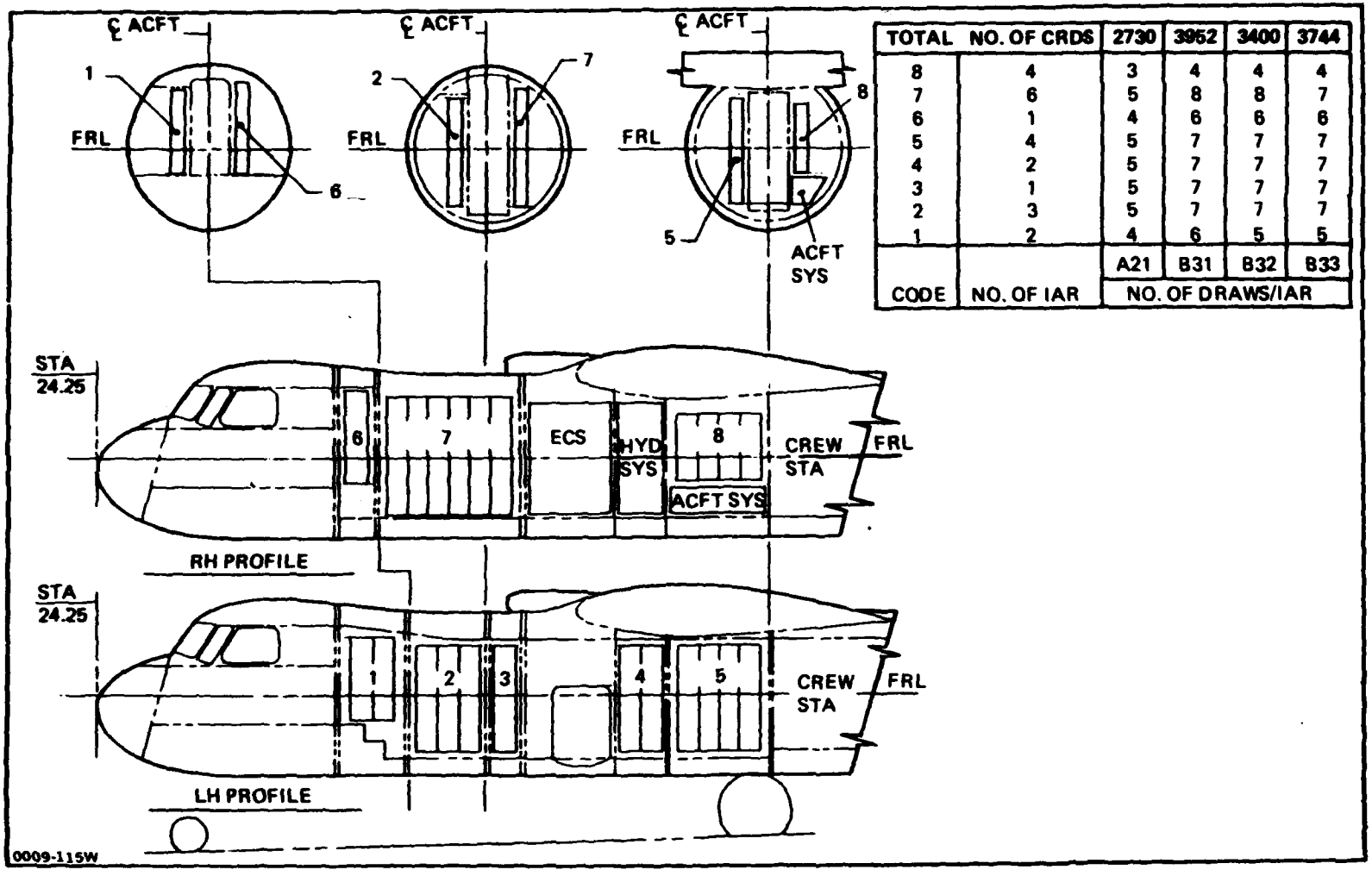

TOTAL	NO. OF CRDS	2730	3952	3400	3744
8	4	3	4	4	4
7	6	5	8	8	7
6	1	4	6	6	6
5	4	5	7	7	7
4	2	5	7	7	7
3	1	5	7	7	7
2	3	5	7	7	7
1	2	4	6	5	5
		A21	B31	B32	B33
CODE	NO. OF IAR	NO. OF DRAWS/IAR			

Figure 122 Integrated Rack Application, E-2C Aircraft

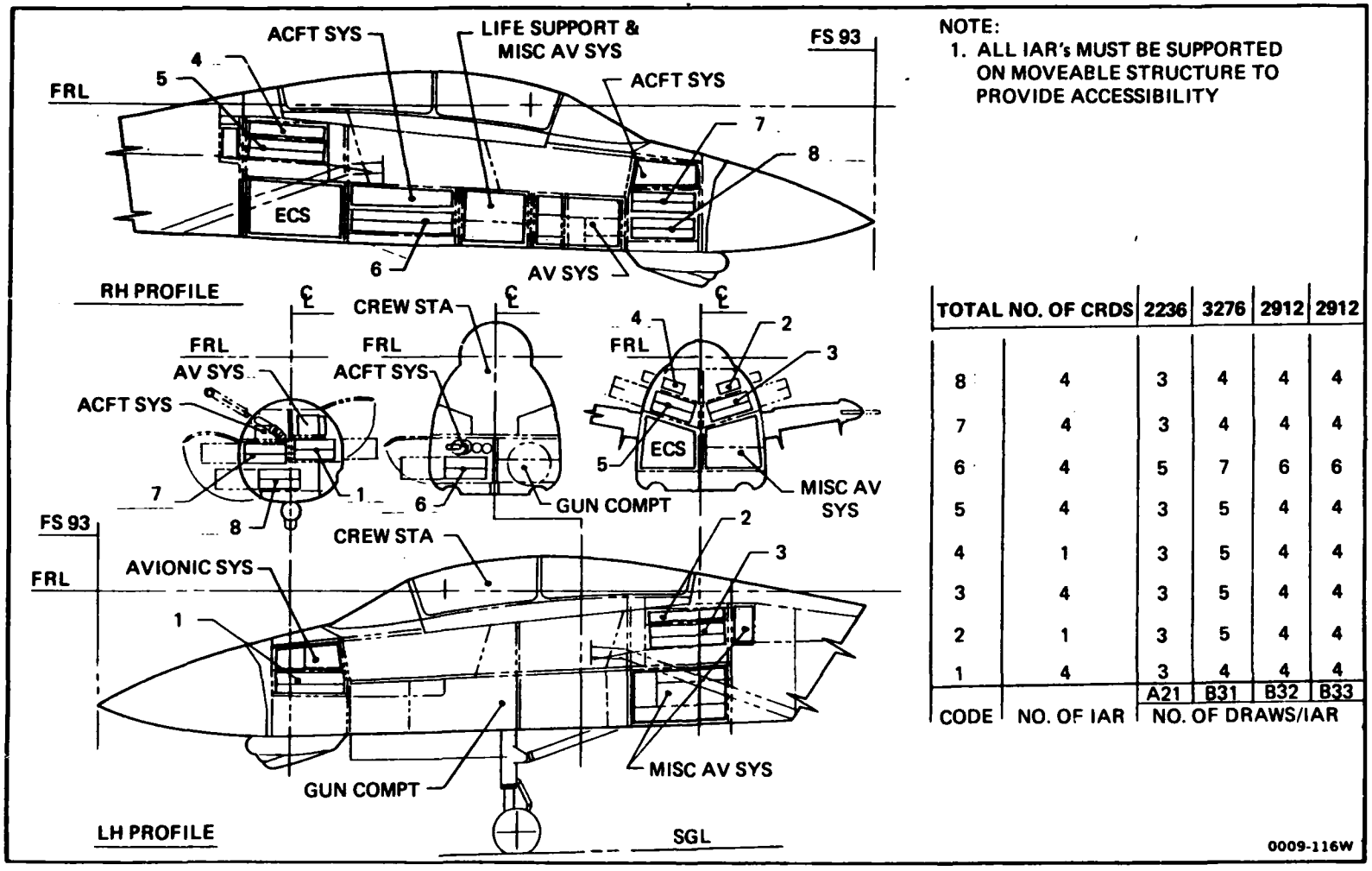

NOTE:

1. ALL IAR's MUST BE SUPPORTED ON MOVEABLE STRUCTURE TO PROVIDE ACCESSIBILITY

TOTAL NO. OF CRDS		2236	3276	2912	2912
8	4	3	4	4	4
7	4	3	4	4	4
6	4	5	7	6	6
5	4	3	5	4	4
4	1	3	5	4	4
3	4	3	5	4	4
2	1	3	5	4	4
1	4	3	4	4	4
		A21	B31	B32	B33
CODE	NO. OF IAR	NO. OF DRAWS/IAR			

0009-116W

Figure 123 Integrated Rack Application, F-14 Aircraft

5 - CONCLUSIONS

5.1 MECHANICAL RACK DESIGN

5.1.1 Material

Although nonmetallic graphite epoxy and Kevlar epoxy are attractive from a weight and stiffness view point, the poor characteristics they have in thermal conductivity and electrical resistivity would require additional complexity in rack design in order to negate these features. Consequently, aluminum alloy (2024 series) is the most viable material to be used for the integrated rack.

5.1.2 Vibration

The use of viscoelastic damping material for the integrated rack will minimize the vibration shock and noise environmental problems. In particular, the results will be:

- control of amplification at structural resonances
- increase of fatigue life of structures
- improvement of equipment reliability.

5.1.3 Rack Configurations

Modular racks concepts have been developed of different tier sizes applicable to both A and B V/STOLs. Rack sizes up to nine tiers are used to partition the avionics in different rack concepts. The use of the smaller rack sizes results in a greater overhead since there is a discrete area required for cooling, power supplies and controllers. Alternately, if only one standard size is available, the total use of rack hardware would greatly diminish as aircraft volume can only provide a limited number of racks of similar dimensions. Thus the implications of a modular rack and its wide application can not be over stated.

5.2 CONCLUSIONS

1. The integrated rack approach is possible from an EMI point of view.
2. The MIL STD 461/462 EMI design and test limits along with EMI test techniques will require modification to cover a V/STOL integrated rack concept (perform a nodal analysis of sources/sinks to identify specification revision requirements).
3. The EMC design requirement must consider onboard generated EMI as well as externally generated EMI for each aircraft type. Specific airframe structural design will have to be defined and analyzed prior to establishing EMC design requirements for the rack.
4. Further development of optical backplanes and miniaturized electrical to optical and optical to electrical interface hardware is required.
5. Analysis of effect of cockpit aperature on Integrated Rack Electromagnetic compatibility is required.

5.3 POWER

The partially redundant sostel system was selected to be incorporated into the Integrated Rack System.

Form factors of 45 and 100 cubic inches were utilized for the 90 and 200-watt supplies. A strong need exists for even higher density supplies.

The 270 Volt System can be used to power the Integrated Racks.

5.4 COOLING CONSIDERATIONS

Conduction cooled racks are far superior to racks which utilize the air impingement concept. When an average power of 5 watts per card is dissipated, then the conduction air guide design B_{32} proves to be the best design. For systems which dissipate 10 watts per card, the same rack design was selected. However, to maintain reasonable maximum and average junction temperatures it is required that the ECS flow rate should be on the order of 5 lb/min/kW. The hollow board rack design shows the most promise when the average power dissipated by the cards becomes greater than 10 watts. The penalties associated with this configuration, (higher pitch resulting in lower packaging efficiency), are offset by the enhanced method the design offers when handling cards of higher power

dissipation. The hollow board design provides lower temperature gradient across the card with slightly less demands on the ECS than other rack concepts.

5.5 RELIABILITY

The conduction air rail (B_{32}) and hollow core (D) concepts, which have essentially the same R&M features, are the preferred integrated rack designs. Because they employ direct injection of cooling air without any intermediate rack heat exchanger they have low complexity and avoid coolant leakage problems.

As the junction temperature is decreased from 125 to 60°C the failure rate of avionics correspondingly decreases, but the rate of decrease (or MTBF improvement) is highest at the upper temperatures and is less significant below 100°C. Thus, reducing avionic junction temperatures much below 80°C results in insignificant LCC benefits.

5.6 DEHUMIDIFICATION

Two forms of dehumidification concepts were developed for the rack designs The heating mode discussed for the B_{32} configuration provides a modest approach to the moisture condensation problem. Since it has not been established what humidity level is important to maintain good reliability, further studies must be conducted during the next phase of Integrated Rack development. This will effect not only the dehumidification schemes but the material selection and coatings that provides moisture protection to the rack and its electronic components.

6 - RECOMMENDATIONS

1. The results of the study show that the B32 conduction air guide rail design is the preferred concept. The analyses included in this report provides a basis for additional investigations since specific areas highlighted in the study can best be further defined by the development of an engineering evaluation unit. For example, problems normally encountered in EMI can be solved by actually developing hardware and conducting tests unique to the rack configuration. Use of heat loads for the 5 and 10 watt module configurations serve to determine the actual junction temperatures and temperature distribution across the cards. Similarly, the cooling requirements for 5 and 10 watt cards can be verified and by use of vibration testing the structural integrity of the rack can be confirmed. Issues associated with back planes and fiber optics/multiplexed data bus concepts when tangible, become more readily resolved.

2. Power supply developments, when compared to other technologies have been slow. The development of supplies which are compatible with the ISEM-2A and the Integrated Rack Form Factor are needed. Only through the development of high density units will the rack packaging efficiency increase.

3. Programs such as VHSIC may push the power dissipation of the circuits considerably. High power modules (greater than 10 watts) should be developed which are compatible and interchangeable with the mounting requirements of the present ISEM-2A. The heat pipe module is such a candidate. The hollow board core concept should also be developed.

4. Secondary back plane technology which integrates Fiber optics (such as 600 - micrometer diameter fibers) with flat circuits is recommended. Although both the optics and the wire technologies are generally well defined, the integration of both into back plane applications has not advanced as rapidly as their own use.

5. SOSTEL provides a workable concept for power management. However the accelerated development of its elements is important so that the benefits can be applied to future Integrated Rack and avionic system efforts.

ABBREVIATIONS & ACRONYMS

AAES	Advanced Aircraft Electrical Systems
ALOFT	Airborne Light Optical Fiber Technology
BIT	Built-in-Test
CMOS	Complementary Metal Oxide Semiconductor
DEMUX	Demultiplexing
DEW	Direct Energy Weapons
DLI	Deck Launch Interceptor
ECL	Emitter Coupled Logic
ECS	Environmental Control System
EMI	Electromagnetic Interference
EMC	Electromagnetic Compatibility
EMP	Electromagnetic Pulse
IAR	Integrated Avionic Rack
ISEM-2A	Improved Standard Electronic Module 2A
LCC	Life Cycle Cost
LHS	Low-Cost High Strength
LIF	Low-Insertion-Force
LSI	Large Scale Integrated Circuit Technology
LEMP	Lightning Electromagnetic Pulse
MAP	Modular Avionic Packaging
MFHBF	Mean Flight Hours between Failures
MTBF	Mean Time Before Failure
MTTR	Mean Time To Repair
MTBMA	Mean Time Before Maintenance Action
MUX	Multiplexing
NAC	Naval Avionic Center
NADC	Naval Air Development Center
NEMP	Nuclear Electromagnetic Pulse
O & S	Operation & Support
RDT&E	Research, Development, Test and Evaluation
rf	Radio Frequency
SEM	Standard Electronic Module
SOSTEL	Solid-State Electric Logic
TSP	Twisted-Shielded-Pair
TOGW	Takeoff Gross Weight
V/STOL	Vertical/Short Takeoff and Landing